Ubiquinone is a key antioxidant during long-chain fatty acid metabolism in *Escherichia coli*

SHASHANK AGRAWAL

Thesis submitted for the partial fulfillment of the degree of

DOCTOR OF PHILOSOPHY

Department of Biological Sciences

Indian Institute of Science Education and Research Mohali

January 2019

Certificate

The work presented in this thesis has been carried out by me under the supervision of Dr. Rachna Chaba at the Department of Biological Sciences, Indian Institute of Science Education and Research (IISER) Mohali, Punjab, India.

This work has not been submitted in part or full for a degree, diploma, or a fellowship to any other university or institute.

Whenever contributions of others are involved, every effort is made to indicate this clearly, with due acknowledgement of collaborative research and discussions. This thesis is a bonafide record of original work done by me and all sources listed within have been detailed in the bibliography.

Date **Place** **Shashank Agrawal**

In my capacity as the supervisor of the candidate's thesis work, I certify that the above statements made by the candidate are true to the best of my knowledge.

Dr. Rachna Chaba

(Supervisor)

Acknowledgements

I express my heartfelt gratitude to my Ph.D. supervisor, Dr. Rachna Chaba for her invaluable guidance, unconditional support, and constant encouragement throughout the period of my research work. I profoundly admire her for being a friend, philosopher and guide, in the truest of their senses, in different phases of my research work. Her leadership has tremendously improved my work abilities and research skills, and taught me the correct ways of implementing ideas and efforts towards achieving success.

I am extremely thankful to my doctoral committee members, Prof. Anand K. Bachhawat and Dr. Shashi B. Pandit for their critical suggestions and motivation that has greatly influenced the quality of my work and crafted my scientific attitude which will be indispensable in my future endeavors.

My sincere gratitude to Prof. Debi P. Sarkar (Director, IISER Mohali) and Prof. N. Sathyamurthy (Former Director, IISER Mohali) for providing me the opportunity to be a part of IISER community. I am thankful to them for providing excellent research facilities, great and competitive research environment, and a cooperative IISER community that has remarkably upgraded my abilities and work.

I thank Dr. Anthony L. Shiver (Stanford University, CA, USA) for analyzing the data obtained from the genetic screen. I greatly admire him for providing all the information and details required for the complete understanding of data analysis.

It gives me immense pleasure to acknowledge and thank Prof. Patricia J. Kiley (University of Wisconsin, Madison, WI, USA) for her precious suggestions that have immensely improved the quality of my work.

I am very grateful to Dr. Dipak Dutta (IMTECH, Chandigarh, India) for sharing reagents and for his constructive feedback on my work. My sincere thanks to Dr. R. Vijaya Anand (IISER Mohali) for help with HPLC experiments. I thank Dr. Gisela Storz (NICHD, Bethesda, MD, USA) for providing pAQ6 construct. I am highly grateful to Dr. Vishal Agrawal (Panjab University, Chandigarh, India) for his critical suggestions and help with some crucial experiments.

Now here are my friends, colleagues, labmates, funmates and foodmates, all in one, i.e. the members of the Chaba lab. If I say, pursing Ph.D. and performing long hour experiments was easily achievable, then I am definitely lying. I would rather say burning mid-night oil is a part of Ph.D. and it's very difficult to pursue without the

help and support of cooperative and trustworthy lab members. I have been really lucky to be a part of Chaba lab, where each member is very generous and upfront for any kind of support or help anytime. I cherished every moment spent with this incredible scientific team. I am very thankful to Bhupinder, Ph.D. student, who was there with me from the very first day in the lab. The experience of setting up the lab together is unforgettable. Very often, Bhupinder's 'all-time ready to help' attitude has helped in overcoming great difficulties. A particular project can only be driven in the right direction if you have skilled and efficient team members. Kanchan Jaswal, Ph.D. student, is exactly the same person one can think of. I thank her for all the help and discussions regarding the project. Garima, Neeladrita, and Swati, Ph.D. students, were helpful and supportive in and out of the lab. The BS-MS students, Himanshi and Megha were always nice and co-operative. I thank Dr. Tapas Patra, former postdoctoral fellow in the lab, for his suggestions and help in standardizing initial experiments.

The Chaba lab started as a part of a five PI lab (Dr. Rachna Chaba, Dr. Mahak Sharma, Dr. Shravan K. Mishra, Dr. Ram Yadav and Dr. Rajesh Ramachandran) in 3TL2 room in Academic Block 1. A majority of my time as a Ph.D. student was spent in the '3TL2 lab'. This arrangement provided a lot of opportunity for inter-group interactions. I thank all the PI's of the '3TL2 lab' and their group members for providing a healthy and interactive research environment.

I am thankful to the Department of Biological Sciences, IISER Mohali for providing a pro-research and scientific environment, which helped in smooth execution of my Ph.D. work. I am indebted to all faculty members for their suggestions during departmental and other presentation events.

Besides excellent research facilities, IISER Mohali has also provided amazing campus enriched with outstanding library, comfortable hostel, nice food courts, eye soothing green and silent campus, that played a hidden but a significant role in successful completion of the project. I thank IISER Mohali for financial support, and all the administrative and other non-academic IISER staff for their help.

I especially thank my batchmates and friends Soumitra, Krishna, and Rohan who constantly stood by me in all ups and downs.

I am fortunate to have an understanding and loving family. I am indebted to my parents whose unconditional support helped me build my strength and enthusiasm during the pursuit of my entire academic career. I thank my wife Paridhi for her silent

efforts and untiring support. My daughter Aadya's effervescent smile helped me rejuvenate after a long and tiring day.

I will always cherish the lifelong associations I have made during my stay at IISER Mohali.

January 2019 *Shashank Agrawal*

Publication

A part of the work embodied in this thesis has been published in:

Agrawal S, Jaswal K, Shiver A. L, Balecha H, Patra T, Chaba R. A genome-wide screen in *Escherichia coli* reveals that ubiquinone is a key antioxidant for metabolism of long-chain fatty acids. **J Biol Chem** 2017; 292: 20086-20099, PMID: 15161972; http://www.jbc.org/content/early/2017/10/17/jbc.M117.806240

Thesis Synopsis

Title – Ubiquinone is a key antioxidant during long-chain fatty acid metabolism in *Escherichia coli*

Supervisor – Dr. Rachna Chaba

Department – Department of Biological Sciences

Institute – Indian Institute of Science Education and Research (IISER)-Mohali

Chapter 1: Introduction

Long-chain fatty acids (LCFAs) are carboxylic acids with an unbranched aliphatic chain comprising 12-20 carbon atoms. Several bacterial pathogens such as *Mycobacterium tuberculosis*, *Pseudomonas aeruginosa*, and *Salmonella typhimurium* metabolize LCFAs derived from host tissues, which enables their survival in harsh environments and contributes to their virulence. From the industrial perspective, due to their highly reduced and anhydrous nature, LCFAs are a promising raw material for production of fuels and chemicals. Although LCFAs are a rich source of energy, they also confer various stresses on bacteria such as acid, membrane and oxidative stress. Therefore, understanding the mechanisms by which LCFAs induce stress in bacteria and in turn the strategies employed by bacteria to counteract such stresses is crucial for identifying targets for the development of new antibacterials and designing novel strategies to promote LCFA-utilization by industrial microbes.

In the present study, using *Escherichia coli* as the model bacterium, we investigated the reason for LCFA-induced oxidative stress and the combat strategies employed by bacteria to mitigate such stress. We showed that LCFA transport and degradation is responsible for elevated levels of reactive oxygen species (ROS) in cells cultured in LCFAs. Our results suggest that a large amount of reduced cofactors produced upon LCFA degradation increase electron flow in the electron transport chain (ETC) thus favoring enhanced production of ROS. Bacteria employ several defense mechanisms to combat ROS that includes both enzymatic players such as superoxide dismutases, catalases and peroxidases, and non-enzymatic players such as glutathione and ubiquinone. The role of ubiquinone, an electron carrier in the ETC, as an antioxidant in bacteria is underappreciated. There is only one report in *E. coli* that

suggests ubiquinone as an antioxidant based on oxidative stress phenotypes of mutants defective in ubiquinone biosynthesis. But, how ubiquinone counteracts ROS, what is the physiological condition under which ubiquinone plays a predominant role as an antioxidant, and what is the relative contribution of ubiquinone to the overall oxidative stress response remains to be assessed. In this study, we analyzed data obtained from a high-throughput genetic screen of *E. coli* single-gene deletion library on oleate, a C18 LCFA. This analysis revealed that amongst various oxidative stress combat players, only the mutants defective in ubiquinone biosynthesis (*ubi* mutants) show significant growth defect in oleate. Through detailed genetic and biochemical experiments we established that ubiquinone is a key antioxidant during LCFA metabolism. Importantly, during the course of our investigation, we characterized *yqiC* as a new player involved in ubiquinone biosynthesis, and showed its genetic interaction with another ubiquinone biosynthesis player, *ubiI*.

Chapter 2: Degradation of long-chain fatty acids generates high levels of reactive oxygen species in *E. coli*

Various mechanisms have been proposed in the literature to explain the correlation between LCFAs and oxidative stress, such as generation of lipid peroxides and peroxyl radicals by oxidative attack on unsaturated fatty acids, stress due to incorporation of fatty acids in the membrane, and β-oxidation of fatty acids. In this section of our study, we investigated the reason for LCFA-induced oxidative stress in *E. coli* by performing a detailed analysis of each individual step involved in LCFA utilization. By assaying ROS levels in various mutants defective in LCFA transport and β-oxidation we established that LCFA degradation is the reason for high levels of ROS in cells grown in LCFAs. Earlier reports suggest that ETC is one of the sites for ROS formation. We proposed that a large amount of reduced cofactors (NADH and $FADH_2$) produced during LCFA metabolism increase electron flow in the ETC thereby increasing the probability of adventitious collision of electrons with O_2 thus contributing to high ROS levels. Our results that ROS levels increase with increase in the chain length of fatty acids, and that both NADH/NAD^+ ratio and the activity of ETC complexes I and II increase in cells utilizing LCFAs are consistent with the above proposal.

Chapter 3: Ubiquinone is a key antioxidant during long-chain fatty acid metabolism in *E. coli*

In this section, we investigated the players involved in counteracting oxidative stress in *E. coli* during LCFA metabolism. For this, we referred to the data obtained from high-throughput genetic screen where the Keio single-gene deletion library of *E. coli* was profiled on the LCFA, oleate. The genetic screen revealed that amongst mutants of various oxidative stress combat players, only mutants defective in ubiquinone biosynthesis (*ubi* mutants) show significant growth defect in oleate. We validated the growth phenotype of various *ubi* mutants in oleate at a candidate level. In candidate studies, we also included succinate that has traditionally been used as a carbon source to screen for genes involved in ubiquinone biosynthesis based on the increased requirement of ubiquinone for growth in succinate compared to glucose. Our results showed that amongst glucose, succinate and oleate, ubiquinone is maximally required for growth in oleate to counteract elevated levels of ROS generated by LCFA degradation. Further, our detailed genetic and biochemical data revealed that amongst various oxidative stress combat players in *E. coli*, ubiquinone is the major antioxidant during LCFA metabolism and acts as the cell's first line of defense against LCFA-induced oxidative stress. Importantly, we observed that ubiquinone accumulates in cells cultured in LCFAs and this accumulation is in response to LCFA degradation. Collectively, our data that LCFA degradation results in elevated levels of ROS and simultaneously signals ubiquinone accumulation suggests that a feedback loop prevents excessive ROS formation during LCFA metabolism.

Chapter 4: Identification of *yqiC* as a novel gene involved in ubiquinone biosynthesis in *E. coli*

Studies in the last several decades have identified eleven ubiquinone biosynthesis genes in *E. coli*. Despite extensive investigations, there are several knowledge gaps in the ubiquinone biosynthesis pathway. For example, the exact role of ubiquinone biosynthesis players, UbiB and UbiJ, is not known and the residual levels of ubiquinone in certain *ubi* mutants suggest redundancy in the ubiquinone biosynthesis pathway. Our results from the previous chapter that the requirement of ubiquinone is maximal in oleate to relieve oxidative stress suggested that oleate is a better carbon source to screen for genes involved in ubiquinone biosynthesis. Therefore, to fill knowledge gaps in the ubiquinone biosynthesis pathway, we again referred to the data

from genetic screen. Amongst the top 100 deletion strains in the screen that showed significant growth defect in oleate were 21 strains that carried deletion in the genes of unknown function (*y* genes). Of these 21 strains, the Δ*yqiC* strain showed maximum growth defect in oleate and was thus selected for detailed analysis. Our search through various databases indicated a strong correlation between *yqiC* and ubiquinone biosynthesis genes. Our results that ubiquinone levels are reduced to ~15-20% in the Δ*yqiC* strain clearly established *yqiC* as a new ubiquinone biosynthesis gene in *E. coli*. Importantly we found that the phenotype of Δ*yqiC* strain was similar to that of Δ*ubiI* strain that lacks a hydroxylase involved in ubiquinone biosynthesis: ubiquinone levels were reduced to ~15-20% in both deletion strains and amongst various carbon sources these strains showed significant growth defect only in oleate. The related phenotypes of *ubiI* and *yqiC* mutants prompted us to examine the phenotype of the *ubiI-yqiC* double mutant. Interestingly, in the *ubiI-yqiC* double mutant, there was no detectable ubiquinone and the strain did not grow either in oleate or succinate. Our results thus provide a strong genetic evidence of the interaction between *yqiC* and *ubiI*.

Table of Contents

Abbreviations

1	µM	Micromolar
2	µmol	Micromoles
3	µl	Microliter
4	4-HB	4-hydroxybenzoate
5	4-HNE	4-hydroxynonenal
6	4-HP_8	3-Octaprenyl-4-hydroxyphenol
7	ATP	Adenosine triphosphate
8	AU	Arbitrary units
9	cDNA	complementary DNA
10	Cit	Citrate
11	CoA	Co-enzyme A
12	Cyd	Cytochrome *bd*
13	Cyo	Cytochrome *bo*
14	DCIP	2,6-Dichlorophenolindophenol
15	$DDMQ_8$	C1-demethyl-C6-demethoxy-Q_8
16	DHE	Dihydroethidium
17	DMAPP	Dimethylallyl diphosphate
18	DMK	Demethylmenaquinone
19	DMQ_8	C6-demethoxy-Q_8
20	DMSO	Dimethyl sulfoxide
21	DNA	Deoxyribonucleic acid
22	ETC	Electron transport chain
23	ETF	Electron transfer flavoprotein
24	$FADH_2$	Flavin adenine dinucleotide

25	FDR	False discovery rate
26	Fum	Fumarate
27	g	grams
28	G3P	Glyceraldehyde-3-phosphate
29	Glo	Glyoxylate
30	GSEA	Gene set enrichment analysis
31	GSH	Glutathione
32	H_2O	Water
33	H_2O_2	Hydrogen peroxide
34	HBSS	Hanks' balanced salt solution
35	HPLC	High Performance Liquid Chromatography
36	IC	Intermediate compound
37	IPP	Isoprenyl diphosphate
38	Isocit	Isocitrate
39	LCFA	Long-chain fatty acid
40	Mal	Malate
41	MDA	Malondialdehyde
42	min	Minutes
43	MK	Menaquinone
44	ml	Milliliter
45	mM	Millimolar
46	MQ	Milli-Q water
47	N.D.	Not determined
48	NA	Not available
49	NADH	Nicotinamide adenine dinucleotide

50	NBT	Nitroblue tetrazolium
51	Ndh	NADH dehydrogenase II
52	NES	Normalized enrichment score
53	nm	Nanometer
54	nmol	Nanomoles
55	Nuo	NADH dehydrogenase I
56	O_2^-	Superoxide ion
57	Oaa	Oxaloacetate
58	OD	Optical density
59	OHB	3-octaprenyl-4-hydroxybenzoate
60	OPP	3-octaprenylphenol
61	PCR	Polymerase chain reaction
62	PMF	Proton motive force
63	pmol	Picomoles
64	Q_{10}	Ubiquinone-10
65	Q_8	Ubiquinone-8
66	Q_8H_2	Ubiquinol-8
67	RNA	Ribonucleic acid
68	ROS	Reactive oxygen species
69	S.D.	Standard deviation
70	Sdh	Succinate dehydrogenase
71	SDS-PAGE	Sodium dodecyl sulphate-polyacrylamide gel electrophoresis
72	SOD	Superoxide dismutase
73	Suc	Succinate
74	Suc-CoA	Succinyl-CoA

75	TB	Tryptone broth
76	TBARS	Thiobarbituric acid responsive substances
77	TCA	Tricarboxylic acid
78	WT	Wild-type
79	α-KG	α-ketoglutrate
80	λ_{max}	Maximum absorbance wavelength

CHAPTER I

Introduction and Review of Literature

1.1 Introduction

Escherichia coli, a gram-negative, facultative anaerobe, exhibits tremendous metabolic flexibility. *E. coli* can utilize a broad range of organic carbon sources for heterotrophic growth, which includes both fermentable (e.g., glucose) and non-fermentable (e.g., fatty acids) carbon sources (Cronan and Laporte, 2005). In this review, we discuss the routes for metabolism of different carbon sources in *E. coli* with a special focus on the metabolism of long-chain fatty acids (LCFAs). Besides *E. coli*, LCFAs serve as an energy-rich nutrient source for several pathogenic bacteria, which contributes to their survival and virulence (Fang et al., 2005; McKinney et al., 2000; Son et al., 2007). In addition to the important role of LCFAs in bacterial pathogenesis, because of the highly reduced and anhydrous nature of LCFAs, its metabolic pathway in *E. coli* is targeted for industrial production of fuels and chemicals (Dellomonaco et al., 2010; Doi et al., 2014). However, there are reports, which suggest that LCFAs confer various stresses on bacteria (Doi et al., 2014; Lennen et al., 2011; Rodriguez et al., 2014). We present existing knowledge on the importance of LCFA metabolism in bacterial pathogenesis and industrial production. We describe instances where LCFA metabolism is linked with stresses in bacteria with a particular emphasis on oxidative stress. The information on the sites of reactive oxygen species (ROS) formation, the damaging effects of ROS and the players involved in combating oxidative stress in *E. coli* is presented Ubiquinone, a lipid-soluble electron carrier in the electron transport chain (ETC), has also been suggested to function as an antioxidant in *E. coli.* We briefly describe the pathway of ubiquinone biosynthesis and our current understanding of its role in mitigating oxidative stress.

1.2 Metabolism of carbon sources in *E. coli*

Energy for various cellular processes and precursors to build cellular components are the two basic requirements for an organism to grow and survive in a particular environment. These requirements are met by the metabolism of carbon sources. *E. coli* is capable of utilizing various carbon sources such as carbohydrates, fatty acids, amino acids, and therefore can grow in diverse environments.

1.2.1 General route for metabolism of carbon sources

Metabolism is a multistep process, which operates in two stages. During the initial stage, carbon sources such as, glucose, fatty acids are degraded into smaller acetyl-CoA (a two-carbon compound; 2C), through a unique degradation pathway mediated by a specific set of proteins and co-factors. For example, glucose and LCFAs are degraded by glycolysis and β-oxidation, respectively. In the final stage, acetyl-CoA is completely degraded into two molecules of CO_2 through tricarboxylic acid (TCA) cycle or metabolized through glyoxylate cycle. The reduced cofactors (NADH and $FADH_2$) produced during both stages of metabolism are oxidized in the ETC. Therefore, metabolism of every carbon source converges into central metabolism, i.e., TCA cycle, glyoxylate cycle and ETC (Clark and Cronan, 2005; Cronan and Laporte, 2005; Romeo and Snoep, 2005; Unden and Dunnwald, 2008) (Fig.1.1).

1.2.1.1 Initial stage: Oxidation of carbon sources to two-carbon compound

Carbohydrates are polyhydroxy aldehydes or ketones, or the compounds that can be hydrolyzed to form the same. These include glucose, mannose, galactose, maltose etc. that differ in complexity, structure or functional groups. Among carbohydrates, glucose is the most simple and preferred carbon source for *E. coli*. Glucose is a six-carbon (6C) compound, which is degraded to produce pyruvate (3C) by the process

called glycolysis. Further, pyruvate dehydrogenase converts pyruvate to acetyl-CoA (2C) generating one molecule of NADH. Glycolysis is a multistep pathway catalyzed by various enzymes yielding ATP, reduced cofactors and several intermediates. The intermediates serve as precursors for the synthesis of various biomolecules. Glycolysis is a nine-step process out of which three steps are irreversible. However, *E. coli* also possesses enzymes that can catalyze the backward reaction at irreversible steps during glycolysis. These enzymes together with other enzymes performing reversible reactions during glycolysis are employed by another pathway, gluconeogenesis. This pathway operates to generate glucose and other glycolytic intermediates from non-carbohydrate substrates. Therefore, gluconeogenesis is important for providing cellular precursors during growth on carbon sources that are not degraded through glycolysis (Romeo and Snoep, 2005) (Fig. 1.1).

Fatty acids consist of an aliphatic hydrocarbon chain with a terminal carboxylic group. Whereas the two-carbon short-chain fatty acid, acetate is directly converted into acetyl-CoA, LCFAs are initially degraded by β-oxidation (Clark and Cronan, 2005). Amino acids have a similar carbon skeleton consisting of an alpha carbon, which is bonded to a carboxyl group, an amino group, and an alkyl (R) group. Amino acids are modified by enzymatic reactions such as transamination, and are converted to various TCA intermediates such as α-ketoglutarate, oxaloacetate and fumarate (Hatfield, 2008; Reitzer, 2005) (Fig. 1.1).

Importantly, acetyl-CoA produced from specific pathways such as glycolysis and β-oxidation is further degraded through TCA and glyoxylate cycles, and reduced cofactors produced are oxidized in the ETC for generation of energy (Clark and Cronan, 2005) (Fig. 1.1).

1.2.1.2 Final stage: Central metabolic pathway for complete degradation of carbon sources

1.2.1.2.1 Tricarboxylic acid cycle

The condensation reaction between acetyl-CoA and oxaloacetate (OAA) marks the first step of TCA cycle. Further, reactions such as dehydration, hydration, decarboxylation, phosphorylation and dehydrogenation degrade acetyl-CoA into two molecules of CO_2 and OAA is regenerated. OAA then condenses again with another molecule of acetyl-CoA. During each round of TCA cycle, three molecules of NADH and one molecule of $FADH_2$ are produced (Cronan and Laporte, 2005). Besides energy generation, TCA intermediates serve as precursors for the synthesis of several cellular components. For example, α-ketoglutarate synthesizes amino acids such as serine and tyrosine, succinyl-CoA is required for the synthesis of cytochromes (an ETC component), OAA is converted to aspartate which is important for the synthesis of pyrimidine nucleotides (Layer et al., 2010; Romano and Nickerson, 1958). Depending upon the environmental condition, *E. coli* can also utilize TCA cycle intermediates such as succinate and malate as carbon source (Lukas et al., 2010) (Fig. 1.1).

1.2.1.2.2 Glyoxylate cycle

During growth of cells on acetate or substrates, such as LCFAs, intermediates for synthesis of cellular components are not generated in the initial stage of degradation. However, under these growth conditions, gluconeogenesis operates to convert OAA to phosphoenolpyruvate (PEP), providing different cellular precursors. Another metabolic pathway, glyoxylate shunt also operates that generates OAA from acetyl-CoA (Cronan and Laporte, 2005).

Glyoxylate pathway is similar to TCA cycle; however, it bypasses the two decarboxylation steps of TCA cycle, thus preventing the loss of carbon from acetyl-CoA as CO_2. Similar to TCA cycle, during glyoxylate shunt, OAA condenses with acetyl-CoA to generate citrate that is further converted to isocitrate. However, in contrast to TCA cycle where isocitrate undergoes decarboxylation, during glyoxylate shunt isocitrate is cleaved to succinate and glyoxylate. Subsequently, glyoxylate reacts with another molecule of acetyl-CoA forming malate, and malate is further oxidized to OAA. Because glyoxylate shunt allows the synthesis of constituents of biomass from two-carbon (2C) substrates, therefore it is an important pathway for growth of *E. coli* on carbon sources such as acetate and LCFAs (Fig. 1.1) (Clark and Cronan, 2005; Cronan and Laporte, 2005). The enzymes for glyoxylate shunt are encoded by the *aceBAK* operon and are tightly regulated. Glyoxylate cycle is active under glucose limitation; *aceBAK* operon is kept repressed by IclR repressor and is regulated by pyruvate and glyoxylate levels (Bernal et al., 2016).

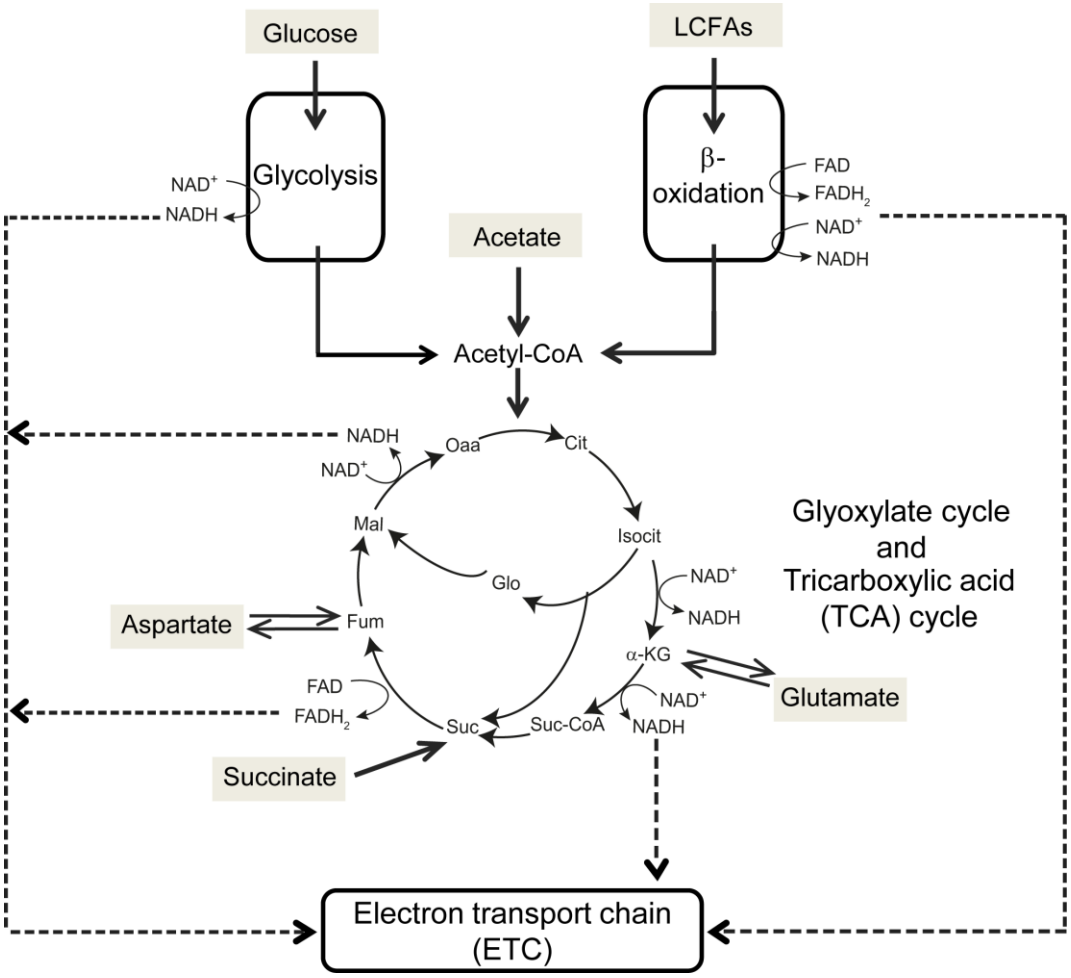

Figure 1.1 Metabolic routes for degradation of different carbon sources. Carbon sources such as Glucose and LCFAs are degraded by Glycolysis and β-oxidation, respectively to acetyl-CoA. Acetyl-CoA feeds into the TCA and Glyoxylate cycle for further metabolism. Amino acids such as Glutamate and Aspartate are converted to TCA intermediates, α-ketoglutarate and fumarate, respectively. Other carbon sources such as Acetate, is converted to acetyl-CoA and fed to TCA cycle for degradation, while Succinate is directly utilized as TCA intermediate. Reduced cofactors (NADH and $FADH_2$) produced during Glycolysis, β-oxidation, TCA cycle and Glyoxylate cycle, are oxidized in ETC to generate energy. Abbreviations: *Oaa*, oxaloacetate; *Cit*, citrate; *Isocit*, isocitrate; *α-KG*, α-ketoglutarate; *Suc-CoA*, succinyl-CoA; *Suc*, succinate; *Fum*, fumarate; *Mal*, malate; *Glo*, glyoxylate.

1.2.2 Electron transport chain (ETC)

In ETC a substrate is oxidized and the electrons are transferred through different ETC components to a final electron acceptor. ETC components, therefore, participate in

redox reactions that are coupled with translocation of protons from the cytoplasm to the periplasm thus generating proton gradient or proton motive force (PMF) across the cytoplasmic membrane. Consequently, certain membrane proteins utilize PMF to perform various physiological processes such as antibiotic resistance, transport of solutes and ATP synthesis (Ezraty et al., 2013; Soballe and Poole, 1999; Unden and Dunnwald, 2008). The process by which PMF generated during ETC is utilized to produce ATP is called oxidative phosphorylation. Besides PMF dependent functions, another important role of ETC is to maintain redox balance. ETC components are present in the inner-membrane and can be divided into three categories, i) substrate-specific dehydrogenases that oxidize different organic substrates and transfer electrons to quinones, ii) quinones that accept electrons from dehydrogenases and transfer these to terminal oxidases, and iii) terminal oxidases which transfer electrons to final electron acceptors (Unden and Bongaerts, 1997) (Fig. 1.2).

1.2.2.1 Diversity of ETC components

ETC can have variable composition depending on the nature of electron donors and electron acceptors. Multiple dehydrogenases, quinones and terminal oxidases are present in *E. coli* that enable transfer of electrons from specific substrates to specific electron acceptors. Substrates such as NADH, succinate, hydrogen, formate, lactate, pyruvate and glycerol-3-phosphate are oxidized by dehydrogenases encoded by *nuoA-N* or *ndh*, *sdhABCD*, *hyaABC* or *hybABC*, *fdnGHI* or *fdoGHI*, *lldD* or *dld*, *poxB* and *glpD* or *glpABC*, respectively. Oxidases encoded by *cyoABCD* or *cydABX* or *appCD*, *narGHI* or *narZYV* or *napABC*, *nrfAB*, *dmsABC*, *torACD*, *frdABCD*, and *phsABC* transfer electrons to the final electron acceptor oxygen, nitrate, nitrite, dimethyl sulfoxide (DMSO), trimethylamine N-oxide (TMAO), fumarate and thiosulphate,

respectively (Unden and Bongaerts, 1997). There are three types of quinones in *E. coli* that function as electron carriers in ETC; whereas ubiquinone mainly functions during aerobic respiration, menaquinone (MK) and demethylmenaquinone (DMK) function under anaerobic conditions (Soballe and Poole, 1999). Certain dehydrogenases and terminal oxidases translocate protons during electron transfer; however, they vary in their efficiency of proton translocation (Imlay, 2003). The PMF generated in the ETC drives ATP synthesis through ATP synthase complex (Capaldi et al., 2000).

During aerobic respiration, the reduced cofactors, NADH and $FADH_2$, produced from the metabolism of carbon sources are oxidized by dehydrogenases NuoA-N or Ndh and SdhABCD, respectively. NuoA-N and Ndh are referred to as ETC complex I, and SdhABCD as ETC complex II. Ubiquinone accepts electrons from complex I and II, and transfers these to the terminal oxidases CyoABCD, CydABX and AppCD (Unden and Bongaerts, 1997) (Fig. 1.2).

1.2.2.2 Complex I: NADH dehydrogenase

There are two types of NADH dehydrogenases in *E. coli,* NADH dehydrogenase I (NDH-1 or Nuo) and NADH dehydrogenase II (NDH-2 or Ndh). During aerobic respiration, both Nuo and Ndh can catalyze the transfer of electrons from NADH to ubiquinone (Unden and Bongaerts, 1997). However, an earlier study showed that the oxygen consumption rate decreases significantly on deleting *ndh,* but not in *nuo* deletion strains, suggesting that Ndh is the major dehydrogenase during aerobic respiration (Tran et al., 1997).

Nuo is a multi-subunit complex constituted by a dozen of proteins present in the inner membrane (Unden and Bongaerts, 1997). The complete Nuo complex can be

divided into three parts: soluble, amphipathic and hydrophobic. Soluble part is composed of NuoE, F and G subunits that contain iron-sulfur clusters and FMN cofactor that catalyzes the oxidation of NADH. The amphipathic part is a connecting segment composed of NuoB, CD and I subunits. The hydrophobic fragment is constituted by NuoA, H, J, K, L, M and N subunits (Braun et al., 1998; Euro et al., 2008; Leif et al., 1995). Importantly, NuoM subunit contains ubiquinone-binding site, and NuoJ, NuoK, NuoM and NuoN subunits together are involved in generation of PMF (Gong et al., 2003; Kaila et al., 2014). Recently, a ratio of $3H^+/2e^-$ has been proposed for oxidation of one molecule of NADH through Nuo (Wikstrom and Hummer, 2012). In contrast to Nuo that can oxidize both NADH and deamino-NADH, Ndh catalyzes the transfer of electrons only from NADH (Matsushita et al., 1987). Ndh is a single-subunit dehydrogenase encoded by *ndh* gene. Ndh does not contribute to PMF generation, as there is no coupling of proton translocation with electron transfer from NADH (Friedrich and Pohl, 2007; Unden and Dunnwald, 2008).

Sequence analysis of Ndh suggests four domains: a FAD-binding domain, a NADH binding domain, a membrane anchoring domain and a copper binding domain (Rapisarda et al., 2002). In the anaerobic ETC, the preference for NADH dehydrogenase varies with terminal electron acceptor; whereas in the presence of nitrate Ndh is preferred, with fumarate or DMSO the oxidation of NADH is more dependent on Nuo (Tran et al., 1997).

1.2.2.3 Complex II: Succinate dehydrogenase

Succinate dehydrogenase (Sdh) catalyzes the oxidation of succinate to fumarate and transfers electrons to ubiquinone (Unden and Dunnwald, 2008). Sdh is a complex

composed of four subunits bound to the membrane. SdhA and SdhB subunits constitute the hydrophilic cytoplasmic part while SdhC and SdhD subunits are two hydrophobic integral membrane proteins (Trezza et al., 2017). SdhB contains three iron-sulfur clusters, whereas SdhA contains covalently bound FAD cofactor. The interface of SdhB, SdhC and SdhD subunits has the quinone-binding site (Tran et al., 2006). Another protein, SdhE enables the assembly of covalent flavin linkage in SdhA subunit (Maklashina et al., 2016). Sdh is a reversible enzyme that functions during both TCA cycle and ETC. Whereas during TCA cycle, Sdh oxidizes succinate to fumarate and simultaneously reduces FAD to $FADH_2$, during ETC it oxidizes $FADH_2$ to FAD and transfers electrons to ubiquinone. In contrast to complex I, oxidation of $FADH_2$ to FAD by Sdh does not contribute to the generation of PMF (Unden and Bongaerts, 1997).

1.2.2.4 Quinones

Quinones are membrane-bound lipids that function as electron carriers in ETC. Structurally, quinone consists of an aromatic quinonoid ring attached to a polyprenyl aliphatic chain. Depending on whether the aromatic ring is benzene or naphthalene, quinones are classified as benzoquinones (e.g. ubiquinone) and naphthoquinones (e.g. MK and DMK), respectively. The number of isoprene units in the polyprenyl chain varies with species. In *E. coli*, the polyprenyl chain of all three quinone species contains eight isoprene units therefore these are termed as ubiquinone-8, MK-8 and DMK-8. Ubiquinone-8 is also referred to as coenzyme-8 or Q_8 (Meganathan, 2001).

Quinones exist in two redox states, quinone and quinol. Quinone accepts electrons from upstream dehydrogenases and gets converted to quinol, which further transfers electrons to terminal oxidases and is oxidized back to quinone (Soballe and

Poole, 1999) (Fig. 1.2). The mid-point potential of quinones determines their specificity for particular electron donors and acceptors in the ETC. Because ubiquinone has high midpoint potential (E'°= +100 mV), therefore it can participate in aerobic respiration, while MK and DMK with low midpoint potentials (E'°= -74 mV and +36 mV respectively) participate in anaerobic respiration (Alvarez et al., 2013). Ubiquinone alongwith terminal oxidases of the ETC is also known to play a critical role in maintaining oxidizing environment in the periplasm by re-oxidizing the disulfide bond forming machinery (the inner membrane disulfide oxidoreductase, DsbB and the periplasmic disulfide oxidoreductase, DsbA) (Bardwell et al., 1991; Kobayashi et al., 1997).

1.2.2.5. Terminal oxidases: CyoABCD, CydABX and AppCD

During aerobic respiration, three enzyme complexes function as terminal oxidases; cytochrome *bo* oxidase (CyoABCD), cytochrome *bd*-I oxidase (CydABX) and cytochrome *bd*-II oxidase (AppCD) (Unden and Bongaerts, 1997). Among these, CyoABCD has less affinity towards oxygen, and it is expressed when oxygen levels are high while CydABX has high affinity towards oxygen and is expressed under oxygen-limited conditions. AppCD complex has not been investigated in detail (Bekker et al., 2009). Both CyoABCD and CydABX contribute to generation of PMF (Puustinen et al., 1991).

CyoABCD complex consists of four subunits, CyoA, CyoB, CyoC, and CyoD that perform catalytic function, however, another protein CyoE is required for the functional expression of cytochrome *bo* oxidase (Minghetti et al., 1992; Saiki et al., 1993). The enzymes contain two heme groups i.e. heme O and heme B which are coupled with copper, therefore forming a heme-copper binuclear center. This center is

the site for reduction of molecular oxygen to water (Mogi et al., 1994). The redox transfer of electrons from ubiquinol to molecular oxygen through CyoABCD is coupled with proton translocation. Oxidation of ubiquinol through CyoABCD translocates four protons into the periplasmic space and two electrons are transferred to oxygen, hence the H^+/e ratio is 2 (Unden and Bongaerts, 1997).

CydABX also catalyzes the two-electron oxidation of ubiquinol and four-electron reduction of molecular oxygen and according to recent reports the H^+/e^- ratio for this enzyme is 0.94 (Borisov et al., 2011a; Borisov et al., 2011b). This complex is a heterodimer, where CydA is the site of ubiquinol oxidation that contains heme b_{558} component. The other two components CydB and CydX together contain heme b_{595} and heme *d*, which is the site for reduction of oxygen to water (Hill et al., 1993; Matsumoto et al., 2006; Miller et al., 1988). CydABX also contributes to generating PMF, but in contrast to CyoABCD, it does not function as a proton pump (Puustinen et al., 1991).

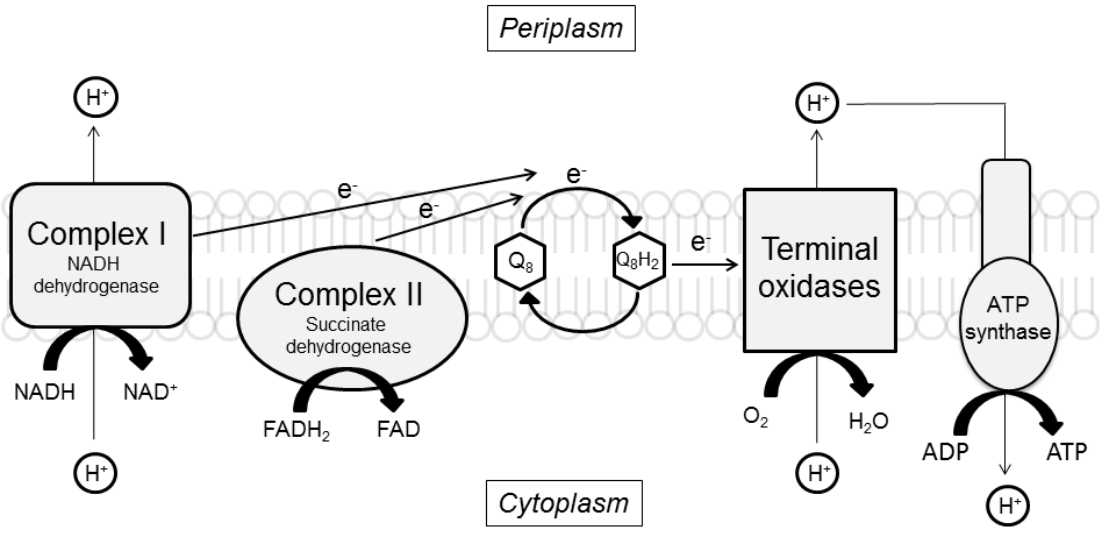

Figure 1.2 Diagrammatic representation of electron transport chain during aerobic respiration. ETC complex I (NADH dehydrogenase) and ETC complex II (Succinate dehydrogenase) oxidizes reduced cofactors, NADH and $FADH_2$, respectively and transfer the

electrons to ubiquinone which is reduced to ubiquinol. Terminal oxidases accept electrons from ubiquinol and oxidize it back to ubiquinone. Molecular oxygen finally accepts electrons from terminal oxidases and gets converted to water molecule. The redox transfer of electrons through complex I and terminal oxidases are coupled with translocation of protons from cytoplasm to periplasm thus generating PMF. ATP synthase utilizes PMF and transfers protons back to cytoplasm from periplasm, and simultaneously generates ATP. Abbreviations: Q_8, ubiquinone-8; Q_8H_2, ubiquinol; H^+, proton; e^-, electron.

1.2.3 Fermentable and Non-fermentable carbon sources

During metabolism, energy (ATP) is generated either through substrate-level phosphorylation or oxidative phosphorylation. Substrate-level phosphorylation is a metabolic chemical reaction that generates ATP by transferring phosphoryl group to ADP from a phosphorylated substrate, while during oxidative phosphorylation PMF generated due to oxidation of reduced substrate in the ETC is accompanied by phosphorylation of ADP to ATP. During the metabolism of fermentable carbon sources (e.g., glucose), energy is derived both by substrate-level phosphorylation during glycolysis and by oxidative phosphorylation in ETC, however, latter process is the sole means of energy production for growth on non-fermentable carbon sources (e.g., succinate, acetate, and fatty acids) (Berger, 1973). Furthermore, in contrast to growth on fermentable carbon sources where metabolic intermediates are generated in glycolysis and TCA cycle, growth on non-fermentable carbon sources is totally dependent on the optimal functioning of gluconeogenesis, TCA and glyoxylate cycles for production of cellular metabolites (Clark and Cronan, 2005; Cronan and Laporte, 2005).

1.3 Long-chain fatty acid metabolism

LCFAs are a rich source of metabolic energy for *E. coli* and are also important components of the membrane. LCFAs once internalized are either degraded to

generate energy and provide precursors for cellular components, or modified to form phospholipids that integrate into the membrane (Iram and Cronan, 2006).

1.3.1 Classification of fatty acids

Fatty acids consist of an aliphatic hydrocarbon chain with a terminal carboxylic group. On the basis of number of carbon atoms present in the aliphatic chain, fatty acids are categorized into short-chain fatty acids (SCFAs; 2 to 4C), medium-chain fatty acids (MCFAs; 5 to 11C) and long-chain fatty acids (LCFAs; 12 to 18C) (Bernal et al., 2016; Mattam and Yazdani, 2013; Nunn et al., 1979). Further, on the basis of saturation of carbon with hydrogen in the aliphatic chain, fatty acids are either saturated or unsaturated (Feng and Cronan, 2009). Of the various fatty acids, *E. coli* K12 can only utilize SCFAs, acetate (2C) and propionate (3C), and LCFAs (Bernal et al., 2016; Wegener et al., 1967). However, certain pathogenic strains of *E. coli* can also metabolize the four-carbon SCFA, butyrate, and MCFAs (Martinez-Vallespin et al., 2016; Tobe et al., 2011).

1.3.2 Pathway of long-chain fatty acid metabolism and its regulation

The initial stage of LCFA metabolism is carried out by proteins encoded by *fad* (fatty acid degradation) genes involved in the transport of LCFAs and its degradation to acetyl-CoA. During the final stage, acetyl-CoA is subsequently metabolized in TCA and glyoxylate cycles (Fig. 1.1). The *fad* genes are regulated by the fatty acid specific transcriptional regulator FadR, ArcAB two-component system and cAMP-CRP global regulator (Fujita et al., 2007).

1.3.2.1 Transport of long-chain fatty acids

Unlike SCFAs that are transported across the outer membrane through diffusion, LCFAs due to its long hydrophobic chain require a specific transporter (Bernal et al., 2016; Maloy et al., 1981). FadL, an outer membrane protein, is a well-established transporter for LCFAs in *E. coli*. Crystal structure shows that FadL is a 14-stranded antiparallel β-barrel, and functions as a ligand-gated diffusion channel that transports LCFAs into periplasm (van den Berg et al., 2004). Long-chain fatty acid CoA-synthetase (FadD) has a dual role in LCFA metabolism. FadD catalyzes the first step of β-oxidation and is also likely involved in the transport of LCFAs through the inner membrane (Fig. 1.3). The process is called 'fatty acid permeation by vectorial acylation' (Fujita et al., 2007; Schmelter et al., 2004). Altogether, exogenous LCFAs are transported into the cytoplasm with the help of FadL and FadD, and the absence of either of these proteins inhibits LCFA transport (Overath et al., 1969).

1.3.2.2 Long-chain fatty acid degradation: β-oxidation

Earlier studies in 1970's reported that the components of LCFA transport and degradation are induced simultaneously, and strains defective in β-oxidation show reduced uptake of LCFAs. Thus LCFA transport and degradation are coupled processes (Klein et al., 1971). During one round of β-oxidation two carbon atoms of LCFAs are released as acetyl-CoA, hence for complete degradation of molecule of LCFA β-oxidation runs multiple times. β-oxidation is broadly a four-step pathway, catalyzed by FadD, FadE, FadB and FadA (Fujita et al., 2007) (Fig. 1.3).

1.3.2.2.1 Fatty acyl-CoA synthetase (FadD)

FadD, fatty acyl-CoA synthetase/ligase, located at both the inner membrane and in the cytoplasm, is the first enzyme involved in β-oxidation. FadD catalyzes the formation of fatty acyl-CoA, at the expense of one molecule of ATP (Schmelter et al., 2004).

fatty acid + ATP + CoA = fatty acyl-CoA + AMP + ipp.

A Δ*fadD* strain of *E. coli* accumulates free fatty acids (Pech-Canul et al., 2011). This observation indicates that in addition to exogenous LCFAs, FadD is also important for degradation of endogenous fatty acids released from membrane lipids (Fig. 1.3).

1.3.2.2.2 Fatty acyl-CoA dehydrogenase (FadE)

FadE is predicted to be an inner membrane protein. Although FadE has not been characterized biochemically, on the basis of sequence motifs and genetic studies FadE has been suggested as the fatty acyl-CoA dehydrogenase in *E. coli*. The enzyme is proposed to catalyze the oxidation of fatty acyl-CoA to 2-enoyl-CoA concomitant with transfer of two electrons from the substrate to FAD cofactor generating $FADH_2$ (Campbell and Cronan, 2002) (Fig. 1.3). In a *fadE* mutant, although β-oxidation is not functional, LCFAs are still transported at reduced rates (Klein et al., 1971).

fatty acyl-CoA + FAD + H^+ = 2-enoyl-CoA + $FADH_2$

Electron transfer flavoproteins (ETF) are reported for mitochondrial acyl-CoA dehydrogenase, which mediate the oxidation of $FADH_2$ to FAD and transfer electrons to ubiquinone in the ETC (Roberts et al., 1996). *Bacillus subtilis* also has ETF proteins, EtfA and EtfB that re-oxidize $FADH_2$ (Matsuoka et al., 2007). However, there are no reports of ETF proteins in *E. coli*. FadE in *E. coli* is almost double the length (814 amino acids) of its mammalian counterpart, where the first 150 and last 400 amino acid residues have no match to the mammalian dehydrogenase. It has been proposed that the extra region in FadE performs the oxidation of $FADH_2$ (Campbell and Cronan, 2002).

1.3.2.2.3 Multienzyme FadAB complex

FadB and FadA together constitute a heterotetrameric multienzyme complex $[(FadB)_2][(FadA)_2]$ located in the cytoplasm. The two α-subunits $[(FadB)_2]$ and two β-subunits $[(FadA)_2]$ are encoded by *fadBA* operon. The FadBA complex has five enzyme activities; enoyl-CoA hydratase, 3-hydroxyacyl-CoA dehydrogenase, 3-hydroxyacyl-CoA epimerase, *cis*-Δ^3-*trans*-Δ^2-enoyl-CoA isomerase and 3-ketoacyl-CoA thiolase. The first four enzyme activities are mediated by FadB while the 3-ketoacyl-CoA thiolase activity is performed by FadA (Pawar and Schulz, 1981; Pramanik et al., 1979; Yang and Elzinga, 1993). Whereas all five enzymatic activities are required for the degradation of unsaturated fatty acids, only three enzymatic activities, enoyl-CoA hydratase, 3-hydroxyacyl-CoA dehydrogenase, and 3-ketoacyl-CoA thiolase are required for the degradation of saturated fatty acids (Clark and Cronan, 2005).

The oxidation product of FadE, 2-enoyl-CoA undergoes hydration and is converted to 3-hydroxyacyl-CoA by the enoyl-CoA hydratase activity of FadB.

$$2\text{-enoyl-CoA} + H_2O = 3\text{-hydroxyacyl-CoA}$$

3-hydroxyacyl-CoA dehydrogenase then oxidizes 3-hydroxyacyl-CoA to 3-oxoacyl-CoA and simultaneously NAD^+ is reduced to NADH.

$$3\text{-hydroxyacyl-CoA} + NAD^+ = 3\text{-oxoacyl-CoA} + NADH + H^+$$

FadA further catalyzes the thiolysis of 3-oxoacyl-CoA to acetyl-CoA, leaving fatty acyl-CoA shortened by two carbons.

$$3\text{-ketoacyl-CoA} + CoA = \text{fatty acyl-CoA} + \text{acetyl-CoA}$$

The fatty acyl-CoA shortened by two carbon atoms is further metabolized by FadE and FadBA complex until it is completely degraded to acetyl-CoA (Clark and Cronan, 2005; Fujita et al., 2007) (Fig. 1.3). In both *fadB* and *fadA* mutants, LCFA transport

and degradation occurs at a reduced rate, however these two processes are much less compromised than the *fadE* mutant (Klein et al., 1971).

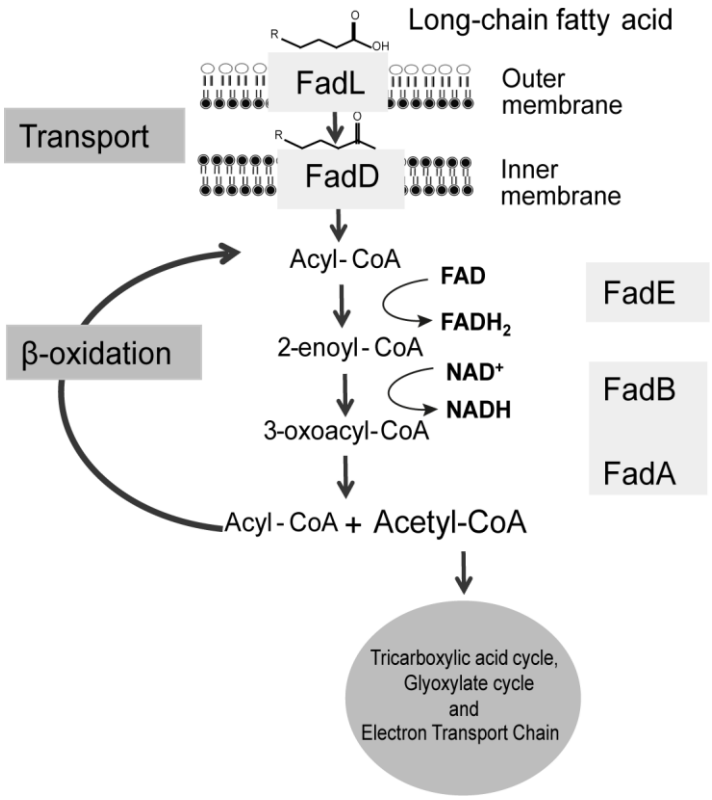

Figure 1.3 Transport and degradation of long-chain fatty acids. Exogenous LCFAs are transported by the outer membrane protein, FadL, and internalized into the cytoplasm via an inner membrane protein, FadD. During transportation, FadD also catalyzes the acylation of fatty acids and converts it to acyl-CoA. Further, acyl-CoA is degraded by β-oxidation pathway mediated by Fad (fatty acid degradation) proteins. FadE, fatty acyl-CoA dehydrogenase, is proposed to oxidize acyl-CoA to 2-enoyl-CoA. During this conversion FAD is reduced to $FADH_2$. Then, enoyl-CoA hydratase/3-hydroxyacyl-CoA dehydrogenase activities of FadB convert 2-enoyl-CoA to 3-oxoacyl-CoA, and one molecule of NADH is produced. 3-oxoacyl-CoA is finally cleaved to release two-carbon acetyl-CoA and two less carbon acyl-CoA, by 3-ketoacyl-CoA thiolase activity of FadA. Acyl-CoA shortened by two carbon atoms undergoes multiple rounds of β-oxidation for complete degradation.

1.3.2.3 Degradation of unsaturated fatty acids

In addition to enzymatic activities that degrade saturated fatty acids (explained above), *cis*-Δ^3-*trans*-Δ^2-enoyl-CoA isomerase and 3-hydroxyacyl-CoA epimerase activities of FadB are required for degradation of unsaturated fatty acids. Unsaturated fatty acids containing double bond at carbon 3 with *cis* configuration undergo a *cis* to *trans* isomerization by *cis*-Δ^3-*trans*-Δ^2-enoyl-CoA isomerase activity.

cis-3-enoyl-CoA ←→ *trans-2-enoyl-CoA*

As explained above, 2-enoyl-CoA undergoes hydration to form 3-hydroxyacyl-CoA. 3-hydroxyacyl-CoA epimerase is further required for conversion of D-3-hydroxyacyl-CoA to L-3-hydroxyacyl-CoA, which is finally degraded to acetyl-CoA by FadA (Clark and Cronan, 2005; Yang et al., 1988). However, for unsaturated fatty acids with double bond at even-numbered carbon, another enzyme, 2,4 dienoyl-CoA reductase encoded by *fadH* performs the reductive removal of double bond (Liang et al., 2000).

1.3.2.4 Anaerobic β-oxidation pathway

E. coli can utilize LCFAs under anaerobic conditions in the presence of electron acceptors such as nitrate, fumarate and TMAO. The anaerobic β-oxidation is carried out by homologues of FadB, FadA, and FadD, i.e., FadJ (YfcX), FadI (YfcY), and FadK (YdiD), respectively. There is no established anaerobic homologue of FadE. However, four of the five proteins encoded by *ydiQRSTD* operon, YdiT, YdiS, and YdiR or YdiQ which are predicted ferrodoxin, flavoprotein and electron transport flavoproteins, respectively, are suggested to perform functions similar to FadE under anaerobic conditions. Whereas, under aerobic conditions, β-oxidation occurs at a reduced rate in Δ*fadB* and Δ*fadA* strains allowing these strains to exhibit delayed growth on LCFAs, double mutants Δ*fadB*Δ*fadJ* and Δ*fadA*Δ*fadI* do not exhibit any

growth on LCFAs. These data show that FadJ and FadI also work sub-optimally under aerobic conditions (Campbell et al., 2003).

1.3.3 Regulation of long-chain fatty acid degradation

The *fad* genes are regulated at a transcriptional level by a fatty-acid specific transcriptional regulator, FadR, the oxygen-sensitive ArcA-ArcB two-component system and the global cyclic AMP receptor protein-cyclic AMP (CRP-cAMP) complex.

FadR is a dual transcriptional regulator that acts as a switch between fatty acid degradation and biosynthesis. Whereas FadR negatively regulates the expression of *fad* genes, it positively regulates the expression of *fab* (fatty acid biosynthesis) genes. In the presence of LCFAs, the acylation product of FadD, long-chain fatty acyl-CoA binds FadR and releases it from the operator of *fad* genes. Because FadR specifically binds long-chain fatty acyl-CoA, exogenous medium-chain fatty acids cannot be utilized by *E. coli* K-12. Under aerobic conditions, the anaerobic *fad* genes, *fadJ* and *fadI*, are repressed by FadR. FadR also regulates genes that encode enzymes of the glyoxylate cycle (*aceBAK* operon), a pathway important for growth on LCFAs (Campbell et al., 2003; Cronan and Subrahmanyam, 1998; Fujita et al., 2007; My et al., 2015; Simons et al., 1980).

ArcAB is a two-component system comprising an inner membrane sensor protein kinase, ArcB, and a cytosolic response regulator, ArcA (Malpica et al., 2006). This system regulates *fad* genes in response to oxygen levels. ArcAB system represses both aerobic *fad* genes, i.e. *fadE*, *fadB*, *fadA* and *fadH*, and anaerobic *fad* genes, i.e. *fadJ*, and *fadI* in the absence of oxygen (Campbell et al., 2003; Cho et al., 2006).

Glucose is a preferred carbon source for *E. coli* compared to LCFAs. The *fad* genes are thus under catabolite repression. In the absence of glucose, cAMP-CRP binds upstream of *fad* genes and positively regulates their expression (Fujita et al., 2007).

1.4 Importance of long-chain fatty acid metabolism in bacterial pathogenesis

Several bacterial pathogens with huge impact on human health use LCFAs as a carbon source that contributes to their survival and virulence. In *S. enterica* serovar Typhimurium, the LCFA pathway is upregulated during infection and contributes to the metabolism of proinflammatory host LCFAs thereby suppressing the innate immune response. Further, the enzyme of glyoxylate cycle, isocitrate lyase, is required for *Salmonella* persistence during chronic infection suggesting an increased dependence on fatty acid utilization during this phase of infection (Black and DiRusso, 2003; Fang et al., 2005). In *P. aeruginosa*, LCFA degradation enzymes are induced during lung infection in cystic fibrosis patients to enable the utilization of lung surfactant lipids. Moreover, *fadD* mutants of *P. aeruginosa* defective in LCFA utilization exhibit decreased *in vivo* fitness in a mouse lung infection model (Kang et al., 2010; Son et al., 2007). In *Mycobacterium tuberculosis*, disruption of the *icl* gene that encodes for isocitrate lyase resulted in attenuation of bacterial persistence and virulence in mouse model implicating fatty acid utilization as an important factor during chronic infection (McKinney et al., 2000). Finally, *Vibrio cholerae* acquires LCFAs from bile, which is suggested to be required for maintenance of the membrane and as a carbon source. Besides, a *fadD* mutant of *V. cholerae* is impaired in the production of virulence factors (Giles et al., 2011; Ray et al., 2011).

1.5 Long-chain fatty acid utilizing bacteria as industrial workhorses

Although lignocellulosic sugars are used as the primary feedstock for the biological production of fuels and chemicals, the availability of fatty acid-rich feedstocks and recent progress in the development of oil-accumulating organisms are drawing attention towards fatty acids as a promising raw material for industrial production (Chisti, 2007; Doi et al., 2014; Lennen et al., 2011). Besides availability, fatty acids offer several advantages when used for fuel and chemical production. Their metabolism to the key intermediate, acetyl-CoA, is very efficient and results in 100% carbon recovery. Because many fuels and chemicals are derived from acetyl-CoA, high product yields are expected if fatty acids are used as the carbon source. However, the highly reduced nature of fatty acids poses a metabolic challenge because these can be metabolized only in the presence of an external electron acceptor. To overcome this challenge, in a recent study, a respiro-fermentative metabolic mode was engineered in *E. coli* to support the synthesis of fermentative products during respiratory metabolism of fatty acids. The engineered strain cultured in medium containing palmitic acid, a C16 LCFA, as a carbon source was shown to produce ethanol, butanol, acetate, and acetone, with yields higher than those produced from fermentation of sugars. Importantly, propionate, which was previously known to be synthesized only by Propionibacteria could also be produced efficiently using the above engineered *E. coli* strain (Dellomonaco et al., 2010). Further, in a separate study, the LCFA, oleate, has been used as a raw material for L-lysine fermentation by emulsification (Doi et al., 2014). Collectively, these studies suggest LCFAs to be an effective carbon source for industrial applications.

1.6 Long-chain fatty acids confer stresses on bacteria

LCFAs are one of the most important classes of high-energy molecules for both bacterial pathogenesis and biotechnology. However, there are a few reports, which suggest that LCFAs confer stresses on bacteria. In a transcriptomics study in *M. tuberculosis* cultured in medium supplemented with a mixture of even-chain-length LCFAs, genes involved in maintaining redox balance were upregulated. Importantly, WhiB3 and DosR, the two heme sensor proteins involved in maintaining intracellular redox balance were overexpressed. Besides, several genes involved in processes that consume reduced cofactors (e.g., complex lipid biosynthesis) were induced, suggesting activation of strategies to counteract redox stress generated by LCFAs (Rodriguez et al., 2014). In a separate study, *E. coli* cultured in oleate (monounsaturated LCFA with 18 carbon atoms; C18) was reported to accumulate 2-fold higher hydrogen peroxide (H_2O_2) levels compared to cultures grown in glucose (Doi et al., 2014). Further, microarray and proteomics studies revealed the induction of acid, membrane and oxidative stress responses in fatty acid overproducing *E. coli* strains (Lennen et al., 2011). However, there has not been any detailed investigation to understand the reason for LCFA-induced stresses, major players/pathways that combat these stresses and the mechanistic details of their activation.

1.7 Oxidative stress

Oxidative stress is a condition that arises due to imbalance between the production of ROS and the ability of oxidative stress defense systems to counteract ROS (Scandalios, 2002). ROS are highly reactive molecules that can oxidize several biomolecules resulting in DNA damage and mutations, lipid peroxidation, disassembly of iron-sulfur clusters, undesired disulfide bond formation in proteins, etc. In its defense bacteria employ various oxidative stress combat players, which are

under tight regulation and enable the cell to survive in harsh environments (Chiang and Schellhorn, 2012; Farr and Kogoma, 1991).

1.7.1 Reactive oxygen species

Because oxygen molecule is a triplet species containing an unpaired electron in each orbital thus it can accept only one electron at a time. Therefore, it is difficult to reduce oxygen molecule by electron donors such as NAD(P)H that transfers two electrons at a time. However, certain enzymes/proteins are capable of transferring univalent electron where adventitious collision of molecular oxygen with single electron generates superoxide ions. Further, superoxide undergoes second, third and fourth electron transfer to produce several types of ROS molecules, i.e. H_2O_2, hydroxyl radical, and finally reduction to water (H_2O), respectively. Under acidic conditions, superoxide ions can also reduce to hydroperoxyl radical ($HOO^{\cdot}$) (Farr and Kogoma, 1991; Messner and Imlay, 1999).

1.7.1.1 Site for ROS formation during metabolism: ETC

Several proteins/enzymes involved in redox reactions that function during ETC and TCA cycles are the major source of ROS. During oxidation-reduction cycle, within these enzymes, the metal centers (e.g., Fe-S cluster), or flavin (FAD or FMN) moieties, or quinone binding sites that are involved in univalent electron transfers might be oxidized by transfer of single electron to oxygen thereby generating ROS. However, multiple studies have shown that among these sites, autoxidation of flavins is the predominant source for ROS formation (Messner and Imlay, 1999, 2002). Inverted membrane vesicles obtained from cells grown in glucose, showed that 0.2% and 0.4% of consumed oxygen is utilized for the formation of superoxide and H_2O_2, respectively (Imlay, 2003). *In vitro* studies showed that ETC accounts for ~87% of

total H_2O_2 produced in the cell. Other experiments, such as change in number of ETC units/cell or the composition of ETC, were found to affect the rate of production of H_2O_2 (Gonzalez-Flecha and Demple, 1995).

In vitro and/or *in vivo* studies have shown that among various ETC dehydrogenases, Nuo, Ndh and Sdh contribute to ROS formation. Nuo accepts an electron from NADH, a reduced cofactor, and transfers to its flavin moiety (FMN). The reduced flavin is exposed to the cytoplasm, which is prone to attack by dissolved oxygen thereby generating ROS (Esterhazy et al., 2008; Messner and Imlay, 1999, 2002; Seaver and Imlay, 2004). During autooxidation of flavoenzymes, single electron transfer to oxygen forms superoxide and flavosemiquinone (FADH·). Further, FADH· either reacts with another oxygen molecule to form superoxide again or it reacts with superoxide to produce a peroxy adduct i.e. H_2O_2 (Imlay, 2003; Seaver and Imlay, 2004). *In vitro* experiments have shown that Ndh generates both superoxide and H_2O_2, where ROS formation was prevented on deleting Ndh while it was enhanced on overexpression of Ndh (Messner and Imlay, 1999). In Sdh, similar to Nuo, reduced flavoprotein contributes to ROS formation. However, Sdh specifically produces superoxide (Messner and Imlay, 2002).

Amongst terminal oxidases, cytochrome oxidases are not reported to generate ROS, although they have metal centers with high electron density. Sulfite reductase, a flavoprotein contains FAD and FMN moieties, and 4Fe-4S metal center. It transfers an electron from NAD(P)H to sulfite. Earlier studies showed that autoxidation of reduced flavins in sulfite reductase is the site for ROS formation, FMN is the primary site, and H_2O_2 is the major ROS produced (Imlay, 2003; Messner and Imlay, 1999). Another ETC component, fumarate reductase (Frd) is involved in single electron redox transfers during anaerobic growth. Frd is structurally and functionally similar to

Sdh, however, it functions as a terminal oxidase and catalyzes the reduction of fumarate. Frd is present in the membrane and contains a flavin cofactor with three Fe-S clusters. Similar to other flavoproteins, Frd has also been shown to contribute to ROS formation through autoxidation of reduced flavins, where it generates both H_2O_2 and superoxide. However, in contrast to Ndh and sulfite reductase, Frd generates more of superoxide than H_2O_2 (Imlay, 2003; Messner and Imlay, 2002).

1.7.1.2 Site for ROS formation during metabolism: Other than ETC

Aspartate oxidase (NadB) catalyzes the FAD-dependent conversion of aspartate to iminoaspartate, the first step of NAD biosynthesis. Structurally, aspartate oxidase is similar to Sdh and Frd, and is a member of succinate:fumarate oxidoreductase family, however, it lacks Fe-S cluster and membrane attachment subunits. Experiments suggest that similar to Sdh and Frd, the flavin moiety of aspartate oxidase is exposed in the cytoplasm that can generate ROS. Aspartate oxidase shows a great deal of similarity with Frd regarding structure, turnover number, and energy of activation, but whereas the predominant ROS produced by Frd is superoxide, NadB generates more H_2O_2 than superoxide. This observation suggests that because aspartate oxidase lacks Fe-S cluster, therefore the mixture of superoxide and H_2O_2 production by Frd is contributed by Fe-S cluster as well (Imlay, 2003; Messner and Imlay, 2002).

Another oxidase, D-amino acid oxidase also contributes to the formation of H_2O_2. Glutathione (GSH) is a tripeptide required for maintaining redox balance in the cell. Glutathione reductase (Gor) reduces oxidized glutathione (GSSG) to reduced glutathione (GSH). Gor is a flavoprotein that uses NADPH as an electron donor and is suggested to generate superoxide during its activity (Farr and Kogoma, 1991).

1.7.2 Oxidative damage

Although ROS are important signaling molecules (Cap et al., 2012), their high intracellular levels can lead to oxidation of biomolecules compromising cell viability. A study has reported that as low as 1 µM H_2O_2 can damage biomolecules in *E. coli* (Jang and Imlay, 2010).

1.7.2.1 Protein Damage

H_2O_2 can spontaneously oxidize the sulfhydryl group of amino acids. Cysteine residues are prone to get oxidized to sulfenic acid adducts which crosslink with other cysteine residues within protein thus forming undesirable disulfide bonds, and hence protein loses its native structure. However, sulfenic acid can also be further oxidized to sulfinic acid (Imlay, 2003). Similar to cysteine, another sulfur-containing amino acid, i.e. methionine is prone to oxidiation by H_2O_2 to form methionine sulfoxide derivatives. Hydroxyl radical oxidizes amino acids leading to protein carbonylation, where residues such as proline, arginine are converted to carbonyl derivatives. These modifications either make proteins more labile to degradation or compromise their function. In addition, certain enzymes that contain metal centers such as fumarase, aconitase, glutamine synthetase, dihydroxy acid dehydratase can be attacked by ROS. Oxidation of metal centers in these enzymes by superoxide or H_2O_2 results in various harmful effects. First, enzymes lose their activity thereby important pathways such as TCA do not function properly, thereby compromising growth on various carbon sources. Second, H_2O_2 oxidizes ferrous ion in metal centers to ferric ion (Fenton reaction) and generates another ROS molecule, i.e. hydroxyl radical that further damages biomolecules (Farr and Kogoma, 1991; Imlay, 2003).

1.7.2.2 Lipid peroxidation

ROS molecules damage lipids through the process called lipid peroxidation. Fatty acids are important constituents of lipids. Unsaturated fatty acids that contain double bond in the aliphatic chain are attacked by various ROS molecules primarily generating lipid hydroperoxides (LOOH) while many different aldehydes such as malondialdehyde (MDA), propanal, hexanal, and 4-hydroxynonenal (4-HNE) are also generated as secondary products (Ayala et al., 2014). The peroxidation of fatty acids alters its ability to rotate and thus makes the membrane more fluid. A change in membrane fluidity interferes with membrane integrity and therefore various physiological processes such as transport, energy generation, and motility are compromised. *In vitro* and *in vivo* studies have shown that ROS molecules such as hydroxyl radicals, hydroperoxy radicals, and singlet oxygen can participate in lipid peroxidation (Farr and Kogoma, 1991).

Lipid peroxidation occurs in three stages: initiation, propagation, and termination. During oxidation of double bond in the fatty acid chain, hydrogen is extracted and a lipid radical is produced ($L^{\cdot}$), which further reacts with molecular oxygen to produce lipid peroxy radical ($ROO^{\cdot}$). During chain propagation step, $ROO^{\cdot}$ further oxidizes another unsaturated fatty acid to produce fatty acid hydroperoxide (ROOH) and an additional molecule of $L^{\cdot}$. The newly formed $L^{\cdot}$ undergoes additional round of propagation step while ROOH is cleaved to $ROO^{\cdot}$ and lipid alkoxy radicals ($LO^{\cdot}$) by reacting with a superoxide molecule or cleaved thermally. Both $ROO^{\cdot}$ and $LO^{\cdot}$ can initiate new rounds of lipid peroxidation or $LO^{\cdot}$ can also be cleaved to form fatty acid aldehydes and alkyl radicals. Therefore, lipid peroxidation generates various end products such as alkanes, epoxides, aldehydes, ketones and products with hydroxyl, carboxyl and peroxyl groups (Ayala et al., 2014; Farr and Kogoma, 1991; Imlay, 2003).

1.7.2.3 DNA damage

Similar to other biomolecules, DNA is also a potent target of various kinds of ROS such as hydroxyl radicals and organic hydroperoxides. DNA consists of nitrogenous bases, adenine, guanine, thymine, and cytosine, and a ribose sugar. Both nitrogenous bases and ribose sugar are prone to attack by ROS molecules. Hydroxyl radicals oxidize ribose sugar leading to DNA fragmentation and induce a double strand break in DNA. ROS molecules react with nitrogenous bases and produce various products such as hydroxymethylurea, urea, thymine glycol, adenine ring-open and ring-saturated products. For example, guanine can be modified to 8-hydroxyguanine, while hydroxylation of thymine produces 5-hydroxymethyluracil. Therefore, whereas modification of ribose sugars by ROS results in DNA strand breaks that interfere with replication, alterations in nitrogenous bases cause mutations. Several lipid peroxidation intermediates and their end products are mutagenic such as 4-HNE, epoxides and other aldehydes that can directly react with DNA, forming intrastrand or interstrand crosslinks (Farr and Kogoma, 1991; Imlay, 2003).

1.7.3 Oxidative stress response players

E. coli employs a number of oxidative stress response players to counteract ROS. These include both enzymatic and non-enzymatic players.

1.7.3.1 Enzymatic players: Catalases and peroxidases

Catalases and peroxidases are enzymatic scavengers that detoxify H_2O_2. Catalases use two molecules of H_2O_2, where one molecule acts as electron donor and the other acts as electron acceptor to produce water and oxygen. In contrast, peroxidases utilize a specific compound other than H_2O_2 as electron donor such as thioredoxin, and convert H_2O_2 to water (Hillar et al., 2000). There is redundancy of catalases and peroxidases

in *E. coli*. The two hydroperoxidases, HPI and HPII, also called as catalase I and catalase II, are encoded by *katG* and *katE*, respectively. HPI is a bifunctional enzyme that has both catalase and peroxidase activities; the peroxidase activity requires lower concentration of H_2O_2 than the catalase activity. In contrast to HPI, HPII is a monofunctional enzyme with only catalase activity (Loewen and Switala, 1986). Another peroxidase, alkyl hydroperoxide reductase (Ahp) encoded by *ahpC* and *ahpF*, scavenges H_2O_2. AhpC and AhpF together constitute an active alkyl hydroperoxide reductase, where AhpF is the peroxiredoxin reductase component and AhpC is the peroxidase component. Therefore, AhpC catalyzes the detoxification of alkyl hydroperoxides or peroxides, while AhpF restores the reduced state of AhpC by transferring electrons from NADH to AhpC (Imlay, 2013; Kamariah et al., 2015). Ahp acts as a primary scavenger of H_2O_2 because it can sense H_2O_2 as low as ~5 µM and saturates at ~20 µM, while catalases are functional at higher H_2O_2 levels (Imlay, 2013)

During oxidative stress, catalases and peroxidases are mainly regulated by the transcriptional regulators, OxyR and RpoS. In the absence of oxidative stress, reduction of disulfide bonds in OxyR by glutathione reductase (*gorA*) and glutaredoxin (*grxA*) keeps the regulator in its inactive form. However, when H_2O_2 levels increase inside the cell, OxyR is directly oxidized by H_2O_2 forming disulfide bonds and thus gets activated (Imlay, 2013). OxyR regulates hundreds of genes. Amongst these, ~40 genes protect the cell from H_2O_2 toxicity, e.g. *ahpCF*, *katG*, *gorA*, *grxA* and *oxyS*. In addition to regulation of genes involved in counteracting H_2O_2 mediated stress, OxyR also governs genes required for protection against damage due to heat stress, near-UV irradiation, lipid peroxidation etc. RpoS is a general stress response regulator in *E. coli*. RpoS regulates ~200 genes including

several genes important for combating oxidative stress such as *oxyR, dps* (DNA-binding protein), *xthA* (exonuclease III), and *sodC* (superoxide dismutase). Importantly, whereas *katG* is regulated by OxyR, *katE* is regulated by RpoS (Chiang and Schellhorn, 2012; Imlay, 2013).

1.7.3.2 Enzymatic players: Superoxide dismutases

Superoxide dismutases (SODs) catalyze the conversion of two superoxide ions into H_2O_2 and H_2O; catalases and peroxidases further detoxify H_2O_2 (Chiang and Schellhorn, 2012). Similar to catalases, there is redundancy in SODs in *E. coli*. SODs exist in three isoforms that mainly differ in their metal cofactors i.e. MnSOD, FeSOD and CuZnSOD, encoded by *sodA, sodB,* and *sodC,* respectively. SodA and SodB are involved in protection against cytoplasmic superoxide while SodC protects against periplasmic superoxide (Benov et al., 1995; Benov and Fridovich, 1994).

sodA is regulated by multiple transcriptional regulators, including the oxygen-sensitive ArcAB two-component system, iron-responsive ferric uptake regulator (Fur) and the SoxRS system. SoxR is a homodimer, where each polypeptide chain contains a [2Fe-2S] cluster. Oxidation of Fe-S cluster of SoxR activates the protein, which then transcriptionally induces the expression of SoxS (Chiang and Schellhorn, 2012; Tardat and Touati, 1993). There are conflicting reports on whether SoxR is directly oxidized by superoxide or it senses redox-cycling agents (Gu and Imlay, 2011). SoxS controls the expression of over 100 genes involved in relieving oxidative stress including superoxide dismutase (*sodA*), endonuclease IV involved in DNA repair (*nfo*) and a protein involved in protection of Fe-S proteins (*yggX*) (Chiang and Schellhorn, 2012). SodB is the only SOD present in *E. coli* under anaerobic conditions (Kargalioglu and Imlay, 1994). *sodB* is negatively regulated by multiple

transcriptional regulators, however it is positively regulated by Fur via the small RNA RyhB (Masse et al., 2005). SodC is repressed during anaerobiosis by Fnr and is induced in stationary phase by RpoS (Gort et al., 1999).

1.7.3.3 Non-enzymatic player: Glutathione

Thiols (R-SH) play a critical role in maintaining redox equilibrium. Glutathione (γ-glutamyl-L-cysteinylglycine) is a tripeptide synthesized by a two-step process mediated by glutamylcysteine synthetase (GshA) and glutathione synthetase (GshB). Glutathione exists in both oxidized (GSSG) and reduced (GSH) forms; however, most of the glutathione pool is kept in its reduced form. The reduced form of glutathione, GSH, plays an important role in combating oxidative stress. (Carmel-Harel and Storz, 2000).

Glutathione-reduction system comprises of glutathione, glutathione reductase (Gor) and a short peptide glutaredoxin (Grx). GSH mediates the reduction of disulfide bonds in proteins either independently or in conjunction with glutaredoxin. During this process two molecules of GSH are oxidized to form GSSG. GSSG is further reduced to GSH by glutathione reductase, which in turn oxidizes one molecule of NADPH. During oxidative stress, ROS molecules cause undesired disulfide bond formation in proteins thereby damaging these biomolecules. GSH helps in combating oxidative stress by restoring thiol groups in proteins (Carmel-Harel and Storz, 2000; Farr and Kogoma, 1991). Various observations support the involvement of glutathione as an antioxidant; *gshA* mutant is hypersensitive to H_2O_2 while *gor* mutant is hypersensitive to paraquat (Carmel-Harel and Storz, 2000). There is a feedback loop between glutathione-reduction system and OxyR. OxyR activates *gor* and *grxA*

(gene encoding one of the glutaredoxins), whereas the latter together reduce and inactivate OxyR (Carmel-Harel and Storz, 2000; Chiang and Schellhorn, 2012).

1.7.3.4 Non-enzymatic player: Ubiquinone

Ubiquinone, an electron carrier in ETC, has also been suggested to function as an antioxidant in *E. coli*. However, till date, there is only one report describing its antioxidant function in bacteria. Søballe and Poole showed that a *ubiCA* double mutant, which produces no detectable ubiquinone, exhibits several oxidative stress phenotypes in LB: accumulation of superoxide and H_2O_2 in membranes, hypersensitivity to oxidative stress inducing agents, $CuSO_4$ and H_2O_2, and up-regulation of catalase. Further supplementation of water-soluble ubiquinones, Ubiquinone-1 and Ubiquinone-2 decreased H_2O_2 levels in the *ubiCA* mutant. To explain the antioxidant function of ubiquinone, authors proposed two mechanisms. First, ubiquinone enables the rapid transfer of electrons from upstream respiratory dehydrogenases to terminal oxidases thereby decreasing the chance of single-electron donation to oxygen limiting the formation of ROS. Second, the reduced form of ubiquinone (ubiquinol) can scavenge ROS (Soballe and Poole, 2000). Recently, another study has demonstrated the *in vitro* quinol peroxidase activity of cytochrome *bd* where quinol serves as a substrate for the terminal oxidase to detoxify H_2O_2 (Al-Attar et al., 2016). However, the exact mechanism by which ubiquinone counteracts ROS, the physiological condition under which ubiquinone plays a predominant role, and the relative contribution of ubiquinone to the overall oxidative stress response remains to be assessed.

1.8 Biosynthesis of ubiquinone-8

The precursors of ubiquinone are 4-hydroxybenzoate (4-HB) and octaprenyl diphosphate. The benzene ring of 4-HB is modified by a series of reactions that include prenylation, decarboxylation, hydroxylation, and methylation to form ubiquinone-8 as the final product. This sequential modification of quinone ring by proteins encoded by *ubi* genes (ubiquinone biosynthesis genes) forms the ubiquinone biosynthesis pathway. In *E. coli* eleven *ubi* genes are reported to participate in ubiquinone biosynthesis (Aussel et al., 2014b). Figure 1.4 shows the ubiquinone biosynthesis pathway.

A very early study suggested that Ubi proteins constitute a large multiprotein complex in *E. coli*. Authors isolated an enzyme complex of ~2000 kDa from the cytoplasmic membrane consisting of at least 12 proteins, ranging from 40 to 80 kDa. The complex contained a high amount of 3-octaprenylphenol (OPP) but no ubiquinone-8. Interestingly, on providing S-Adenosylmethionine (SAM), NADPH, and O_2 to the complex, ubiquinone-8 could be synthesized from OPP (Knoell, 1979). However, till date, the ubiquinone biosynthesis complex is not well established.

1.8.1 Biosynthesis of 4-hydroxybenzoate (4-HB)

Chorismate pyruvate-lyase, UbiC catalyzes the aromatization of chorismate to 4-HB, which is the first committed step in the biosynthesis of ubiquinone (Fig. 1.4). Chorismate is the end product of the shikimate pathway, which uses D-erythrose-4-phosphate as a precursor (Meganathan, 2001).

1.8.2 Biosynthesis of Polyprenyl chain

The two glycolytic intermediates, pyruvate and glyceraldehyde-3-phosphate (G3P) serve as precursors for the synthesis of isoprenyl diphosphate (IPP) and dimethylallyl pyrophosphate (DMAPP) by methylerythritol phosphate pathway (MEP). Various

genes such as *dxr*, *dxs*, *ispD*, *ispE*, and *ispF* encode enzymes required for the MEP pathway. IPP and DMAPP act as precursors for the synthesis of octaprenyl diphosphate, and this process is catalyzed by proteins encoded by *ispA* and *ispB*. Octaprenyl diphosphate is finally attached to the quinone ring (Aussel et al., 2014b; Meganathan, 2001) (Fig. 1.4).

1.8.3 Modification of quinone ring: Prenylation

ubiA is the first gene involved in the modification of quinone ring and encodes 4-hydroxybenzoate octaprenyltransferase that catalyzes the prenylation of 4-HB to 3-octaprenyl-4-hydroxybenzoate (OHB) (Young et al., 1972) (Fig. 1.4).

1.8.4 Modification of quinone ring: Decarboxylation

Decarboxylation of OHB to OPP is mediated by the enzyme 3-octaprenyl-4-hydroxybenzoate decarboxylase. It is suggested that both UbiD and UbiX are required for decarboxylase activity, where UbiX is presumed to serve as a necessary partner for the decarboxylase, UbiD (Gulmezian et al., 2007) (Fig. 1.4).

1.8.5 Modification of quinone ring: Hydroxylation and Methylation

The alternate three hydroxylation and methylation reactions mediated by hydroxylases, UbiI, UbiH and UbiF, and methylases, UbiG and UbiE, further modifiy the quinone ring (Fig. 1.4). OPP is hydroxylated at C5 position to form an intermediate compound (IC1) by a monooxygenase, UbiI, while UbiG, a methyltransferase, catalyzes the O-methylation of IC1 at its C5 position (Hajj Chehade et al., 2013; Hsu et al., 1996) that produces another intermediate compound (IC2). The methylated product (IC2) again undergoes hydroxylation at C1 position, proposed to be catalyzed by UbiH to form C1-demethyl-C6-demethoxy-Q_8 ($DDMQ_8$)

(Aussel et al., 2014b; Nakahigashi et al., 1992). Second methyltransferase i.e. UbiE then transfers the methyl group at C2 position of $DDMQ_8$ converting it to C6-demethoxy-Q_8 (DMQ_8) (Lee et al., 1997). Both UbiG and UbiE are dependent on SAM for their activity (Aussel et al., 2014b). UbiF catalyzes third hydroxylation of the quinone ring, at the C6 position of DMQ_8, generating IC3 (Kwon et al., 2000). Further, above hydroxylated product (IC3) undergoes O-methylation at C6 position by UbiG to synthesize ubiquinone-8. UbiG thus functions as a methyltransferase at two positions i.e. C5 and C6. UbiF, UbiH and UbiI are flavin-containing monooxygenases (Aussel et al., 2014b; Pelosi et al., 2016).

UbiB and UbiJ are two additional players involved in ubiquinone biosynthesis; however, their exact function in the pathway is unclear. UbiB shows similarity with proteins belonging to eukaryotic-type protein kinase family and is proposed to be involved in regulation of ubiquinone biosynthesis through its kinase activity. On the basis of sequence similarity, UbiJ is proposed to be a carrier protein involved in ubiquinone biosynthesis (Aussel et al., 2014b).

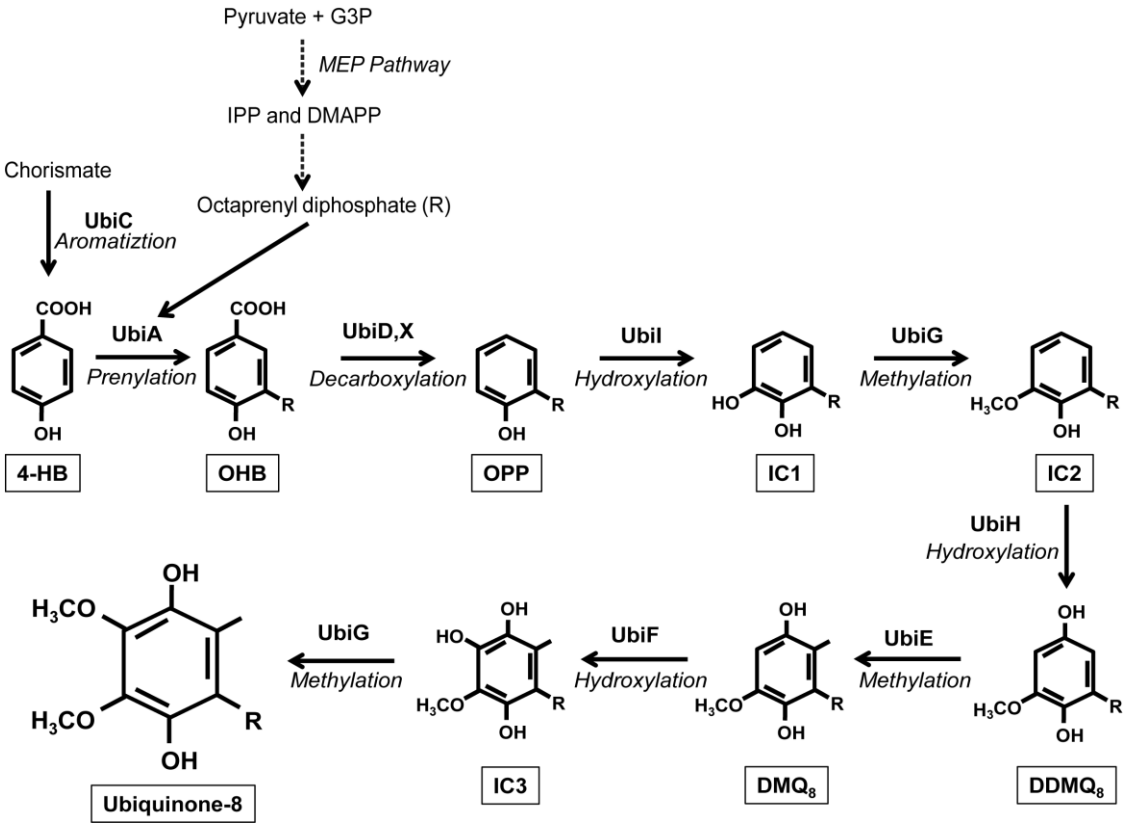

Figure 1.4 Ubiquinone biosynthesis pathway in *E. coli*. Biosynthesis of ubiquinone-8 is mediated by Ubi proteins. Octaprenyl chain of ubiquinone-8 is synthesized from the precursors IPP and DMAPP. IPP and DMAPP are produced from MEP pathway using Pyruvate and G3P as precursors. Chorismate is aromatized by UbiC protein to form 4-HB. 4-HB undergoes prenylation by UbiA and produces OHB. Further, the ring modification reactions such as decarboxylation and three alternate hydroxylation and methylation reactions mediated by several Ubi proteins generate ubiquinone-8. Dotted arrows indicate multistep process. Abbreviations: *G3P*, glyceraldehyde-3-phosphate; *IPP*, isoprenyl diphosphate; DMAPP, dimethylallyl diphosphate; *4-HB*, 4-hydroxybenzoate; *OHB*, 3-octaprenyl-4-hydroxybenzoate; *OPP*, 3-octaprenylphenol; *IC1*, intermediate compound 1; *IC2*, intermediate compound 2; *$DDMQ_8$*, C1-demethyl-C6-demethoxy-Q_8; *DMQ_8*, C6-demethoxy-Q_8; *IC3*, intermediate compound 3.

1.8.6 Growth phenotypes, ubiquinone levels and accumulation of pathway intermediates in *ubi* mutants

For the last several decades, the increased requirement of ETC and hence ubiquinone for energy generation during aerobic growth on non-fermentable carbon sources, succinate and malate, compared to a fermentable carbon source, glucose, has been used as the rationale for identifying genes involved in ubiquinone biosynthesis (Stroobant et al., 1972; Wu et al., 1993). In addition, reduction in ubiquinone levels and accumulation of ubiquinone pathway intermediates in mutant strains has enabled identification of *ubi* genes (Cox et al., 1968; Cox et al., 1969; Hajj Chehade et al., 2013; Stroobant et al., 1972). Table 1.1 lists our current information on ubiquinone levels and intermediates that accumulate in mutants affected in different steps of ubiquinone biosynthesis pathway along with their reported growth phenotype on glucose and a non-fermentable carbon source, succinate.

Gene	Mutant type[a]/ Q_8 content[b]		Mutant type[a]/Accumulated Q_8 intermediate[c]		Mutant type[a]/Growth on Glucose		Mutant type[a]/Growth on Succinate		References
ubiC	PM	Low levels detected	PM	None	PM	Growth	PM	Growth defect	(Lawrence et al., 1974; Siebert et al., 1994)
ubiA	KO	Not detected	--	Not known	PM	Growth	PM	No growth	(Cox et al., 1968; Wu et al., 1993)
ubiD	RM	~25%[#]	RM	OHB	RM	Growth	RM	Growth defect	(Cox et al., 1969)
ubiX	KO	Low[#] levels detected	KO	OHB	KO	Growth defect	KO	Growth defect	(Gulmezian et al., 2007)
ubiI	KO	~15%	KO	4-HP_8	KO	Growth	KO	Growth	(Hajj Chehade et al., 2013; Pelosi et al., 2016)
ubiG	PM	~5%	PM	OPP and IC3	PM	Growth	PM	No growth	(Stroobant et al., 1972)
ubiH	KO	Not detected	PM	OPP, IC1, and IC2	KO	Growth	KO	No growth	(Pelosi et al., 2016; Young et al., 1973)
ubiE	KO	Not detected	PM	$DDMQ_8$	PM	Growth defect	PM	No growth	(Aussel et al., 2014a; Lee et al., 1997; Swearingen et al., 2006)
ubiF	KO	Not detected	KO	DMQ_8	KO	Growth defect	KO	No growth	(Kwon et al., 2000; Pelosi et al., 2016)
ubiB	KO	Not detected	KO	OPP	KO	Growth	KO	No growth	(Macinga et al., 1998; Poon et al., 2000)
ubiJ	KO	Not detected	--	Not known	KO	Growth defect	KO	No growth	(Aussel et al., 2014a; Xia et al., 2017)

Table 1.1 Ubiquinone content, accumulated ubiquinone intermediates and growth phenotypes of different *ubi* mutants in *E. coli*. It is important to note that in studies referred

in the table, there are differences in terms of the *E. coli* K12 strains used, the techniques employed for quantifying ubiquinone levels, and the composition of growth medium. All these studies were performed under aerobic conditions.

[a] Mutants reported in this table vary from random mutant (RM) to point mutant (PM) to gene knockout (KO).

[b] Percentage (%) of Q_8 content in different *ubi* mutants is in comparison to wild-type (WT) Q_8 content

[c] Accumulated Q_8 intermediate: *4-HP*$_8$, 3-Octaprenyl-4-hydroxyphenol; *OHB*, 3-octaprenyl-4-hydroxybenzoate; *OPP*, 3-octaprenylphenol; *IC1*, intermediate compound 1; *IC2*, intermediate compound 2; *DDMQ*$_8$, C1-demethyl-C6-demethoxy-Q_8; *DMQ*$_8$, C6-demethoxy-Q_8; *IC3*, intermediate compound 3.

[#] In *ubiD* and *ubiX* mutants, whereas ubiquinone levels are reduced in log phase cells, these mutants have ubiquinone levels equivalent to WT in stationary phase cells. The decarboxylase that functions in place of UbiD and UbiX in stationary phase is not known.

1.9 Thesis Objective

The success of bacteria as pathogens and as industrial workhorses relies largely on their ability to utilize energy-rich nutrients and their resistance to stress conditions. LCFAs are one of the most important classes of energy-rich molecules for both bacterial pathogenesis and industrial production (Dellomonaco et al., 2010; Doi et al., 2014; Ray et al., 2011; Son et al., 2007). However, there are a few reports, which suggest that LCFAs confer stresses on bacteria, including oxidative stress (Doi et al., 2014; Lennen et al., 2011). Till date, there has not been any detailed investigation to understand the reason for LCFA-induced stresses and the major players/pathways employed by bacteria to combat such stresses. These studies besides being relevant from a fundamental perspective are also important for identifying novel antibacterial targets to control LCFA-utilization by bacterial pathogens and design metabolic engineering strategies to promote LCFA-utilization by industrial microbes.

LCFA metabolism has been studied in *E. coli* since 1960's and the players involved in its transport and degradation have largely been characterized (Fujita et al.,

2007). Despite such extensive investigations, the connection of LCFA metabolism with stress response pathways is still unexplored. In the present work, we used *E. coli* as a model bacterium to understand the interconnection between LCFA metabolism and oxidative stress. Our specific objectives in the first part of the thesis are: 1) investigate the reason for LCFA-induced oxidative stress, and 2) investigate strategies used by *E. coli* to mitigate oxidative stress generated by LCFAs. Our results from the first two objectives established that LCFA transport and degradation is responsible for elevated levels of ROS in LCFA-utilizing bacteria and that ubiquinone, an electron carrier in the ETC, is a key antioxidant during LCFA metabolism. The maximal requirement of ubiquinone for growth on LCFAs compared to other tested carbon sources encouraged us to use LCFAs as a carbon source for the identification of new players in ubiquinone biosynthesis pathway. In the second part of the thesis, we identified *yqiC* as a novel ubiquinone biosynthetic player and showed its genetic interaction with another gene involved in ubiquinone biosynthesis, *ubiI*.

CHAPTER II

Materials and Methods

2.1 Bacterial strains, plasmids, and primers

Experiments were conducted in BW25113 background. Deletion strains were obtained from the Keio deletion library. Either both independent clones from the library and/or fresh transductants were analyzed to rule out genetic errors. Strains and plasmids, used in this study are listed in Table 2.1. Primers used for plasmid construction and for confirmation of gene disruption are listed in Table 2.2.

Table 2.1 Strains and plasmids used in this study

Strains/plasmids	***Relevant genotype***	***Source/reference***
Strains		
BW25113 (WT)	*lacI*^{q} *rrnB*$_{T14}$ Δ*lacZ*$_{WJ16}$ *hsdR514* Δ*araBAD*$_{AH33}$ Δ*rhaBAD*$_{LD78}$	Genetic Stock Center (Datsenko and Wanner, 2000)
RC1025 (Δ*fadL*)	*fadL*::*kan* in BW25113	Keio collection (Baba et al., 2006)
RC1026 (Δ*fadD*)	*fadD*::*kan* in BW25113	Keio collection (Baba et al., 2006)
RC1117 (Δ*fadE*)	*fadE*::*kan* in BW25113	Keio collection (Baba et al., 2006)
RC1116 (Δ*fadB*)	*fadB*::*kan* in BW25113	Keio collection (Baba et al., 2006)
RC1115 (Δ*fadA*)	*fadA*::*kan* in BW25113	Keio collection (Baba et al., 2006)
RC1167 (Δ*fadJ*)	*fadJ*::*kan* in BW25113	Keio collection (Baba et al., 2006)
RC1166 (Δ*fadI*)	*fadI*::*kan* in BW25113	Keio collection (Baba et al., 2006)
RC1173	RC1116; *kan* cassette flipped out	This work
RC1176	P1 (BW25113 *fadJ*::*kan*) x	This work

	RC1173, Kan^R	
RC1169	RC1115; *kan* cassette flipped out	This work
RC1174	P1 (BW25113 *fadI*::*kan*) x RC1169, Kan^R	This work
RC1104 (Δ*ubiC*)	*ubiC*::*kan* in BW25113	Keio collection (Baba et al., 2006)
RC1082 (Δ*ubiE*)	*ubiE*::*kan* in BW25113	Keio collection (Baba et al., 2006)
RC1081 (Δ*ubiF*)	*ubiF*::*kan* in BW25113	Keio collection (Baba et al., 2006)
RC1083 (Δ*ubiH*)	*ubiH*::*kan* in BW25113	Keio collection (Baba et al., 2006)
RC1041 (Δ*ubiI*)	*ubiI*::*kan* in BW25113	Keio collection (Baba et al., 2006)
RC1084 (Δ*ubiX*)	*ubiX*::*kan* in BW25113	Keio collection (Baba et al., 2006)
RC1092 (Δ*ahpC*)	*ahpC*::*kan* in BW25113	Keio collection (Baba et al., 2006)
RC1105 (Δ*soxR*)	*soxR*::*kan* in BW25113	Keio collection (Baba et al., 2006)
RC1106 (Δ*sodA*)	*sodA*::*kan* in BW25113	Keio collection (Baba et al., 2006)
RC1091 (Δ*katE*)	*katE*::*kan* in BW25113	Keio collection (Baba et al., 2006)
RC1093 (Δ*gshB*)	*gshB*::*kan* in BW25113	Keio collection (Baba et al., 2006)
RC1080 (Δ*yqiC*)	*yqiC*::*kan* in BW25113	Keio collection (Baba et al., 2006)
RC5114 (Δ*nuoK*)	*nuoK*::*kan* in BW25113	Keio collection (Baba et al., 2006)
RC5116 (Δ*sdhB*)	*sdhB*::*kan* in BW25113	Keio collection (Baba et al., 2006)

RC8007	RC1041; *kan* cassette flipped out	Chaba lab
RC8009	P1 (BW25113 *yqiC*::*kan*) x RC8007, Kan^R	Chaba lab
Plasmids		
pACYC184	Vector, p15A ori, Cm^R , Tet^R	New England Biolabs (Chang and Cohen, 1978; Rose, 1988)
pBAD24	Vector, f1 ori, pBR322 ori, Amp^R	(Guzman et al., 1995)
pAQ6	*sodA* promoter and *sodA* in pACYC184, Cm^R	Gisela Storz lab (Storz et al., 1987)
pKJ7	*ubiI*-6His in pBAD24, Amp^R	Chaba lab
pSA4	putative *yqiC* promoter and *yqiC*-6His in pACYC184, Tet^R	This work

* Restriction sites are underlined

'This work' refers to strains/plasmids that were made as part of thesis and 'Chaba lab' refers to strains/plasmids made by other lab members

Table 2.2 Primers used in this study

Primers: for cloning

Primers	***Sequence (from 5' to 3')***	***Purpose***
SA 55	CATGCCATGGAAAAGAGGAAAGTAGCGT CTGATTCATGGTAAAAAAACCTCAC	Froward Primer: for cloning *yqiC*-6His with putative *yqiC* promoter in pACYC184
SA 56	CCGGAATTCTTAGTGATGATGATGATGAT GCAGCGTTGGGGGGAGAGTCTCTGGATCT GG	Reverse Primer: for cloning *yqiC*-6His with putative *yqiC* promoter in pACYC184

Primers: for confirmation of gene disruption with kanamycin cassette

Primers	***Sequence (from 5' to 3')***	***Purpose***
KJ 63	TCGCCACTGGTCTGATTTCTAAG	Forward Primer: *fadL*::*kan*
KJ 64	AGGACACTACTTTCGGTGAAGTGG	Reverse Primer: *fadL*::*kan*

KJ 65	ATGTTAACGGCATGTATATCATTTGG	Forward Primer: *fadD*::*kan*
KJ 66	CGTCCGTGGTAATCATTTGGTAATTC	Reverse Primer: *fadD*::*kan*
KJ 67	CACTACAACCATATCATCACAAGTGG	Forward Primer: *fadE*::*kan*
KJ 68	TAGCGGATAAAGAAACGGAGCC	Reverse Primer: *fadE*::*kan*
KJ 69	TACACACTTCGACTCATCTGGTACG	Forward Primer: *fadB*::*kan*
KJ 70	ATCTTCTGCACGCACGTTACG	Reverse Primer: *fadB*::*kan*
KJ 71	TACTATCCTCCGGTTGAGCCAGC	Forward Primer: *fadA*::*kan*
KJ 72	TCTTATCAGGCCTACATTGGTGC	Reverse Primer: *fadA*::*kan*
SA 79	CGGCGGTGGATTTGGTTTAGTTA	Forward Primer: *fadJ*::*kan*
SA 80	GACCAACACTCCGCCATTCAGC	Reverse Primer: *fadJ*::*kan*
SA 77	CACTTTCCCTTTTCTCCACTTGGC	Forward Primer: *fadI*::*kan*
SA 78	ACGGCAATGTTGTCCAGACGAAC	Reverse Primer: *fadI*::*kan*
HB01	CACTTAATTTGCTTTACATCTCCCG	Forward Primer: *ubiC*::*kan*
HB02	CAATTGGCTTATCCGTACGC	Reverse Primer: *ubiC*::*kan*
SA 65	CCGGGTAGAAATCTAGGGCATCG	Forward Primer: *ubiE*::*kan*
SA 66	GCGGGTGAGCGATACAGGAAGG	Reverse Primer: *ubiE*::*kan*
SA 67	GCCGTTGTGACCAGTATGAGCG	Forward Primer: *ubiF*::*kan*
SA 68	CGACCTACGGTTGGCACGCA	Reverse Primer: *ubiF*::*kan*
GA 18	ATGCAGAAGTGCCAGAACAATATCG	Forward Primer: *ubiH*:*kan*
GA 19	AATGGCTACATCAACACTTTG	Reverse Primer: *ubiH*::*kan*
SA 36	GCTGATGACGATGGAATTATTC	Forward Primer: *ubiI*:*kan*
SA 37	GAGATGAAAGTGTGATGGGTATC	Reverse Primer: *ubiI*::*kan*
HB 03	TTGCAACTCCCGCCGAAATC	Forward Primer: *ubiX*::*kan*
HB 04	AGCGTTTCGATTGAATGGCAG	Reverse Primer: *ubiX*::*kan*
SA 53	CGGCAGCAACGCATAGCTTCAC	Forward Primer: *yqiC*::*kan*
SA 54	TGGTTTTCTGAATGGGATTACGCG	Reverse Primer: *yqiC*::*kan*
SAK1	GAGGCTATTCGGCTATGACTG	Forward Primer: for confirming kanamycin gene in strains harboring gene disruption with kanamycin cassette
SAK2	TTCCATCCGAGTACGTGCTC	Reverse Primer: for confirming kanamycin gene in strains harboring gene disruption with kanamycin cassette

2.2 Media composition and growth conditions

Strains were cultured in Lysogeny broth (LB; 5 g/liter of yeast extract, 10 g/liter of Bacto-Tryptone, and 5 g/liter NaCl), in Tryptone broth (TB; 10 g/liter of Bacto-Tryptone, and 5 g/liter of NaCl), and in M9 minimal medium (5.3 g/liter of Na_2HPO_4,

3 g/liter of KH_2PO_4, 0.5 g/liter of NaCl, 1 g/liter of NH_4Cl, 0.12 g/liter of $MgSO_4$, 2 mg/liter of biotin, 2 mg/liter of nicotinamide, 0.2 mg/liter of riboflavin, and 2 mg/liter of thiamine). Unless otherwise specified, when required, TB medium or M9 minimal medium was supplemented with one of the following carbon sources at a final concentration of 5 mM: glucose or sodium salt of acetate, succinate, laurate, stearate or oleate. Laurate (50 mM), oleate (50 mM) and stearate (33 mM) were solubilized in 5.0% Brij-58 (Lepore et al., 2011). Media were solidified using 1.5% (w/v) bacto agar. For chemical genomics screen, minimal medium was supplemented either with 5 mM oleate or 0.2% glucose with 0.5% Brij-58.

Cultures were incubated at 37°C. For experiments in liquid medium, unless indicated otherwise, primary cultures were grown in 3 ml TB, which were further re-inoculated either in TB or TB supplemented with desired carbon source to an initial OD_{600} of ~0.01. These secondary cultures were grown for defined time periods. For the detection of Q_8 in Δ*ubiI*Δ*yqiC* double mutant, strains were grown in LB supplemented with 0.2% glucose.

2.3 Recombinant DNA work and gel electrophoresis

General protocols for cloning techniques, colony PCR, agarose gel electrophoresis, and SDS-PAGE were adapted from 'Sambrook Molecular cloning: A Laboratory manual'. Plasmid isolation, purification of PCR products and gel extraction of DNA was performed using kits purchased from Thermo scientific and protocols were followed as per manufacturer's instruction manual.

2.4 P1 Lysate preparation and transduction

P1 lysate was prepared using protocol mentioned in (Miller, 1972) with slight modifications. Overnight cultures of desired strains were sub-cultured with 1:100

ratio in 2 ml LB containing 5 mM $CaCl_2$, and incubated at 37°C for 90 min. 20 µl of P1 lysate was added to cultures and cultures were again incubated at 37°C for 3-4 hours. 50 µl of chloroform was added to lysed cultures and vortexed for 30 seconds. Cell debris was pelleted and supernatant (lysate) was transferred to fresh MCT containing 50 µl of chloroform, and stored at 4°C until use.

P1 transduction was preformed using protocol mentioned in (Miller, 1972) with slight modifications. 1 ml of overnight culture was pelleted and re-suspended in 500 µl of solution containing 5 mM $MgSO_4$ and 10 mM $CaCl_2$. 100 µl of re-suspended cells were aliquoted in two MCTs. 60 µl of P1 lysate was added to first aliquot while second aliquot was left untreated, and samples were incubated at 30°C for 30 min in a water bath. 1 ml LB containing 10 mM of sodium citrate was added to the samples and incubated at 37°C for 1 hour in a water bath. Cells were pelleted and washed twice with 1 ml LB and then suspended in 100 µl of LB. Suspended cells were spread on LB agar plates supplemented with 10 mM of sodium citrate and suitable antibiotic, and incubated at 30°C for 16-18 hours. 60 µl of P1 lysate was also spread on LB agar plates as control. Colonies obtained were re-streaked twice on LB agar plates with 10 mM sodium citrate and suitable antibiotic and incubated at 37°C. Transductants were confirmed by colony PCR.

2.5 Growth curves

Overnight cultures grown in TB were pelleted, and cells were re-inoculated in 50 ml of TB or TB medium supplemented with oleate or Brij-58 detergent. Secondary cultures were setup with initial OD_{600} of ~0.01 in 250 ml shake flasks and incubated at 37°C in a water bath shaker. OD_{600} of secondary cultures was measured at regular time intervals and OD_{600} was plotted against time to generate growth curves.

2.6 Dilution spotting

Overnight cultures were pelleted by centrifugation, washed and re-suspended in M9 minimal medium (without any carbon source) and OD_{450} of each strain was normalized. Several dilutions of cultures were spotted on M9 minimal medium agar supplemented with desired carbon source. Antibiotics were added whenever required. Plates were incubated and imaged at various time intervals using the Gel Doc XR+ imaging system from BioRad. A representative image with apparent growth differences is shown in the figures.

2.7 RNA isolation, cDNA preparation and quantitative RT-PCR

Secondary cultures (15 ml) were grown in 125 ml flasks to OD_{600} ~0.5 or 1. Samples (8 ml) were added to ice-cold 5% water-saturated phenol (in ethanol), and centrifuged at 8200 X g for 2 min. Cell pellets were flash-frozen in liquid nitrogen and stored at -80°C until required. RNA was extracted using the hot-phenol method, with slight modifications. Briefly, pellets were re-suspended in 500 µl lysis solution (320 mM Na acetate pH 4.6, 8% SDS, 16 mM EDTA), followed by mixing with 1 ml water buffered phenol. Samples were incubated at 65°C for 5 min with intermittent vortexing. Samples were kept on ice for 5 min and centrifuged at 4°C for 10 min. The supernatant was extracted twice with phenol-chloroform, precipitated with 2.5 volumes of absolute ethanol and washed with 70% ethanol. The RNA pellet was air dried and re-suspended in 85 µl RNase free water. DNA-free Turbo DNase was used to remove genomic DNA from samples according to the manufacturer's instructions for rigorous DNase treatment (Applied Biosystems, USA). cDNA was prepared for qRT-PCR using 5 µg of input RNA as described previously (Cummings et al., 2006). Quantitative RT-PCR reactions were carried out using Power Sybrgreen PCR master

mix according to the manufacturer's instructions (Applied Biosystems, USA), and 5 pmol of forward and reverse primers (Integrated DNA Technologies). Real-time PCR was performed with a Quant Studio 6 Flex system (Applied Biosystems, USA). Data were analyzed as described (Vandesompele et al., 2002) using *recA* and *gyrA* as control.

2.8 Nitroblue tetrazolium (NBT) assay

Secondary cultures (3 ml) were grown in TB or TB medium supplemented with desired carbon source or Brij-58 detergent for ~16 hours. ROS levels were determined by NBT reduction assay following the protocol described in (Albesa et al., 2004) with slight modifications. 1 ml of overnight secondary cultures were pelleted and re-suspended in 1 ml of M9 minimal medium (without any carbon source). OD_{450} was measured and cells were normalized to OD 1.0. 1 ml of normalized cultures were pelleted and re-suspended in 200 µl of Hanks' balanced salt solution (HBSS). 200 µl of cultures in HBSS were split in two equal aliquots: 0.5 ml NBT (1 mg/ml) was added to one aliquot and the other aliquot was left untreated. Both aliquots were incubated at 37°C for 30 min in water bath. 100 µl of 0.1 M HCl was added and samples were centrifuged at 18,400 X *g* for 15 min. Supernatant was discarded, and pellet was treated with 0.4 ml dimethyl sulfoxide (DMSO) to dissolve reduced NBT (formazan blue), followed by addition of 0.8 ml HBSS. Formazan blue was quantified at 575 nm. To determine the absorbance corresponding to formazan blue, absorbance of aliquot without NBT was deducted from absorbance obtained for NBT treated sample. For experiments where ROS levels were determined in different phases of growth, 15 ml secondary cultures were grown in 125 ml flasks. Independent cultures (from the same primary culture) were set-up for each time point. The composition of

HBSS solution is mentioned in the following Table 2.3. The HBSS solution was filter sterilized after preparation.

Table 2.3 Composition of HBSS solution

Components	**Amount (1 L)**
NaCl	8 gm
KCl	400 mg
$CaCl_2.2H_2O$	186 mg
$MgSO_4.7H_2O$	10 mg
$MgCl_2.6H_2O$	100 mg
Na_2HPO_4	480 mg
Glucose	1 gm
$NaHCO_3$	350 mg
KH_2PO_4	60 mg

2.9 Dihydroethidium (DHE) assay

Secondary cultures (3 ml) were grown in TB supplemented with either oleate or Brij-58 detergent for ~16 hours. ROS levels were measured using the dihydroethidium (DHE) assay as described previously (Sevin and Sauer, 2014), with slight modifications. 1 ml of overnight cells were pelleted and washed with 1X PBS solution (pH 7.4) and normalized to OD_{450} 1.0. Two aliquots of the suspension, each of 100 µl was taken in two MCTs. To one aliquot 100 µl of 1X PBS containing 20 µM DHE and to the other 100 µl of 1X PBS (control for background fluorescence) was added. Under dark conditions, cells were incubated at 37°C for 1 hour in water bath to allow uptake and oxidation of DHE by ROS. Samples were then immediately transferred to ice. DHE oxidation was measured using BD Accuri C6 flow cytometer. Data are shown after subtracting the background fluorescence.

2.10 NADH and NAD^+ quantification

Secondary cultures (3 ml) were grown in TB supplemented with either oleate or Brij-58 detergent for ~16 hours. Extraction of NAD^+ and NADH was carried out following the procedure described in (San et al., 2002) with slight modification. Briefly, 2 ml of overnight secondary cultures were pelleted, and washed three times with 1 ml cold 1X PBS, and normalized to OD_{450} 1.0. Immediately, 1 ml of each sample was taken in two MCTs, pelleted and re-suspended either in 300 µl of 0.2 M NaOH (for NADH) or 300 µl of 0.2 M HCl (for NAD^+). Samples were incubated at 50°C in water bath for 10 min and were immediately transferred to ice for 5 min. 300 µl of 0.1 M HCl (for NADH) or 0.1 M NaOH (for NAD^+) was added drop-wise to the samples with vortexing. Cell debris was removed by centrifugation at 18,400 X g for 5 min at 4°C, and the supernatant was transferred to a fresh MCT and kept in ice. Samples with extracted NADH or NAD^+ were de-proteinized using a 9 kDa cut-off filter by centrifugation at 6,900 X g for 15 min at 4°C, and kept in ice. NAD^+/NADH quantification kit (Sigma) was further used for quantifying amount of NADH and NAD^+ in samples. Briefly, 150 µl reaction mix was prepared in 96-well plates (transparent with clear bottom) according to manufacturer's instruction. Each reaction mix contained 50 µl sample (above extracted sample), 98 µl cycling buffer, and 2 µl cycling enzyme mix. The reaction mix was incubated at room temperature (RT) for 10 min and then 10 µl of NADH developer was added in dark. After two hours, absorbance was measured at 450 nm (Thermo scientific Multiskan Go). Standard curve was generated using NADH standard provided in the kit, and the amount of NADH or NAD^+ in the samples was determined.

2.11 Enzyme activity assays

2.11.1 *Preparation of cell extract*

Secondary cultures (3 ml) were grown either in TB or TB supplemented with oleate for ~16 hours. Cultures were washed at least three times with assay buffer. 1.5 ml of 5 x 10^9 cells were re-suspended and sonicated. Samples were centrifuged at 18,400 X g for 40 min at 4°C, supernatant was collected and kept in ice. Protein in the cell extracts was quantified using Bradford assay.

2.11.2 *NADH dehydrogenase assay*

The protocol adapted from (Wang and Maier, 2004) was slightly modified. 1 ml reaction mixture was set up containing 50 mM Tris-Cl (pH 8.0), 250 µM Menadione, and 1 µg protein. Reaction was initiated by adding 250 µM NADH. Enzyme activity was calculated from the decrease in absorbance of NADH (extinction coefficient: 6.22 mM^{-1} cm^{-1}) at 340 nm over a period of 5 min. Activity was expressed as nmoles of NADH oxidized per min per mg protein. Reaction mixture without NADH was taken as blank.

2.11.3 *Succinate dehydrogenase assay*

The protocol adapted from (McNeil et al., 2012) was followed with few modifications. 1 ml reaction mixture was set up containing 0.1 M NaPO4 (pH 7.0), 0.1 M sodium succinate (pH 7.5), 0.12 M sodium azide, 0.1 mM ubiquinone-2 (Sigma, 10 mM stock was prepared in ethanol) and 50 µg protein. Reaction was followed by adding 0.05 mM DCIP (2,6-Dichlorophenolindophenol). Enzyme activity was calculated from the decrease in absorbance of DCIP (extinction coefficient: 22 mM^{-1} cm^{-1}) at 600 nm over a period of 15 min. Activity was expressed as nmoles of DCIP reduced per min per mg protein. Reaction mixture without DCIP was taken as blank.

2.12 Thiobarbituric acid responsive substance (TBARS) assay

TBARS assay measures MDA (malondialdehyde), a byproduct of lipid peroxidation. Quantification of MDA level was carried out following the procedure described in (Rael et al., 2004) with few modifications. Secondary cultures (3 ml) were grown in TB and TB supplemented with either oleate or Brij-58 detergent for ~16 hours. 1.5 ml of overnight cultures were washed three times with 20 mM KH_2PO_4 (pH 7.4) buffer containing .01M $CuCl_2$. OD_{450} of each sample was measured and 1.5 ml of 5 x 10^9 cells was sonicated. The sonicated samples were centrifuged at 18,400 X g for 20 min at 4°C, cell debris was removed and supernatant was collected. In 400 µl of supernatant, 0.5 mM ascorbate and 2 mM sucrose was added, and incubated at 37°C for 60 min. In this mixture, 400 µl of 1% TBA, 400 µl of conc. acetic acid was added, and incubated in boiling water for 30 min. Samples were left at room temperature for 20 min. The absorbance of 1ml reaction mixture was then measured at 532 nm in spectrophotometer. Acetone was taken (instead of sonicated sample) as a positive control. Protein in the cell extracts after sonication was quantified using Bradford assay.

2.13 Library screening and data processing

The chemical genomics screen was performed using the same methodology as reported previously with slight modifications (Nichols et al., 2011). Briefly, the Keio deletion library was arrayed in 1536-format and pinned onto plates containing minimal medium agar supplemented either with oleate or glucose with Brij-58, using a Singer Rotor robot. Plates were incubated at 37°C for 21 hours for glucose with Brij-58 and 42 hours for oleate. Time points were chosen such that fitness differences were apparent but growth had not saturated. Pictures of the plates were taken using a

Canon G10 digital camera. Colony size was quantified from plate images using the HT Colony Grid Analyzer software package (Collins et al., 2006). Colony sizes were filtered and normalized using established methods for chemical genomics in *E. coli* K-12 (Shiver et al., 2016). To account for potential effects of Brij-58 on growth, fitness scores for the oleate condition were generated by directly comparing colony size between oleate and glucose with Brij-58 control using the same statistical test as the S-score (Collins et al., 2006).

2.14 Preparation of ubiquinol-8 standard

Ubiquinone-8 (Avantis Polar Lipids) was reduced to ubiquinol-8 following the procedure used for reduction of ubiquinone-10 (Kotnik, 2013). In 125 ml conical flask, 19 ml hexane, 1 ml methanol and 200 mg of sodium borohydride was added to a freshly prepared 1 ml ubiquinone-8 solution (1 mg/ml in hexane). The mixture was covered to avoid light, stirred, and kept for 5 min. Disappearance of yellowish color of ubiquinone indicated the conversion of ubiquinone to ubiquinol. The mixture was transferred to 50 ml falcon tube and 2 ml MQ water was added and mixed thoroughly by shaking to dissolve sodium borohydride in water. The mixture was centrifuged at 2050 X g for 5 min. Upper layer of organic solvent containing ubiquinol-8 was transferred into a fresh tube and stored at -20°C.

2.15 Extraction of quinones from *E. coli* cells

Quinones were extracted using the protocol described in (Hajj Chehade et al., 2013) with slight modifications. 15 ml of secondary cultures grown either in TB or TB supplemented with oleate or Brij-58 detergent were incubated at 37°C for ~16 hours in a water bath shaker. Equal numbers of cells (~3 X 10^{10} cells) were pelleted by centrifugation and pellet mass was determined. Pellets were re-suspended in 100 µl of

0.1 M KCl, and then 200 µl of glass beads (acid washed ≥106 µm, Sigma), 600 µl of methanol and 12 µg of ubiquinone-10 standard (used as internal control for normalizing extraction efficiency) were added sequentially. Samples were vortexed for 15 min followed by addition of 400 µl n-Hexane (petroleum ether). Samples were vortexed again for 3 min and the topmost layer of hexane (containing dissolved lipid mix) was transferred gently into fresh MCT. 100 µl of this hexane layer with dissolved lipids was completely dried under vacuum and lipid mix was re-suspended in 100 µl of mobile phase.

2.16 Detection of quinones by HPLC-photodiode array analysis

The extracted lipid mix was separated and analyzed by reversed-phase HPLC using C18 column (Waters Sunfire 5 µm columns, 4.6 X 250 mm). Mobile phase was prepared using 40% ethanol, 40% acetonitrile, and 20% of a mix of 90% isopropyl alcohol and 10% of 1 M lithium perchlorate (Hajj Chehade et al., 2013). Samples were injected with the running mobile phase, at a flow rate of 1 ml/min, temperature 25°C and monitoring at wavelength range of 240 nm to 400 nm. A chromatogram containing various peaks was obtained for each sample at a particular wavelength. Using standards for ubiquinone-8 (Q_8) and ubiquinol-8 (Q_8H_2) the peaks of quinones in samples were identified at respective wavelengths. For each sample, the Q_8 peak area per unit mass was calculated, and to account for the difference in extraction efficiency between samples, the Q_8 peak area per unit mass was divided by ubiquinone-10 peak area.

CHAPTER III

Degradation of long-chain fatty acids generates high levels of reactive oxygen species in *E. coli*

3.1 Introduction

Long-chain fatty acids (LCFAs) are carboxylic acids with an unbranched aliphatic chain comprising 12-20 carbon atoms. LCFAs serve as a rich source of metabolic energy for *Escherichia coli* and several other important pathogens such as *Pseudomonas aeruginosa*, *Mycobacterium tuberculosis*, *Salmonella enterica* serovar Typhimurium and *Vibrio cholerae.* These bacteria utilize fatty acids derived from host, for example, *P. aeruginosa* utilizes lipids from lung surfactants of cystic fibrosis patients (Son et al., 2007), *M. tuberculosis* utilizes fatty acids as a major carbon source from chronically infected lung tissues (McKinney et al., 2000), *S. enterica* serovar Typhimurium derives fatty acids from phagosomes during chronic infection (Fang et al., 2005) and *V. cholerae* acquires fatty acids from bile (Giles et al., 2011). The utilization of LCFAs enables the survival of these pathogens in the harsh environments of host tissues and contributes to their virulence (Fang et al., 2005; Kang et al., 2010; Son et al., 2007). In addition to their important role in bacterial pathogenesis, LCFAs serve as a raw material for industrial production of various fuels and chemicals. *E. coli* has been engineered for aerobic fermentation of LCFAs to produce ethanol, butanol, acetate, propionate and acetone, with yields higher than those obtained from sugar fermentation (Dellomonaco et al., 2010). Further, in a separate study, the LCFA, oleate (monounsaturated LCFA with 18 carbon atoms; C18), has been used as a raw material for L-lysine fermentation by emulsification (Doi et al., 2014). Although LCFAs are rich energy source they confer various stresses on bacteria such as acid stress, redox stress, envelope stress as indicated by upregulation of stress response genes in bacteria grown in LCFAs or over-producing free fatty acids (Lennen et al., 2011; Rodriguez et al., 2014). Importantly, the connection between LCFAs and redox stress has been indicated in several studies. A

global transcriptome of *M. tuberculosis* cultured in medium supplemented with a mixture of even-length LCFAs, showed significant overexpression of genes involved in maintaining redox balance. Notably, WhiB3 and DosR, the two heme sensor proteins that regulate intracellular redox balance were overexpressed. In addition, several genes involved in cellular processes that consume reduced cofactors (e.g., complex lipid biosynthesis) were upregulated, suggesting induction of combat strategies to handle redox stress generated by LCFAs (Rodriguez et al., 2014). In another study, *E. coli* grown in oleate was reported to accumulate higher level of reactive oxygen species (ROS) compared to cultures grown in glucose (Doi et al., 2014). Further, a study in *E. coli* aimed at overproducing free fatty acids showed that fatty acid accumulation is accompanied by induction of several regulon members of SoxS, the major transcriptional regulator of oxidative stress combat players (Lennen et al., 2011).

Various mechanisms have been suggested in the literature to explain the correlation between fatty acids and ROS, which include stress due to fatty acid incorporation in the membrane, generation of lipid peroxides and peroxyl radicals by oxidative attack on fatty acids, and β-oxidation of fatty acids (Doi et al., 2014; Pradenas et al., 2012; Schonfeld and Wojtczak, 2008). Which of the above mechanism(s) account for increased levels of ROS in bacteria cultured in LCFAs has not been investigated. Given the importance of LCFAs in bacterial pathogenesis and industrial production, a detailed investigation of the reason(s) for LCFA-mediated ROS generation and of the strategies employed by bacteria to mitigate LCFA-induced stress is required.

In this chapter, we describe our work aimed at understanding the reason for generation of elevated levels of ROS in *E. coli* cultured in LCFAs. We used *E. coli* as

a model because the pathway of LCFA transport and degradation has been extensively characterized in this bacterium. LCFA degradation is mediated by proteins encoded by the *fad* (fatty acid degradation) genes (Clark and Cronan, 2005). Briefly, exogenous LCFAs are transported inside the cell by an outer membrane protein, FadL, followed by extraction from the inner membrane and esterification to acyl-CoA by the inner membrane-associated fatty acyl-CoA synthetase, FadD. Acyl-CoAs are degraded to acetyl-CoA via the β-oxidation pathway mediated by the enzymatic activities of FadE, FadB, and FadA. For the degradation of one molecule of LCFA the β-oxidation pathway runs multiple times, and thus the number of β-oxidation cycles for a particular LCFA depends on the number of carbon atoms in its aliphatic chain. Acetyl-CoA feeds into the tricarboxylic acid (TCA) cycle and glyoxylate pathway for further metabolism (Cronan and Laporte, 2005). The reduced cofactors (NADH and $FADH_2$) generated during β-oxidation and TCA cycle are oxidized in the electron transport chain (ETC) resulting in the production of ATP.

We investigated the reason for oxidative stress in *E. coli* grown in LCFAs by measuring ROS levels in several *fad* deletion strains. We convincingly established that LCFA transport and degradation is the reason for generation of high levels of ROS. Our results further suggest that a large amount of reduced cofactors generated during LCFA metabolism increase the flow of electrons in ETC resulting in elevated levels of ROS.

3.2 Results

3.2.1 LCFAs supplemented in tryptone broth (TB) are used as a carbon source by *E. coli* and generate oxidative stress in bacteria

Because *E. coli* grown in minimal medium containing oleate generates high levels of ROS (Doi et al., 2014), we sought to investigate whether high ROS levels is due to LCFA transport and degradation. This required determining ROS levels in *fad* knockouts, which do not grow in minimal medium containing LCFAs as the sole carbon source (Campbell et al., 2003). We chose tryptone broth (TB) medium, a mixture of amino acids, for experiments with the idea that TB would support the growth of *fad* knockouts, and since TB causes mild catabolite repression (Petit-Koskas and Contesse, 1976), LCFAs supplemented in TB would be co-utilized with carbon components of TB. We first confirmed the co-utilization of LCFAs with TB and then measured ROS levels in desired strains.

3.2.1.1 Oleate supplemented in TB is co-utilized with carbon components of TB medium

We used oleate as a representative LCFA for our experiments and first checked the growth of wild-type (WT) *E. coli* cells cultured in TB and TB supplemented with oleate (TB-Ole). Since oleate was solubilized in the detergent, Brij-58, we also determined the growth of cells in TB supplemented with Brij (TB-Brij). Cells grown in TB-Ole had higher biomass than cultures grown in TB and TB-Brij (Fig. 3.1A). We further measured the transcript levels of *fadL* (gene encoding the outer membrane transporter for LCFAs) and *fadE* (gene encoding the fatty acyl-CoA dehydrogenase) in WT cells grown in TB, TB-Brij and TB-Ole media at time points, T1 and T2, as indicated in the growth curve (Fig. 3.1A). The *fad* genes are negatively regulated by the transcriptional regulator, FadR, repression of which is relieved by acyl-CoA; hence *fad* genes are induced in the presence of LCFAs (Clark and Cronan, 2005). Compared to the TB medium, we observed ~2 fold increase in *fadL* transcript levels

and ~15 to 20 fold increase in *fadE* transcript levels in WT cells grown in TB-Ole (Figs. 3.1, B and C). Brij-58 alone did not affect the transcript levels of *fad* genes. Collectively, the increase in biomass, and transcript levels of *fadL* and *fadE* in WT grown in TB-Ole confirmed the co-utilization of oleate with carbon components of TB medium.

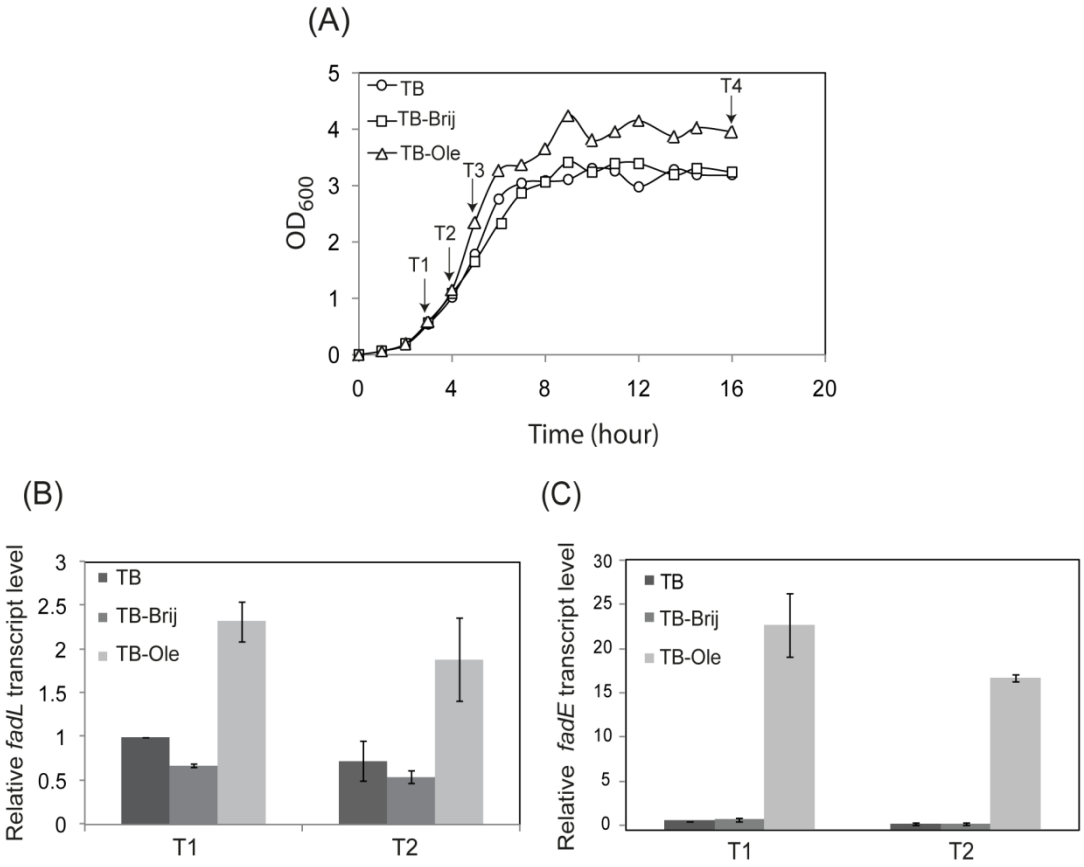

Figure 3.1 Oleate is co-utilized with carbon components of TB medium. (A) Increase in biomass of WT cells in TB-Ole confirms the co-utilization of oleate with TB. WT was grown in TB, TB-Brij and TB-Ole. OD_{600} of the cultures was measured and growth curves were plotted. The experiment was done 3 times. A representative dataset is shown. T1, T2, T3 and T4 indicate time points where cultures were harvested for various assays. (B) *fadL* and (C) *fadE* are transcriptionally induced in *E. coli* grown in TB-Ole. WT was grown in TB, TB-Brij and TB-Ole. Samples were harvested for RNA isolation at time points T1 and T2 shown in Fig. 3.1A, cDNA was prepared, and transcript abundance was assayed by qRT-PCR. Data were normalized to transcript levels in TB at time point T1 and represent average (± S.D.) of 3 independent experiments.

3.2.1.2 *E. coli* cultured in TB supplemented with oleate generates high levels of ROS

E. coli grown in minimal medium supplemented with oleate is reported to accumulate ~2-fold higher levels of hydrogen peroxide (H_2O_2) compared with cultures grown in glucose (Doi et al., 2014). Because our follow-up experiments required the use of TB medium, we first checked whether *E. coli* cells also generate high levels of ROS in TB-Ole compared to a basal medium. We used Nitroblue tetrazolium (NBT) reduction assay for determining ROS levels. NBT is a yellow colored positively charged compound, which crosses the cell membrane (Berridge et al., 2005), and gets reduced by superoxide ion to form a blue colored compound, formazan (Albesa et al., 2004; Perez-Pantoja et al., 2013) (Fig. 3.2A). Under our experimental conditions, we observed that with an increase in the number of cells the absorbance of formazan increases linearly, suggesting that NBT is not limiting for the assay (Fig. 3.2B). We measured ROS levels in WT cultured in TB and TB-Ole at different phases of growth (Fig. 3.1A). ROS levels were consistently higher in TB-Ole (~1.3 to 1.8-fold) compared to TB in each phase of growth with a maximum difference in stationary phase (Fig. 3.2C). Hence for our downstream single time point experiments cultures were sampled in stationary phase. Brij-58 alone did not result in increased ROS (Fig. 3.2C inset). NBT has been extensively used in *E. coli* and other gram-negative bacteria to measure intracellular superoxide (Albesa et al., 2004; Berridge et al., 2005; Marathe et al., 2013; Perez-Pantoja et al., 2013). We independently validated that the reduction of NBT reports on intracellular superoxide levels by overexpressing superoxide dismutase, SodA, from plasmid pAQ6 (a gift from Gisela Storz lab) (Storz et al., 1987) in WT cells cultured in TB, TB-Brij and TB-Ole (Fig. 3.2D). We observed ~30% decrease in NBT signal in all media conditions (Fig. 3.2E).

As an additional evidence for elevated ROS levels in cells grown in oleate, we used a fluorometric approach based on the oxidation of the cell-permeable non-fluorescent dye, dihydroethidium (DHE) by superoxide ion to a fluorescent product, hydroxyl ethidium (Zhao et al., 2003). We measured ROS levels in WT cells grown in TB-Brij and TB-Ole media conditions. In comparison to TB-Brij, we observed ~2.5 fold higher ROS levels in WT cells grown in TB-Ole (Fig. 3.2F). Thus, similar to the colorimetric NBT assay, the fluorometric DHE assay also reported higher levels of ROS in *E. coli* cells grown in TB-Ole.

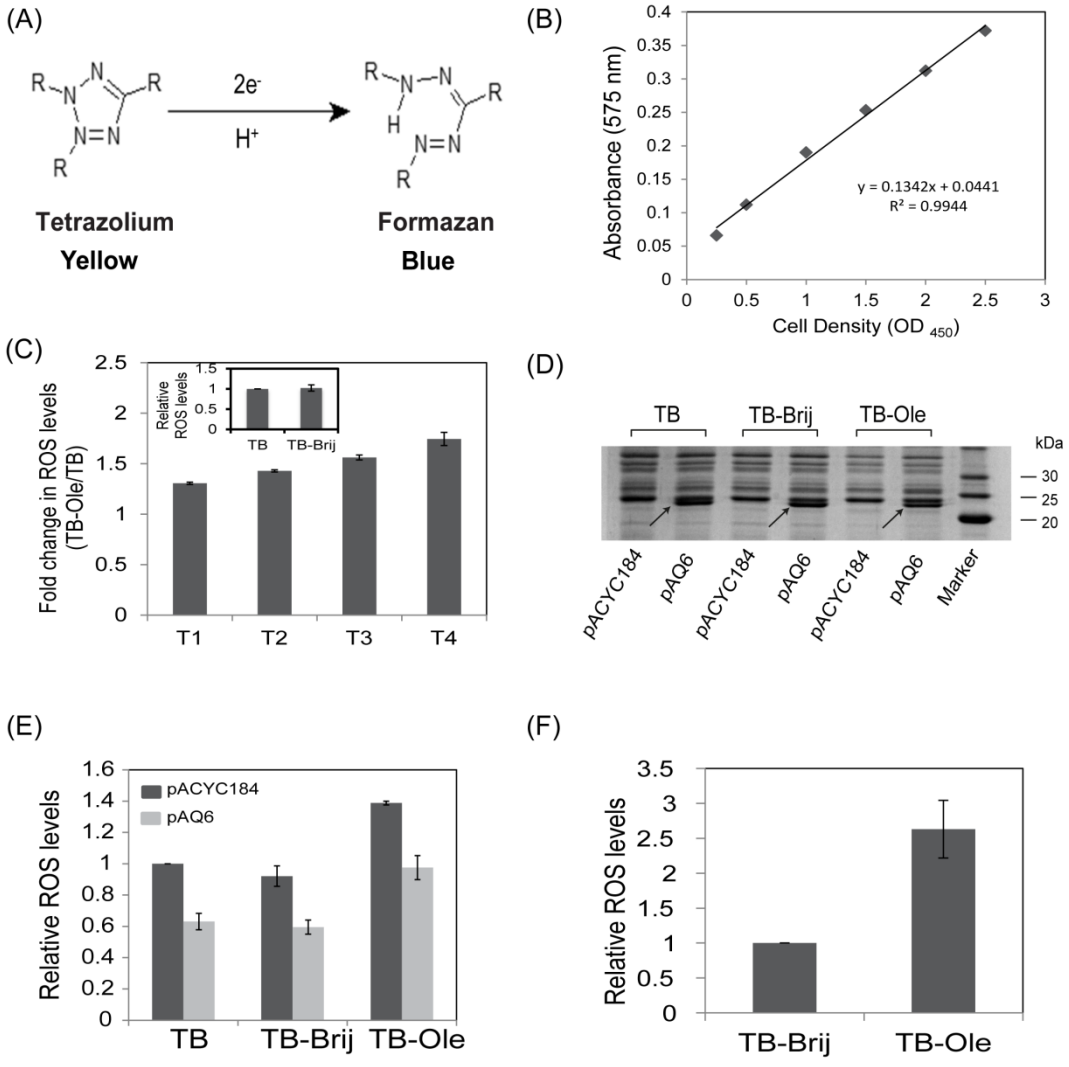

Figure 3.2 *E. coli* cultured in tryptone broth supplemented with oleate generates high levels of ROS. (A) Yellow colored NBT dye is reduced to blue colored formazan by superoxide, which can be detected at 575 nm. (Adapted from – Tim Vickers, https://commons.wikimedia.org/w/index.php?curid=4427975). (B) Curve showing a linear increase in absorbance of formazan with increase in number of cells. (C) Difference in ROS levels between TB and TB-Ole. WT was grown either in TB or TB-Ole, and cultures were harvested at different phases of growth as indicated in Fig. 3.1A. Fold change in ROS levels (TB-Ole/TB) was calculated. Data represent average (± S.D.) of 3 independent experiments. (Inset) Brij-58 does not interfere with ROS assay. ROS levels were determined by NBT assay in WT grown in TB and TB-Brij. Data were normalized to the ROS level of WT in TB and represent average (± S.D.) of 3 independent experiments. (D) SodA expression from the plasmid. WT cells carrying either pACYC184 (empty plasmid) or pAQ6 (pACYC184 carrying *sodA*) were grown in TB, TB-Brij and TB-Ole. Cells were harvested, lysates were prepared and samples were run on 15% SDS-PAGE. The band corresponding to SodA is indicated (Mol. wt. ~24 kDa). (E) Overexpression of SodA from plasmid reduces NBT signal. WT was transformed either with pACYC184 or pAQ6. Cultures were grown in TB, TB-Brij and TB-Ole. ROS levels were determined by NBT assay. Data were normalized to the ROS level of WT transformed with pACYC184 in TB medium and represent average (± S.D.) of 3 independent experiments. (F) Fold-increase in ROS levels in TB-Ole compared to TB-Brij as determined by DHE assay is similar to that observed by NBT assay. WT was grown either in TB-Brij or TB-Ole. ROS levels were determined. Data were normalized to the ROS level of WT in TB-Brij and represent average (± S.D.) of 3 independent experiments.

3.2.2. LCFA metabolism is the reason for high levels of ROS in *E. coli* cultured in oleate

In order to investigate the reason for LCFA-mediated oxidative stress, we sought to analyze each individual step involved in the transport and β-oxidation of LCFAs. We thus determined ROS levels in *fad* deletion strains defective in LCFA transport and degradation.

3.2.2.1 Verification of *fad* deletion strains obtained from the Keio deletion library

We obtained *fad* deletion strains from the Keio deletion library, which is a collection of single-gene knockouts of all non-essential genes (~4000) in *E. coli*, and each

deletion strain has two independent clones (Baba et al., 2006). Before measuring ROS levels in various *fad* strains, we first verified each *fad* deletion strain by colony PCR using four sets of primers (Fig. 3.3A). A representative gel image for the PCR verification of Δ*fadB* strain is shown in Fig. 3.3B. We further confirmed the known growth phenotypes of *fad* deletion strains on minimal medium containing oleate as the sole carbon source (Campbell and Cronan, 2002; Campbell et al., 2003; Nunn and Simons, 1978). As expected, whereas all *fad* knockouts exhibited normal growth in minimal medium supplemented with glucose, none of the deletion strains showed growth in minimal medium supplemented with oleate (Fig. 3.3C). Collectively, our above results verified *fad* deletion strains from the library. For all follow-up experiments either both independent clones from the library and/or fresh transductants were analyzed to rule out genetic errors.

(A)

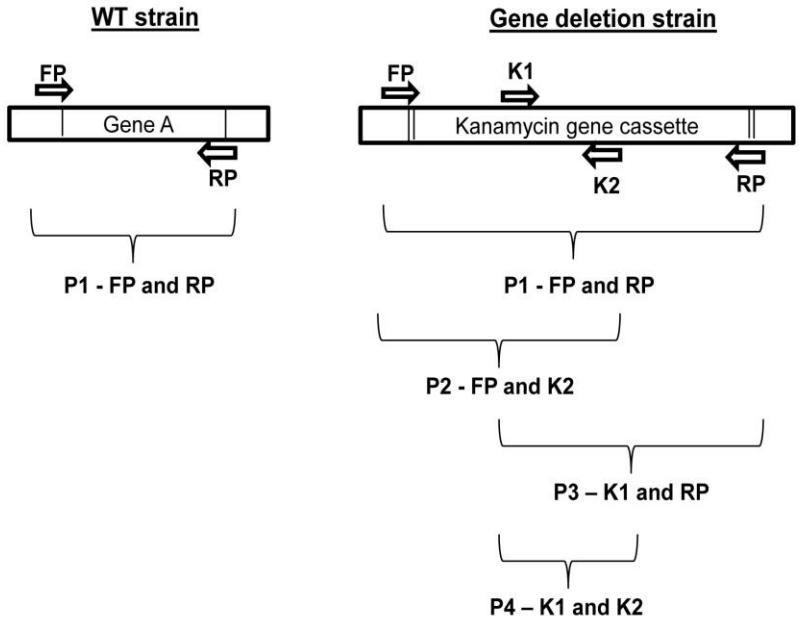
WT strain
Gene deletion strain
FP
Gene A
RP
FP
K1
Kanamycin gene cassette
K2
RP
P1 - FP and RP
P1 - FP and RP
P2 - FP and K2
P3 – K1 and RP
P4 – K1 and K2

(B)

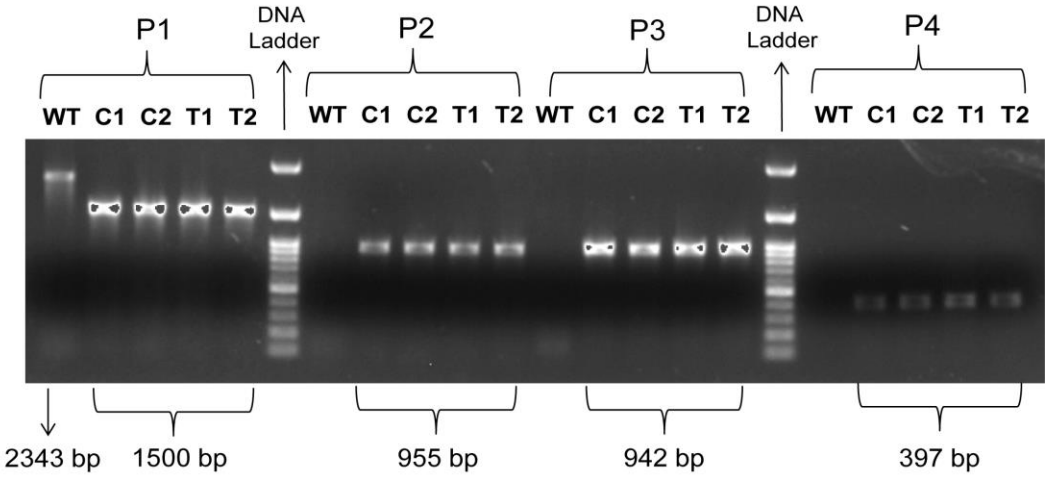
P1
DNA Ladder
P2
P3
DNA Ladder
P4
WT C1 C2 T1 T2
WT C1 C2 T1 T2
WT C1 C2 T1 T2
WT C1 C2 T1 T2
2343 bp
1500 bp
955 bp
942 bp
397 bp

(C)

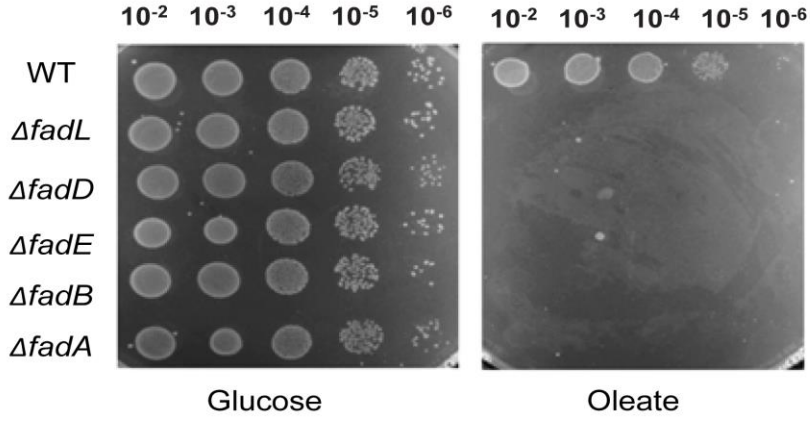
10-2 10-3 10-4 10-5 10-6
10-2 10-3 10-4 10-5 10-6
WT
ΔfadL
ΔfadD
ΔfadE
ΔfadB
ΔfadA
Glucose
Oleate

Figure 3.3 Verification of *fad* deletion strains. (A) A diagrammatic representation of four primer sets (P1 to P4), used to confirm the insertion of kanamycin gene cassette, replacing the gene of interest from WT. FP: Forward primer and RP: Reverse primer (gene specific primers); K1 and K2: kanamycin cassette specific primers. (B) *fad* deletion strains were verified by PCR and a representative gel image for PCR verification of *fadB*::*kan* strain is shown. Both parents (C1 and C2) and transductants (T1 and T2) were verified by four sets of primers P1 to P4. Requisite bands were obtained in each lane. (C) Dilutions of the cultures of various *fad* deletion strains were spotted on minimal medium containing either glucose or oleate as a carbon source. Minimal medium with glucose also had Brij-58.

3.2.2.2 Transport and β-oxidation of exogenously supplied LCFAs accounts for high levels of ROS in *E. coli*

Exogenous LCFAs are transported inside the cell by an outer-membrane protein, FadL. Subsequently, the inner-membrane associated acyl-CoA synthetase, FadD, extracts LCFAs from the inner-membrane concomitant with esterification to acyl-CoA (Fig. 3.4A). Acyl-CoA is oxidized to 2-enoyl-CoA by the fatty acyl-CoA dehydrogenase, FadE. 2-enoyl-CoA is further converted to 3-oxoacyl-CoA by enoyl-CoA hydratase/3-hydroxyacyl-CoA dehydrogenase, FadB and finally 3-oxoacyl-CoA is cleaved to acetyl-CoA by the 3-ketoacyl-CoA thiolase, FadA (Clark and Cronan, 2005). Whereas LCFAs are not at all transported inside the cell in *fadL* and *fadD* mutants, *fadE*, *fadB*, and *fadA* mutants are able to transport LCFAs at reduced rates but are defective in β-oxidation (Klein et al., 1971). We, therefore, suggested that determining ROS levels in *fad* deletion strains would help us to determine whether LCFA transport and degradation is the reason for LCFA-induced oxidative stress.

ROS levels in *fad* knockouts were measured by NBT assay. In comparison to WT, where ROS levels increased by ~1.6 fold in the presence of oleate, Δ*fadL* strain exhibited similar ROS levels in both TB and TB-Ole. Further, ROS levels did not show a considerable increase in Δ*fadD* strain in TB-Ole compared to TB medium

(Fig. 3.4B). Collectively, data from Δ*fadL* and Δ*fadD* strains clearly validate that LCFA transport inside the cell is required for elevated ROS levels in the presence of oleate. An additional observation from Δ*fadD* strain was that ROS levels were higher even in TB basal medium. We suggest that since in addition to degradation of exogenous LCFAs, FadD is also required for utilization of endogenous fatty acids released from membrane lipids (Pech-Canul et al., 2011), therefore in a Δ*fadD* strain accumulation of intracellular free fatty acids is the reason for higher ROS levels. Our result that Δ*fadD* grown in TB medium has increased ROS levels is consistent with the proposal that accumulation of fatty acids can cause oxidative stress in bacteria (Pradenas et al., 2012).

A Δ*fadE* strain, which is defective in β-oxidation but can still transport LCFAs although at a reduced rate (Klein et al., 1971) did not exhibit a considerable increase in ROS levels in TB-Ole in comparison to TB medium. This result suggests that transport and subsequent degradation of oleate is the reason for LCFA-induced oxidative stress. Surprisingly, unlike Δ*fadE* the deletion of either *fadB* or *fadA* showed nearly WT ROS levels, i.e. ~1.6 fold increase in ROS levels in the presence of oleate compared to TB medium (Fig. 3.4B). Here, it is important to consider that FadJ and FadI are the homologues of FadB and FadA, respectively, that mainly function during anaerobic β-oxidation; however, these enzymes also work sub-optimally under aerobic conditions (Campbell et al., 2003). We speculated that in Δ*fadB* and Δ*fadA* strains the increase in ROS levels in TB-Ole is due to the suboptimal activity of FadJ and FadI. To investigate this proposal, we measured ROS levels in strains deleted for both the aerobic and anaerobic forms of enzymes, i.e., Δ*fadB*Δ*fadJ* and Δ*fadA*Δ*fadI* strains. As expected, Δ*fadJ* and Δ*fadI* strains showed ROS levels similar to WT due to

the enzymatic activity of FadB and FadA. Importantly, the double mutants Δ*fadB*Δ*fadJ* and Δ*fadA*Δ*fadI* exhibited no increase in ROS levels in the presence of oleate compared to TB medium (Fig. 3.4C). Collectively, the above data clearly establish that LCFA transport and degradation is the reason for elevated levels of ROS in the presence of oleate.

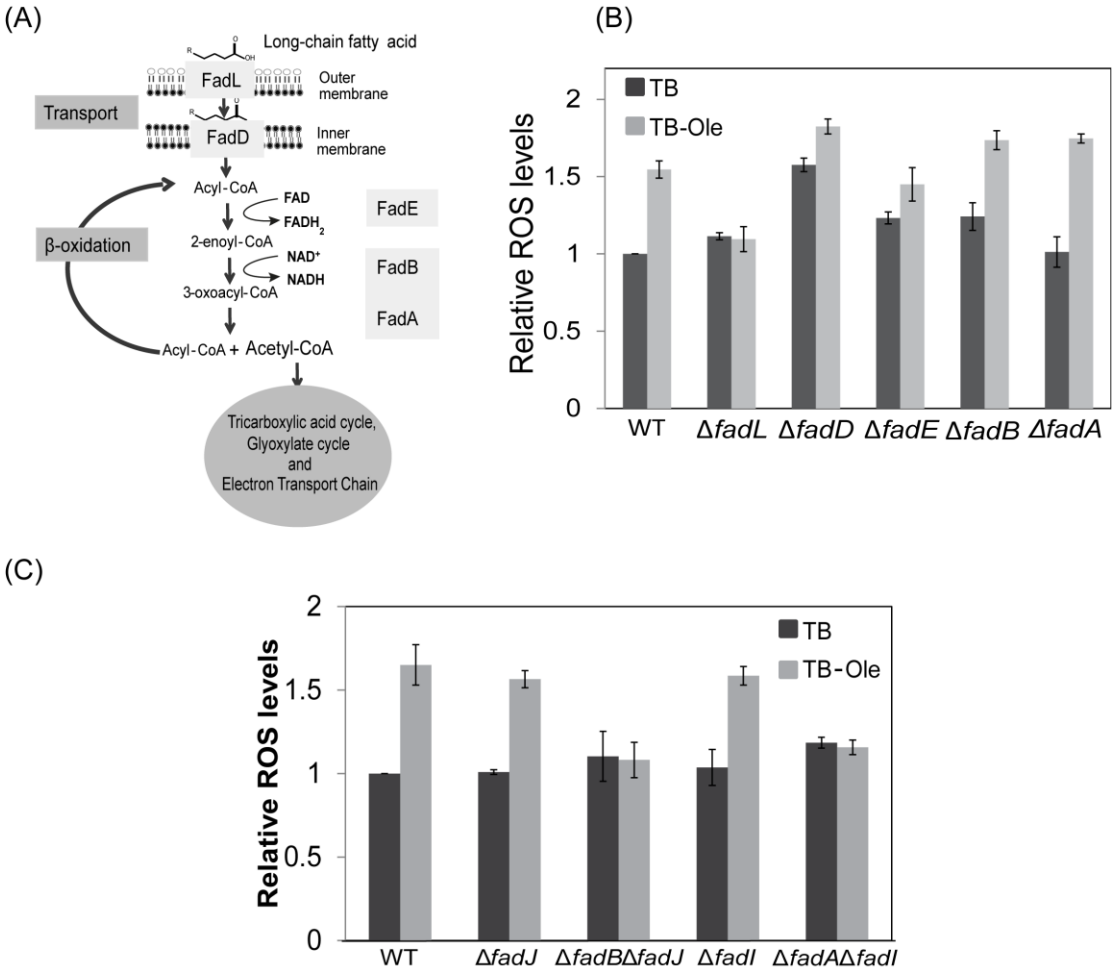

Figure 3.4 ROS levels do not increase in strains defective in LCFA uptake and degradation. (A) A schematic of the LCFA degradation pathway is shown. Exogenous LCFAs are transported inside the cell by an outer-membrane protein, FadL. The inner-membrane associated fatty acyl-CoA synthetase, FadD, extracts LCFAs from the inner-membrane concomitant with esterification to acyl-CoA. Acyl-CoA is oxidized to 2-enoyl-CoA by the fatty acyl-CoA dehydrogenase, FadE, generating one molecule of $FADH_2$. Further, 2-enoyl-CoA is converted to 3-oxoacyl-CoA by FadB, generating one molecule of

NADH. Finally, 3-oxoacyl-CoA is cleaved to acetyl-CoA by a 3-ketoacyl-CoA thiolase, FadA. Acetyl-CoA is further degraded by TCA and glyoxylate cycles. The reduced cofactors produced during β-oxidation and TCA cycle are oxidized in the ETC for generation of energy. (B) WT and various *fad* deletion strains were grown either in TB or TB-Ole. ROS levels were determined by NBT assay. Data were normalized to the ROS level of WT in TB and represent average (± S.D.) of 3 independent experiments. (C) ROS levels were measured in single and double mutants of various *fad* genes. WT and various *fad* deletion strains (Δ*fadJ*, Δ*fadB*Δ*fadJ*, Δ*fadI* and Δ*fadA*Δ*fadI*) were grown either in TB or TB-Ole, and ROS levels were determined by NBT assay. Data were normalized to the ROS level of WT in TB and represent average (± S.D.) of 3 independent experiments.

3.2.3 Increased production of reduced cofactors during LCFA metabolism likely contributes to elevated levels of ROS

Several mechanisms have been proposed to explain the formation of ROS during metabolism, such as extraction of electrons from reduced metal centers of dehydrogenases by molecular O_2, leakage of electrons during oxidation-reduction cycles of ETC promoting the reaction of free electrons with O_2, and auto-oxidation of flavoproteins (Imlay, 2003). The probability of above-mentioned events favoring intervention of O_2 with electrons would logically be higher in cells that produce a large number of reduced cofactors, i.e. high NADH/NAD^+ and $FADH_2$/FAD ratios, thereby generating high levels of ROS. Based on the metabolic pathway of LCFAs, a large number of reduced cofactors are expected to generate during LCFA degradation; however, there is no experimental evidence for the same in *E. coli.* Thus we investigated whether a large amount of reduced cofactors are indeed generated during LCFA metabolism that increases electron flow in the ETC favoring high ROS formation. Because fatty acids of varying carbon chain length are expected to produce different amount of reduced cofactors, we first determined whether ROS levels correlate with the chain length of fatty acids. Next, we directly measured intracellular

$NADH/NAD^+$ ratio in cells utilizing LCFAs. Finally, to assess whether there is an increase in electron flow in the ETC during LCFA metabolism we measured the activity of ETC complex I and complex II.

3.2.3.1 ROS levels directly correlate with the carbon chain length of fatty acids

In each round of β-oxidation, one molecule of $FADH_2$ and NADH are produced, and two carbon atoms are released as acetyl-CoA (Fig. 3.4A). Reduced cofactors are further generated by the metabolism of acetyl-CoA in the TCA cycle. For complete degradation of one molecule of LCFA, β-oxidation and TCA cycle runs multiple times, therefore, amount of reduced cofactors produced would vary with the chain length of fatty acids (Fig. 3.5A). We argued that if reduced cofactors are the reason for high ROS levels generated by fatty acid metabolism, then ROS levels should increase with an increase in the chain length of fatty acids. We determined ROS levels in WT cells grown in TB supplemented with either, a short-chain fatty acid, acetate (2C); or long-chain fatty acids, laurate (12C); or oleate (18C). *E. coli* K12 does not utilize butyrate (4C) and medium-chain fatty acids (5C to 10C), and hence these fatty acids could not be compared. As expected, ROS levels were highest in TB-Ole followed by TB-Lau; acetate utilization did not result in increase in ROS level over the level observed with TB alone, or TB supplemented with glucose (TB-Glu). Hence with increase in the chain length of fatty acids ROS levels increase in the order: TB-Ole >TB-Lau >TB-Ace (Fig. 3.5B).

A previous study has reported that monounsaturated fatty acids are prone to oxidative attack at the double bond resulting in the generation of peroxyl radicals (Pradenas et al., 2012). Therefore we tested if the highest level of ROS in TB-Ole is because oleate is a monounsaturated fatty acid. We compared ROS levels between *E.*

coli grown in TB-Ole and bacteria grown in TB containing stearate (TB-Ste), a saturated C18 LCFA. ROS levels were comparable in TB-Ole and TB-Ste (Fig. 3.5B) indicating that high ROS level in TB-Ole is not due to the unsaturated nature of oleate. Taken together, these results suggest that reduced cofactors generated by LCFA degradation are the reason for increased ROS formation during growth of *E. coli* in LCFAs.

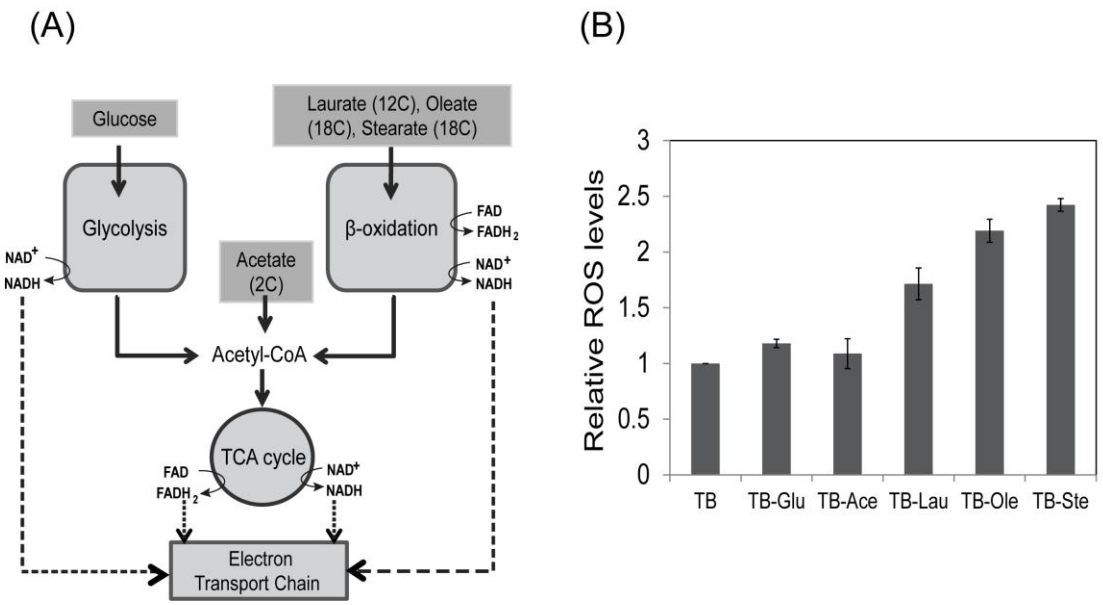

Figure 3.5 ROS levels increase with an increase in the chain length of fatty acids. (A) A schematic of the metabolic route of LCFAs, acetate (2C) and glucose is shown. LCFAs, such as oleate (18C), stearate (18C), and laurate (12C) are degraded by β-oxidation. The end product of β-oxidation, acetyl-CoA enters TCA cycle for further degradation. Acetate is converted to acetyl-CoA which is catabolized by TCA cycle. Glucose is primarily catabolized by glycolysis followed by TCA cycle. The reduced cofactors produced through β-oxidation, glycolysis and TCA cycle are fed to ETC for energy generation. (B) WT was grown either in TB or TB supplemented with one of the indicated carbon sources: glucose (TB-Glu), acetate (TB-Ace), laurate (TB-Lau), oleate (TB-Ole) or stearate (TB-Ste). ROS levels were determined by NBT assay. Data were normalized to the ROS level of WT in TB and represent average (± S.D.) of 3 independent experiments.

3.2.3.2 NADH/NAD$^+$ ratio increases in LCFA-utilizing cells

We next determined whether reduced cofactors increase in LCFA-utilizing cells. For this, we measured the intracellular concentration of NADH and NAD$^+$ by a colorimetric assay (Sigma). Fig. 3.6A shows the NADH standard curve used for quantification of intracellular levels of NAD$^+$ and NADH. We observed ~2.5-fold increase in NADH in TB-Ole compared to TB-Brij (Fig. 3.6B); however, there was no significant change in NAD$^+$ levels (Fig. 3.6C). Overall, this resulted in ~2.5 fold higher NADH/NAD$^+$ ratio in TB-Ole compared to TB-Brij (Fig. 3.6D). Compared to WT, in the *fadL* knockout, both NADH and NAD$^+$ levels were similar in TB-Brij and TB-Ole (Figs. 3.6, B and C). This result clearly shows that the amount of reduced cofactors significantly increases during LCFA metabolism.

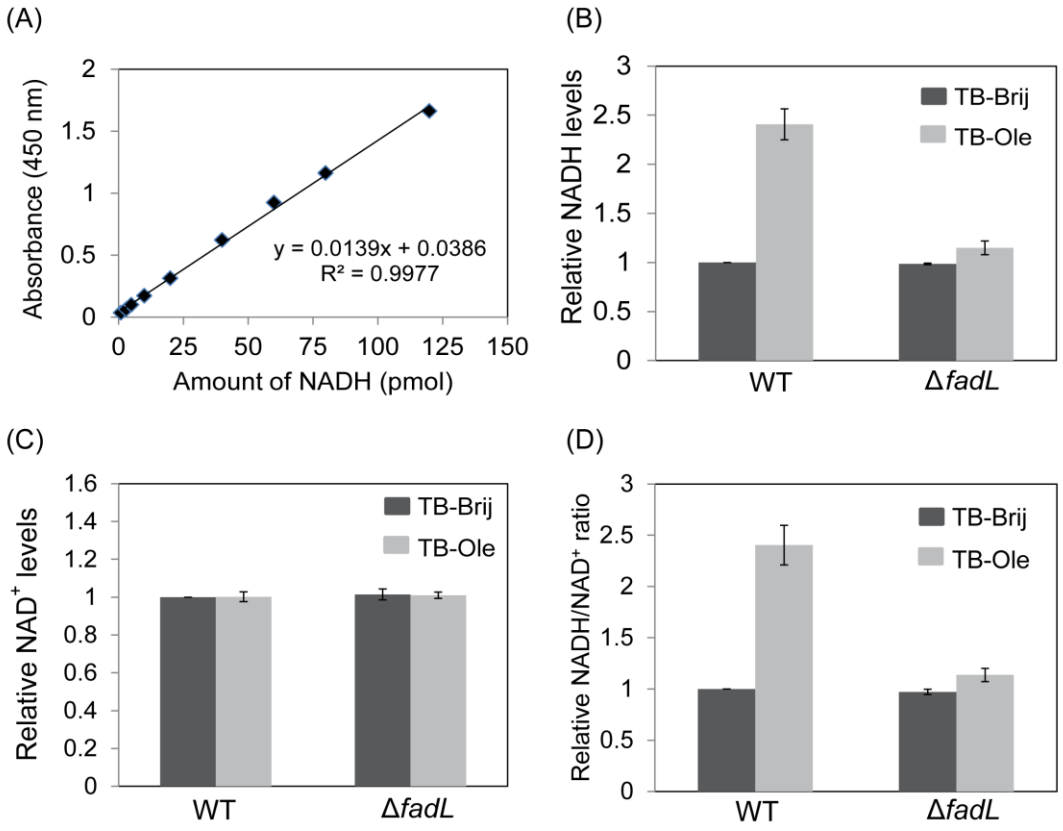

Figure 3.6 NADH/NAD^+ ratio increases significantly during LCFA metabolism. (A) A standard curve for NADH based on colorimetric detection (Sigma). Absorbance at 450 nm increases linearly with increasing amount of NADH. (B to D) WT and Δ*fadL* strains were grown either in TB-Brij or TB-Ole. The amount of NADH (B) and NAD^+ (C), and NADH/NAD^+ ratio (D) was determined. Data were normalized to WT in TB-Brij and represent average (± S.D.) of 3 independent experiments.

3.2.3.3 The activity of ETC complex I and complex II increases in LCFA metabolizing cells

We observed that cells metabolizing LCFAs generate a large amount of reduced cofactors. Next, we wanted to determine whether the increased amount of reduced cofactors results in an increase in electron flow in the ETC. Therefore, we measured the enzyme activities of ETC complex I and ETC complex II in extracts prepared from cells grown in TB and TB-Ole. During aerobic respiration, ETC complex I (NADH dehydrogenase) and ETC complex II (succinate dehydrogenase) oxidize NADH and $FADH_2$, respectively, and transfer electrons to ubiquinone. *nuoK* and *sdhB* code for a subunit of NADH dehydrogenase (Erhardt et al., 2012) and succinate dehydrogenase, (Cheng et al., 2006), respectively. Hence Δ*nuoK* and Δ*sdhB* strains were used as controls in the assay for complex I and complex II, respectively. The activity of complex I was quantified by measuring the rate of NADH decay at 340 nm; the linear range of detection of NADH was estimated by monitoring the absorbance of varying amounts of NADH (Fig. 3.7A). In WT cells, the activity of complex I increased by ~1.4 fold in the presence of oleate (Figs. 3.7, B and C). The activity of complex II was quantified by measuring the rate of 2,6-dichlorophenolindophenol (DCIP) reduction. Complex II oxidizes $FADH_2$ and transfers electrons to DCIP which is a blue colored artificial electron acceptor that gets converted to colorless compound upon reduction. Hence the activity of complex

II can be quantified by measuring the rate of decay of DCIP absorbance at 600 nm. The linear range of detection of DCIP was estimated by monitoring the absorbance with varying amounts of DCIP (Fig. 3.8A). Similar to complex I, the activity of complex II increased ~1.5 fold in the presence of oleate (Figs. 3.8, B and C). Increase in the activity of respiratory complexes was dependent on oleate transport inside the cells since the increase in activity of both complex I and complex II was abolished in a Δ*fadL* strain (Figs. 3.7, B and D; Figs. 3.8, B and D). As expected, complex I and complex II activity was significantly decreased in Δ*nuoK* and Δ*sdhB* strains, respectively (Fig. 3.7B and Fig. 3.8B). Brij-58 did not interfere with the assays (Fig. 3.7B inset, Fig. 3.8B inset). Altogether, increase in activity of complex I and complex II in LCFA metabolizing cells shows that there is an increase in electron flow in the ETC due to a large amount of reduced cofactors generated by LCFA degradation.

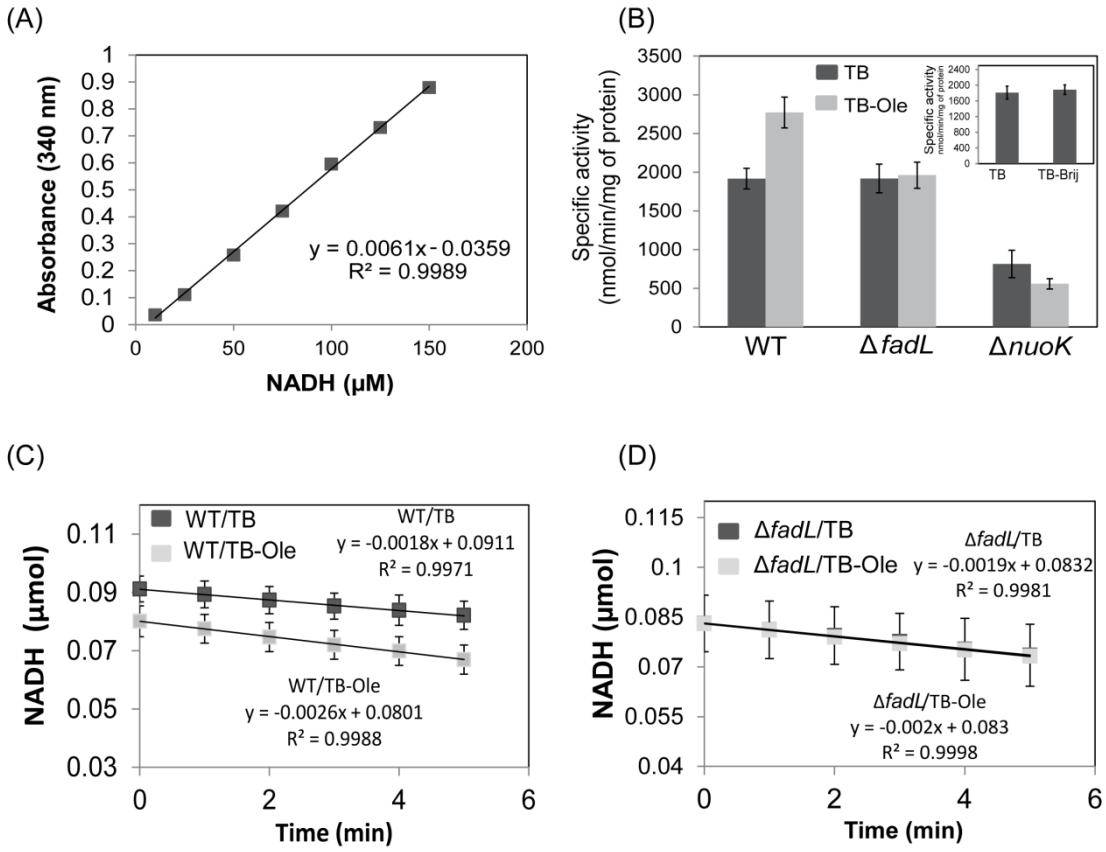

Figure 3.7 Activity of respiratory complex I increase in cells utilizing LCFAs. (A) Curve showing linear range detection of NADH. (B) WT, Δ*fadL* and Δ*nuoK* strains were grown either in TB or TB-Ole and complex I activity was measured. Data represent average (± S.D.) of 3 independent experiments. (Inset) Brij-58 does not interfere with complex I assay. Complex I activity was measured in WT grown in TB and TB-Brij. Data represent average (± S.D.) of 3 independent experiments. (C) and (D) NADH decay rate for WT (C) and Δ*fadL* (D) in TB and TB-Ole was plotted. Data represent average (± S.D.) of 3 independent experiments.

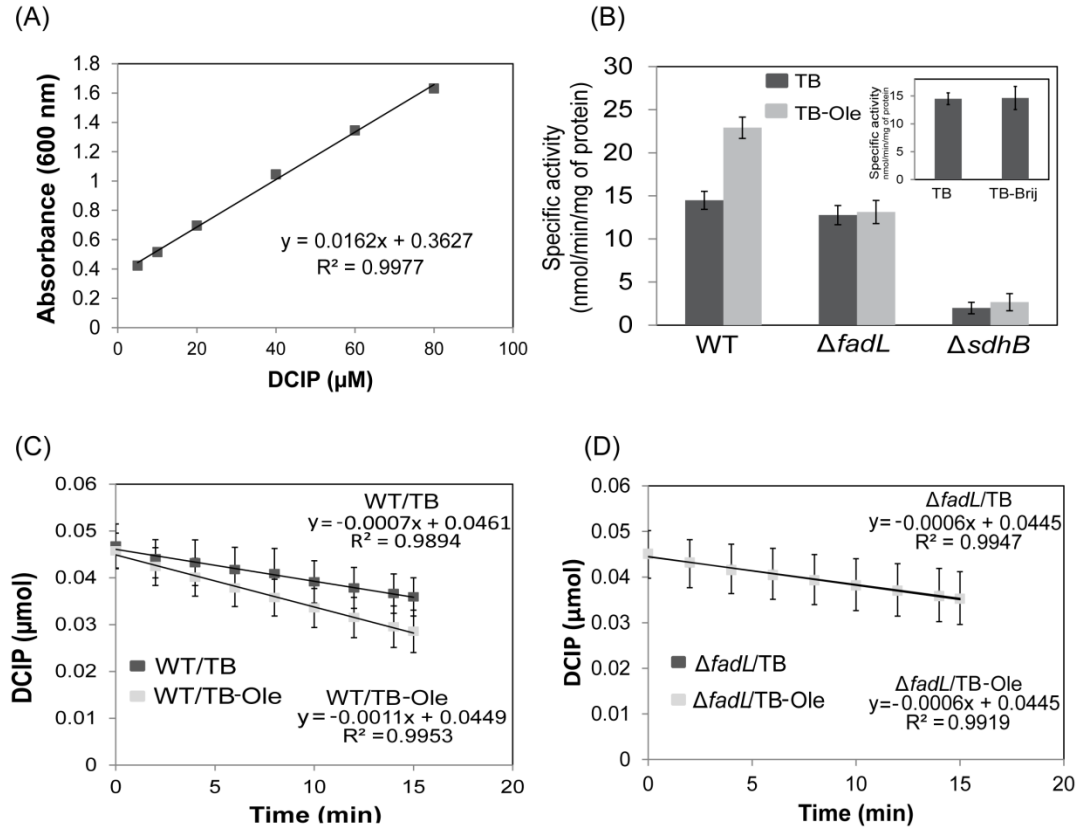

Figure 3.8 Activity of respiratory complex II increases in cells utilizing LCFAs. (A) Curve showing linear range detection of DCIP. (B) WT, Δ*fadL* and Δ*sdhB* strains were grown either in TB or TB-Ole and complex II activity was measured. Data represent average (± S.D.) of 3 independent experiments. (Inset) Brij-58 does not interfere with complex II assay. Complex II activity was measured in WT grown in TB and TB-Brij. Data represent average (± S.D.) of 3 independent experiments. (C) and (D) Rate of DCIP reduction for WT (C) and Δ*fadL* (D) in TB and TB-Ole was plotted. Data represent average (± S.D.) of 3 independent experiments.

3.2.4. LCFA utilization results in increased lipid peroxidation

ROS is a byproduct of metabolism and participates in various signaling cascades and physiological processes (Cap et al., 2012). However, a significant increase in ROS levels can oxidize biomolecules such as lipids, proteins and DNA (Imlay, 2003). We investigated whether the increase in ROS levels during LCFA metabolism results in increased oxidation of biomolecules. For this, we observed the extent of lipid peroxidation in oleate utilizing cells. During lipid peroxidation, fatty acid component of lipids in cellular membrane is attacked by free radicals and converted to lipid peroxides and other reactive aldehydes such as malondialdehyde (MDA); MDA thus acts as a bioactive marker for lipid peroxidation. We measured MDA levels by thiobarbituric acid responsive substances (TBARS) assay (Yoon et al., 2002). MDA levels increased by ~2 fold in WT cells cultured in TB-Ole compared to TB medium. Brij-58 did not interfere with the assay; the MDA levels in TB and TB-Brij were similar. In contrast to WT, in *fadL* knockout, MDA levels were comparable in both TB and TB-Ole medium (Fig. 3.9). This result clearly shows the harmful effect of LCFA-induced oxidative stress on cellular biomolecules in *E. coli*.

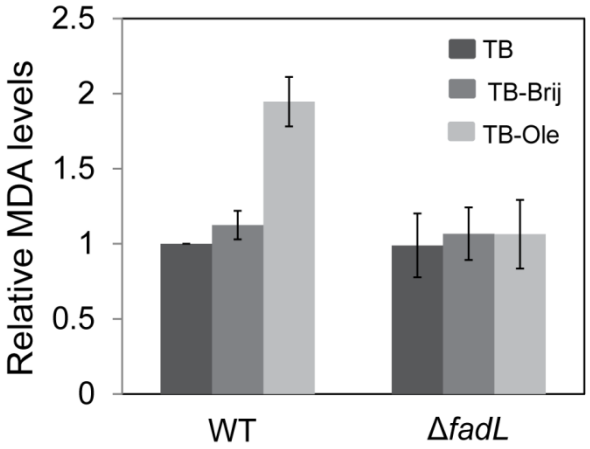

Figure 3.9 Thiobarbituric acid responsive substance (TBARS) measures oxidative damage in LCFA-utilizing cells. MDA acts as a bioactive marker for lipid peroxidation. WT

and Δ*fadL* strains were grown in TB, TB-Brij and TB-Ole. MDA levels were determined by TBARS assay. Data were normalized to the MDA level of WT in TB and represent average (± S.D.) of 3 independent experiments.

3.3 Discussion

Recent studies have indicated the connection between LCFAs and redox stress, where bacterial cells grown in the presence of LCFAs either showed significant overexpression of genes that are involved in maintaining redox balance (Rodriguez et al., 2014), or generated high levels of ROS (Doi et al., 2014). To explain the correlation between fatty acids and ROS, various mechanisms have been suggested such as generation of lipid peroxides and peroxyl radicals by oxidative attack on fatty acids, β-oxidation of fatty acids, and stress due to fatty acid incorporation in the membrane (Doi et al., 2014; Pradenas et al., 2012; Schonfeld and Wojtczak, 2008). We investigated the reason for oxidative stress in *E. coli* cultured in LCFAs. To address this, we used several *fad* knockouts defective in LCFA transport and degradation. Because *fad* deletion strains do not grow in minimal medium supplemented with LCFAs as a sole carbon source, we performed experiments in TB medium supplemented with LCFAs. We observed an increase in biomass and transcript levels of *fadL* and *fadE* in WT grown in TB-Ole medium that confirmed the co-utilization of oleate with TB (Fig. 3.1). We used NBT assay to determine intracellular superoxide levels and observed increase in ROS levels in *E. coli* grown in oleate compared to bacteria grown in basal medium (Fig. 3.2C). We validated our results from NBT assay by using a fluorescent dye, DHE that also detects superoxide (Fig. 3.2F). Our results that *fad* deletion strains defective in LCFA metabolism do not exhibit an increase in ROS convincingly established that LCFA transport and degradation is the reason for oxidative stress in cells grown in this carbon source (Fig.

3.4). The biological significance of elevated ROS levels in LCFA-utilizing cells was evident from the increase MDA levels, a by-product of lipid peroxidation and a hallmark of oxidative damage (Fig. 3.9).

ROS is a by-product of aerobic metabolism. The reduced cofactors, NADH and $FADH_2$ generated during metabolism are oxidized by respiratory dehydrogenases enabling electron flow in the ETC. Concomitantly, ROS is formed by extraction of electrons from reduced metal centers of dehydrogenases by molecular O_2, leakage of electrons during oxidation-reduction cycles of ETC or auto-oxidation of flavoproteins (Imlay, 2003). We suggested that high $NADH/NAD^+$ and $FADH_2$/FAD ratios attained during LCFA degradation would increase electron flow in the ETC thereby increasing the probability of ROS formation through the above-mentioned events. Our results that ROS levels directly correlate with the chain length of fatty acids (Fig. 3.5), higher $NADH/NAD^+$ ratio in LCFA-utilizing cells (Fig. 3.6), and increased enzyme activities of ETC complex I and II in cells cultured in oleate (Figs. 3.7 and 3.8), collectively support the above proposal.

Importantly, a predominant source of ROS during LCFA degradation could be the acyl-CoA dehydrogenase, FadE, which catalyzes the oxidation of acyl-CoA to enoyl-CoA concomitant with the reduction of FAD to $FADH_2$ (Campbell and Cronan, 2002). Because the step catalyzed by FadE would result in a high $FADH_2$/FAD ratio and auto-oxidation of flavins is suggested to be a source of ROS, it is important to investigate whether FadE is a major site of ROS during growth in LCFAs. FadE has not been biochemically characterized till date; it has been considered to be the acyl-CoA dehydrogenase in *E. coli* based on genetic studies and the presence of characteristic sequence motifs (Campbell and Cronan, 2002). Additionally, whether FadE re-oxidizes $FADH_2$ and directly transfers electrons to ubiquinone or requires

electron transfer flavoprotein (ETF) is also unclear. Therefore, detailed studies would be required to investigate the contribution of FadE to ROS formation. Experiments such as measuring ROS levels, dehydrogenase activity of FadE and re-oxidation of $FADH_2$ by FadE or ETF would have to be conducted in parallel in *fad* mutants, blocked in steps downstream of FadE. Our work described in this chapter provides an important basis to address these issues in future studies.

CHAPTER IV

Ubiquinone is a key antioxidant during long-chain fatty acid metabolism in *E. coli*

4.1 Introduction

In the previous chapter, we established that long-chain fatty acid (LCFA) transport and degradation in *Escherichia coli* results in elevated levels of reactive oxygen species (ROS). However, despite their ability to cause oxidative stress, *E. coli* and several other important pathogens utilize LCFAs derived from host tissues that contribute to their survival and virulence (Fang et al., 2005; McKinney et al., 2000; Son et al., 2007). This suggests that bacteria must have strategies to mitigate LCFA-induced oxidative stress. In this chapter, we investigated the players employed by *E. coli* to counteract oxidative stress during LCFA metabolism. *E. coli* harbors various oxidative stress combat players that include transcriptional regulators, OxyR, SoxRS and RpoS, which govern the expression of >100 oxidative stress response genes including ROS scavenging enzymes, such as superoxide dismutases (SOD) and peroxidases (catalase and alkyl hydroperoxide reductase) to combat the damaging effects of ROS [reviewed in (Chiang and Schellhorn, 2012; Imlay, 2013)]. SOD converts superoxide to hydrogen peroxide (H_2O_2), which is further detoxified to oxygen and water by peroxidases. Catalases (Kat) and alkyl hydroperoxide reductase (Ahp) are H_2O_2 scavengers in *E. coli*. Importantly, these enzymatic players are redundant, for e.g., there are two catalases in *E. coli*, catalase I (KatG) and catalase II (KatE) (Loewen and Switala, 1986). Similarly, there are three SOD isozymes MnSOD, FeSOD and CuZnSOD encoded by *sodA, sodB* and *sodC,* respectively, which differ in their requirement of metal cofactors (Benov and Fridovich, 1994). In addition to enzymatic defenses, *E. coli* also uses non-enzymatic antioxidants, such as glutathione and ubiquinone (Farr and Kogoma, 1991; Soballe and Poole, 2000). Glutathione (GSH) or L-γ-glutamyl-L-cysteinylglycine, is a tripeptide non-protein thiol molecule which is synthesized in two steps through γ-glutamylcysteine

synthetase and glutathione synthetase encoded by *gshA* and *gshB* genes, respectively (Carmel-Harel and Storz, 2000). GSH functions to reduce cellular disulfide bonds and control the redox state of cysteine residues in various proteins. Ubiquinone is a lipid-soluble electron carrier in the electron transport chain (ETC) and has also been suggested to be an antioxidant in *E. coli*. An earlier study showed that a *ubiCA* knockout which produces no detectable ubiquinone exhibits several oxidative stress phenotypes in LB: accumulation of superoxide and H_2O_2 in membranes, hypersensitivity to oxidative stress inducing agents, and upregulation of catalases (Soballe and Poole, 2000). However, what is the physiological condition under which ubiquinone plays a predominant role as an antioxidant, how ubiquinone counteracts ROS and what is the relative contribution of ubiquinone to the overall oxidative stress response remains to be assessed.

To investigate players involved in counteracting oxidative stress during LCFA metabolism, we referred to the data obtained from a high-throughput genetic screen of the *E. coli* gene deletion library (Keio deletion library) on the LCFA, oleate. The genetic screen revealed that amongst various oxidative stress combat players, genes involved in the biosynthesis of ubiquinone, are highly required for growth on LCFAs. Our detailed genetic and biochemical experiments showed that the increased requirement of ubiquinone for growth on oleate is to counter elevated levels of ROS generated by LCFA degradation. Moreover, we find that amongst various oxidative stress combat players in *E. coli*, ubiquinone is the major antioxidant and acts as the cell's first line of defense against LCFA-induced oxidative stress. Importantly, we showed that ubiquinone accumulates in cells grown in LCFAs and degradation of LCFAs provides the signal for upregulation of ubiquinone. Taken together, our results emphasize that ubiquinone is a key antioxidant during LCFA metabolism and

therefore provides a rationale for investigating its role in LCFA-utilizing pathogenic bacteria.

4.2 Results

4.2.1 High-throughput genetic screen reveals that ubiquinone biosynthesis genes are highly required for growth of *E. coli* in oleate

A high-throughput genetic screen was performed by Dr. Rachna Chaba to test the ability of 3994 gene deletion strains from the Keio deletion library to grow on oleate as the sole carbon source. The requirement of various oxidative stress response players for growth on oleate was assessed by analyzing data from the genetic screen.

4.2.1.1 Screening mutants from Keio deletion library for growth on oleate

The genetic screen was performed to identify genes required for successful growth of *E. coli* on oleate. For this, the Keio deletion library containing 3994 mutants was pinned on M9 minimal agar plates containing oleate as the sole carbon source (Fig. 4.1A). As a control, the library was also pinned on M9 minimal agar plates containing glucose as carbon source. Since oleate was solubilized in the detergent Brij-58, the minimal medium containing glucose was also supplemented with Brij-58. Plates were incubated at 37ºC and the images of the plates were captured at a single time point, chosen such that growth had not saturated and the fitness differences were apparent. The colony size was quantified using image analysis software (Collins et al., 2006). Fitness-score was assigned to the strains in the oleate condition by calculating the statistical significance of the difference in colony size between oleate and the glucose control (in collaboration with Dr. Anthony L. Shiver). The fitness-scores thus reported represent the statistical significance of a change in colony size on oleate as compared

to growth on glucose with positive and negative fitness-scores representing increased and decreased colony size, respectively. A full list of fitness scores of Keio library strains in oleate (normalized to a glucose control) is available in Appendix 1. Here, the mutants are ranked according to their fitness scores. Mutants ranked at the top in the LCFA dataset are those with negative fitness scores indicating the severe requirement of the gene for growth in oleate. In contrast, the mutants ranked at the bottom in the LCFA dataset are those with positive fitness scores indicating growth advantage, where deleting a gene results in better growth of cells in oleate.

The screen was setup in triplicate and each replicate had two independent clones of each strain. The reproducibility of the colony size measurements from the replicates was checked by determining the Pearson's correlation coefficient. Fig. 4.1B depicts the scatter plot for colony size obtained from the replicates. The plot is linear with a Pearson's coefficient of 0.86 (R-value) which depicts highly reproducible data from the replicates.

(A) (B)

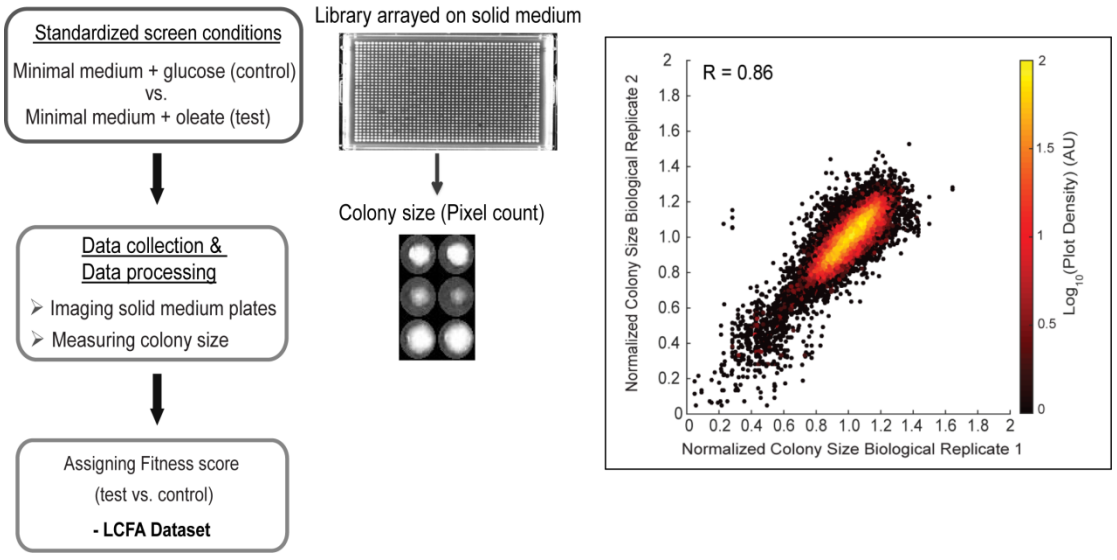

Figure 4.1 Screening Keio deletion library on oleate and data processing. (A) Strains from Keio deletion library were arrayed in 1536-format on minimal medium plates containing either oleate (test) or glucose with Brij-58 (control) as carbon source. Plates were incubated and imaged at appropriate time point. Colony size was determined by using image analysis software. On the basis of colony size, fitness score was assigned to each strain. (B) Colony sizes of individual mutants are normalized to the plate average and replicates (n > 3) are plotted for the two conditions tested: oleate and glucose with Brij-58. Points are colored by the logarithm of local density in the plot. Normalized colony sizes from replicates are highly correlated (R = 0.86, Pearson's coefficient). The screen was set-up by Dr. Rachna Chaba and the statistical analysis of the data was done in collaboration with Dr. Anthony L. Shiver.

Before performing a detailed analysis of the LCFA dataset to probe players required to mitigate LCFA-induced oxidative stress, we first verified the accuracy of our dataset by ensuring that genes already known to play a role in LCFA metabolism are required for growth on oleate in our screen. Hence, we checked the ranks of *fad* deletion strains in our LCFA dataset because *fad* genes are absolutely required for degradation of LCFAs. Importantly, we found that strains carrying deletion of *fad* genes involved in aerobic β-oxidation i.e., Δ*fadL*, Δ*fadD*, Δ*fadE*, Δ*fadB* and Δ*fadA* were amongst the top 25 candidates in the LCFA dataset (Table 4.1). The phenotype of *fad* strains validates the robustness of our high-throughput genetic screen and our statistical approach to calculate the fitness scores, and emphasizes that our LCFA dataset can serve as a rich source to identify genes involved in LCFA-related pathways.

Strain	Rank
fadL::kan	1
fadE::kan	4
fadA::kan	16
fadB::kan	18
fadD::kan	23

Table 4.1 Positions of various *fad* deletion strains in the LCFA dataset. All *fad* knockouts were present amongst the top 25 candidates in the LCFA dataset. It shows that *fad* genes are highly required for growth in oleate.

4.2.1.2 Genetic screen reveals the pathways used by *E. coli* to metabolize oleate

Oleate, an LCFA, is a non-fermentable carbon source which is degraded to acetyl-CoA by β-oxidation pathway. Acetyl-CoA is further metabolized by tricarboxylic acid (TCA) and glyoxylate cycles that provide cellular metabolites required for growth of cell. Reduced cofactors generated during β-oxidation and TCA cycle are oxidized in the ETC to generate ATP. During growth in oleate, ATP is solely generated by oxidative phosphorylation in the ETC. In contrast to oleate, glucose is a fermentable carbon source which is metabolized by glycolysis to pyruvate. Pyruvate is further converted to acetyl-CoA that finally enters TCA cycle for degradation. During glucose metabolism, ATP is produced through both, substrate-level phosphorylation in glycolysis and oxidative-phosphorylation in ETC (Clark and Cronan, 2005; Cronan and Laporte, 2005; Romeo and Snoep, 2005). To understand the physiological basis of deletion strains that showed growth defect in oleate in comparison to glucose, a global analysis using Gene Set Enrichment Analysis (GSEA) and gold-standard biological pathways (Keseler et al., 2013; Mootha et al., 2003; Subramanian et al., 2005) was performed to find pathways that play a significant role in growth on oleate (in collaboration with Dr. Anthony L. Shiver). Table 4.2 enlists the significantly

enriched pathways during LCFA metabolism. Importantly, global analysis highlighted the β-oxidation pathway (FDR q-value: 1.1%), critical for the utilization of LCFAs as an energy source, as a signature of growth in oleate. In addition, significant enrichment in the TCA and glyoxylate cycles (FDR q-value <5%) was obtained, a result consistent with these pathways being critical for the generation of reduced cofactors and metabolites for growth in oleate. Furthermore, oleate utilization exhibited enrichment in multiple pathways for electron transfer activity (FDR q-value <5%), underscoring the importance of ETC for energy generation during growth in oleate (Table 4.2).

S. No.	NAME (Pathways)	SIZE	NES	NOM p-val	FDR q-val
1.	ADENOSINE RIBONUCLEOTIDES <I>DE NOVO</I> BIOSYNTHESIS	10	-2.1666	0	2.71E-04
2.	NADH TO CYTOCHROME <I>BO</I> OXIDASE ELECTRON TRANSFER I	15	-2.1199	0	2.83E-04
3.	SUPERPATHWAY OF GLYCOLYSIS, PYRUVATE DEHYDROGENASE, TCA, AND GLYOXYLATE BYPASS	40	-2.1241	0	3.24E-04
4.	SUPERPATHWAY OF ADENOSINE NUCLEOTIDES <I>DE NOVO</I> BIOSYNTHESIS II	18	-2.1684	0.00208768	3.61E-04
5.	SUPERPATHWAY OF PURINE NUCLEOTIDES <I>DE NOVO</I> BIOSYNTHESIS II	29	-2.0929	0	3.66E-04
6.	NADH TO TRIMETHYLAMINE <I>N</I>-OXIDE ELECTRON TRANSFER	13	-2.1311	0	3.78E-04
7.	TCA CYCLE I (PROKARYOTIC)	16	-2.1334	0	4.53E-04
8.	NADH TO FUMARATE ELECTRON TRANSFER	15	-2.0843	0	5.37E-04
9.	NADH TO DIMETHYL SULFOXIDE ELECTRON TRANSFER	14	-2.1763	0	5.42E-04
10.	SUPERPATHWAY OF GLYOXYLATE BYPASS AND TCA	20	-2.2165	0	0.00108333
11.	NADH TO CYTOCHROME <I>BD</I> OXIDASE ELECTRON TRANSFER I	14	-2.0328	0	0.00142584
12.	NITRATE REDUCTION VIII (DISSIMILATORY)	17	-1.9966	0	0.00256972
13.	FATTY ACID &BETA;-OXIDATION I	6	-1.896	0	0.01091814
14.	SUCCINATE TO CYTOCHROME <I>BO</I> OXIDASE ELECTRON TRANSFER	7	-1.8866	0.0021645	0.01169031
15.	SUPERPATHWAY OF LIPOPOLYSACCHARIDE BIOSYNTHESIS	19	-1.8734	0.00230415	0.01279964
16.	GLUCONEOGENESIS I	16	-1.8633	0.00431035	0.01290186
17.	GLYOXYLATE CYCLE	5	-1.8511	0	0.0147448
18.	SUPERPATHWAY OF UBIQUINOL-8 BIOSYNTHESIS (PROKARYOTIC)	5	-1.8378	0	0.0167636
19.	UBIQUINOL-8 BIOSYNTHESIS (PROKARYOTIC)	4	-1.7842	0	0.029801
20.	LIPID A-CORE BIOSYNTHESIS	8	-1.734	0.02169197	0.0526685
21	SUCCINATE TO CYTOCHROME <I>BD</I> OXIDASE ELECTRON TRANSFER	6	-1.7145	0.01535088	0.06141216
22.	PANTOTHENATE AND COENZYME A BIOSYNTHESIS I	4	-1.6766	0.00217391	0.08356956

Table 4.2 Gene set enrichment analysis (GSEA) of metabolic pathways in *E. coli* during LCFA metabolism. Statistical significance of the enrichment of pathways in *E. coli* for strains defective in growth on oleate as a carbon source. Name is the pathway name as reported from Ecocyc. Size is the number of genes within this group. The Normalized Enrichment Score (NES) reflects the maximal enrichment of a pathway for defective mutants,

normalized for set size and average enrichment across the dataset. NES is the primary metric for comparing significance between gene sets. The Nominal p-value reflects the statistical significance of a given NES score without multiple hypothesis correction. The False Discovery Rate (FDR) q-value reflects the fraction of gene sets with a given NES score that are expected to be false-positives. Pathways with FDR q-value <10% are listed. The GSEA analysis was performed in collaboration with Dr. Anthony L. Shiver.

4.2.1.3 The requirement of ubiquinone is higher in cells grown in oleate compared to another non-fermentable carbon source, succinate

Our GSEA analysis showed that along with other ETC components, ubiquinone biosynthesis pathway is also enriched during LCFA metabolism (Table 4.2). Biosynthesis of ubiquinone requires eleven *ubi* genes (Aussel et al., 2014b). Of these, knockouts of *ubiA, ubiD* and *ubiJ* are not present in the Keio deletion library (Baba et al., 2006). Additionally, for *ubiB* only the SPA-tagged strain is available in the library. Therefore in the absence of a clean deletion strain it is difficult to interpret the growth requirement of *ubiB* on oleate. Importantly, out of the seven *ubi* deletion strains present in the Keio deletion library, *ubiE, ubiF* and *ubiH* knockouts showed no growth in oleate, and *ubiI* and *ubiX* mutants exhibited growth defect in oleate. These *ubi* deletion strains had significant negative fitness scores and ranked amongst the top 60 candidates in our LCFA dataset (Appendix 1 and Table 4.3). Oleate and succinate are non-fermentable carbon sources, which unlike glucose, a fermentable carbon source, require optimal functioning of ETC (Berger, 1973; Campbell et al., 2003). Traditionally, the increased requirement of ubiquinone for energy generation during growth with succinate compared to glucose has been the rationale for identifying genes involved in ubiquinone biosynthesis (Stroobant et al., 1972; Wu et al., 1993). However, it was surprising that a recent study showed that a *ubiI* deletion strain that produces only 10-15% ubiquinone compared to wild-type (WT) cells exhibited

normal growth in succinate (Hajj Chehade et al., 2013; Pelosi et al., 2016). The growth defect of *ubiI* knockout in oleate suggested that in addition to energy generation through electron carrier function of ubiquinone in ETC, it might have an additional role in oleate. Because ubiquinone has been suggested to be an antioxidant in *E. coli* (Soballe and Poole, 2000), we argued that the higher requirement of ubiquinone in oleate might be to mitigate LCFA-induced oxidative stress. To ascertain the requirement of ubiquinone in comparison to the overall oxidative stress response processes in *E. coli*, in addition to *ubi* deletion strains we also checked the rank of knockouts of other oxidative stress combat players in our LCFA dataset (Table 4.3). Surprisingly, we found that none of the mutants defective in oxidative stress combat players other than *ubi* deletion strains showed significant fitness defects in our screen on oleate. The above results prompted us to investigate the role of ubiquinone in relieving oxidative stress during LCFA metabolism.

S.No.	Strain	Rank (LCFA Dataset)	Fitness Score
1	*ubiF::kan*	8	-10.26617679
2	*ubiH::kan*	9	-9.734733222
3	*ubiE::kan*	11	-9.115755198
4	*ubiI::kan*	32	-3.870561205
5	*ubiX::kan*	57	-2.668101812
6	*ubiG::kan*	N.D.	N.D.
7	*ubiB-SPA*	3342	1.081911962
8	*ubiC::kan*	2701	0.49555802
9	*ubiA::kan*	NA	NA
10	*ubiD::kan*	NA	NA
11	*ubiJ::kan*	NA	NA
12	*sodC::kan*	262	-1.530049407
13	*sodB::kan*	388	-1.276927013
14	*gshA::kan*	626	-0.976178701
15	*oxyR::kan*	724	-0.858656147
16	*ahpF::kan*	751	-0.833439092
17	*katE::kan*	987	-0.631357017
18	*katG::kan*	1019	-0.608962983
19	*soxR::kan*	1048	-0.584468719
20	*ahpC::kan*	1397	-0.332999557
21	*gshB::kan*	1593	-0.198633163
22	*sodA::kan*	2582	0.403063458
23	*oxyS::kan*	2893	0.654399208
24	*soxS::kan*	3082	0.803484881
25	*rpoS::kan*	3905	2.703599014

Table 4.3 Relative positions of deletion strains of various oxidative stress combat players in LCFA dataset. The relative fitness score for oleate compared to glucose control was obtained for strains in the Keio deletion library. Table shows the fitness score of strains deleted individually for oxidative stress combat players. Description of the function of these players is provided in Chapter 1 (Section 1.7.3). Negative and positive fitness scores represent growth defect and growth advantage, respectively, of mutants in oleate compared to glucose control. N.D.: Not determined; NA: Not available.

4.2.2 Validation of growth phenotype of ubiquinone deficient strains on oleate in candidate studies

Although high-throughput genetic screens are a rapid and efficient tool to study a large number of strains/conditions at a time, but it also has certain limitations that

must be considered while analyzing the data. Problems include presence of incorrect strains in the library, suppressors and cross-contamination. Therefore, before investigating the role of ubiquinone in LCFA metabolism in detail, we first verified the growth phenotypes of various *ubi* mutants at a candidate level. This was important especially considering that out of the seven *ubi* deletion strains in the Keio deletion library, Δ*ubiC* did not show growth defect in oleate and the fitness score of Δ*ubiG* strain could not be determined. The compromised growth of these *ubi* mutants has been reported on succinate in earlier candidate studies (Hsu et al., 1996; Lawrence et al., 1974). We thus tested the growth phenotype of one of these *ubi* deletion strains (Δ*ubiC*) in candidate studies along with five other *ubi* mutants (Δ*ubiE*, Δ*ubiF*, Δ*ubiH*, Δ*ubiI* and Δ*ubiX*) that had shown growth phenotypes in our genetic screen. We made several transductants of the six *ubi* deletion strains and confirmed these by colony PCR. To determine the growth behavior of *ubi* mutants, similar to screen conditions, we used minimal medium containing either glucose or oleate as carbon source. In this study, we also included succinate as a control carbon source where the growth phenotype of various *ubi* mutants is reported in the literature (Gulmezian et al., 2007; Lawrence et al., 1974; Pelosi et al., 2016; Swearingen et al., 2006), and thus would serve as additional control to validate the phenotypes. The experiment was performed in six different sets where each set represents one *ubi* deletion strain. Figs. 4.2, A to F show the images of each *ubi* mutant spotted on solid minimal medium plates containing different carbon sources. The growth phenotype of all tested *ubi* mutants corroborated with their known phenotype in succinate; whereas *ubiE*, *ubiF* and *ubiH* mutants exhibited no growth, *ubiC* and *ubiX* mutants showed growth defect and *ubiI* mutant displayed growth equivalent to WT. In glucose, *ubiC, ubiE*, *ubiF*, *ubiH* and *ubiX* mutants showed growth defect while *ubiI* mutant had growth equivalent to WT.

However, in oleate, in comparison to WT, *ubi* mutants either did not grow at all (*ubiC, ubiE, ubiF,* and *ubiH*) or showed a significant growth defect (*ubiI* and *ubiX*). In a separate set of experiments conducted in our lab (Kanchan Jaswal, Ph.D. student), the growth profile of *ubiH* and *ubiI* deletion strains was compared in liquid minimal medium. Corroborating with our results on solid medium, whereas *ubiH* mutant showed growth defect in glucose, and did not grow at all with oleate and succinate, the *ubiI* mutant showed a significant growth defect only in oleate (Fig. 3A, Agrawal S et al., *JBC* 2017). Taken together, the growth phenotype of various *ubi* mutants (*ubiE*, *ubiF*, *ubiH, ubiI* and *ubiX*) obtained from genetic screen was reproducible in candidate studies. Moreover, the no growth phenotype of *ubiC* mutant in oleate in candidate studies suggests that its unexpected growth behavior in screen was due to problems associated with high-throughput studies.

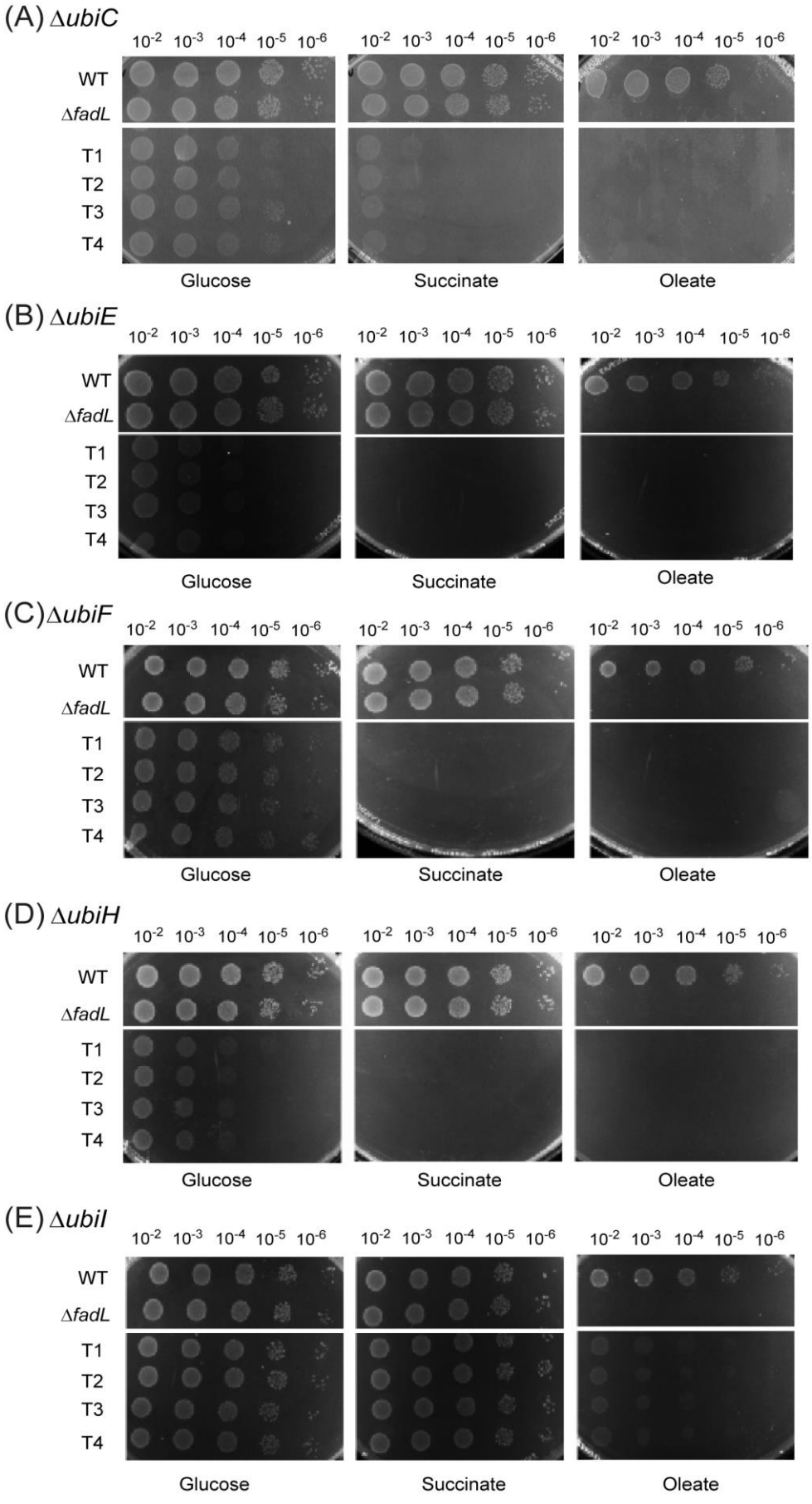
(A) ΔubiC
(B) ΔubiE
(C) ΔubiF
(D) ΔubiH
(E) ΔubiI
10-2 10-3 10-4 10-5 10-6
WT
ΔfadL
T1
T2
T3
T4
Glucose
Succinate
Oleate

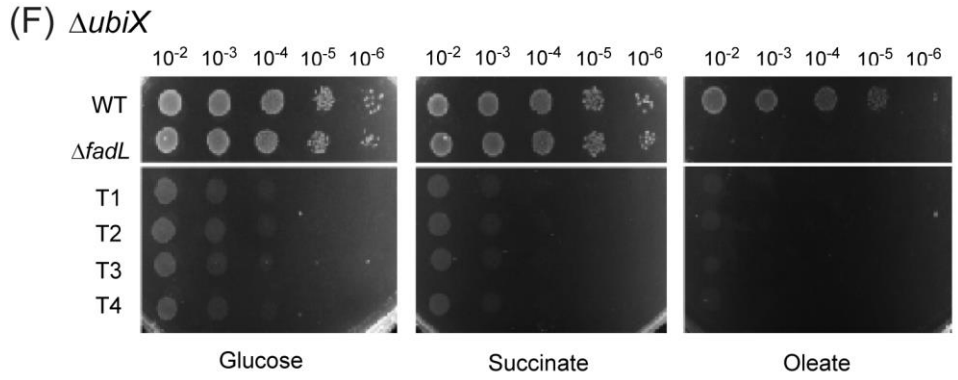

Figure 4.2 Growth defect of *ubi* deletion strains in different carbon sources. (A to F) Dilutions of the cultures were spotted on minimal medium containing one of the carbon sources. Each minimal medium condition had Brij-58. Δ*fadL* (FadL is the outer membrane transporter for LCFAs), which does not grow on oleate was used as a control. T1, T2, T3 and T4 represent four transductants of *ubi* deletion strains. WT, Δ*fadL* and the four transductants of each *ubi* deletion strain were spotted on the same plate with a particular carbon source and imaged.

Upon relating the growth profile of *ubi* deletion strains observed in our study with their ubiquinone levels reported in the literature, we find that mutants with no detectable ubiquinone (*ubiE*, *ubiF*, and *ubiH*) (Kwon et al., 2000; Pelosi et al., 2016; Swearingen et al., 2006) show growth defect in glucose and do not grow at all in succinate and oleate, whereas a *ubiI* mutant, which produces reduced levels of ubiquinone (Hajj Chehade et al., 2013), exhibits growth defect only in oleate. Importantly, these results suggest that there is a differential requirement of ubiquinone for growth on various carbon sources, requirement being maximal in oleate.

4.2.3 Maximal requirement of ubiquinone for growth of *E. coli* in oleate is to mitigate elevated levels of ROS generated by LCFA degradation

The higher requirement of ubiquinone for growth in oleate compared to other carbon sources, succinate and glucose, and the significant requirement of ubiquinone biosynthesis genes in oleate compared to various other oxidative stress combat

players led us to investigate the role of ubiquinone in relieving LCFA-induced oxidative stress. We performed a series of experiments to test this idea. We argued that if the higher requirement of ubiquinone in oleate is to counter oxidative stress, then cells cultured in oleate should have higher level of ROS compared to succinate and glucose. In a recent study, *E. coli* grown in oleate has been reported to accumulate higher levels of ROS compared to cultures grown in glucose (Doi et al., 2014), however the comparison of ROS levels in cells cultured in oleate and succinate has not been reported. Here, we measured intracellular ROS levels in WT cultured in Tryptone broth (TB) supplemented with glucose, succinate or oleate by a colorimetric assay using nitroblue tetrazolium (NBT) dye. We found that WT had the highest ROS levels in oleate (Fig. 4.3A). Moreover, ROS levels further increased in Δ*ubiI* in all media conditions with maximal ROS levels again in TB-Ole grown cells. Next, we investigated whether the growth defect of ubiquinone deficient strains in oleate is due to elevated levels of ROS. Therefore we checked the growth of Δ*ubiI* strain in oleate medium supplemented with antioxidants. We used thiourea and vitamin C (ascorbate) as antioxidants (Dwyer et al., 2014; Fuentes and Amabile-Cuevas, 1998), where thiourea scavenges hydroxyl radicals (Chueca et al., 2014) and ascorbate acts as a lipid hydroperoxyl radical scavenger (Traber and Stevens, 2011). Both thiourea and ascorbate partially recovered the growth defect of Δ*ubiI* strain in oleate (Fig. 4.3B). Consistent with our results in solid medium, in another set of experiments performed in liquid medium in our lab (Kanchan Jaswal, Ph.D. student), the supplementation of antioxidants, glutathione and thiourea, partially recovered the growth defect of Δ*ubiI* in oleate (Figs. 3, B and C, Agrawal S et al., *JBC* 2017). We did not observe a complete recovery because another factor responsible for the poor growth of Δ*ubiI* in

oleate would be reduced energy generation due to lowering of ETC function. To further examine the antioxidant function of ubiquinone in countering ROS in oleate grown cells, we checked the effect of ubiquinone supplementation on ROS levels. We measured ROS levels in WT and *ubiI* mutant grown either in TB or TB-Ole with or without exogenous supplementation of ubiquinone-8. Importantly, ROS levels decreased by ~15–25% in WT grown in TB-Ole and *ubiI* mutant grown either in TB or TB-Ole upon ubiquinone-8 supplementation (Fig. 4.3C), reiterating that ubiquinone relieves oxidative stress.

In order to confirm that all the above phenotypes of Δ*ubiI* strain are due to the loss of function of UbiI, we performed complementation experiments using clone, pKJ7, which carries *ubiI* gene on plasmid pBAD24. Transformation of pKJ7 in Δ*ubiI* strain restored ROS levels of cells grown in TB and TB-Ole to WT levels (Fig. 4.3D), as well as rescued the growth defect of Δ*ubiI* in oleate (Fig. 4.3E).

Collectively, our above results validate that the higher requirement of ubiquinone in oleate is to relieve oxidative stress generated by LCFA metabolism.

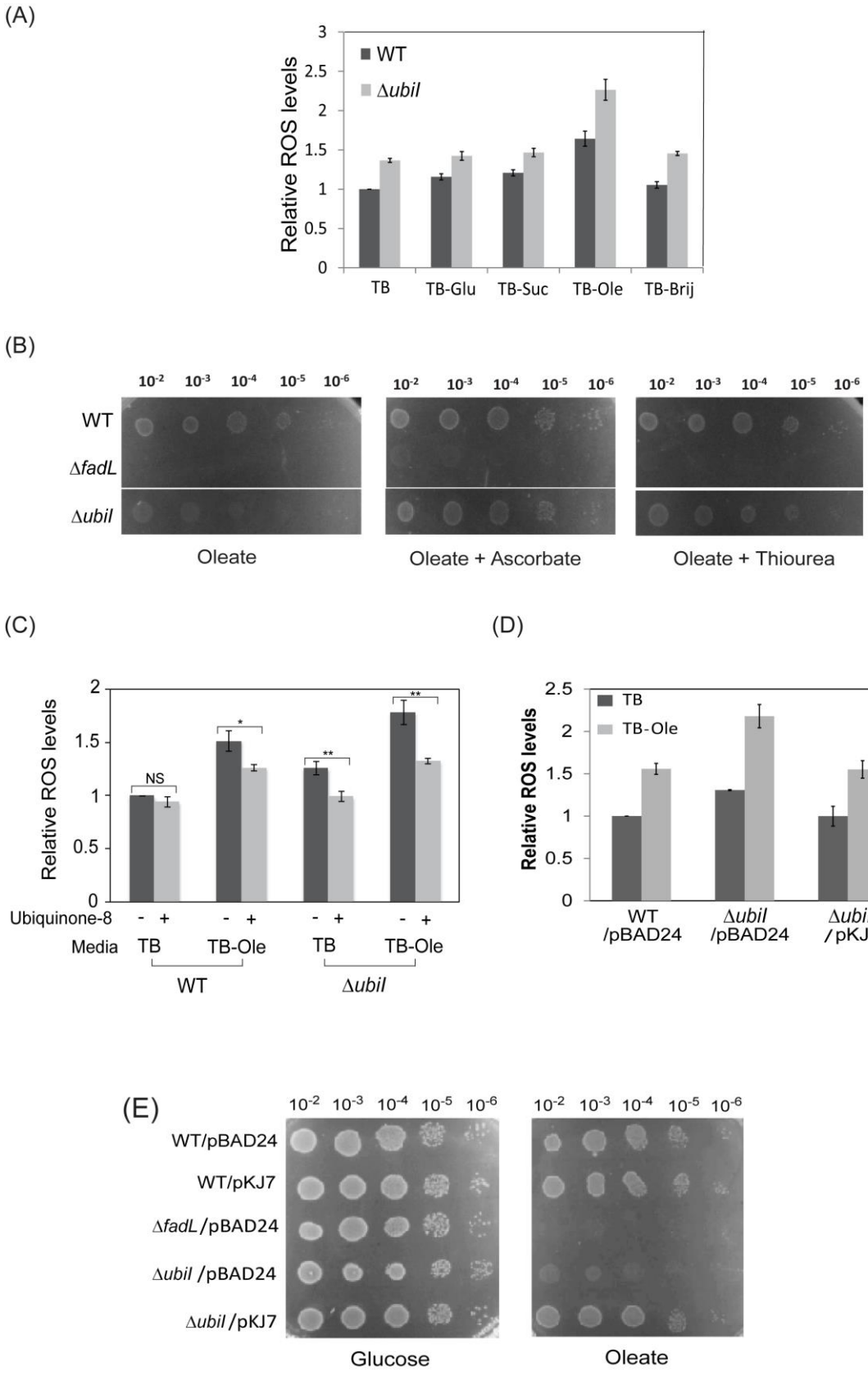

Figure 4.3 The increased requirement of ubiquinone for growth in oleate is to mitigate elevated levels of ROS. (A) WT and Δ*ubiI* strains exhibit maximum ROS levels in TB-Ole.

WT and Δ*ubiI* were grown either in TB or TB supplemented with carbon sources or Brij-58: glucose (TB-Glu), succinate (TB-Suc), oleate (TB-Ole), and Brij-58 (TB-Brij). ROS levels were determined by NBT assay. Data were normalized to the ROS level of WT in TB and represent average (± S.D.) of 5 independent experiments. (B) The growth defect of Δ*ubiI* in minimal medium containing oleate is partially recovered by supplementing antioxidants. WT, Δ*fadL* and Δ*ubiI* strains were grown in minimal medium containing oleate with or without 0.5 mM ascorbate or 1 mM thiourea. (C) Supplementation of ubiquinone-8 suppresses ROS levels. WT and Δ*ubiI* were grown either in TB or TB-Ole. Medium contained either 20 µM ubiquinone-8 or 0.1% ethanol (solvent for ubiquinone-8). ROS levels were determined by NBT assay. Data were normalized to the ROS level of WT in TB containing 0.1% ethanol and represent average (± S.D.) of 3 independent experiments. *, $p < 0.05$; **, $p < 0.005$; NS, not significant (unpaired two-tailed Student's t test). (D) Restoring ubiquinone in ubiquinone deficient strain decreases the elevated levels of ROS. WT carrying empty plasmid (pBAD24), and Δ*ubiI* carrying either pBAD24 or pBAD24 with *ubiI* (pKJ7) were grown either in TB or TB-Ole. ROS levels were determined by NBT assay. Data were normalized to the ROS level of WT carrying pBAD24 in TB and represent average (± S.D.) of 3 independent experiments. (E) *ubiI* cloned on plasmid complements the growth defect of Δ*ubiI* in oleate. Dilutions of WT and Δ*ubiI* carrying either empty plasmid (pBAD24) or pBAD24 with *ubiI* (pKJ7) were spotted on minimal medium containing either glucose or oleate as the sole carbon source. Δ*fadL* transformed with pBAD24 was used as a control.

4.2.4 Ubiquinone is a major antioxidant during LCFA metabolism

E. coli has a suite of oxidative stress combat players, both enzymatic and non-enzymatic. We compared the requirement of various known oxidative stress combat systems in managing ROS in *E. coli* during LCFA metabolism. We selected representative players from each of the known oxidative stress response systems: OxyR regulon member AhpC; SoxR and its regulated target SodA; a RpoS regulon member KatE; enzyme involved in glutathione biosynthesis, GshB (Cheng et al., 2006; Imlay, 2003); and four out of the eleven players involved in ubiquinone biosynthesis (Aussel et al., 2014b; Soballe and Poole, 2000). All these strains deleted either for genes encoding regulatory proteins or enzymes were grown in TB and TB-

Ole, and ROS levels were determined. In TB medium, ROS levels were ~1.3 to 1.5 fold higher when strains lacked either the *ubi* genes or other oxidative stress combat players (Fig. 4.4). In contrast, in TB-Ole medium, ROS levels increased only in *ubi* deletion strains; >2-fold in comparison to WT in TB medium. These results indicate that whereas all oxidative stress response systems play a role in protecting cells against ROS generated during basal metabolism, ubiquinone plays a major role in counteracting ROS produced during oleate metabolism. We considered two possibilities for the TB-Ole results: i) there is redundancy of enzymatic scavengers and their regulators; thus deleting any one of the components does not have a major effect, and ii) as long as ubiquinone is present, it does not allow ROS to build-up further in TB-Ole; thus cells are not dependent on other oxidative stress players. Consistent with the second possibility, from a separate line of experiments in our lab (Kanchan Jaswal, Ph.D. student), we find that the enzymatic scavengers, *katG* and *ahpC* are induced (~2-fold) during oleate metabolism only in a *ubiI* mutant and this increased expression is reduced by ~25% upon exogenous supplementation of ubiquinone-8 (Figs. 4, B to D, Agrawal S et al., *JBC* 2017). Therefore, we conclude that ubiquinone is a key antioxidant and acts as the cell's first line of defense against LCFA-mediated oxidative stress.

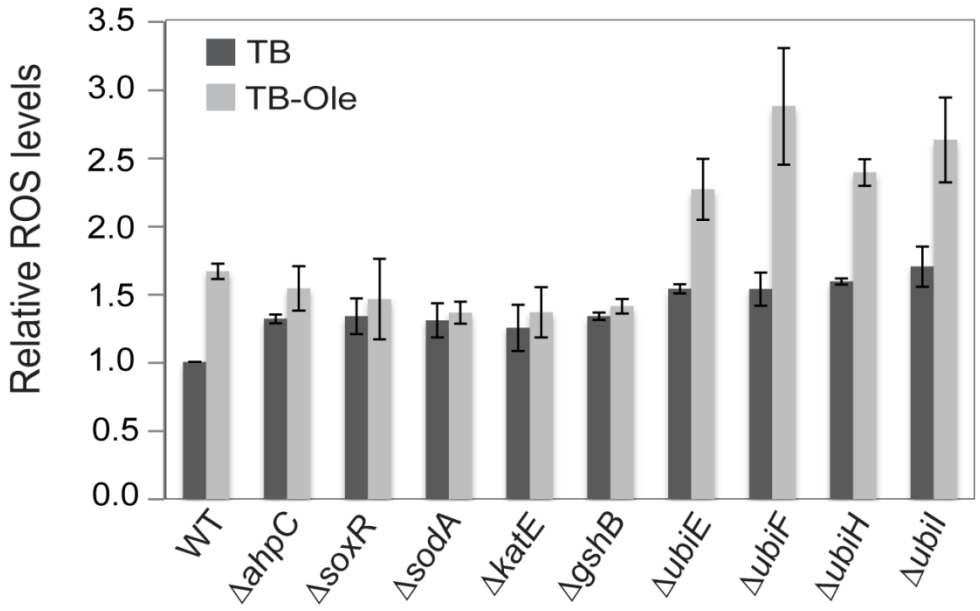

Figure 4.4 Ubiquinone is a major player that counteracts oxidative stress during LCFA metabolism. WT and various deletion strains were grown either in TB or TB-Ole. ROS levels were determined by NBT assay. Data were normalized to the ROS level of WT in TB and represent average (± S.D.) of 3 independent experiments.

4.2.5 Ubiquinone accumulates in response to LCFA degradation in *E. coli*

Our above data showed that ubiquinone is a major player that mitigates LCFA-mediated oxidative stress and therefore we examined whether this defense system is also induced by LCFAs. Ubiquinone is a benzoquinone that contains a polyisoprene chain attached to a quinone ring, where the number of isoprene units in a ubiquinone molecule varies in different organisms. In *E. coli*, ubiquinone has eight isoprene units hence termed as ubiquinone-8 or Q_8 or Coenzyme Q_8 or CoQ_8 (Meganathan, 2001). Ubiquinone is present in the inner membrane and exists in two redox states; the oxidized form is ubiquinone and the reduced form is ubiquinol. The upregulation of ubiquinone in LCFA-utilizing cells was investigated by measuring the total ubiquinone content in these cells, i.e. ubiquinone and ubiquinol by High Performance Liquid Chromatography-photodiode array detector analysis (HPLC-PDA).

4.2.5.1 Assigning peaks to ubiquinone-8 and ubiquinol-8 in HPLC chromatograms

In order to measure the total ubiquinone content in *E. coli* cells, we extracted lipids from cultures and injected these in HPLC system. The chromatogram obtained showed various peaks corresponding to different compounds. In HPLC, each compound is detected at an appropriate wavelength (lambda max; λ_{max}) and displayed in the form of a peak with a specific elution time. We assigned peaks for ubiquinone-8 and ubiquinol-8 in the chromatograms of lipid extracts based on the behavior of pure standards i.e., elution time at λ_{max}. The λ_{max} for ubiquinone-8 standard was found to be 275 nm (Fig. 4.5A). Since ubiquinol-8 standard was not available commercially, ubiquinone-8 was treated with sodium borohydride and reduced to ubiquinol-8. The λ_{max} of ubiquinol-8 was found to be 290 nm (Fig. 4.5B). Analysis of these quinone standards on HPLC showed that ubiquinone-8 at 275 nm had a single peak with elution time ~14.0 min (Fig. 4.5C), and ubiquinol-8 at 290 nm had the elution time ~11 min (Fig. 4.5D). We also injected lipid extracts from Δ*ubiI* strain as a control where ubiquinone levels are reported to be only 10-15% of WT (Hajj Chehade et al., 2013) and thus manifests as a reduction in ubiquinone and ubiquinol peaks in the chromatogram (Figs. 4.5, C and D). A previous study has shown that a compound, 3-octaprenyl-4-hydroxyphenol (4-HP_8), accumulates in Δ*ubiI* strain and the peak corresponding to 4-HP_8 lies next to ubiquinone-8 (Hajj Chehade et al., 2013). In our experiments, we also observed a peak (Peak X) next to ubiquinone-8 with elution time ~15 min in the Δ*ubiI* strain, which we suggest corresponds to 4-HP_8 (Fig. 4.5C).

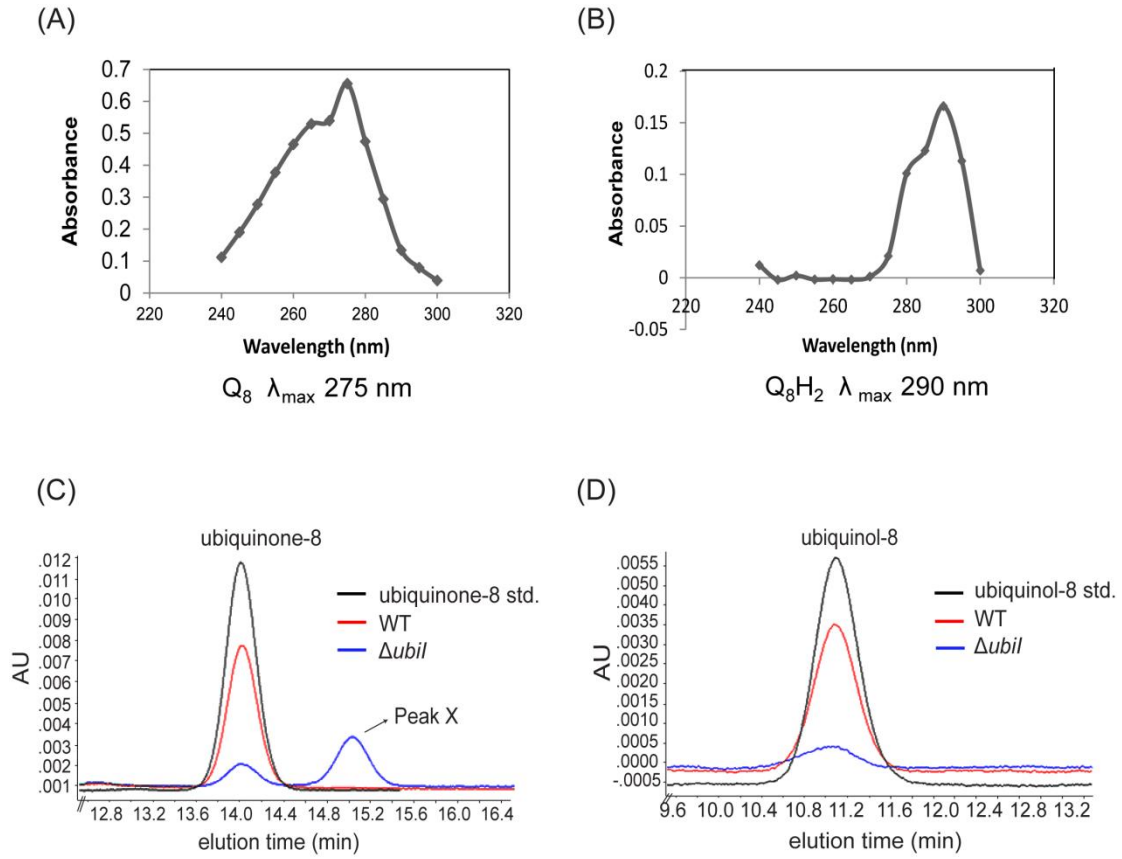

Figure 4.5 Determining peaks for ubiquinone-8 and ubiquinol-8 in HPLC-PDA analysis. (A and B) Absorbance of ubiquinone-8 (Q_8) and ubiquinol-8 (Q_8H_2) standards was monitored in the wavelength range of 240 to 300 nm. λ_{max} for ubiquinone-8 and ubiquinol-8 was found to be 275 nm and 290 nm, respectively. (C and D) HPLC-PDA analysis of ubiquinone-8 and ubiquinol-8. Lipid extracts from WT and Δ*ubiI* strains were run on HPLC system and the peaks for ubiquinone-8 and ubiquinol-8 were assigned at 275 nm and 290 nm, respectively, based on the elution time of standards and reduction of peaks in Δ*ubiI*. Peak corresponding to an additional compound (peak X) was observed in Δ*ubiI*, next to the ubiquinone-8 peak at 275 nm.

4.2.5.2 Ubiquinone-8 accumulates in cells grown in oleate

Ubiquinone content in the cell can be quantified by measuring the corresponding peak area, however certain parameters such as difference in the number of cells and difference in the extraction efficiency amongst various samples have to be normalized. We accounted for the difference in cell number amongst samples by normalizing ‘peak area’ with ‘the mass of cell pellet before extraction’. Variation in

'extraction efficiency' amongst samples was taken care by using ubiquinone-10 (Q_{10}) as an internal control. Various features of Q_{10} allow it to serve as a good internal control. First, Q_{10} does not exist naturally in *E. coli* (Meganathan, 2001). Second, the elution time of Q_{10} (~25 min, λ_{max} 275 nm) (Figs. 4.6, A and B) is well apart from both ubiquinone-8 and ubiquinol-8. The known and equal amount of Q_{10} was added to each sample before extraction of lipids. The 'peak area per unit pellet mass' was further normalized with 'peak area of Q_{10}' for each sample. The amount of ubiquinone-8 or ubiquinol-8 in a particular sample was calculated as:

Amount of ubiquinone-8 = (peak area of Q_8/pellet mass)/peak area of Q_{10}

Amount of ubiquinol-8 = (peak area of Q_8H_2/pellet mass)/peak area of Q_{10}

The total ubiquinone content in the cell was calculated as:

$$Total\ Q8\ content = \frac{\frac{peak\ area\ of\ Q8}{pellet\ mass}}{peak\ area\ of\ \mathrm{Q10}} + \frac{\frac{peak\ area\ of\ Q8H2}{pellet\ mass}}{peak\ area\ of\ \mathrm{Q10}}$$

We measured total Q_8 content in WT cells grown either in TB or TB-Ole. We observed ~1.8 fold higher Q_8 levels in cells grown in TB-Ole compared to cells grown in TB. There was no change in the total Q_8 content in TB-Brij in comparison to cells grown in TB medium (Fig. 4.6C). Our results thus show that ubiquinone accumulates in the presence of oleate.

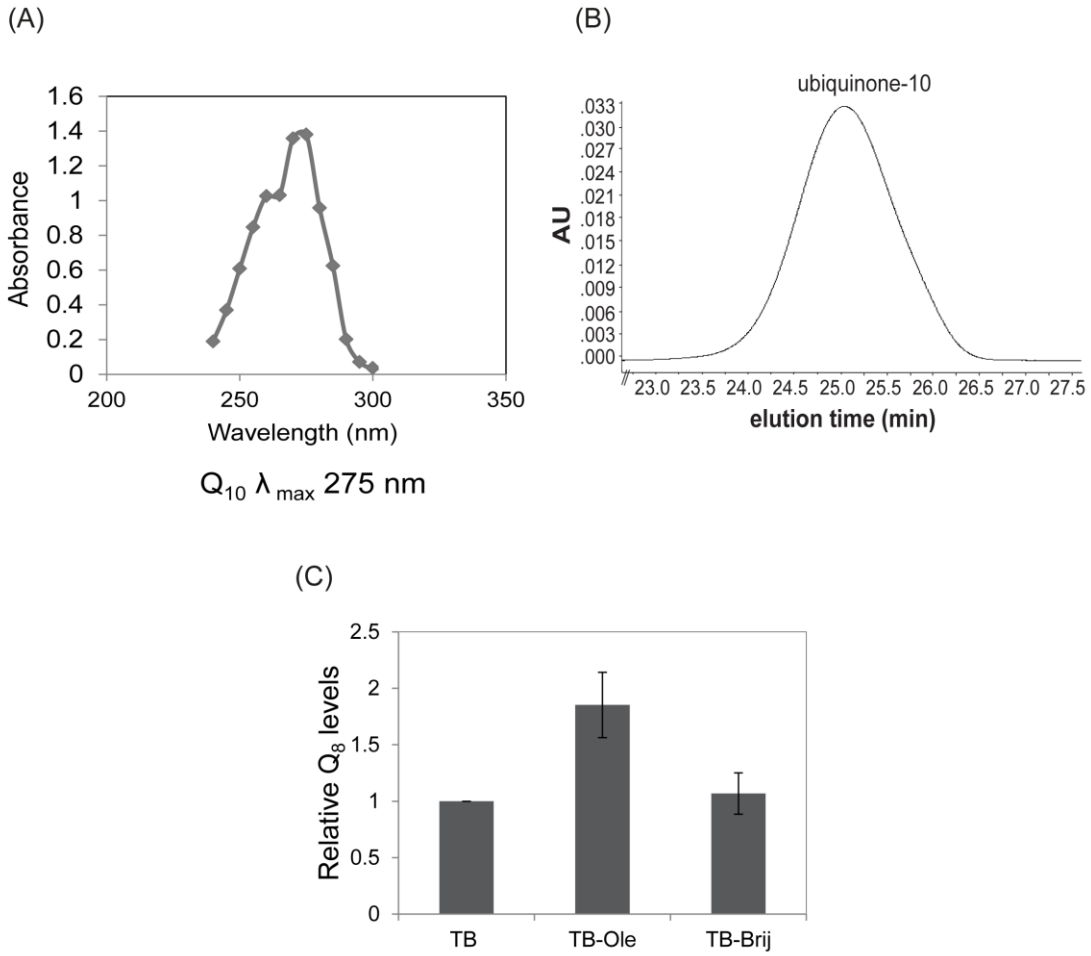

Figure 4.6 Ubiquinone accumulates in *E. coli* cells grown in oleate. (A) Absorbance of ubiquinone-10 (Q_{10}) standard was monitored in the wavelength range of 240 to 300 nm and λ_{max} was found to be 275 nm. (B) HPLC-PDA analysis of ubiquinone-10 standard, showing peak at elution time ~ 25 min. (C) Ubiquinone accumulates in WT cells grown in oleate. The total Q_8 level in lipid extracts from WT grown in TB, TB-Ole and TB-Brij was determined. Q_8 levels were normalized to the Q_8 level of WT in TB and represent average (± S.D.) of at least 4 independent experiments.

4.2.5.3. Accumulation of ubiquinone-8 in cells cultured in oleate is in response to LCFA degradation

We investigated the reason for upregulation of ubiquinone during LCFA metabolism. For this, we checked ubiquinone levels in various *fad* knockouts, which are defective in LCFA transport and degradation (Δ*fadL*, Δ*fadD*, and Δ*fadE*) (Clark and Cronan, 2005; Klein et al., 1971). Each mutant was grown either in TB or TB-Ole medium,

lipid mix was extracted and run on the HPLC system. In contrast to WT cells, Q_8 levels did not increase in TB-Ole in *fad* knockouts (Fig. 4.7). These results show that LCFA degradation signals the accumulation of ubiquinone in oleate utilizing cells.

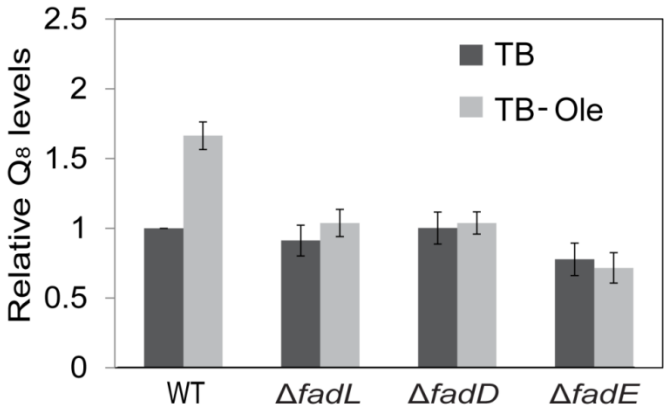

Figure 4.7 LCFA degradation signals the accumulation of ubiquinone in oleate utilizing cells. The total Q_8 level in lipid extracts from WT and various *fad* deletion strains grown either in TB or TB-Ole was determined. Q_8 levels were normalized to the Q_8 level of WT in TB and represent average (± S.D.) of at least 4 independent experiments.

4.3 Discussion

4.3.1 Ubiquinone relieves oxidative stress generated by LCFAs

We investigated the combat strategies employed by *E. coli* to counter LCFA-induced oxidative stress. For this, we analyzed data from high-throughput genetic screen of the *E. coli* Keio deletion library on an LCFA, oleate. The GSEA analysis of the LCFA dataset showed that ubiquinone biosynthesis pathway is significantly enriched during LCFA metabolism (Table 4.2). Further, our detailed analysis showed that ubiquinone is maximally required in oleate to mitigate elevated levels of ROS. Compared with WT cells, ROS levels were ~1.5-fold higher in a Δ*ubiI* strain grown in glucose or succinate (Fig. 4.3A) but there was no difference in the growth profile of WT and Δ*ubiI* in these carbon sources (Fig. 4.2E). The utilization of oleate resulted in a ~1.5-

fold increase in ROS levels in WT cells compared with other carbon sources that further increased to ~2.5-fold in a Δ*ubiI* strain (Fig. 4.3A). Importantly, this elevated level of ROS (~2.5-fold) was deleterious as evident from the significant growth defect of the Δ*ubiI* strain in oleate and that the growth defect could be partially recovered by chemical antioxidants (Fig. 4.3B). These data clearly indicate that in oleate-utilizing cells optimum levels of ubiquinone are required to manage ROS below a toxic threshold. Furthermore, we find that among various oxidative stress combat players, ubiquinone is the key antioxidant during LCFA metabolism. This is supported by the observation that strains deleted for oxidative stress combat players other than *ubi* genes do not exhibit an increase in ROS in oleate-utilizing cells (Fig. 4.4). Moreover, whereas ubiquinone accumulates in the presence of oleate (Fig. 4.6), other players are induced only in a mutant defective in ubiquinone biosynthesis (Figs. 4, B and C, Agrawal S et al., *JBC* 2017). Interestingly, oleate degradation generates ROS (Fig. 3.4, Chapter 3) and also provides a signal for ubiquinone accumulation (Fig. 4.7). These results suggest a feedback loop that prevents excessive ROS formation during growth in LCFAs. An earlier study has shown that ubiquinone is present in excess over flavins and cytochromes in the *E. coli* inner membrane (Cox et al., 1970). Thus under normal conditions ubiquinone is not limiting for its electron transfer function. Considering this, ~2-fold increase in ubiquinone levels in cells utilizing oleate could bring a significant physiological response. Few *ubi* genes are regulated by the ArcA–ArcB two-component system and catabolite repression (Gibert et al., 1988; Zhang and Javor, 2003). It will be interesting to investigate the mechanisms that regulate ubiquinone levels during LCFA degradation. We suggest that ROS itself might not be the signal for upregulation of ubiquinone, because despite exhibiting a higher level of

ROS the Δ*fadD* strain had basal ubiquinone levels in TB medium (compare Fig. 3.4B, Chapter 3 and Fig. 4.7).

4.3.2 Mechanisms by which ubiquinone might counteract LCFA-mediated oxidative stress

Several mechanisms have been suggested for ROS formation in the ETC that includes extraction of electrons from reduced metal centers of certain enzymes by molecular O_2, leakage of electrons during oxidation-reduction cycles of ETC promoting the reaction of free electrons with O_2, and autoxidation of flavoproteins (Imlay, 2003). Søballe and Poole first demonstrated the role of ubiquinone in counteracting ROS in bacteria and proposed two mechanisms to explain its antioxidant function. First, ubiquinone limits ROS formation due to its ability to rapidly transfer electrons from upstream respiratory dehydrogenases to terminal oxidases thereby decreasing the chance of single-electron donation to oxygen. Second, the reduced form of ubiquinone (ubiquinol) can scavenge ROS (Soballe and Poole, 2000).

The predominant mechanism by which ubiquinone combats ROS during LCFA degradation would depend on the major site of ROS formation. Fig. 4.8 shows the probable sites of ROS formation during growth of *E. coli* in LCFAs and the mechanisms by which ubiquinone might counteract LCFA-induced oxidative stress. Our results from chapter 3 suggests that the large amount of reduced cofactors generated by LCFA degradation increases electron flow in ETC increasing the probability of adventitious collision of electrons with O_2 resulting in elevated levels of ROS (Figs. 3.5, 3.6, 3.7 and 3.8, Chapter 3). Thus one would speculate that during LCFA metabolism ubiquinone limits ROS formation by rapidly transferring electrons from upstream respiratory dehydrogenases to terminal oxidases. If this is the sole

mechanism by which ubiquinone functions during LCFA metabolism, then similar to ubiquinone, the requirement of other ETC components should also be higher in oleate in comparison to other non-fermentable carbon sources. However, additional studies from our lab where LCFA dataset was compared with already published genome-wide screens of various carbon sources has revealed that unlike respiratory dehydrogenases and terminal oxidases whose requirement for growth is inversely correlated with the energy yield of non-fermentable carbon sources, the requirement of ubiquinone correlates with oxidative stress. Acetate is a poorer carbon source than oleate in terms of energy yield (Clark and Cronan, 2005), whereas oleate metabolism generates higher ROS levels than acetate (Fig. 3.5B, Chapter 3). In a comparison of acetate and oleate, studies from our lab has shown that the requirement of the NADH dehydrogenase, Nuo, and the terminal oxidase, Cyo, is higher in acetate to meet energy requirement whereas ubiquinone requirement is higher in oleate to counteract oxidative stress (Kanchan Jaswal, Ph.D. student) (Agrawal S et al., *JBC* 2017). Therefore, these studies suggest that at least in LCFA metabolism the antioxidant role of ubiquinone cannot be explained solely by its known electron carrier function in ETC. Importantly, a predominant source of ROS during LCFA degradation could be the predicted acyl-CoA dehydrogenase, FadE, which is suggested to catalyze the oxidation of acyl-CoA to enoyl-CoA concomitant with reduction of FAD to $FADH_2$ (Campbell and Cronan, 2002). It is likely that ubiquinone limits ROS formation at FadE by transferring electrons from FadE to the ETC. In addition, a recent study has demonstrated the *in vitro* quinol peroxidase activity of Cyd where quinol serves as a substrate for the peroxidase to detoxify H_2O_2 (Al-Attar et al., 2016). Thus, during LCFA catabolism, besides decreasing ROS formation because of its electron shuttling role in ETC, ubiquinone might promote the peroxidase activity of terminal oxidase to

detoxify ROS. Because ETC is one of the sites for ROS formation, it might be advantageous for the cell to have antioxidants in the membrane to detoxify ROS locally. Ubiquinone in conjunction with Cyd might fulfill this role.

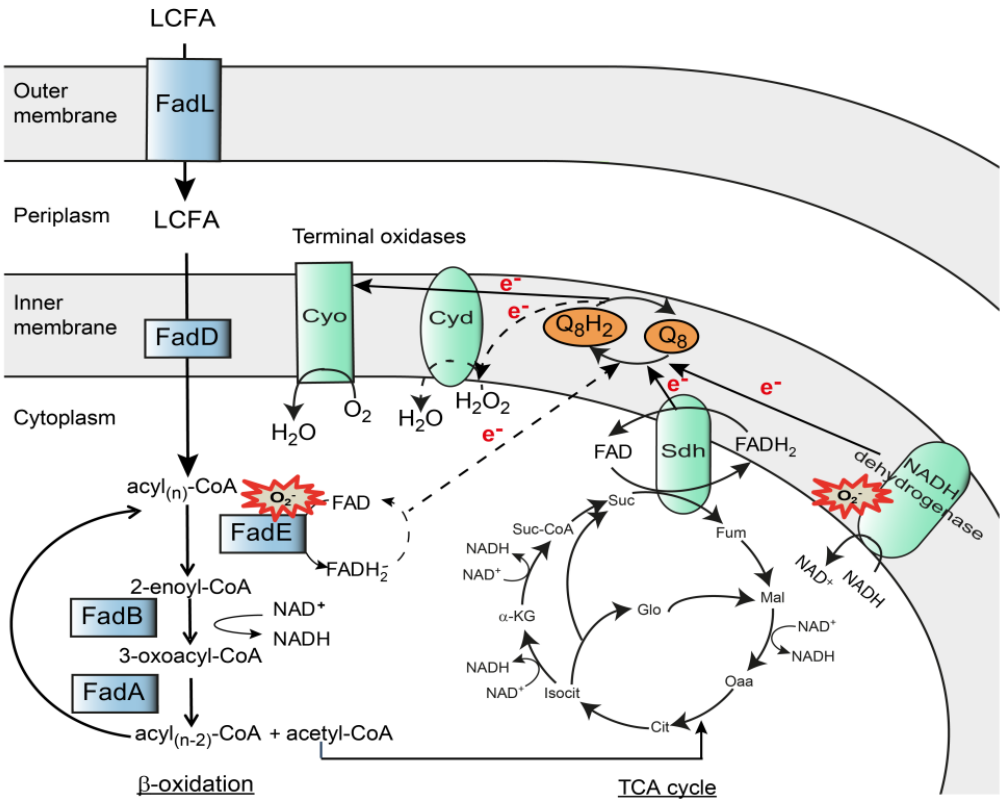

Figure 4.8 Probable sites of ROS formation during LCFA degradation and the mechanisms employed by ubiquinone to mitigate LCFA-induced oxidative stress. Exogenous LCFAs are transported inside the cell by an outer membrane protein, FadL. Subsequently, the inner membrane-associated acyl-CoA synthetase, FadD, extracts LCFAs from the inner membrane concomitant with esterification to acyl-CoA. Acyl-CoAs are degraded to acetyl-CoA via the β-oxidation pathway mediated by enzymatic activities of FadE, FadB, and FadA. Acetyl-CoA feeds into the TCA cycle for further metabolism. High NADH/NAD^+ and $FADH_2$/FAD ratios during β-oxidation and TCA cycle increase the electron flow in the ETC thereby increasing electron leakage and autoxidation of the reduced form of NADH dehydrogenase resulting in ROS formation. In addition, a predominant source of ROS could be the acyl-CoA dehydrogenase, FadE, which reduces FAD to $FADH_2$. Ubiquinone limits ROS formation by rapidly transferring electrons from upstream dehydrogenases to terminal oxidases (Cyo and Cyd) thus preventing electron leakage and

autoxidation of the reduced form of dehydrogenases. In addition, the quinol peroxidase activity of Cyd will detoxify H_2O_2. *Arrows* with e^- labeled on the line show the direction of electron transfer. *Dotted arrows* indicate reactions for which either the components involved are not known (oxidation of FadE and electron transfer from FadE to the ETC) or the mechanisms are not established *in vivo* (detoxification of H_2O_2 by Cyd). Abbreviations: *Oaa*, oxaloacetate; *Cit*, citrate; *Isocit*, isocitrate; *α-KG*, α-ketoglutarate; *Suc-CoA*, succinyl-CoA; *Suc*, succinate; *Fum*, fumarate; *Mal*, malate; *Glo*, glyoxylate; O_2^-, superoxide; *Sdh*, succinate dehydrogenase; Q_8, ubiquinone-8; Q_8H_2, ubiquinol-8; *Cyd*, cytochrome bd; *Cyo*, cytochrome bo.

Several bacterial pathogens use LCFAs derived from host tissues as their nutrient source (Fang et al., 2005; McKinney et al., 2000; Son et al., 2007). It will be interesting to examine whether ubiquinone participates in managing LCFA-mediated oxidative stress in these pathogens. In fact, a few *ubi* mutants of *S. typhimurium* are impaired for intracellular proliferation in macrophages (Aussel et al., 2014a). Because *S. typhimurium* utilizes fatty acids in macrophages during chronic infection (Fang et al., 2005), it is possible that ubiquinone is required by this intracellular pathogen to combat oxidative stress generated by LCFAs.

CHAPTER V

Identification of *yqiC* as a novel gene involved in ubiquinone biosynthesis in *E. coli*

5.1 Introduction

Ubiquinone is a redox-active lipid located in the inner membrane of *Escherichia coli* and plays important role in various physiological processes in the cell (Aussel et al., 2014b). Ubiquinone being an electron carrier in the electron transport chain (ETC) is critical for energy generation and governs various proton motive force (PMF) dependent processes such as antibiotic resistance and motility (Bar-Tana et al., 1980; Ezraty et al., 2013). Ubiquinone also modulates redox sensing of the two-component system, ArcAB (Georgellis et al., 2001), which mediates the response of *E. coli* to varying respiratory growth conditions by acting as a global regulator of gene expression under microaerobic and anaerobic conditions (Bekker et al., 2010). Various studies have also shown the requirement of ubiquinone in bacterial virulence (Aussel et al., 2014a; Gomez et al., 2012). Besides this, prior to our work, there has been only one report in *E. coli* that suggested ubiquinone to function as an antioxidant (Soballe and Poole, 2000). From our work presented in the previous chapter we established that ubiquinone is a key antioxidant during metabolism of long-chain fatty acids (LCFAs).

Structurally, ubiquinone consists of an aromatic benzene ring and polyprenyl hydrophobic chain, where number of isoprene units in the polyprenyl chain varies among organisms (Meganathan, 2001). Because *E. coli* ubiquinone contains eight isoprene units it is termed as ubiquinone-8 (Meganathan, 2001). Ubiquinone is synthesized in *E. coli* by a dedicated ubiquinone biosynthesis pathway involving eleven *ubi* genes (Aussel et al., 2014b) (Fig. 1.4, Chapter 1). The precursors for ubiquinone biosynthesis, 4-hydroxybenzoate (4-HB) and octaprenyl diphosphate, are synthesized from shikimate pathway and methylerythritol phosphate pathway (MEP), respectively (Meganathan, 2001). 4-HB contains an aromatic benzene ring that is

modified by one prenylation, one decarboxylation, three hydroxylation, and three methylation reactions to synthesize ubiquinone-8. UbiC catalyzes the first committed step converting chorismate to 4-HB (Meganathan, 2001). Next, UbiA catalyzes the prenylation of 4-HB with octaprenyl diphosphate chain to form 3-octaprenyl-4-hydroxybenzoate (OHB). Further, OHB undergoes decarboxylation by both UbiD and UbiX to form 3-octaprenylphenol (OPP). Next, three hydroxylation (by UbiI, UbiH and UbiF) and three methylation (by UbiG and UbiE) reactions occur in alternate fashion in the benzene ring forming ubiquinone-8 (Aussel et al., 2014b; Meganathan, 2001).

Despite decades of active research on the identification and characterization of players involved in ubiquinone biosynthesis in *E. coli* there are obvious knowledge gaps in the pathway. Although UbiB and UbiJ have been shown to be involved in ubiquinone biosynthesis, their exact role in the pathway remains elusive (Aussel et al., 2014b). UbiJ has been predicted to bind lipids and thus could serve as an accessory factor in ubiquinone biosynthesis (Aussel et al., 2014a). Further, residual levels of ubiquinone in certain *ubi* mutants suggest that there is redundancy in the ubiquinone biosynthesis pathway (Cox et al., 1969; Gulmezian et al., 2007; Hajj Chehade et al., 2013; Stroobant et al., 1972). A very early study suggested that Ubi proteins constitute a large multiprotein complex. Authors isolated a soluble enzyme complex of ~2000 kDa, comprising at least 12 proteins, from the cytoplasmic membrane of *E. coli*. The complex contained high amount of OPP but no ubiquinone-8. Interestingly, on providing S-Adenosylmethionine (SAM), NADPH, and O_2 to the complex, ubiquinone-8 could be synthesized from OPP (Knoell, 1979). However, till date, the ubiquinone biosynthesis complex has not been established. It is likely that certain Ubi

proteins such as UbiJ and as yet unidentified Ubi players are involved in the assembly of the mega ubiquinone biosynthesis complex in the membrane.

In the last several years, classical genetic approaches have been employed to identify ubiquinone biosynthesis genes. Because the requirement of ubiquinone for growth on non-fermentable carbon sources (where energy generation occurs only by oxidative phosphorylation in the ETC) is higher compared to growth on fermentable carbon sources (where energy generation happens both by substrate-level and oxidative phosphorylation), this rationale has been used to screen for genes involved in ubiquinone biosynthesis (Stroobant et al., 1972; Wu et al., 1993). Thus, *E. coli* mutants that were more defective for growth on non-fermentable carbon sources such as malate or succinate, compared to the fermentable carbon source, glucose, were investigated further for their role in ubiquinone biosynthesis. However, a recent study showed that a *ubiI* deletion strain, where ubiquinone levels are reduced to 10-15% of wild-type WT levels exhibits normal growth in succinate (Hajj Chehade et al., 2013) (Pelosi et al., 2016), indicating that *ubi* deletion strains that have residual ubiquinone levels might not be identified by their phenotype using this carbon source. Importantly, from our work presented in the previous chapter we found that *ubiI* deletion strain shows significant growth defect in oleate. Therefore, we suggest that oleate is a better carbon source than succinate for identifying *ubi* players especially ones that have a partial effect on ubiquinone levels. Because there is redundancy in the ubiquinone biosynthesis pathway and possibility of accessory factors required for building the multiprotein complex in the inner membrane, we analyzed our LCFA dataset obtained from the genetic screen on oleate, to identify new genes involved in ubiquinone biosynthesis. Our detailed investigation identified *yqiC* as a novel gene

required for ubiquinone biosynthesis. In addition, our results provide a strong genetic evidence of the interaction between *ubiI* and *yqiC*.

5.2 Results

5.2.1 High-throughput genetic screen reveals the requirement of several genes of unknown function for optimal growth in oleate

To identify new players involved in ubiquinone biosynthesis, we examined the data obtained from genetic screen in oleate (Result section 4.2.1.1, Chapter 4). We analyzed top 100 candidates from the LCFA dataset, constituting ~2.5% of the LCFA-responsive genome. Amongst top 100 candidates there were 21 'genes of unknown or putative function' ('*y*' genes) (Appendix 2). *yqiC* deletion strain had the most severe defect in oleate (17^{th} rank in the LCFA dataset) amongst deletion strains of the 21 'y' genes. We thus pursued with investigating the role of *yqiC* in LCFA metabolism.

5.2.2. Validation of the growth phenotype of Δ*yqiC* strain in oleate at a candidate level

Due to problems associated with high-throughput genetic screens (Result section 4.2.2, Chapter 4), before any detailed investigation, we first verified the growth phenotype of Δ*yqiC* strain at a candidate level. We made fresh transductants of the strain and confirmed these by colony PCR. We further checked the growth of Δ*yqiC* strain in minimal medium containing either glucose or oleate as the sole carbon source. *yqiC* deletion strain showed growth equivalent to WT in minimal medium with glucose but exhibited growth defect in oleate (Fig. 5.1A). Thus our results at a candidate level corroborated with the phenotype of Δ*yqiC* strain in high-throughput screens. Further, the growth phenotype of Δ*yqiC* in oleate could be complemented by

providing *yqiC* gene on a plasmid, pACYC184 (pSA4) (Fig. 5.1B). We next investigated the role of *yqiC* in LCFA metabolism.

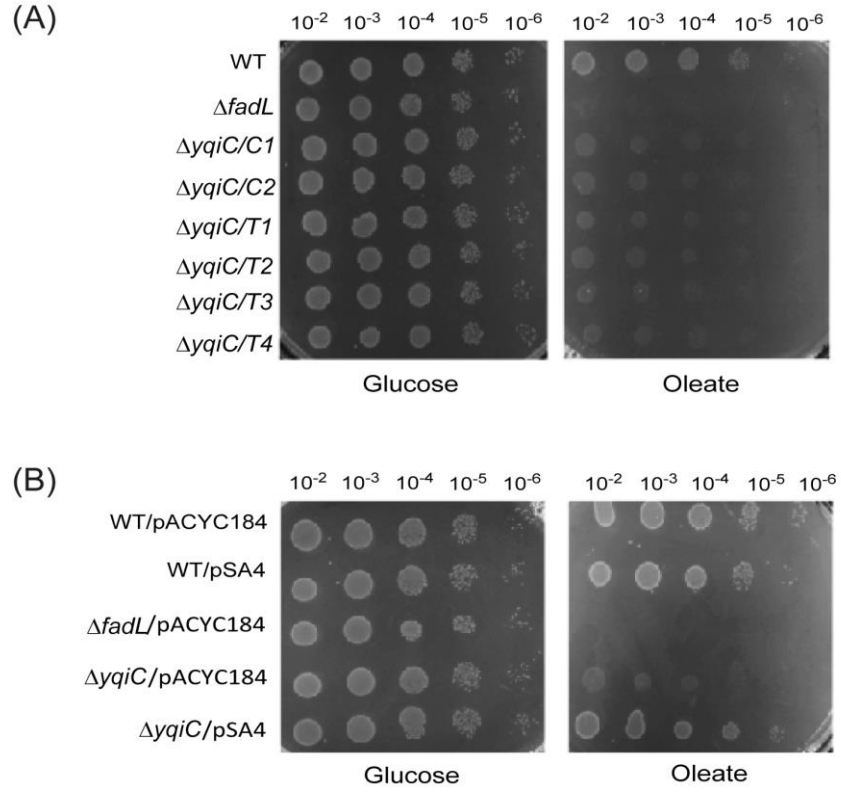

Figure 5.1 Verification of the growth phenotype of Δ*yqiC* strain in oleate. (A) Δ*yqiC* shows significant growth defect in oleate. Dilutions of the cultures were spotted on minimal medium containing either glucose or oleate. Minimal medium with glucose had Brij-58. Δ*fadL* was used as a control. C1 and C2 represent two independent clones of Δ*yqiC* from the Keio deletion library and T1, T2, T3 and T4 are their transductants. (B) *yqiC* cloned on plasmid complements the growth defect of Δ*yqiC* in oleate. Dilutions of WT and Δ*yqiC* carrying either empty plasmid (pACYC184) or pACYC184 with *yqiC* (pSA4) were spotted on minimal medium containing either glucose or oleate as the sole carbon source. Minimal medium with glucose had Brij-58. Δ*fadL* transformed with pACYC184 was used as a control.

5.2.3. *yqiC* is a novel ubiquinone-8 biosynthesis gene in *E. coli*

In order to predict the function of *yqiC* we searched for known or predicted interacting partners of YqiC or the genes with similar phenotypic profile as *yqiC* in

various available databases. This analysis led us to investigate the role of *yqiC* in ubiquinone biosynthesis. Various genetic and biochemical experiments were further performed to elucidate its involvement in ubiquinone biosynthesis.

5.2.3.1 Search through various databases indicates strong correlation between *yqiC* and ubiquinone biosynthesis genes

String is a database of known and predicted protein-protein interactions for an organism (Szklarczyk et al., 2017). For each interacting partner a 'score' is designated, which represents the extent of likelihood of a candidate to interact with the desired protein. Analysis of YqiC in 'String' gave a list of predicted interacting partners with significant scores. Fig. 5.2 shows the protein-protein interaction network for top 10 YqiC interacting proteins, and Table 5.1 provides their interaction scores. Interestingly, amongst the 10 predicted interacting partners, seven proteins are those that are known to be involved in ubiquinone biosynthesis. UbiF is the topmost protein with a score of 0.736 and UbiE is the 10th protein with a score of 0.592.

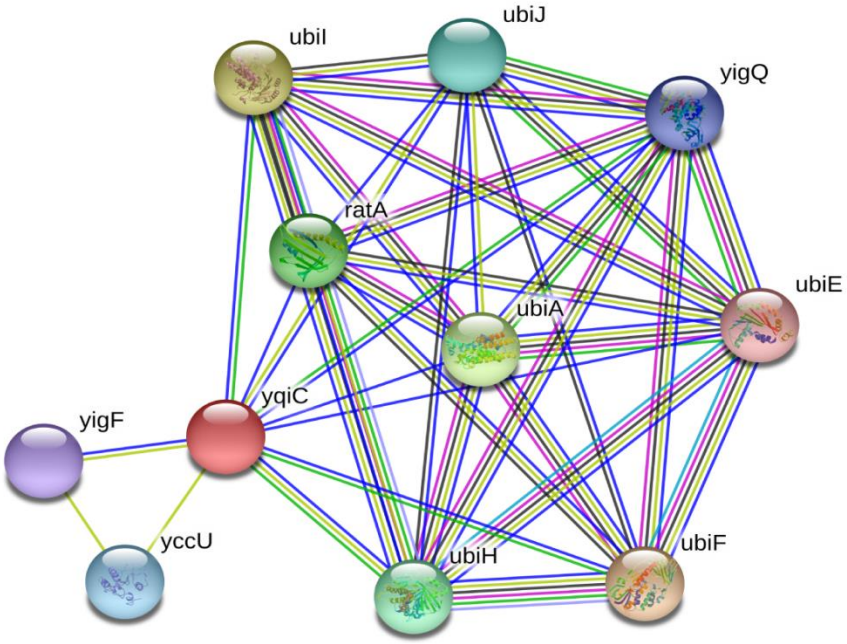

Figure 5.2 Predicted protein-protein interaction network for YqiC. Proteins interacting with YqiC were predicted from String database and interaction network is shown for top 10 proteins. Nodes represent proteins and Edges represent protein-protein associations. Cyan and pink represents known interactions; Cyan: from curated databases, and Pink: experimentally determined. Green, red or blue represents predicted interactions; Green: gene neighborhood, Red: gene fusions, and Blue: gene co-occurrence. Others are represented by Yellow: text mining, Black: co-expression, and light blue: protein homology.

S. No.	Protein	Score
1	UbiF	0.736
2	UbiI	0.732
3	UbiA	0.722
4	RatA	0.712
5	UbiH	0.711
6	UbiJ	0.695
7	YccU	0.658
8	YigQ (UbiB)	0.642
9	YigF	0.634
10	UbiE	0.592

Table 5.1 List of proteins predicted to interact with YqiC. Scores of top 10 proteins predicted to interact with YqiC protein from String database is shown. Amongst top ten proteins, seven proteins (shaded in grey) are involved in ubiquinone biosynthesis.

In a previous study, authors tested the growth of Keio deletion library in around 300 different media conditions. Growth phenotype for each strain in various conditions is given a score and is available in a dataset "High-Throughput Phenotype Data Analysis" [(Nichols et al., 2011), http://www.porteco.org/phenotypes/]. In this dataset, correlation between two strains is indicated by the Pearson correlation coefficient of the scores of two strains across all conditions. Therefore a positive and negative correlation coefficient between two strains represents related and anti-correlated growth phenotypes, respectively. Analysis of Δ*yqiC* strain in this dataset

revealed a positive correlation of various *ubi* genes with *yqiC* (Table 5.2). Importantly, the highest correlation of *yqiC* was observed with *ubiI* with a correlation coefficient of 0.776. Together, the analysis of *yqiC* in various databases strongly suggested its involvement in ubiquinone biosynthesis.

Strain	Correlation coefficient
ubiI::*kan*	0.775682
ubiC::*kan*	0.472577
ubiX::*kan*	0.321542
ubiH::*kan*	0.317641
ubiE::*kan*	0.310051
ubiF::*kan*	0.278182

Table 5.2 Correlation between Δ*yqiC* strain and various *ubi* deletion strains. High-Throughput Phenotype Data Analysis was used to analyze the correlation between Δ*yqiC* and other *ubi* deletion strains in the Keio library. Out of seven *ubi* deletion strains in the Keio library, six *ubi* strains showed a positive correlation coefficient with Δ*yqiC*.

5.2.3.2 Δ*ubiI* and Δ*yqiC* have related phenotypes

Our results from previous chapter showed that amongst the tested non-fermentable carbon sources, succinate and oleate, Δ*ubiI* exhibits growth defect only in oleate (Fig. 4.2 E, Chapter 4). Because, *yqiC* shows highest correlation with *ubiI* in the High-Throughput Phenotype Dataset (Table 5.2), we investigated whether similar to Δ*ubiI* the growth defect of Δ*yqiC* is also specific to oleate. Fig. 5.3A shows the images of Δ*yqiC* and Δ*ubiI* strains spotted on solid medium containing different carbon sources. We observed that similar to Δ*ubiI*, Δ*yqiC* has growth equivalent to WT in minimal medium with either glucose or succinate, however it showed growth defect in oleate. Because we had observed that one of the reasons for the growth defect of Δ*ubiI* in

oleate is oxidative stress (Result section 4.2.3, Chapter 4), we wanted to determine whether high ROS levels is also a reason for the growth defect of Δ*yqiC* strain in oleate. Therefore, we assessed the growth of Δ*yqiC* in oleate medium supplemented with antioxidants, thiourea and vitamin C (ascorbate) (Dwyer et al., 2014; Fuentes and Amabile-Cuevas, 1998). For better comparison we also included Δ*ubiI* in this experiment. The growth defects of both *ubiI* and *yqiC* deletion strains in oleate were partially recovered by thiourea and ascorbate (Fig. 5.3B). Further, using NBT assay, we observed that similar to Δ*ubiI*, Δ*yqiC* also has elevated ROS levels. Δ*yqiC* showed ~1.3 fold increase in ROS levels in TB and ~2 fold higher ROS levels in TB-Ole in comparison to WT grown in TB (Fig. 5.3C). Altogether, these results indicate that *yqiC* functions in a pathway similar to *ubiI* and thus prompted us to investigate its role in ubiquinone biosynthesis.

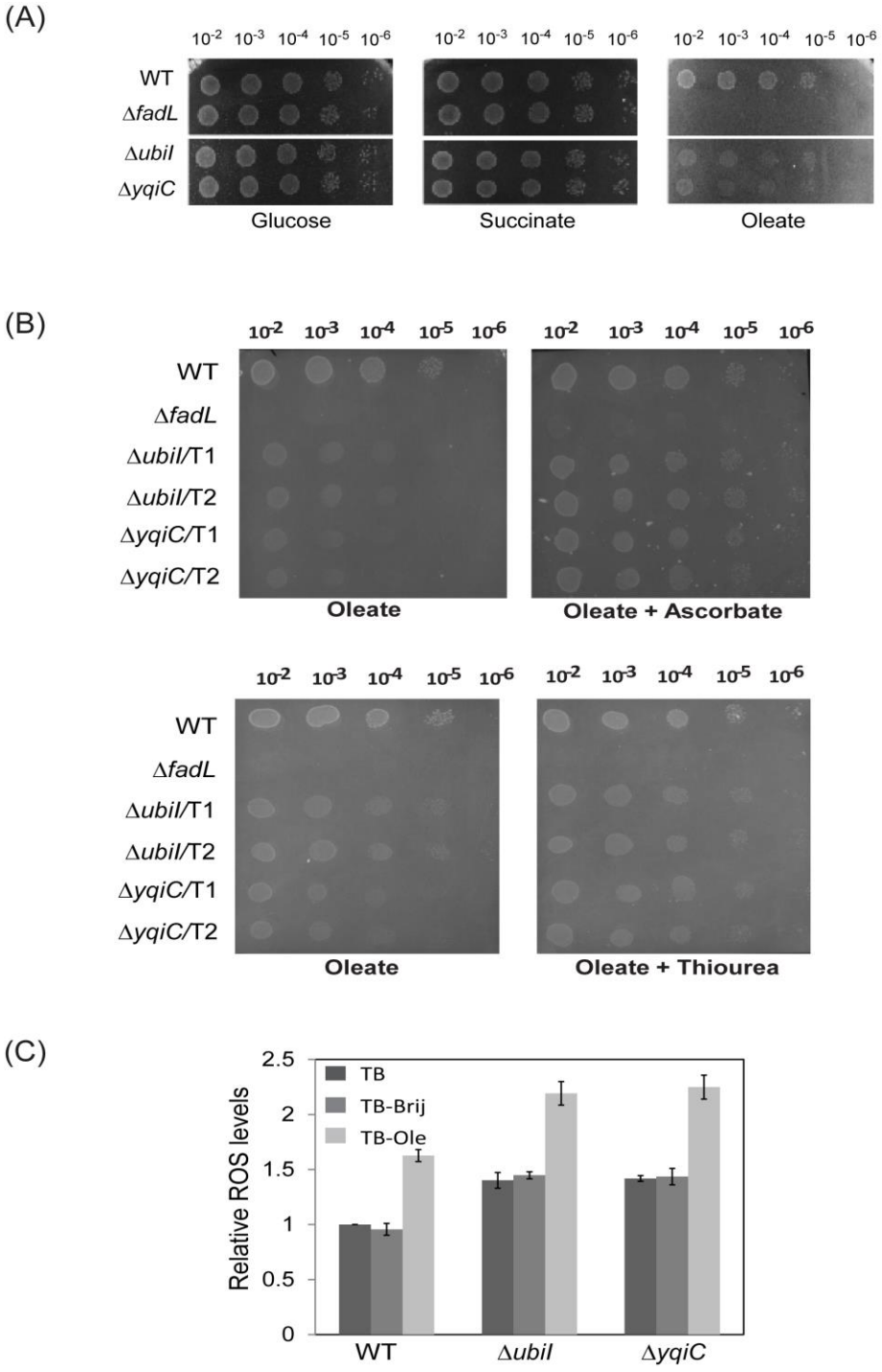

Figure 5.3 Δ*yqiC* exhibits phenotypes similar to Δ*ubiI*. (A) Δ*yqiC* shows significant growth defect only in oleate. Dilutions of the cultures were spotted on minimal medium containing one of the carbon sources: glucose, succinate or oleate. Each minimal medium condition had Brij-58. Δ*fadL* was used as a control. (B) The growth defect of Δ*yqiC* in minimal medium containing oleate is partially recovered by supplementing antioxidants. WT, Δ*fadL*, Δ*ubiI* and Δ*yqiC* strains were grown in minimal medium containing oleate with or without 0.5 mM ascorbate or 1 mM thiourea. T1 and T2 represent transductants of parent strains obtained from

the Keio library. (C) Δ*yqiC* has elevated ROS levels. WT, Δ*ubiI* and Δ*yqiC* strains were grown in TB, TB-Brij and TB-Ole. ROS levels were determined by NBT assay. Data were normalized to the ROS level of WT in TB and represent average (± S.D.) of 3 independent experiments.

5.2.3.3 *yqiC* is a novel ubiquinone biosynthesis gene

We determined ubiquinone levels in Δ*yqiC* strain through HPLC analysis. Because *yqiC* has strong correlation with *ubiI*, for comparison we also included Δ*ubiI* strain in our experiments. WT, Δ*ubiI* and Δ*yqiC* strains were grown in TB medium, lipid extracts were prepared and run on HPLC system. We found that similar to Δ*ubiI*, the total ubiquinone content in Δ*yqiC* was 15-20% of WT level (Fig. 5.4A). This result shows that *yqiC* is involved in ubiquinone biosynthesis. Figs. 5.4, B and C represent the merge chromatograms of lipid extracts from WT, Δ*ubiI* and Δ*yqiC* strains grown in TB medium with ubiquinone-8 standard at 275 nm (Fig. 5.4B) and with ubiquinol-8 standard at 290 nm (Fig. 5.4C). Δ*ubiI* and Δ*yqiC* strains show diminished peak for both ubiquinone-8 and ubiquinol-8. Intriguingly, similar to Δ*ubiI*, Δ*yqiC* also has a peak (Peak X) next to the peak for ubiquinone-8 (Result section 4.2.5.1, Chapter 4) (Hajj Chehade et al., 2013). Collectively, the similar growth pattern of *ubiI* and *yqiC* deletion strains in various carbon sources, elevated levels of ROS and same HPLC profile suggests involvement of these players in a common step of ubiquinone biosynthesis.

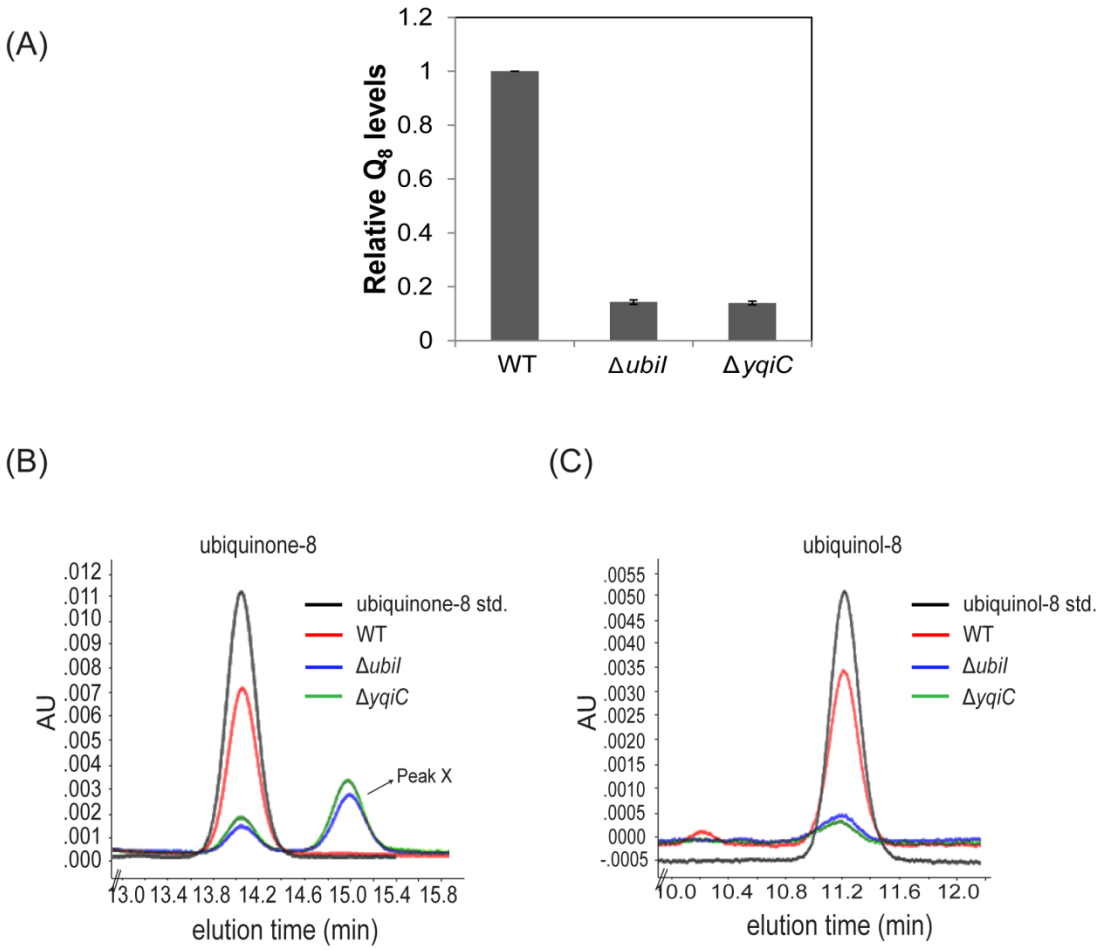

Figure 5.4 *yqiC* is identified as a new gene involved in ubiquinone biosynthesis. (A) WT, Δ*ubiI* and Δ*yqiC* cells were grown in TB, and the total Q_8 level in lipid extracts was determined. Q_8 levels were normalized to the Q_8 level of WT in TB and represent average (±S.D.) of 3 independent experiments. (B) HPLC-PDA analysis of ubiquinone-8 standard, lipid extracts from WT, Δ*ubiI* and Δ*yqiC* cells. Absorbance of ubiquinone-8 was determined at 275 nm. Peaks corresponding to ubiquinone-8, and an additional compound (Peak X) observed in Δ*ubiI* and Δ*yqiC* are indicated. (C) HPLC-PDA analysis of ubiquinol-8 standard, lipid extracts from WT, Δ*ubiI* and Δ*yqiC* cells. Absorbance of ubiquinol-8 was determined at 290 nm. Peak corresponding to ubiquinol-8 is indicated. The HPLC data was independently reproduced in (Balecha, 2017).

We ensured that the reduced level of ubiquinone in Δ*yqiC* strain was due to loss of YqiC by determining ubiquinone levels in Δ*yqiC* transformed with plasmid carrying *yqiC* (pSA4). Ubiquinone levels were restored to WT (Fig. 5.5A). Also, there

was no accumulation of the compound corresponding to Peak X in the complemented strain (Fig. 5.5B). Figs. 5.5, B and C represent the merge chromatograms for various strains for ubiquinone-8 at 275 nm (Fig. 5.5B) and ubiquinol-8 at 290 nm (Fig. 5.5C).

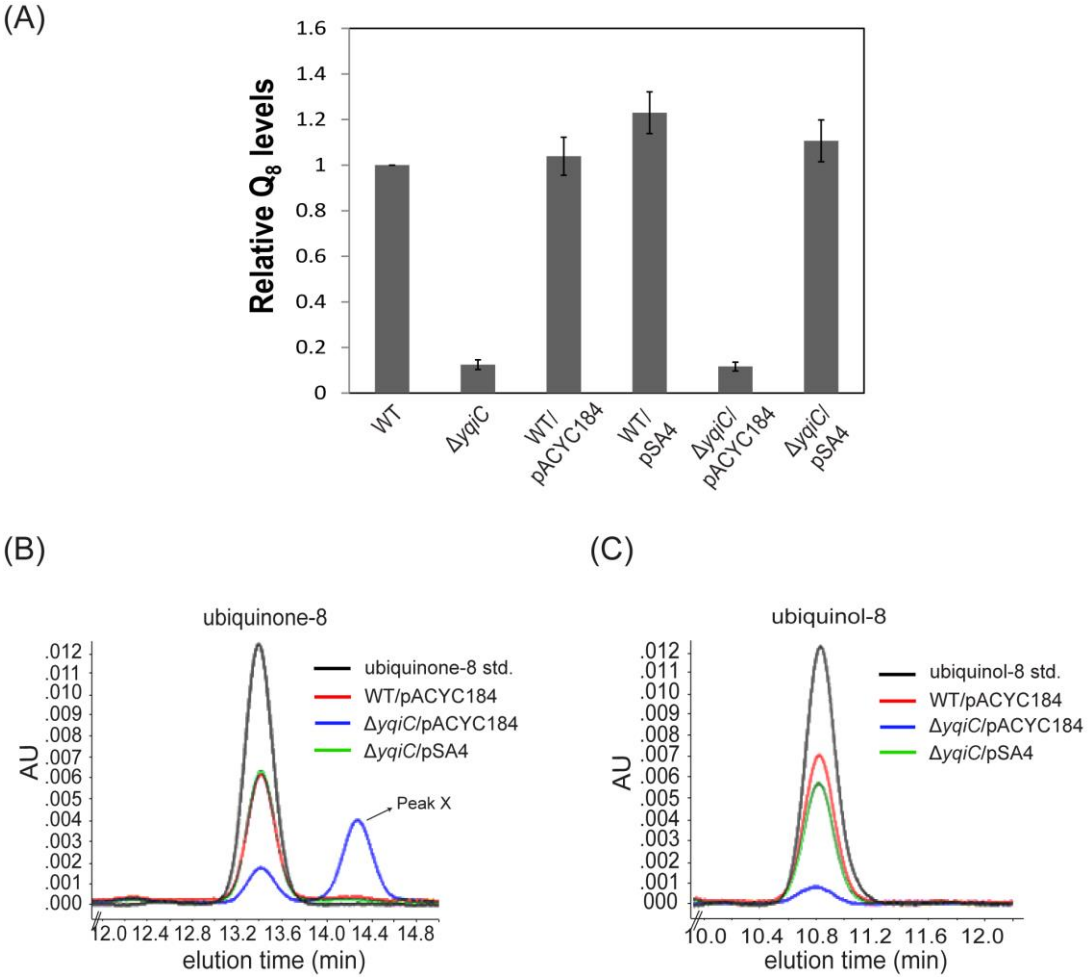

Figure 5.5 Q_8 levels are restored to WT in Δ*yqiC* cells transformed with plasmid carrying *yqiC*. (A) WT, Δ*yqiC*, WT carrying either pACYC184 or pSA4 and Δ*yqiC* cells transformed either with pACYC184 or pSA4 were grown in TB, and the total Q_8 level in lipid extracts was determined. Q_8 levels were normalized to the Q_8 level of WT in TB and represent average (± S.D.) of ≥4 independent experiments. (B) HPLC-PDA analysis of ubiquinone-8 standard, lipid extracts from WT transformed with pACYC184 and lipid extracts from Δ*yqiC* cells transformed either with pACYC184 or pSA4. Absorbance of ubiquinone-8 was determined at 275 nm. Peaks corresponding to ubiquinone-8 and an additional compound (Peak X) are indicated. (C) HPLC-PDA analysis of ubiquinol-8 standard, lipid extracts from WT transformed with pACYC184 and lipid extracts from Δ*yqiC*

cells transformed either with pACYC184 or pSA4. Absorbance of ubiquinol-8 was determined at 290 nm. Peak corresponding to ubiquinol-8 is indicated. The HPLC data was independently reproduced in (Balecha, 2017).

5.2.4. A novel genetic interaction between ubiquinone biosynthesis genes, *yqiC* and *ubiI*

The related phenotypes of Δ*ubiI* and Δ*yqiC* strains prompted us to examine the phenotype of the *ubiI-yqiC* double mutant. In this direction, we determined ubiquinone levels of the double mutant in LB-glucose medium as well as assessed its growth in various carbon sources.

5.2.4.1. *ubiI-yqiC* double mutant produces no detectable ubiquinone

In contrast to the normal growth of Δ*ubiI* and Δ*yqiC* strains in LB medium, the *ubiI-yqiC* double mutant formed tiny colonies on LB. Therefore, we resorted to growing the cultures in a rich LB-glucose medium where there is reduced dependence on ubiquinone for growth. WT, Δ*ubiI*, Δ*yqiC* and Δ*ubiI*Δ*yqiC* strains were grown in LB with 0.2% glucose, lipids were extracted and run on the HPLC system. In Δ*ubiI* and Δ*yqiC* strains the total ubiquinone content was reduced to ~30% of WT levels. Interestingly, there was no detectable ubiquinone in the *ubiI-yqiC* double mutant (Fig. 5.6A), suggesting redundancy in the ubiquinone biosynthesis pathway. Figs. 5.6, B and C show the merge chromatograms of lipid extracts from WT, Δ*ubiI*, Δ*yqiC* and Δ*ubiI*Δ*yqiC* strains for ubiquinone-8 at 275 nm (Fig. 5.6B) and ubiquinol-8 at 290 nm (Fig. 5.6C). Similar to Δ*ubiI* and Δ*yqiC* strains, an additional peak (Peak X) was also observed in the *ubiI-yqiC* double mutant (Fig. 5.6B).

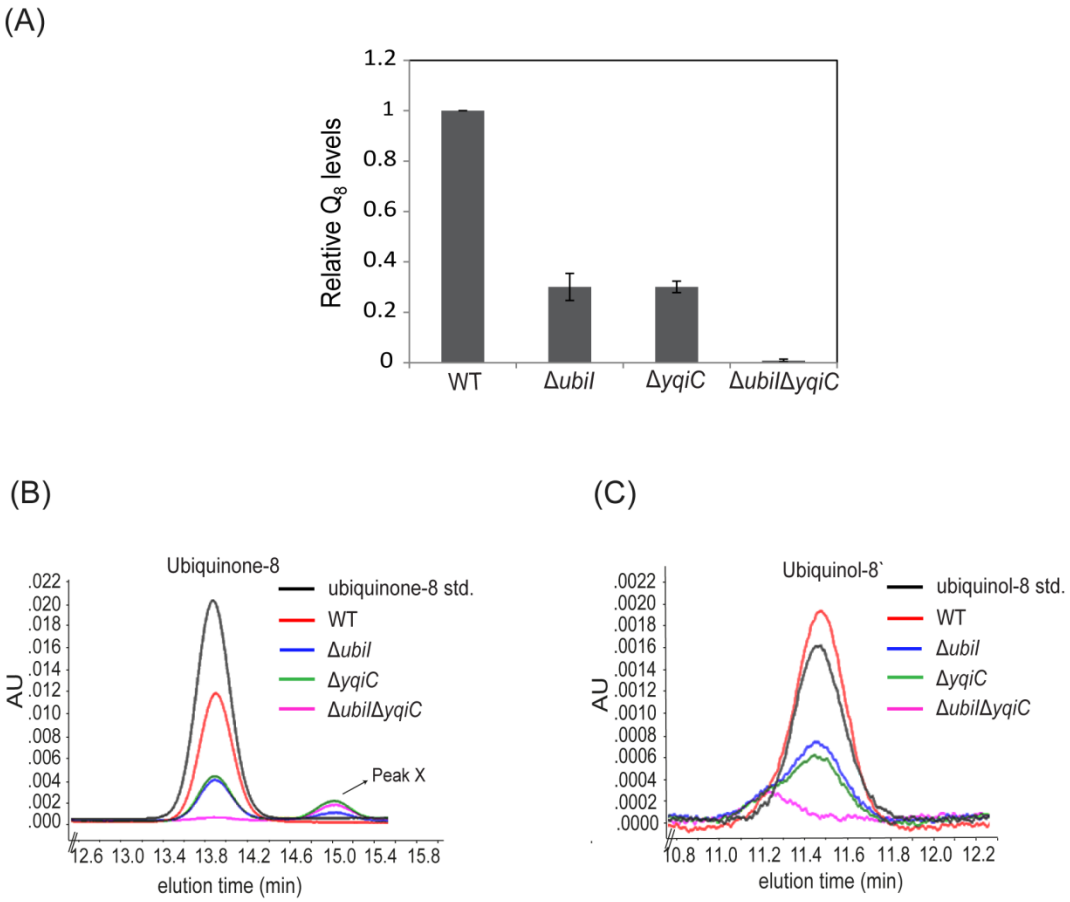

Figure 5.6 Ubiquinone is not detected in the *ubiI-yqiC* double mutant. (A) Total Q_8 level in lipid extracts from WT, Δ*ubiI*, Δ*yqiC* and Δ*ubiI*Δ*yqiC* cells grown in LB-glucose was determined. Q_8 levels were normalized to the Q_8 level of WT in LB-glucose and represent the average (± S.D.) of 3 independent experiments. (B) HPLC-PDA analysis of ubiquinone-8 standard, and lipid extracts from WT, Δ*ubiI*, Δ*yqiC* and Δ*ubiI*Δ*yqiC* cells. Absorbance of ubiquinone-8 was determined at 275 nm. Peaks corresponding to ubiquinone-8 and an additional compound (Peak X) are indicated. (C) HPLC-PDA analysis of ubiquinol-8 standard, and lipid extracts from WT, Δ*ubiI*, Δ*yqiC* and Δ*ubiI*Δ*yqiC* cells. Absorbance of ubiquinol-8 was determined at 290 nm. Peak corresponding to ubiquinol-8 is indicated. The HPLC data was independently reproduced in (Balecha, 2017).

5.2.4.2. *ubiI-yqiC* double mutant does not grow on non-fermentable carbon sources

Our results presented in chapter 4 showed that whereas *ubi* deletion strains with no detectable ubiquinone (Δ*ubiE*, Δ*ubiF* and Δ*ubiH*) exhibit growth defect in glucose, these strains do not grow at all in non-fermentable carbon sources, succinate and

oleate (Figs. 4.2, B, C and D, Chapter 4). Here, we created a double mutant, Δ*ubiI*Δ*yqiC* that produces no detectable ubiquinone. We therefore investigated whether this synthetic strain has a similar growth profile on different carbon sources as the single *ubi* deletion strains that do not produce ubiquinone. In this experiment, we included Δ*ubiE* strain for comparison. Similar to Δ*ubiE*, the *ubiI-yqiC* double mutant showed growth defect in glucose but did not grow at all in oleate and succinate (Fig. 5.7). Collectively, our results that a double mutant of *yqiC* and *ubiI*, shows synthetic sick/lethal phenotype with no detectable ubiquinone provides strong genetic evidence of the interaction between YqiC and UbiI.

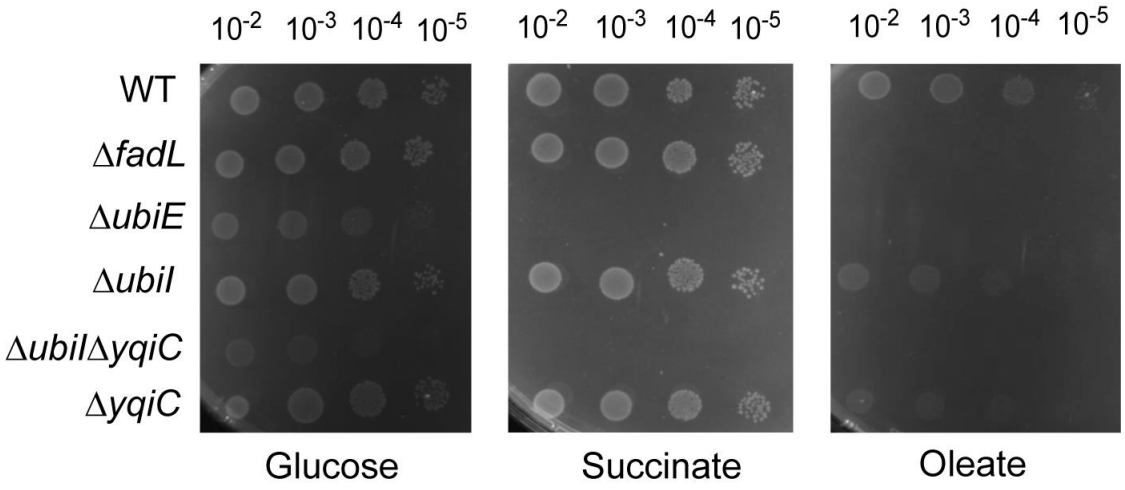

Figure 5.7 Δ*ubiI*Δ*yqiC* shows a synthetic sick/lethal phenotype in different carbon sources. Dilutions of the cultures were spotted on minimal medium containing one of the carbon sources; glucose, succinate or oleate. Each minimal medium condition had Brij-58. Δ*fadL* was used as a control.

5.3 Discussion

The increased requirement of ubiquinone for growth of *E. coli* in oleate compared to other carbon sources led us to analyze data from our LCFA screen with the objective to identify novel players involved in ubiquinone biosynthesis. In this chapter, we

established *yqiC* as a new ubiquinone biosynthesis gene. Importantly, we found that the phenotypes of *ubiI* and *yqiC* deletion strains are related. Both strains show ~80% reduction in ubiquinone levels, accumulate same pathway compound, show significant growth defect only in oleate and exhibit elevated levels of ROS (Figs. 5.3 and 5.4). The related phenotypes of *ubiI* and *yqiC* mutants led us to investigate the phenotype of *ubiI-yqiC* double mutant. Importantly, the double mutant showed no detectable ubiquinone (Fig. 5.6), and whereas it exhibited growth defect in glucose, the double mutant did not grow at all with oleate and succinate (Fig. 5.7). These data suggest functional redundancy between *ubiI* and *yqiC*. To further explore this, in another set of experiments in our lab, we find that whereas transforming *ubiI* on multicopy plasmid does not recover the growth of Δ*yqiC* strain on oleate, multicopy *yqiC* recovers the growth of Δ*ubiI* strain after prolonged incubation (Balecha 2017). Collectively, our results besides identifying *yqiC* as a novel ubiquinone biosynthesis player provide a genetic evidence of the redundancy between *ubiI* and *yqiC*.

On the basis of biochemical and biophysical features such as high α-helical content, coiled-coil domain involved in trimerization and membrane fusions *in vitro*, YqiC from *Salmonella typhimurium* was reported to be a member of the *Brucella* membrane fusogenic protein (BMFP) family. Further, in this study, the *yqiC* deletion strain was severely attenuated for virulence in the murine model (Carrica et al., 2011). While our work was in progress, in another study in *S. typhimurium*, *yqiC* was shown to be involved in bacterial colonization and invasion, biofilm formation, motility, regulation of flagella and fimbriae expression, and induction of host innate immunity post-infection. Further, in the same study, based on the absence of menaquinone-8 peak in HPLC in *yqiC* mutant, *yqiC* was reported to be a menaquinone biosynthesis player (Wang et al., 2016). Contrary to the above report, a recent study in *E. coli*

showed that menaquinone biosynthesis is not impaired in a *yqiC* mutant, however, ubiquinone-8 levels are reduced by ~80% (Loiseau et al., 2017). The discrepancy between the two studies is suggested to be due to the erroneous identification of *S. typhimurium* endogenous menaquinone (Wang et al., 2016) since these authors used vitamin K2 (menaquinone-4) as a standard to assign menaquinone-8 peak in HPLC of *S. typhimurium* lipid extracts, even though menaquinone-4 and menaquinone-8 have very different retention times on C-18 column. Our findings that *yqiC* deletion strain has ~20% ubiquinone-8 levels (Fig. 5.4) are entirely consistent with the results of Loiseau et al. (Loiseau et al., 2017). Hence, *yqiC* is a bona fide ubiquinone biosynthesis player. Because of its involvement in ubiquinone biosynthesis, YqiC has been renamed as UbiK (Loiseau et al., 2017).

E. coli UbiK was reported to physically interact with a non-enzymatic ubiquinone biosynthesis player, UbiJ, and proposed to be an assembly factor for additional Ubi proteins. Further, the UbiK–UbiJ complex was shown to interact with palmitoleic acid, a major lipid in *E. coli*; an observation consistent with the idea that the UbiK-UbiJ complex might serve as a platform for the assembly of mega complex of ubiquinone biosynthesis players in the membrane (Loiseau et al., 2017). Our result that a double mutant of *ubiK* and *ubiI* shows synthetic sick/lethal phenotype with no detectable ubiquinone provides strong genetic evidence of the interaction between UbiK and other Ubi proteins. Furthermore, additional data from our lab that multicopy *ubiK* recovers the growth of Δ*ubiI* strain in oleate suggest that overexpression of UbiK in Δ*ubiI* strain stabilizes a Ubi protein which has functional redundancy with UbiI. In fact, in a previous study, the residual level of ubiquinone in a Δ*ubiI* strain was attributed to the suboptimal C5-hydroxylase activity of a C6-monooxygenase, UbiF (Hajj Chehade et al., 2013). Therefore, overexpression of

UbiK might stabilize UbiF in the mega complex, which allows for suboptimal ubiquinone biosynthesis in the absence of UbiI.

Despite extensive study of the ubiquinone biosynthesis pathway over the past several decades, our high-throughput genetic screen on LCFAs identified a new ubiquinone biosynthesis player, *yqiC*. We suggest that our LCFA dataset can be mined further to identify additional missing players of the ubiquinone biosynthesis pathway.

CHAPTER VI

Bibliography

Al-Attar, S., Yu, Y., Pinkse, M., Hoeser, J., Friedrich, T., Bald, D., and de Vries, S. (2016). Cytochrome bd Displays Significant Quinol Peroxidase Activity. Scientific reports *6*, 27631.

Albesa, I., Becerra, M.C., Battan, P.C., and Paez, P.L. (2004). Oxidative stress involved in the antibacterial action of different antibiotics. Biochemical and biophysical research communications *317*, 605-609.

Alvarez, A.F., Rodriguez, C., and Georgellis, D. (2013). Ubiquinone and menaquinone electron carriers represent the yin and yang in the redox regulation of the ArcB sensor kinase. Journal of bacteriology *195*, 3054-3061.

Aussel, L., Loiseau, L., Hajj Chehade, M., Pocachard, B., Fontecave, M., Pierrel, F., and Barras, F. (2014a). *ubiJ*, a new gene required for aerobic growth and proliferation in macrophage, is involved in coenzyme Q biosynthesis in *Escherichia coli* and *Salmonella enterica* serovar Typhimurium. J Bacteriol *196*, 70-79.

Aussel, L., Pierrel, F., Loiseau, L., Lombard, M., Fontecave, M., and Barras, F. (2014b). Biosynthesis and physiology of coenzyme Q in bacteria. Biochimica et biophysica acta *1837*, 1004-1011.

Ayala, A., Munoz, M.F., and Arguelles, S. (2014). Lipid peroxidation: production, metabolism, and signaling mechanisms of malondialdehyde and 4-hydroxy-2-nonenal. Oxidative medicine and cellular longevity *2014*, 360438.

Baba, T., Ara, T., Hasegawa, M., Takai, Y., Okumura, Y., Baba, M., Datsenko, K.A., Tomita, M., Wanner, B.L., and Mori, H. (2006). Construction of *Escherichia coli* K-12 in-frame, single-gene knockout mutants: the Keio collection. Mol Syst Biol *2*, 2006 0008.

Balecha, H. (2017). Identifying new players involved in ubiquinone biosynthesis in *Escherichia coli* (Thesis submitted to Indian Institute of Science Education and Research Mohali, India, for BS-MS dual degree).

Bar-Tana, J., Howlett, B.J., and Hertz, R. (1980). Ubiquinone synthetic pathway in flagellation of *Salmonella typhimurium*. Journal of bacteriology *143*, 637-643.

Bardwell, J.C., McGovern, K., and Beckwith, J. (1991). Identification of a protein required for disulfide bond formation in vivo. Cell *67*, 581-589.

Bekker, M., Alexeeva, S., Laan, W., Sawers, G., Teixeira de Mattos, J., and Hellingwerf, K. (2010). The ArcBA two-component system of *Escherichia coli* is regulated by the redox state of both the ubiquinone and the menaquinone pool. Journal of bacteriology *192*, 746-754.

Bekker, M., de Vries, S., Ter Beek, A., Hellingwerf, K.J., and de Mattos, M.J. (2009). Respiration of *Escherichia coli* can be fully uncoupled via the nonelectrogenic terminal cytochrome bd-II oxidase. Journal of bacteriology *191*, 5510-5517.

Benov, L., Chang, L.Y., Day, B., and Fridovich, I. (1995). Copper, zinc superoxide dismutase in *Escherichia coli*: periplasmic localization. Archives of biochemistry and biophysics *319*, 508-511.

Benov, L.T., and Fridovich, I. (1994). *Escherichia coli* expresses a copper- and zinc-containing superoxide dismutase. The Journal of biological chemistry *269*, 25310-25314.
Berger, E.A. (1973). Different mechanisms of energy coupling for the active transport of proline and glutamine in *Escherichia coli*. Proceedings of the National Academy of Sciences of the United States of America *70*, 1514-1518.
Bernal, V., Castano-Cerezo, S., and Canovas, M. (2016). Acetate metabolism regulation in *Escherichia coli:* carbon overflow, pathogenicity, and beyond. Appl Microbiol Biotechnol *100*, 8985-9001.
Berridge, M.V., Herst, P.M., and Tan, A.S. (2005). Tetrazolium dyes as tools in cell biology: new insights into their cellular reduction. Biotechnology annual review *11*, 127-152.
Black, P.N., and DiRusso, C.C. (2003). Transmembrane movement of exogenous long-chain fatty acids: proteins, enzymes, and vectorial esterification. Microbiology and molecular biology reviews : MMBR *67*, 454-472, table of contents.
Borisov, V.B., Gennis, R.B., Hemp, J., and Verkhovsky, M.I. (2011a). The cytochrome bd respiratory oxygen reductases. Biochimica et biophysica acta *1807*, 1398-1413.
Borisov, V.B., Murali, R., Verkhovskaya, M.L., Bloch, D.A., Han, H., Gennis, R.B., and Verkhovsky, M.I. (2011b). Aerobic respiratory chain of *Escherichia coli* is not allowed to work in fully uncoupled mode. Proceedings of the National Academy of Sciences of the United States of America *108*, 17320-17324.
Braun, M., Bungert, S., and Friedrich, T. (1998). Characterization of the overproduced NADH dehydrogenase fragment of the NADH:ubiquinone oxidoreductase (complex I) from *Escherichia coli*. Biochemistry *37*, 1861-1867.
Campbell, J.W., and Cronan, J.E., Jr. (2002). The enigmatic *Escherichia coli fadE* gene is *yafH*. Journal of bacteriology *184*, 3759-3764.
Campbell, J.W., Morgan-Kiss, R.M., and Cronan, J.E., Jr. (2003). A new *Escherichia coli* metabolic competency: growth on fatty acids by a novel anaerobic beta-oxidation pathway. Molecular microbiology *47*, 793-805.
Cap, M., Vachova, L., and Palkova, Z. (2012). Reactive oxygen species in the signaling and adaptation of multicellular microbial communities. Oxidative medicine and cellular longevity *2012*, 976753.
Capaldi, R.A., Schulenberg, B., Murray, J., and Aggeler, R. (2000). Cross-linking and electron microscopy studies of the structure and functioning of the *Escherichia coli* ATP synthase. The Journal of experimental biology *203*, 29-33.
Carmel-Harel, O., and Storz, G. (2000). Roles of the glutathione- and thioredoxin-dependent reduction systems in the *Escherichia coli* and saccharomyces cerevisiae responses to oxidative stress. Annu Rev Microbiol *54*, 439-461.
Carrica, M.C., Craig, P.O., Garcia-Angulo, V.A., Aguirre, A., Garcia-Vescovi, E., Goldbaum, F.A., and Cravero, S.L. (2011). YqiC of *Salmonella enterica* serovar Typhimurium is a membrane fusogenic protein required for mice colonization. BMC microbiology *11*, 95.

Chang, A.C., and Cohen, S.N. (1978). Construction and characterization of amplifiable multicopy DNA cloning vehicles derived from the P15A cryptic miniplasmid. Journal of bacteriology *134*, 1141-1156.
Cheng, V.W., Ma, E., Zhao, Z., Rothery, R.A., and Weiner, J.H. (2006). The iron-sulfur clusters in *Escherichia coli* succinate dehydrogenase direct electron flow. The Journal of biological chemistry *281*, 27662-27668.
Chiang, S.M., and Schellhorn, H.E. (2012). Regulators of oxidative stress response genes in *Escherichia coli* and their functional conservation in bacteria. Archives of biochemistry and biophysics *525*, 161-169.
Chisti, Y. (2007). Biodiesel from microalgae. Biotechnology advances *25*, 294-306.
Cho, B.K., Knight, E.M., and Palsson, B.O. (2006). Transcriptional regulation of the *fad* regulon genes of *Escherichia coli* by ArcA. Microbiology *152*, 2207-2219.
Chueca, B., Pagan, R., and Garcia-Gonzalo, D. (2014). Differential mechanism of *Escherichia coli* Inactivation by (+)-limonene as a function of cell physiological state and drug's concentration. PloS one *9*, e94072.
Clark, D.P., and Cronan, J.E. (2005). Two-Carbon Compounds and Fatty Acids as Carbon Sources. EcoSal Plus *1*.
Collins, S.R., Schuldiner, M., Krogan, N.J., and Weissman, J.S. (2006). A strategy for extracting and analyzing large-scale quantitative epistatic interaction data. Genome biology *7*, R63.
Cox, G.B., Gibson, F., and Pittard, J. (1968). Mutant strains of *Escherichia coli* K-12 unable to form ubiquinone. Journal of bacteriology *95*, 1591-1598.
Cox, G.B., Newton, N.A., Gibson, F., Snoswell, A.M., and Hamilton, J.A. (1970). The function of ubiquinone in *Escherichia coli*. The Biochemical journal *117*, 551-562.
Cox, G.B., Young, I.G., McCann, L.M., and Gibson, F. (1969). Biosynthesis of ubiquinone in Escherichia coli K-12: location of genes affecting the metabolism of 3-octaprenyl-4-hydroxybenzoic acid and 2-octaprenylphenol. J Bacteriol *99*, 450-458.
Cronan, J.E., Jr., and Laporte, D. (2005). Tricarboxylic Acid Cycle and Glyoxylate Bypass. EcoSal Plus *1*.
Cronan, J.E., Jr., and Subrahmanyam, S. (1998). FadR, transcriptional co-ordination of metabolic expediency. Molecular microbiology *29*, 937-943.
Cummings, C.A., Bootsma, H.J., Relman, D.A., and Miller, J.F. (2006). Species- and strain-specific control of a complex, flexible regulon by *Bordetella* BvgAS. Journal of bacteriology *188*, 1775-1785.
Datsenko, K.A., and Wanner, B.L. (2000). One-step inactivation of chromosomal genes in *Escherichia coli* K-12 using PCR products. Proceedings of the National Academy of Sciences of the United States of America *97*, 6640-6645.
Dellomonaco, C., Rivera, C., Campbell, P., and Gonzalez, R. (2010). Engineered respiro-fermentative metabolism for the production of biofuels and biochemicals from fatty acid-rich feedstocks. Appl Environ Microbiol *76*, 5067-5078.
Doi, H., Hoshino, Y., Nakase, K., and Usuda, Y. (2014). Reduction of hydrogen peroxide stress derived from fatty acid beta-oxidation improves fatty acid utilization in *Escherichia coli*. Appl Microbiol Biotechnol *98*, 629-639.

Dwyer, D.J., Belenky, P.A., Yang, J.H., MacDonald, I.C., Martell, J.D., Takahashi, N., Chan, C.T., Lobritz, M.A., Braff, D., Schwarz, E.G.*, et al.* (2014). Antibiotics induce redox-related physiological alterations as part of their lethality. Proceedings of the National Academy of Sciences of the United States of America *111*, E2100-2109.
Erhardt, H., Steimle, S., Muders, V., Pohl, T., Walter, J., and Friedrich, T. (2012). Disruption of individual *nuo*-genes leads to the formation of partially assembled NADH:ubiquinone oxidoreductase (complex I) in *Escherichia coli*. Biochimica et biophysica acta *1817*, 863-871.
Esterhazy, D., King, M.S., Yakovlev, G., and Hirst, J. (2008). Production of reactive oxygen species by complex I (NADH:ubiquinone oxidoreductase) from *Escherichia coli* and comparison to the enzyme from mitochondria. Biochemistry *47*, 3964-3971.
Euro, L., Bloch, D.A., Wikstrom, M., Verkhovsky, M.I., and Verkhovskaya, M. (2008). Electrostatic interactions between FeS clusters in NADH:ubiquinone oxidoreductase (Complex I) from *Escherichia coli*. Biochemistry *47*, 3185-3193.
Ezraty, B., Vergnes, A., Banzhaf, M., Duverger, Y., Huguenot, A., Brochado, A.R., Su, S.Y., Espinosa, L., Loiseau, L., Py, B.*, et al.* (2013). Fe-S cluster biosynthesis controls uptake of aminoglycosides in a ROS-less death pathway. Science *340*, 1583-1587.
Fang, F.C., Libby, S.J., Castor, M.E., and Fung, A.M. (2005). Isocitrate lyase (AceA) is required for *Salmonella* persistence but not for acute lethal infection in mice. Infect Immun *73*, 2547-2549.
Farr, S.B., and Kogoma, T. (1991). Oxidative stress responses in E*scherichia coli* and *Salmonella typhimurium.* Microbiological reviews *55*, 561-585.
Feng, Y., and Cronan, J.E. (2009). *Escherichia coli* unsaturated fatty acid synthesis: complex transcription of the *fabA* gene and in vivo identification of the essential reaction catalyzed by FabB. The Journal of biological chemistry *284*, 29526-29535.
Friedrich, T., and Pohl, T. (2007). NADH as Donor. EcoSal Plus *2*.
Fuentes, A.M., and Amabile-Cuevas, C.F. (1998). Antioxidant vitamins C and E affect the superoxide-mediated induction of the *soxRS* regulon of *Escherichia coli*. Microbiology *144 (Pt 7)*, 1731-1736.
Fujita, Y., Matsuoka, H., and Hirooka, K. (2007). Regulation of fatty acid metabolism in bacteria. Molecular microbiology *66*, 829-839.
Georgellis, D., Kwon, O., and Lin, E.C. (2001). Quinones as the redox signal for the arc two-component system of bacteria. Science *292*, 2314-2316.
Gibert, I., Llagostera, M., and Barbe, J. (1988). Regulation of *ubiG* gene expression in *Escherichia coli*. Journal of bacteriology *170*, 1346-1349.
Giles, D.K., Hankins, J.V., Guan, Z., and Trent, M.S. (2011). Remodelling of the *Vibrio cholerae* membrane by incorporation of exogenous fatty acids from host and aquatic environments. Mol Microbiol *79*, 716-728.
Gomez, F., Monsalve, G.C., Tse, V., Saiki, R., Weng, E., Lee, L., Srinivasan, C., Frand, A.R., and Clarke, C.F. (2012). Delayed accumulation of intestinal coliform bacteria enhances life span and stress resistance in *Caenorhabditis elegans* fed respiratory deficient *E. coli*. BMC microbiology *12*, 300.

Gong, X., Xie, T., Yu, L., Hesterberg, M., Scheide, D., Friedrich, T., and Yu, C.A. (2003). The ubiquinone-binding site in NADH:ubiquinone oxidoreductase from *Escherichia coli*. The Journal of biological chemistry *278*, 25731-25737.
Gonzalez-Flecha, B., and Demple, B. (1995). Metabolic sources of hydrogen peroxide in aerobically growing *Escherichia coli*. The Journal of biological chemistry *270*, 13681-13687.
Gort, A.S., Ferber, D.M., and Imlay, J.A. (1999). The regulation and role of the periplasmic copper, zinc superoxide dismutase of *Escherichia coli*. Molecular microbiology *32*, 179-191.
Gu, M., and Imlay, J.A. (2011). The SoxRS response of *Escherichia coli* is directly activated by redox-cycling drugs rather than by superoxide. Molecular microbiology *79*, 1136-1150.
Gulmezian, M., Hyman, K.R., Marbois, B.N., Clarke, C.F., and Javor, G.T. (2007). The role of UbiX in *Escherichia coli* coenzyme Q biosynthesis. Archives of biochemistry and biophysics *467*, 144-153.
Guzman, L.M., Belin, D., Carson, M.J., and Beckwith, J. (1995). Tight regulation, modulation, and high-level expression by vectors containing the arabinose PBAD promoter. Journal of bacteriology *177*, 4121-4130.
Hajj Chehade, M., Loiseau, L., Lombard, M., Pecqueur, L., Ismail, A., Smadja, M., Golinelli-Pimpaneau, B., Mellot-Draznieks, C., Hamelin, O., Aussel, L.*, et al.* (2013). *ubiI*, a new gene in *Escherichia coli* coenzyme Q biosynthesis, is involved in aerobic C5-hydroxylation. The Journal of biological chemistry *288*, 20085-20092.
Hatfield, G.W. (2008). Amino Acid Metabolism and Fluxes. EcoSal Plus *3*.
Hill, J.J., Alben, J.O., and Gennis, R.B. (1993). Spectroscopic evidence for a heme-heme binuclear center in the cytochrome bd ubiquinol oxidase from *Escherichia coli*. Proceedings of the National Academy of Sciences of the United States of America *90*, 5863-5867.
Hillar, A., Peters, B., Pauls, R., Loboda, A., Zhang, H., Mauk, A.G., and Loewen, P.C. (2000). Modulation of the activities of catalase-peroxidase HPI of *Escherichia coli* by site-directed mutagenesis. Biochemistry *39*, 5868-5875.
Hsu, A.Y., Poon, W.W., Shepherd, J.A., Myles, D.C., and Clarke, C.F. (1996). Complementation of coq3 mutant yeast by mitochondrial targeting of the *Escherichia coli* UbiG polypeptide: evidence that UbiG catalyzes both O-methylation steps in ubiquinone biosynthesis. Biochemistry *35*, 9797-9806.
Imlay, J.A. (2003). Pathways of oxidative damage. Annu Rev Microbiol *57*, 395-418.
Imlay, J.A. (2013). The molecular mechanisms and physiological consequences of oxidative stress: lessons from a model bacterium. Nature reviews Microbiology *11*, 443-454.
Iram, S.H., and Cronan, J.E. (2006). The beta-oxidation systems of *Escherichia col*i and *Salmonella enterica* are not functionally equivalent. Journal of bacteriology *188*, 599-608.
Jang, S., and Imlay, J.A. (2010). Hydrogen peroxide inactivates the *Escherichia coli* Isc iron-sulphur assembly system, and OxyR induces the Suf system to compensate. Molecular microbiology *78*, 1448-1467.
Kaila, V.R., Wikstrom, M., and Hummer, G. (2014). Electrostatics, hydration, and proton transfer dynamics in the membrane domain of respiratory complex

I. Proceedings of the National Academy of Sciences of the United States of America *111*, 6988-6993.
Kamariah, N., Manimekalai, M.S., Nartey, W., Eisenhaber, F., Eisenhaber, B., and Gruber, G. (2015). Crystallographic and solution studies of NAD(+)- and NADH-bound alkylhydroperoxide reductase subunit F (AhpF) from *Escherichia coli* provide insight into sequential enzymatic steps. Biochimica et biophysica acta *1847*, 1139-1152.
Kang, Y., Zarzycki-Siek, J., Walton, C.B., Norris, M.H., and Hoang, T.T. (2010). Multiple FadD acyl-CoA synthetases contribute to differential fatty acid degradation and virulence in *Pseudomonas aeruginosa*. PloS one *5*, e13557.
Kargalioglu, Y., and Imlay, J.A. (1994). Importance of anaerobic superoxide dismutase synthesis in facilitating outgrowth of *Escherichia coli* upon entry into an aerobic habitat. Journal of bacteriology *176*, 7653-7658.
Keseler, I.M., Mackie, A., Peralta-Gil, M., Santos-Zavaleta, A., Gama-Castro, S., Bonavides-Martinez, C., Fulcher, C., Huerta, A.M., Kothari, A., Krummenacker, M.*, et al.* (2013). EcoCyc: fusing model organism databases with systems biology. Nucleic acids research *41*, D605-612.
Klein, K., Steinberg, R., Fiethen, B., and Overath, P. (1971). Fatty acid degradation in *Escherichia coli*. An inducible system for the uptake of fatty acids and further characterization of old mutants. Eur J Biochem *19*, 442-450.
Knoell, H.E. (1979). Isolation of a soluble enzyme complex comprising the ubiquinone-8 synthesis apparatus from the cytoplasmic membrane of *Escherichia coli*. Biochemical and biophysical research communications *91*, 919-925.
Kobayashi, T., Kishigami, S., Sone, M., Inokuchi, H., Mogi, T., and Ito, K. (1997). Respiratory chain is required to maintain oxidized states of the DsbA-DsbB disulfide bond formation system in aerobically growing *Escherichia coli* cells. Proceedings of the National Academy of Sciences of the United States of America *94*, 11857-11862.
Kotnik, D., J.-K. P., Krizman, M., Zibert, T., Prosek, M., and Smidovnik, A. (2013). Rapid and sensitive HPLC-MS/MS method for quantitative determination of CoQ10. Res Precision Instrument Mach *2*, 6-13.
Kwon, O., Kotsakis, A., and Meganathan, R. (2000). Ubiquinone (coenzyme Q) biosynthesis in *Escherichia coli*: identification of the *ubiF* gene. FEMS microbiology letters *186*, 157-161.
Lawrence, J., Cox, G.B., and Gibson, F. (1974). Biosynthesis of ubiquinone in *Escherichia coli* K-12: biochemical and genetic characterization of a mutant unable to convert chorismate into 4-hydroxybenzoate. J Bacteriol *118*, 41-45.
Layer, G., Reichelt, J., Jahn, D., and Heinz, D.W. (2010). Structure and function of enzymes in heme biosynthesis. Protein science : a publication of the Protein Society *19*, 1137-1161.
Lee, P.T., Hsu, A.Y., Ha, H.T., and Clarke, C.F. (1997). A C-methyltransferase involved in both ubiquinone and menaquinone biosynthesis: isolation and identification of the *Escherichia coli ubiE* gene. Journal of bacteriology *179*, 1748-1754.
Leif, H., Sled, V.D., Ohnishi, T., Weiss, H., and Friedrich, T. (1995). Isolation and characterization of the proton-translocating NADH: ubiquinone oxidoreductase from *Escherichia coli*. European journal of biochemistry *230*, 538-548.

Lennen, R.M., Kruziki, M.A., Kumar, K., Zinkel, R.A., Burnum, K.E., Lipton, M.S., Hoover, S.W., Ranatunga, D.R., Wittkopp, T.M., Marner, W.D., 2nd*, et al.* (2011). Membrane stresses induced by overproduction of free fatty acids in *Escherichia coli*. Appl Environ Microbiol *77*, 8114-8128.
Lepore, B.W., Indic, M., Pham, H., Hearn, E.M., Patel, D.R., and van den Berg, B. (2011). Ligand-gated diffusion across the bacterial outer membrane. Proceedings of the National Academy of Sciences of the United States of America *108*, 10121-10126.
Liang, X., Thorpe, C., and Schulz, H. (2000). 2,4-Dienoyl-CoA reductase from *Escherichia coli* is a novel iron-sulfur flavoprotein that functions in fatty acid beta-oxidation. Archives of biochemistry and biophysics *380*, 373-379.
Loewen, P.C., and Switala, J. (1986). Purification and characterization of catalase HPII from Escherichia coli K12. Biochemistry and cell biology = Biochimie et biologie cellulaire *64*, 638-646.
Loiseau, L., Fyfe, C., Aussel, L., Hajj Chehade, M., Hernandez, S.B., Faivre, B., Hamdane, D., Mellot-Draznieks, C., Rascalou, B., Pelosi, L.*, et al.* (2017). The UbiK protein is an accessory factor necessary for bacterial ubiquinone (UQ) biosynthesis and forms a complex with the UQ biogenesis factor UbiJ. The Journal of biological chemistry *292*, 11937-11950.
Lukas, H., Reimann, J., Kim, O.B., Grimpo, J., and Unden, G. (2010). Regulation of aerobic and anaerobic D-malate metabolism of *Escherichia coli* by the LysR-type regulator DmlR (YeaT). Journal of bacteriology *192*, 2503-2511.
Macinga, D.R., Cook, G.M., Poole, R.K., and Rather, P.N. (1998). Identification and characterization of *aarF*, a locus required for production of ubiquinone in *Providencia stuartii* and *Escherichia coli* and for expression of 2'-N-acetyltransferase in P. stuartii. Journal of bacteriology *180*, 128-135.
Maklashina, E., Rajagukguk, S., Starbird, C.A., McDonald, W.H., Koganitsky, A., Eisenbach, M., Iverson, T.M., and Cecchini, G. (2016). Binding of the Covalent Flavin Assembly Factor to the Flavoprotein Subunit of Complex II. The Journal of biological chemistry *291*, 2904-2916.
Maloy, S.R., Ginsburgh, C.L., Simons, R.W., and Nunn, W.D. (1981). Transport of long and medium chain fatty acids by *Escherichia coli* K12. The Journal of biological chemistry *256*, 3735-3742.
Malpica, R., Sandoval, G.R., Rodriguez, C., Franco, B., and Georgellis, D. (2006). Signaling by the arc two-component system provides a link between the redox state of the quinone pool and gene expression. Antioxidants & redox signaling *8*, 781-795.
Marathe, S.A., Kumar, R., Ajitkumar, P., Nagaraja, V., and Chakravortty, D. (2013). Curcumin reduces the antimicrobial activity of ciprofloxacin against *Salmonella typhimurium* and *Salmonella typhi*. The Journal of antimicrobial chemotherapy *68*, 139-152.
Martinez-Vallespin, B., Vahjen, W., and Zentek, J. (2016). Effects of medium-chain fatty acids on the structure and immune response of IPEC-J2 cells. Cytotechnology *68*, 1925-1936.
Masse, E., Vanderpool, C.K., and Gottesman, S. (2005). Effect of RyhB small RNA on global iron use in *Escherichia coli*. Journal of bacteriology *187*, 6962-6971.

Matsumoto, Y., Murai, M., Fujita, D., Sakamoto, K., Miyoshi, H., Yoshida, M., and Mogi, T. (2006). Mass spectrometric analysis of the ubiquinol-binding site in cytochrome bd from *Escherichia coli*. The Journal of biological chemistry *281*, 1905-1912.
Matsuoka, H., Hirooka, K., and Fujita, Y. (2007). Organization and function of the YsiA regulon of *Bacillus subtilis* involved in fatty acid degradation. The Journal of biological chemistry *282*, 5180-5194.
Matsushita, K., Ohnishi, T., and Kaback, H.R. (1987). NADH-ubiquinone oxidoreductases of the *Escherichia coli* aerobic respiratory chain. Biochemistry *26*, 7732-7737.
Mattam, A.J., and Yazdani, S.S. (2013). Engineering *E. coli* strain for conversion of short chain fatty acids to bioalcohols. Biotechnology for biofuels *6*, 128.
McKinney, J.D., Honer zu Bentrup, K., Munoz-Elias, E.J., Miczak, A., Chen, B., Chan, W.T., Swenson, D., Sacchettini, J.C., Jacobs, W.R., Jr., and Russell, D.G. (2000). Persistence of *Mycobacterium tuberculosis* in macrophages and mice requires the glyoxylate shunt enzyme isocitrate lyase. Nature *406*, 735-738.
McNeil, M.B., Clulow, J.S., Wilf, N.M., Salmond, G.P., and Fineran, P.C. (2012). SdhE is a conserved protein required for flavinylation of succinate dehydrogenase in bacteria. The Journal of biological chemistry *287*, 18418-18428.
Meganathan, R. (2001). Ubiquinone biosynthesis in microorganisms. FEMS microbiology letters *203*, 131-139.
Messner, K.R., and Imlay, J.A. (1999). The identification of primary sites of superoxide and hydrogen peroxide formation in the aerobic respiratory chain and sulfite reductase complex of *Escherichia coli*. The Journal of biological chemistry *274*, 10119-10128.
Messner, K.R., and Imlay, J.A. (2002). Mechanism of superoxide and hydrogen peroxide formation by fumarate reductase, succinate dehydrogenase, and aspartate oxidase. The Journal of biological chemistry *277*, 42563-42571.
Miller, J.H. (1972). Experiments in molecular genetics. Cold Spring Harbor Laboratory, NY.
Miller, M.J., Hermodson, M., and Gennis, R.B. (1988). The active form of the cytochrome d terminal oxidase complex of *Escherichia coli* is a heterodimer containing one copy of each of the two subunits. The Journal of biological chemistry *263*, 5235-5240.
Minghetti, K.C., Goswitz, V.C., Gabriel, N.E., Hill, J.J., Barassi, C.A., Georgiou, C.D., Chan, S.I., and Gennis, R.B. (1992). Modified, large-scale purification of the cytochrome o complex (*bo*-type oxidase) of *Escherichia coli* yields a two heme/one copper terminal oxidase with high specific activity. Biochemistry *31*, 6917-6924.
Mogi, T., Nakamura, H., and Anraku, Y. (1994). Molecular structure of a heme-copper redox center of the *Escherichia coli* ubiquinol oxidase: evidence and model. Journal of biochemistry *116*, 471-477.
Mootha, V.K., Lindgren, C.M., Eriksson, K.F., Subramanian, A., Sihag, S., Lehar, J., Puigserver, P., Carlsson, E., Ridderstrale, M., Laurila, E.*, et al.* (2003). PGC-1alpha-responsive genes involved in oxidative phosphorylation

are coordinately downregulated in human diabetes. Nature genetics *34*, 267-273.
My, L., Ghandour Achkar, N., Viala, J.P., and Bouveret, E. (2015). Reassessment of the Genetic Regulation of Fatty Acid Synthesis in *Escherichia coli*: Global Positive Control by the Dual Functional Regulator FadR. Journal of bacteriology *197*, 1862-1872.
Nakahigashi, K., Miyamoto, K., Nishimura, K., and Inokuchi, H. (1992). Isolation and characterization of a light-sensitive mutant of *Escherichia coli* K-12 with a mutation in a gene that is required for the biosynthesis of ubiquinone. Journal of bacteriology *174*, 7352-7359.
Nichols, R.J., Sen, S., Choo, Y.J., Beltrao, P., Zietek, M., Chaba, R., Lee, S., Kazmierczak, K.M., Lee, K.J., Wong, A.*, et al.* (2011). Phenotypic landscape of a bacterial cell. Cell *144*, 143-156.
Nunn, W.D., and Simons, R.W. (1978). Transport of long-chain fatty acids by *Escherichia coli*: mapping and characterization of mutants in the fadL gene. Proceedings of the National Academy of Sciences of the United States of America *75*, 3377-3381.
Nunn, W.D., Simons, R.W., Egan, P.A., and Maloy, S.R. (1979). Kinetics of the utilization of medium and long chain fatty acids by mutant of *Escherichia coli* defective in the *fadL* gene. The Journal of biological chemistry *254*, 9130-9134.
Overath, P., Pauli, G., and Schairer, H.U. (1969). Fatty acid degradation in *Escherichia coli*. An inducible acyl-CoA synthetase, the mapping of old-mutations, and the isolation of regulatory mutants. European journal of biochemistry *7*, 559-574.
Pawar, S., and Schulz, H. (1981). The structure of the multienzyme complex of fatty acid oxidation from Escherichia coli. The Journal of biological chemistry *256*, 3894-3899.
Pech-Canul, A., Nogales, J., Miranda-Molina, A., Alvarez, L., Geiger, O., Soto, M.J., and Lopez-Lara, I.M. (2011). FadD is required for utilization of endogenous fatty acids released from membrane lipids. J Bacteriol *193*, 6295-6304.
Pelosi, L., Ducluzeau, A.L., Loiseau, L., Barras, F., Schneider, D., Junier, I., and Pierrel, F. (2016). Evolution of Ubiquinone Biosynthesis: Multiple Proteobacterial Enzymes with Various Regioselectivities To Catalyze Three Contiguous Aromatic Hydroxylation Reactions. mSystems *1*.
Perez-Pantoja, D., Nikel, P.I., Chavarria, M., and de Lorenzo, V. (2013). Endogenous stress caused by faulty oxidation reactions fosters evolution of 2,4-dinitrotoluene-degrading bacteria. PLoS genetics *9*, e1003764.
Petit-Koskas, E., and Contesse, G. (1976). Stimulation in trans of synthesis of E. coli gal operon enzymes by lambdoid phages during low catabolite repression. Mol Gen Genet *143*, 203-209.
Poon, W.W., Davis, D.E., Ha, H.T., Jonassen, T., Rather, P.N., and Clarke, C.F. (2000). Identification of *Escherichia coli ubiB*, a gene required for the first monooxygenase step in ubiquinone biosynthesis. Journal of bacteriology *182*, 5139-5146.
Pradenas, G.A., Paillavil, B.A., Reyes-Cerpa, S., Perez-Donoso, J.M., and Vasquez, C.C. (2012). Reduction of the monounsaturated fatty acid content of

Escherichia coli results in increased resistance to oxidative damage. Microbiology *158*, 1279-1283.
Pramanik, A., Pawar, S., Antonian, E., and Schulz, H. (1979). Five different enzymatic activities are associated with the multienzyme complex of fatty acid oxidation from *Escherichia coli*. Journal of bacteriology *137*, 469-473.
Puustinen, A., Finel, M., Haltia, T., Gennis, R.B., and Wikstrom, M. (1991). Properties of the two terminal oxidases of *Escherichia coli*. Biochemistry *30*, 3936-3942.
Rael, L.T., Thomas, G.W., Craun, M.L., Curtis, C.G., Bar-Or, R., and Bar-Or, D. (2004). Lipid peroxidation and the thiobarbituric acid assay: standardization of the assay when using saturated and unsaturated fatty acids. J Biochem Mol Biol *37*, 749-752.
Rapisarda, V.A., Chehin, R.N., De Las Rivas, J., Rodriguez-Montelongo, L., Farias, R.N., and Massa, E.M. (2002). Evidence for Cu(I)-thiolate ligation and prediction of a putative copper-binding site in the *Escherichia coli* NADH dehydrogenase-2. Archives of biochemistry and biophysics *405*, 87-94.
Ray, S., Chatterjee, E., Chatterjee, A., Paul, K., and Chowdhury, R. (2011). A *fadD* mutant of Vibrio cholerae is impaired in the production of virulence factors and membrane localization of the virulence regulatory protein TcpP. Infect Immun *79*, 258-266.
Reitzer, L. (2005). Catabolism of Amino Acids and Related Compounds. EcoSal Plus *1*.
Roberts, D.L., Frerman, F.E., and Kim, J.J. (1996). Three-dimensional structure of human electron transfer flavoprotein to 2.1-A resolution. Proceedings of the National Academy of Sciences of the United States of America *93*, 14355-14360.
Rodriguez, J.G., Hernandez, A.C., Helguera-Repetto, C., Aguilar Ayala, D., Guadarrama-Medina, R., Anzola, J.M., Bustos, J.R., Zambrano, M.M., Gonzalez, Y.M.J., Garcia, M.J.*, et al.* (2014). Global adaptation to a lipid environment triggers the dormancy-related phenotype of Mycobacterium tuberculosis. MBio *5*, e01125-01114.
Romano, A.H., and Nickerson, W.J. (1958). Utilization of amino acids as carbon sources by *Streptomyces fradiae*. Journal of bacteriology *75*, 161-166.
Romeo, T., and Snoep, J.L. (2005). Glycolysis and Flux Control. EcoSal Plus *1*.
Rose, R.E. (1988). The nucleotide sequence of pACYC184. Nucleic acids research *16*, 355.
Saiki, K., Mogi, T., Ogura, K., and Anraku, Y. (1993). In vitro heme O synthesis by the cyoE gene product from *Escherichia coli*. The Journal of biological chemistry *268*, 26041-26044.
San, K.Y., Bennett, G.N., Berrios-Rivera, S.J., Vadali, R.V., Yang, Y.T., Horton, E., Rudolph, F.B., Sariyar, B., and Blackwood, K. (2002). Metabolic engineering through cofactor manipulation and its effects on metabolic flux redistribution in *Escherichia coli*. Metabolic engineering *4*, 182-192.
Scandalios, J.G. (2002). Oxidative stress responses--what have genome-scale studies taught us? Genome biology *3*, REVIEWS1019.
Schmelter, T., Trigatti, B.L., Gerber, G.E., and Mangroo, D. (2004). Biochemical demonstration of the involvement of fatty acyl-CoA synthetase in

fatty acid translocation across the plasma membrane. The Journal of biological chemistry *279*, 24163-24170.
Schonfeld, P., and Wojtczak, L. (2008). Fatty acids as modulators of the cellular production of reactive oxygen species. Free Radic Biol Med *45*, 231-241.
Seaver, L.C., and Imlay, J.A. (2004). Are respiratory enzymes the primary sources of intracellular hydrogen peroxide? The Journal of biological chemistry *279*, 48742-48750.
Sevin, D.C., and Sauer, U. (2014). Ubiquinone accumulation improves osmotic-stress tolerance in Escherichia coli. Nature chemical biology *10*, 266-272.
Shiver, A.L., Osadnik, H., Kritikos, G., Li, B., Krogan, N., Typas, A., and Gross, C.A. (2016). A Chemical-Genomic Screen of Neglected Antibiotics Reveals Illicit Transport of Kasugamycin and Blasticidin S. PLoS genetics *12*, e1006124.
Siebert, M., Severin, K., and Heide, L. (1994). Formation of 4-hydroxybenzoate in *Escherichia coli*: characterization of the ubiC gene and its encoded enzyme chorismate pyruvate-lyase. Microbiology *140 (Pt 4)*, 897-904.
Simons, R.W., Egan, P.A., Chute, H.T., and Nunn, W.D. (1980). Regulation of fatty acid degradation in Escherichia coli: isolation and characterization of strains bearing insertion and temperature-sensitive mutations in gene fadR. Journal of bacteriology *142*, 621-632.
Soballe, B., and Poole, R.K. (1999). Microbial ubiquinones: multiple roles in respiration, gene regulation and oxidative stress management. Microbiology *145 (Pt 8)*, 1817-1830.
Soballe, B., and Poole, R.K. (2000). Ubiquinone limits oxidative stress in Escherichia coli. Microbiology *146 (Pt 4)*, 787-796.
Son, M.S., Matthews, W.J., Jr., Kang, Y., Nguyen, D.T., and Hoang, T.T. (2007). In vivo evidence of *Pseudomonas aeruginosa* nutrient acquisition and pathogenesis in the lungs of cystic fibrosis patients. Infect Immun *75*, 5313-5324.
Storz, G., Christman, M.F., Sies, H., and Ames, B.N. (1987). Spontaneous mutagenesis and oxidative damage to DNA in Salmonella typhimurium. Proc Natl Acad Sci U S A *84*, 8917-8921.
Stroobant, P., Young, I.G., and Gibson, F. (1972). Mutants of *Escherichia coli* K-12 blocked in the final reaction of ubiquinone biosynthesis: characterization and genetic analysis. J Bacteriol *109*, 134-139.
Subramanian, A., Tamayo, P., Mootha, V.K., Mukherjee, S., Ebert, B.L., Gillette, M.A., Paulovich, A., Pomeroy, S.L., Golub, T.R., Lander, E.S.*, et al.* (2005). Gene set enrichment analysis: a knowledge-based approach for interpreting genome-wide expression profiles. Proceedings of the National Academy of Sciences of the United States of America *102*, 15545-15550.
Swearingen, J.W., Jr., Fuentes, D.E., Araya, M.A., Plishker, M.F., Saavedra, C.P., Chasteen, T.G., and Vasquez, C.C. (2006). Expression of the *ubiE* gene of *Geobacillus stearothermophilus* V in *Escherichia coli* K-12 mediates the evolution of selenium compounds into the headspace of selenite- and selenate-amended cultures. Appl Environ Microbiol *72*, 963-967.

Szklarczyk, D., Morris, J.H., Cook, H., Kuhn, M., Wyder, S., Simonovic, M., Santos, A., Doncheva, N.T., Roth, A., Bork, P.*, et al.* (2017). The STRING database in 2017: quality-controlled protein-protein association networks, made broadly accessible. Nucleic acids research *45*, D362-D368.
Tardat, B., and Touati, D. (1993). Iron and oxygen regulation of Escherichia coli MnSOD expression: competition between the global regulators Fur and ArcA for binding to DNA. Molecular microbiology *9*, 53-63.
Tobe, T., Nakanishi, N., and Sugimoto, N. (2011). Activation of motility by sensing short-chain fatty acids via two steps in a flagellar gene regulatory cascade in enterohemorrhagic *Escherichia coli.* Infect Immun *79*, 1016-1024.
Traber, M.G., and Stevens, J.F. (2011). Vitamins C and E: beneficial effects from a mechanistic perspective. Free Radic Biol Med *51*, 1000-1013.
Tran, Q.H., Bongaerts, J., Vlad, D., and Unden, G. (1997). Requirement for the proton-pumping NADH dehydrogenase I of *Escherichia coli* in respiration of NADH to fumarate and its bioenergetic implications. European journal of biochemistry *244*, 155-160.
Tran, Q.M., Rothery, R.A., Maklashina, E., Cecchini, G., and Weiner, J.H. (2006). The quinone binding site in *Escherichia coli* succinate dehydrogenase is required for electron transfer to the heme b. The Journal of biological chemistry *281*, 32310-32317.
Trezza, A., Bernini, A., Langella, A., Ascher, D.B., Pires, D.E.V., Sodi, A., Passerini, I., Pelo, E., Rizzo, S., Niccolai, N.*, et al.* (2017). A Computational Approach From Gene to Structure Analysis of the Human ABCA4 Transporter Involved in Genetic Retinal Diseases. Investigative ophthalmology & visual science *58*, 5320-5328.
Unden, G., and Bongaerts, J. (1997). Alternative respiratory pathways of Escherichia coli: energetics and transcriptional regulation in response to electron acceptors. Biochimica et biophysica acta *1320*, 217-234.
Unden, G., and Dunnwald, P. (2008). The Aerobic and Anaerobic Respiratory Chain of *Escherichia coli* and *Salmonella enterica*: Enzymes and Energetics. EcoSal Plus *3*.
van den Berg, B., Black, P.N., Clemons, W.M., Jr., and Rapoport, T.A. (2004). Crystal structure of the long-chain fatty acid transporter FadL. Science *304*, 1506-1509.
Vandesompele, J., De Preter, K., Pattyn, F., Poppe, B., Van Roy, N., De Paepe, A., and Speleman, F. (2002). Accurate normalization of real-time quantitative RT-PCR data by geometric averaging of multiple internal control genes. Genome biology *3*, RESEARCH0034.
Wang, G., and Maier, R.J. (2004). An NADPH quinone reductase of *Helicobacter pylori* plays an important role in oxidative stress resistance and host colonization. Infect Immun *72*, 1391-1396.
Wang, K.C., Huang, C.H., Ding, S.M., Chen, C.K., Fang, H.W., Huang, M.T., and Fang, S.B. (2016). Role of *yqiC* in the Pathogenicity of *Salmonella* and Innate Immune Responses of Human Intestinal Epithelium. Frontiers in microbiology *7*, 1614.
Wegener, W.S., Reeves, H.C., and Ajl, S.J. (1967). Propionate oxidation in Escherichia coli. Archives of biochemistry and biophysics *121*, 440-442.
Wikstrom, M., and Hummer, G. (2012). Stoichiometry of proton translocation by respiratory complex I and its mechanistic implications. Proceedings of the

National Academy of Sciences of the United States of America *109*, 4431-4436.
Wu, G., Williams, H.D., Gibson, F., and Poole, R.K. (1993). Mutants of Escherichia coli affected in respiration: the cloning and nucleotide sequence of *ubiA*, encoding the membrane-bound p-hydroxybenzoate:octaprenyltransferase. Journal of general microbiology *139*, 1795-1805.
Xia, H., Yang, X., Tang, Q., Ye, J., Wu, H., and Zhang, H. (2017). EsrE-A yigP Locus-Encoded Transcript-Is a 3' UTR sRNA Involved in the Respiratory Chain of *E. coli*. Frontiers in microbiology *8*, 1658.
Yang, S.Y., and Elzinga, M. (1993). Association of both enoyl coenzyme A hydratase and 3-hydroxyacyl coenzyme A epimerase with an active site in the amino-terminal domain of the multifunctional fatty acid oxidation protein from *Escherichia coli.* The Journal of biological chemistry *268*, 6588-6592.
Yang, S.Y., Li, J.M., He, X.Y., Cosloy, S.D., and Schulz, H. (1988). Evidence that the *fadB* gene of the fadAB operon of *Escherichia coli* encodes 3-hydroxyacyl-coenzyme A (CoA) epimerase, delta 3-cis-delta 2-trans-enoyl-CoA isomerase, and enoyl-CoA hydratase in addition to 3-hydroxyacyl-CoA dehydrogenase. Journal of bacteriology *170*, 2543-2548.
Yoon, S.J., Park, J.E., Yang, J.H., and Park, J.W. (2002). OxyR regulon controls lipid peroxidation-mediated oxidative stress in *Escherichia coli*. J Biochem Mol Biol *35*, 297-301.
Young, I.G., Leppik, R.A., Hamilton, J.A., and Gibson, F. (1972). Biochemical and genetic studies on ubiquinone biosynthesis in *Escherichia coli* K-12:4-hydroxybenzoate octaprenyltransferase. Journal of bacteriology *110*, 18-25.
Young, I.G., Stroobant, P., Macdonald, C.G., and Gibson, F. (1973). Pathway for ubiquinone biosynthesis in *Escherichia coli* K-12: gene-enzyme relationships and intermediates. Journal of bacteriology *114*, 42-52.
Zhang, H., and Javor, G.T. (2003). Regulation of the isofunctional genes ubiD and *ubiX* of the ubiquinone biosynthetic pathway of *Escherichia coli*. FEMS microbiology letters *223*, 67-72.
Zhao, H., Kalivendi, S., Zhang, H., Joseph, J., Nithipatikom, K., Vasquez-Vivar, J., and Kalyanaraman, B. (2003). Superoxide reacts with hydroethidine but forms a fluorescent product that is distinctly different from ethidium: potential implications in intracellular fluorescence detection of superoxide. Free Radic Biol Med *34*, 1359-1368.

APPENDIX

Appendix 1:

S. No.	Strain	Fitness score
1	*fadL*	-16.32178544
2	*atpD*	-13.65342117
3	*aceA*	-12.9569136
4	*fadE*	-12.52043798
5	*fbp*	-11.94722863
6	*waaF*	-11.48653067
7	*crr*	-10.56125334
8	*ubiF*	-10.26617679
9	*ubiH*	-9.734733222
10	*atpC*	-9.699998
11	*ubiE*	-9.115755198
12	*lpcA*	-8.871246607
13	*atpF*	-8.871081181
14	*acnB*	-8.169206373
15	*yqiC*	-7.930827442
16	*fadA*	-7.905753027
17	*sdhC*	-7.697426745
18	*fadB*	-7.456658761
19	*rfaE*	-6.493110498
20	*sdhB*	-6.491103127
21	*pgm*	-5.489921682
22	*ihfA*	-5.075449668
23	*fadD*	-4.913557842
24	*dgoR*	-4.69322012
25	*atpB*	-4.69110191
26	*rfaD*	-4.651227964
27	*atpE*	-4.621628264
28	*cysQ*	-4.594318183
29	*sdhA*	-4.423356259
30	*bamA{del(64)}*	-4.280288381
31	*tolC*	-3.999431466
32	*ubiI*	-3.870561205
33	*sucD*	-3.820607408
34	*sucC*	-3.725962391
35	*yhcB*	-3.463785296
36	*aceK*	-3.462361809
37	*yebK*	-3.350374101
38	*hemY*	-3.226217943
39	*sdaC*	-3.163393818
40	*lpxM*	-3.101357581
41	*dnaJ*	-3.045563285
42	*gor*	-3.042199597
43	*nuoN*	-3.016217619
44	*nuoF*	-3.011756327
45	*fdrA*	-3.00500556
46	*ybhP*	-2.982895156
47	*pdxH*	-2.957958666
48	*sdhE*	-2.951473555
49	*gfcC*	-2.913517263
50	*fepC*	-2.895343045
51	*fimI*	-2.887526401
52	*ybgA*	-2.882884174
53	*yqaA*	-2.808089583
54	*fur*	-2.79195901
55	*panD*	-2.687325442
56	*nuoL*	-2.670489511
57	*ubiX*	-2.668101812
58	*nuoE*	-2.642539283
59	*ddpA*	-2.634170437
60	*nuoK*	-2.611256296
61	*nuoB*	-2.603869018
62	*aceB*	-2.580987902
63	*lpxC{G210S}*	-2.579964405
64	*ydeS*	-2.567089378
65	*ygeH*	-2.516479173
66	*yidK*	-2.4970406
67	*pck*	-2.493718268
68	*ygcR*	-2.490318244
69	*ihfB*	-2.47864082
70	*yhbT*	-2.475555298
71	*imp4213*	-2.447895786
72	*cbrC*	-2.440214408
73	*uidC*	-2.373264155
74	*yjjM*	-2.372056062
75	*purN*	-2.351262395
76	*yeaN*	-2.329523891
77	*yqiH*	-2.317737963
78	*ogt*	-2.300827659
79	*ydfU*	-2.29781441
80	*yjcZ*	-2.282334121
81	*cra*	-2.277429372
82	*intS*	-2.276840312
83	*cspD*	-2.274728501
84	*nuoG*	-2.272982649
85	*yegT*	-2.272849708
86	*ybaP*	-2.256804121
87	*waaI*	-2.252993561
88	*fepB*	-2.249845351
89	*tdcG*	-2.19671543
90	*rydB*	-2.196646786
91	*ytfL*	-2.1943005
92	*wcaJ*	-2.190732645
93	*nudK*	-2.18899908
94	*fryC*	-2.187743374
95	*nuoJ*	-2.173164905
96	*yeaD*	-2.170368682
97	*yfcS*	-2.169103768
98	*phoH*	-2.16619703
99	*yfjS*	-2.149523939
100	*ptrB*	-2.139666563
101	*nuoA*	-2.134631026
102	*ulaA*	-2.122828103
103	*yncH*	-2.118301074
104	*metH*	-2.114514383
105	*amiD*	-2.103586643
106	*dhaK*	-2.10282821
107	*mdlB*	-2.087188227
108	*yhhZ*	-2.078058913
109	*malQ*	-2.069249576
110	*ybdF*	-2.065838194
111	*panC*	-2.060880747
112	*ybjT*	-2.060430177
113	*ybhJ*	-2.059939833
114	*imp-DAS*	-2.057022829
115	*argI*	-2.048457206
116	*ycjT*	-2.048420451
117	*gspO*	-2.045998715
118	*tfaD*	-2.038761287
119	*waaC*	-2.038431239
120	*tisB*	-2.032790477
121	*envY*	-2.032205676
122	*asmA*	-2.031865832
123	*barA*	-2.021693679
124	*nuoM*	-2.019204834
125	*yeaO*	-2.014040909
126	*hyfR*	-1.998575842
127	*wcaC*	-1.996922819
128	*panB*	-1.990551367
129	*birA-SPA*	-1.986833714
130	*etp*	-1.974332451
131	*ydbK*	-1.970919693
132	*pheS-SPA*	-1.959837183
133	*csgC*	-1.959206887
134	*dedD*	-1.954215324
135	*slmA*	-1.949556208
136	*casA*	-1.949419899
137	*ycfP*	-1.949198604
138	*yfdE*	-1.935057641
139	*dsbB*	-1.930793475
140	*yihP*	-1.929008313
141	*sgcQ*	-1.927206242
142	*yejK*	-1.926097184
143	*ompX*	-1.921283292
144	*ymfH*	-1.918315911
145	*yegQ*	-1.917640427
146	*yhjD-kan*	-1.913677361
147	*inaA*	-1.910567586
148	*rnpA-SPA*	-1.904490584
149	*secB*	-1.90351884
150	*elfD*	-1.899391921
151	*yobA*	-1.89749308
152	*nikR*	-1.89089384
153	*sfmA*	-1.88963003
154	*rsmA*	-1.875747348
155	*ybgL*	-1.874104223
156	*yfjJ*	-1.873915396
157	*ymjA*	-1.866825937
158	*ygfI*	-1.86403201
159	*ycgX*	-1.860120702
160	*tktA*	-1.852839313
161	*hslV*	-1.85102681
162	*pinH*	-1.850532425
163	*yecH*	-1.843191516
164	*gcvA*	-1.837420316
165	*rutB*	-1.836733961
166	*yigM*	-1.836203678
167	*fecD*	-1.834806226
168	*lar*	-1.833299777
169	*ydcM*	-1.830489837
170	*yedZ*	-1.82654177
171	*ybbB*	-1.825925272
172	*ushA*	-1.819166567
173	*kdgR*	-1.803754183
174	*yncL*	-1.802738195
175	*ptsA*	-1.798458753
176	*tauB*	-1.797396657
177	*yedK*	-1.79168791
178	*lon*	-1.790750417
179	*phnM*	-1.787102064
180	*relA*	-1.781082082
181	*phnK*	-1.776777803
182	*amn*	-1.776765157
183	*feaB*	-1.775245315
184	*yiaB*	-1.763050696
185	*pepE*	-1.762971601
186	*ynjE*	-1.760415608
187	*kdpF*	-1.756153892
188	*ydjN*	-1.754791451
189	*ygaP*	-1.74583082
190	*ybeR*	-1.743702067
191	*chbR*	-1.737555202
192	*glcF*	-1.732863021
193	*yjfN*	-1.723710766
194	*grxB*	-1.714917877
195	*arpA*	-1.713062627
196	*yiiS*	-1.70885625

197	*adk-SPA*	-1.705742355	271	*ychO*	-1.510032214	345	*ccmH*	-1.339674197
198	*yifN*	-1.702841822	272	*truC*	-1.507527105	346	*treA*	-1.336254507
199	*yneL*	-1.700379418	273	*rihC*	-1.501713313	347	*aroK*	-1.335210188
200	*yciB*	-1.699810654	274	*mgsA*	-1.496748066	348	*ddpF*	-1.333796973
201	*lolB-SPA*	-1.69750327	275	*yehR*	-1.496411263	349	*potE*	-1.332942041
202	*ydiM*	-1.697424393	276	*gsiB*	-1.496115416	350	*bdm*	-1.332862624
203	*phoB*	-1.693572247	277	*hybB*	-1.493463051	351	*imp-kan*	-1.330166021
204	*pflA*	-1.691410654	278	*yjdN*	-1.493046701	352	*nhaA*	-1.330055191
205	*yehQ*	-1.68835186	279	*nfuA*	-1.490371833	353	*agaS*	-1.329836799
206	*ydcN*	-1.684361181	280	*ygbN*	-1.488928201	354	*yghJ*	-1.327027545
207	*fucK*	-1.684285523	281	*fcl*	-1.488713476	355	*yqeA*	-1.325077607
208	*flgB*	-1.682897365	282	*ymfQ*	-1.487028231	356	*fadK*	-1.3243346
209	*rutF*	-1.682506481	283	*sgcC*	-1.486234326	357	*yccB*	-1.324319228
210	*narL*	-1.681016239	284	*eutR*	-1.485686108	358	*ftsA-kan*	-1.324280873
211	*ilvB*	-1.673209588	285	*ycbC*	-1.483808762	359	*yeeP*	-1.324060031
212	*yfiR*	-1.666984573	286	*yoaD*	-1.474491098	360	*ydhB*	-1.323838232
213	*mdh*	-1.663534805	287	*fimF*	-1.473752801	361	*viaA*	-1.323263551
214	*sufE*	-1.651953941	288	*rsmB*	-1.471699581	362	*yfeH*	-1.322678398
215	*yfjD*	-1.649079598	289	*ddlB*	-1.471379439	363	*ybjX*	-1.322561458
216	*fadM*	-1.645483656	290	*yphH*	-1.469862277	364	*yigF*	-1.322464172
217	*nrdD*	-1.64226246	291	*frmB*	-1.468634205	365	*yedF*	-1.320919864
218	*ybgP*	-1.640260962	292	*srmB*	-1.465439066	366	*treF*	-1.318539319
219	*nuoH*	-1.639300583	293	*citC*	-1.460997712	367	*ybaV*	-1.317498659
220	*xylF*	-1.637694199	294	*entB*	-1.457278505	368	*chbF*	-1.313191529
221	*sdhD*	-1.636740216	295	*lamB*	-1.454549849	369	*yebV*	-1.310225085
222	*aspA*	-1.636374904	296	*waaA-A*	-1.452167497	370	*yidJ*	-1.309705986
223	*glxR*	-1.63464058	297	*yhiS_1*	-1.450774264	371	*cybB*	-1.309595377
224	*phnC*	-1.630021838	298	*yhcM*	-1.450606506	372	*potA*	-1.307006553
225	*yafX*	-1.622606515	299	*yehW*	-1.445959949	373	*yebG*	-1.306761504
226	*casE*	-1.620047432	300	*menE*	-1.445022845	374	*yoeF*	-1.306746997
227	*ndk*	-1.619426124	301	*wcaB*	-1.444042612	375	*yeiS*	-1.30449337
228	*envR*	-1.619117096	302	*ygfZ*	-1.44273213	376	*gspF*	-1.301354594
229	*sieB*	-1.617798636	303	*isrC*	-1.441694407	377	*hofO*	-1.300718998
230	*cdd*	-1.617039999	304	*yjaB*	-1.438823394	378	*tyrB*	-1.300130633
231	*asnB*	-1.605343051	305	*ybhB*	-1.438343479	379	*ydhJ*	-1.298003338
232	*mukB-SPA*	-1.603928515	306	*mglC*	-1.436136148	380	*ligA-SPA*	-1.297904443
233	*ymbA*	-1.600022166	307	*ycaP*	-1.436030746	381	*ftsE-SPA*	-1.297214644
234	*paaA*	-1.598021865	308	*tfaS*	-1.431546919	382	*bama-kan*	-1.296890275
235	*yfaE*	-1.597584271	309	*rhaS*	-1.43106981	383	*mcaS*	-1.293626778
236	*yjjB*	-1.596633663	310	*casD*	-1.428812849	384	*panZ*	-1.292158231
237	*yejB*	-1.596463137	311	*citF*	-1.423025692	385	*flgF*	-1.28891628
238	*rcdA*	-1.596132281	312	*casC*	-1.42043548	386	*pptA*	-1.284734309
239	*yhjX*	-1.59370658	313	*ves*	-1.418822977	387	*yihD*	-1.284418277
240	*cobC*	-1.591374964	314	*narH*	-1.414617861	388	*cpxP*	-1.284218869
241	*feoA*	-1.591039772	315	*yjfZ*	-1.414508782	389	*holC*	-1.283492629
242	*yiiM*	-1.586298492	316	*fbaA-SPA*	-1.411000585	390	*ptrA*	-1.282682133
243	*adhE*	-1.585531986	317	*ydfW*	-1.408047152	391	*ydhL*	-1.281988187
244	*ymjC*	-1.583508679	318	*cpdA*	-1.406525905	392	*fucA*	-1.281662109
245	*ppiD*	-1.580622244	319	*ykgI*	-1.402918116	393	*yibT*	-1.281622659
246	*yeiG*	-1.574722098	320	*rutR*	-1.398165569	394	*ycjU*	-1.28103408
247	*citD*	-1.573875129	321	*ybbN*	-1.396720122	395	*allB*	-1.280809848
248	*yidH*	-1.568353428	322	*yfhL*	-1.396378698	396	*yaeI*	-1.279317325
249	*yibL*	-1.567227799	323	*yphC*	-1.394520273	397	*uxuR*	-1.277267862
250	*cyoB*	-1.563833078	324	*ybcH*	-1.392085737	398	*sodB*	-1.276927013
251	*yehC*	-1.553602063	325	*bglF*	-1.391071381	399	*npr*	-1.274591507
252	*cspH*	-1.552170301	326	*mngB*	-1.388174117	400	*ydcL*	-1.273763217
253	*yaiZ*	-1.548487649	327	*pheT-SPA*	-1.387638322	401	*glnL*	-1.273426803
254	*yceK*	-1.54713134	328	*yeeA*	-1.386200299	402	*ycfZ*	-1.27153009
255	*fimD*	-1.5437336	329	*fau*	-1.383951066	403	*yihM*	-1.271137754
256	*waaP*	-1.538767584	330	*rarA*	-1.3835017	404	*gfcE*	-1.26892775
257	*marC*	-1.538282886	331	*yraJ*	-1.376338103	405	*tqsA*	-1.267824643
258	*hyfC*	-1.537975747	332	*yhaC*	-1.373529977	406	*gnsB*	-1.263890236
259	*bacA*	-1.535226746	333	*yoaK*	-1.370615494	407	*ydfP*	-1.260867992
260	*ybhH*	-1.534471466	334	*ydiS*	-1.368977373	408	*yqgC*	-1.258162861
261	*hycC*	-1.531765519	335	*mutT*	-1.366446698	409	*cmtB*	-1.256725698
262	*sodC*	-1.530049407	336	*ygeI*	-1.365319764	410	*tehA*	-1.253065906
263	*yccM*	-1.526561549	337	*yfbN*	-1.365238426	411	*yfiM*	-1.252588242
264	*yaiF*	-1.523277291	338	*dacC*	-1.364398905	412	*wzxE*	-1.25159901
265	*metN*	-1.521519244	339	*ybcM*	-1.363728772	413	*garK*	-1.248838102
266	*yagN*	-1.517873131	340	*purK*	-1.355882824	414	*ypfM*	-1.248821138
267	*acpH*	-1.514708575	341	*yegH*	-1.354242975	415	*dinB*	-1.248757542
268	*waaG*	-1.514610798	342	*ycaC*	-1.35119886	416	*norV*	-1.237984658
269	*yceH*	-1.514016218	343	*paaX*	-1.347485147	417	*ubiG*	N.D.
270	*gmm*	-1.513499901	344	*ycjF*	-1.346898377	418	*yfbO*	-1.237469094

419	*rsxC*	-1.234277238	493	*yggC*	-1.110370416	567	*cptA*	-1.03147611
420	*anmK*	-1.231718225	494	*fabZ{F101Y}*	-1.108861142	568	*marR*	-1.031305614
421	*ydeK*	-1.229212061	495	*fis*	-1.108574481	569	*ybeQ*	-1.030288099
422	*hipB*	-1.228335146	496	*ryfD/clpB*	-1.106498033	570	*dcm*	-1.029246315
423	*eno-SPA*	-1.227194715	497	*speF*	-1.106377024	571	*yagB*	-1.028998596
424	*cycA*	-1.227155279	498	*hyi*	-1.104594344	572	*alsE*	-1.027514797
425	*yjbR*	-1.220290653	499	*eutE*	-1.104593148	573	*gltS*	-1.027488671
426	*manZ*	-1.216735512	500	*dsrA*	-1.103682908	574	*lpoB*	-1.027242261
427	*aaeR*	-1.216231299	501	*atpH*	-1.102556117	575	*nrdI*	-1.026828534
428	*ygeO*	-1.214861409	502	*flhA*	-1.102369985	576	*ykgE*	-1.026260134
429	*elfC*	-1.213017236	503	*kefF*	-1.102056605	577	*yddA*	-1.022235897
430	*fixB*	-1.212051493	504	*glpX*	-1.10135699	578	*pgaD*	-1.022019052
431	*ymfJ*	-1.211576594	505	*yciC*	-1.100964918	579	*pitB*	-1.020600976
432	*solA*	-1.207970034	506	*ymdB*	-1.100134747	580	*chbC*	-1.019446754
433	*tdh*	-1.204925485	507	*relB*	-1.099345587	581	*yaiP*	-1.018892356
434	*kdtA-SPA*	-1.203694732	508	*menF*	-1.097865997	582	*napH*	-1.018766079
435	*sgcE*	-1.20201786	509	*yjbF*	-1.097708738	583	*yhdT*	-1.017487382
436	*rbsB*	-1.199791162	510	*ypjM_2*	-1.096353103	584	*yjaG*	-1.01530941
437	*yqeK*	-1.199576478	511	*yneG*	-1.096307609	585	*kdpB*	-1.012147835
438	*ybaE*	-1.198212977	512	*yhdJ*	-1.095784333	586	*ybgK*	-1.011714263
439	*nagK*	-1.196946287	513	*frlR*	-1.093061793	587	*fimH*	-1.009895362
440	*rdoA*	-1.196185056	514	*ydjM*	-1.092439877	588	*ydiN*	-1.008190557
441	*frdC*	-1.195166848	515	*ccmA*	-1.090814115	589	*sucA*	-1.007932476
442	*torS*	-1.193120115	516	*ohsC*	-1.089432549	590	*wzc*	-1.003280153
443	*lysP*	-1.191774529	517	*yeiP*	-1.087799649	591	*waaJ*	-1.000162932
444	*cpdB*	-1.188646851	518	*putA*	-1.086599587	592	*yfbL*	-0.998523353
445	*mdoD*	-1.186573625	519	*murP*	-1.086568055	593	*livF*	-0.998334726
446	*dnaK*	-1.185483665	520	*ygcE*	-1.085907751	594	*yoaI*	-0.99759702
447	*murI-SPA*	-1.184680962	521	*polB*	-1.085037716	595	*appB*	-0.997196125
448	*yghF*	-1.182541558	522	*puuE*	-1.084069851	596	*kch*	-0.997176697
449	*rutD*	-1.18055812	523	*yniD*	-1.083207473	597	*mqsA-SPA*	-0.997079693
450	*torT*	-1.17879661	524	*yggD*	-1.081722597	598	*ghrB*	-0.995607178
451	*ytfT*	-1.177852142	525	*micM*	-1.075971668	599	*hofM*	-0.994301935
452	*yiiG*	-1.177017764	526	*ribE-SPA*	-1.075767518	600	*dksA*	-0.993886566
453	*smrB*	-1.176596608	527	*cusB*	-1.0756168	601	*ynfN*	-0.993749248
454	*cfa*	-1.176353399	528	*yhjA*	-1.07479079	602	*ttcA*	-0.993676156
455	*ycaR*	-1.175554867	529	*yciS*	-1.074437335	603	*yihV*	-0.99314229
456	*nuoC*	-1.170660376	530	*bcsQ*	-1.071483644	604	*emrB*	-0.993130016
457	*yliE*	-1.170491386	531	*waaQ*	-1.067787293	605	*yhgA*	-0.993043847
458	*ydhS*	-1.156495636	532	*yqhA*	-1.065555112	606	*ygbL*	-0.992580216
459	*ybjL*	-1.155450347	533	*yajO*	-1.063147046	607	*yaiS*	-0.992090047
460	*ftsK-SPA*	-1.152834609	534	*yghO*	-1.061666429	608	*cbl*	-0.990627873
461	*yzcX*	-1.152458531	535	*ybeX*	-1.059796489	609	*ydiY*	-0.990285544
462	*clsA*	-1.151611084	536	*rlmI*	-1.059780132	610	*rsmD*	-0.9899273
463	*ybjN*	-1.149134308	537	*efeB*	-1.057886607	611	*yiaM*	-0.989082701
464	*rimP*	-1.148610721	538	*cutA*	-1.057198745	612	*hyfD*	-0.98765033
465	*yciW*	-1.148092194	539	*mpaA*	-1.056671244	613	*gloB*	-0.987198309
466	*gcvT*	-1.144958375	540	*napF*	-1.055110007	614	*ucpA*	-0.986955277
467	*nrdG*	-1.143336203	541	*yebS*	-1.053775071	615	*carB*	-0.986696759
468	*tynA*	-1.1423031	542	*pepA*	-1.053190151	616	*yciI*	-0.985497365
469	*hemX*	-1.141024333	543	*yhdU*	-1.052817276	617	*yciO*	-0.98441999
470	*ycdY*	-1.136434774	544	*cysK*	-1.051703644	618	*ynbC*	-0.98346561
471	*vsr*	-1.136026641	545	*ydaY*	-1.051636377	619	*hflK*	-0.981435685
472	*msrC*	-1.135626583	546	*ccmC*	-1.051523425	620	*hemN*	-0.981362193
473	*mepA*	-1.135507258	547	*ydfX*	-1.047665323	621	*ycjV*	-0.979058542
474	*yliI*	-1.134801876	548	*yqgA*	-1.047045211	622	*yhhH*	-0.979049124
475	*yfdI*	-1.132096992	549	*hypE*	-1.046998265	623	*ribD-SPA*	-0.978210692
476	*caiE*	-1.128347011	550	*ybhL*	-1.045120714	624	*ycfK*	-0.977043089
477	*chaB*	-1.126928891	551	*sufA*	-1.044676661	625	*ydfE*	-0.976570308
478	*ibpA*	-1.126379147	552	*ygcN*	-1.04450959	626	*gshA*	-0.976178701
479	*murB-SPA*	-1.124222835	553	*arnE*	-1.043404195	627	*sfmH*	-0.974757553
480	*fumA*	-1.123959718	554	*yfcZ*	-1.041153672	628	*gdhA*	-0.974730509
481	*mdoH*	-1.123559075	555	*fabR*	-1.041099774	629	*qor*	-0.973882828
482	*rluE*	-1.122831872	556	*hfq*	-1.038784525	630	*yjdI*	-0.973443331
483	*ybeF*	-1.121818746	557	*nusG-SPA*	-1.0386969	631	*waaB*	-0.965081203
484	*yjgM*	-1.120791285	558	*hdeB*	-1.037060351	632	*yfjW*	-0.96455333
485	*rtcB*	-1.11675332	559	*yicN*	-1.036907928	633	*elfA*	-0.963669782
486	*tktB*	-1.11565851	560	*yfjR*	-1.036753598	634	*ybaO*	-0.962865006
487	*rcnB*	-1.115356352	561	*hns*	-1.034799349	635	*ygeM*	-0.962251917
488	*yfaW*	-1.114640142	562	*fliF*	-1.033989277	636	*mdoG*	-0.958683188
489	*dmsB*	-1.114143255	563	*ylbH*	-1.033870874	637	*bcp*	-0.958494496
490	*araE*	-1.113333793	564	*ynaK*	-1.03287748	638	*sbp*	-0.958493629
491	*fliZ*	-1.112943518	565	*ppdC*	-1.032850628	639	*cbtA*	-0.957740263
492	*hisA-SPA*	-1.111403584	566	*nmpC*	-1.031523268	640	*ybiP*	-0.956152585

641	*serS-SPA*	-0.955566959	715	*nadK-SPA*	-0.866391884	789	*cyoE*	-0.792448979
642	*otsA*	-0.955005966	716	*fkpA*	-0.864697668	790	*gudX*	-0.791076536
643	*ycgL*	-0.954819177	717	*entF*	-0.863824884	791	*nagD*	-0.790620155
644	*gss*	-0.954421945	718	*yraR*	-0.86132762	792	*yhhY*	-0.790246882
645	*yihY*	-0.954173309	719	*intB*	-0.860639706	793	*ygfQ*	-0.789339994
646	*fecC*	-0.952048147	720	*yfjL*	-0.860608372	794	*eutJ*	-0.788852593
647	*rmf*	-0.949490308	721	*yjgH*	-0.859489053	795	*idnT*	-0.787577395
648	*gcvR*	-0.948859273	722	*yqfE*	-0.858918232	796	*pflD*	-0.787520828
649	*yeiW*	-0.947070496	723	*cpxR*	-0.858899667	797	*wbbI*	-0.78709276
650	*cyoC*	-0.946624326	724	*oxyR*	-0.858656147	798	*yiaT*	-0.784385948
651	*nikB*	-0.946442239	725	*ompF*	-0.857380701	799	*mazG*	-0.784258735
652	*entE*	-0.946189131	726	*pdhR*	-0.856974819	800	*mgrB*	-0.783731526
653	*arnD*	-0.943907418	727	*allA*	-0.856817754	801	*argF*	-0.782037575
654	*ssuD*	-0.943221813	728	*tppB*	-0.856047492	802	*ygeW*	-0.780838061
655	*gltI*	-0.939704684	729	*atpG*	-0.854308102	803	*proB*	-0.780835626
656	*yifB*	-0.936761767	730	*ymfA*	-0.853519803	804	*yjeF*	-0.778693935
657	*ycfH*	-0.936699848	731	*rnt*	-0.853146534	805	*yfeR*	-0.777218104
658	*pldA*	-0.93503126	732	*fieF*	-0.853046163	806	*yfjK*	-0.777016688
659	*ycbJ*	-0.929142522	733	*yfgD*	-0.851103994	807	*atpA*	-0.77493486
660	*greA*	-0.928177983	734	*aroH*	-0.850100335	808	*sapC*	-0.774273147
661	*yecT*	-0.928139594	735	*hycA*	-0.845556468	809	*sgcA*	-0.773633331
662	*fliO*	-0.927485656	736	*yacC*	-0.844941263	810	*yciN*	-0.77311105
663	*dps*	-0.927457548	737	*acnA*	-0.844897799	811	*ykgM*	-0.772538407
664	*yjbE*	-0.926593704	738	*tusD*	-0.844052485	812	*ydhP*	-0.772516595
665	*pspA*	-0.925827248	739	*yphE*	-0.844003124	813	*ydgU*	-0.772298188
666	*yhbS*	-0.925101254	740	*ycdU*	-0.840730383	814	*ymdE*	-0.771249113
667	*pepT*	-0.923743974	741	*mnmC*	-0.840416789	815	*ampG*	-0.770990221
668	*ltaE*	-0.922626704	742	*yehS*	-0.838823924	816	*gspG*	-0.770796969
669	*galU*	-0.920020515	743	*torA*	-0.838257991	817	*eutB*	-0.769563316
670	*yoaB*	-0.916192225	744	*ybeM_2*	-0.838125638	818	*ppsA*	-0.767547508
671	*ypaA*	-0.914454674	745	*yebE*	-0.837515739	819	*yceD*	-0.766734041
672	*yfdP*	-0.913265705	746	*yjiL*	-0.836864553	820	*pfkB*	-0.765168502
673	*kilR*	-0.913033663	747	*lysC*	-0.836506568	821	*lexA-SPA*	-0.764331489
674	*mprA*	-0.912594132	748	*ycjD*	-0.834442829	822	*gcvB*	-0.764144278
675	*topA-SPA*	-0.912456128	749	*csdE*	-0.834388039	823	*nhoA*	-0.763693889
676	*isrB*	-0.912183178	750	*modF*	-0.833446888	824	*ycfJ*	-0.761656652
677	*yfgI*	-0.910870111	751	*ahpF*	-0.833439092	825	*mhpD*	-0.761656101
678	*gstA*	-0.910747134	752	*pstB*	-0.832079877	826	*tpx*	-0.761215017
679	*emrE*	-0.910203076	753	*treC*	-0.830268029	827	*prpC*	-0.759611824
680	*ung*	-0.909972568	754	*ymgF*	-0.82939127	828	*alaA*	-0.757433818
681	*cyoA*	-0.909008954	755	*betI*	-0.829105926	829	*rodZ*	-0.756726852
682	*dcuS*	-0.908266526	756	*malY*	-0.827522575	830	*fucI*	-0.7565841
683	*ybdZ*	-0.907342574	757	*ydcY*	-0.822319673	831	*ybdN*	-0.755976471
684	*yjdK*	-0.906834959	758	*fliH*	-0.820680784	832	*ycjR*	-0.755472969
685	*clcA*	-0.906155515	759	*rhsD*	-0.820186725	833	*entS*	-0.753322919
686	*yegD*	-0.905047648	760	*yccU*	-0.817733833	834	*maeB*	-0.752890514
687	*phnE_2*	-0.904610931	761	*efeU_1*	-0.817270944	835	*ykgA*	-0.752527249
688	*ymfR*	-0.902771975	762	*yfcU*	-0.815425698	836	*fruB*	-0.750697756
689	*gatD*	-0.901858461	763	*dmsA*	-0.814782642	837	*hdeD*	-0.750477122
690	*gspL*	-0.901166276	764	*bluF*	-0.814780171	838	*yjdO*	-0.750274841
691	*greB*	-0.898967527	765	*mntP*	-0.812677684	839	*potH*	-0.749899091
692	*aslA*	-0.898762418	766	*uxuA*	-0.811931535	840	*gph*	-0.748970623
693	*yiaJ*	-0.897387994	767	*nrdH*	-0.810941864	841	*aaeX*	-0.748903952
694	*tdcD*	-0.893892558	768	*yegW*	-0.81036917	842	*hspQ*	-0.748382945
695	*aslB*	-0.890071745	769	*tsaE-SPA*	-0.809693837	843	*yqcA*	-0.748167338
696	*ydfZ*	-0.889288925	770	*hyaF*	-0.806723136	844	*ispF-SPA*	-0.745659187
697	*imp-DAS+4*	-0.888072216	771	*adiC*	-0.805535907	845	*mdtF*	-0.745505104
698	*fdhF*	-0.886826772	772	*elaB*	-0.805018613	846	*ecnB*	-0.744796189
699	*nadB*	-0.883983403	773	*bcr*	-0.804860944	847	*aas*	-0.743960958
700	*narI*	-0.883033922	774	*yggI*	-0.804722706	848	*yeeD*	-0.743887809
701	*paaC*	-0.882882204	775	*ygcQ*	-0.803326501	849	*mazF*	-0.741860899
702	*bcsA*	-0.881394038	776	*ygdH*	-0.801231937	850	*tatD*	-0.74090193
703	*ysaA*	-0.880103352	777	*iraM*	-0.800786108	851	*yohD*	-0.738620495
704	*ydeR*	-0.879736304	778	*yhcO*	-0.800340383	852	*yegR*	-0.738616722
705	*sucB*	-0.8781514	779	*ynhG*	-0.799214159	853	*mipA*	-0.737886176
706	*ybgF*	-0.877217897	780	*ynbE*	-0.796895585	854	*chaA*	-0.736412551
707	*ychN*	-0.876623011	781	*tbpA*	-0.796832438	855	*rbsD*	-0.734939904
708	*ypjD*	-0.876206796	782	*comR*	-0.796769317	856	*ddpD*	-0.7337619
709	*yaiY*	-0.875417563	783	*yafJ*	-0.796706855	857	*ybbW*	-0.733180965
710	*menD*	-0.873351588	784	*hokD*	-0.795577904	858	*hrpA*	-0.733123441
711	*ydgJ*	-0.871053513	785	*ydiZ*	-0.795470837	859	*yiiF*	-0.732323622
712	*yojI*	-0.870626985	786	*lldR*	-0.794429815	860	*nagE*	-0.731851639
713	*smg*	-0.867204977	787	*cyaA*	-0.794087158	861	*yhdE*	-0.731569123
714	*pgpC*	-0.867189566	788	*ytfJ*	-0.792967034	862	*sbcD*	-0.731176735

863	*agaR*	-0.730461323	937	*phoQ*	-0.670147292	1011	*bioH*	-0.615306106
864	*bioA*	-0.729721778	938	*micA*	-0.669277503	1012	*hycH*	-0.615301916
865	*murQ*	-0.727014353	939	*pepD*	-0.666861711	1013	*ybfN*	-0.614462618
866	*yoaE*	-0.725969151	940	*murG-SPA*	-0.666481564	1014	*appC*	-0.614257882
867	*ghrA*	-0.725515287	941	*argR*	-0.664050699	1015	*ypeC*	-0.613734023
868	*zraR*	-0.724154785	942	*ybgO*	-0.66349182	1016	*btuR*	-0.612733531
869	*hofP*	-0.723534351	943	*arnA*	-0.663052588	1017	*sufS*	-0.611744803
870	*ecpC*	-0.721815499	944	*yddG*	-0.662771501	1018	*yebA*	-0.609158256
871	*pabC*	-0.720835795	945	*fliJ*	-0.662560152	1019	*katG*	-0.608962983
872	*tfaE*	-0.719789848	946	*lysU*	-0.662487913	1020	*ynfO*	-0.607314954
873	*aer*	-0.719145037	947	*agaV*	-0.661779041	1021	*yhjY*	-0.605716697
874	*yfgO*	-0.719072466	948	*ykiA*	-0.6589917	1022	*sibD*	-0.60363499
875	*ymfL*	-0.717829687	949	*phnL*	-0.656894045	1023	*stfR*	-0.602285273
876	*ygaQ_4*	-0.717820959	950	*wbbH*	-0.65519064	1024	*yfjI*	-0.601833831
877	*ypjM_3*	-0.716889617	951	*mhpR*	-0.654733495	1025	*yghX_2*	-0.599754643
878	*mcbR*	-0.715665345	952	*flgI*	-0.653974314	1026	*ybaB*	-0.598778425
879	*yegI*	-0.715642852	953	*mltB*	-0.653910677	1027	*ygiS*	-0.5977251
880	*ogrK*	-0.715436514	954	*fliR*	-0.653821624	1028	*ydfG*	-0.597096485
881	*tdcA*	-0.713577756	955	*yiaU*	-0.652657799	1029	*lit*	-0.597060794
882	*ybdD*	-0.71300935	956	*abrB*	-0.651407882	1030	*norW*	-0.596508729
883	*hyuA*	-0.71223501	957	*yidA*	-0.649036096	1031	*fumB*	-0.596103723
884	*sohB*	-0.712130996	958	*php*	-0.64898309	1032	*ygjR*	-0.596086275
885	*aqpZ*	-0.711981511	959	*ygjI*	-0.648257274	1033	*lpxT*	-0.595781872
886	*ccmE*	-0.711844867	960	*oppA*	-0.648033084	1034	*wzzB*	-0.595725392
887	*uraA*	-0.709292872	961	*elaA*	-0.647828814	1035	*ymjC*	-0.594960036
888	*glmU-SPA*	-0.709071058	962	*mscM*	-0.643427497	1036	*cvrA*	-0.594889005
889	*narK*	-0.708982239	963	*cadB*	-0.642688862	1037	*smpB*	-0.594435012
890	*yedY*	-0.707584025	964	*mutM*	-0.642318025	1038	*pcm*	-0.593274725
891	*srlA*	-0.706516162	965	*ybcN*	-0.641620493	1039	*def-SPA*	-0.593083662
892	*gfcD*	-0.705034737	966	*srlD*	-0.641212105	1040	*yddH*	-0.592861652
893	*cyoD*	-0.703668994	967	*tas*	-0.639619093	1041	*hofN*	-0.592783691
894	*ecpD*	-0.703173667	968	*chbG*	-0.639229172	1042	*hyfI*	-0.591625001
895	*torR*	-0.702902595	969	*umuC*	-0.638507757	1043	*narX*	-0.590275982
896	*xseA*	-0.702858891	970	*yjcO*	-0.637801059	1044	*sfmF*	-0.590266184
897	*ydeT*	-0.701341283	971	*cho*	-0.63776208	1045	*panF*	-0.587236608
898	*dgkA*	-0.701116077	972	*hycF*	-0.637684487	1046	*sdiA*	-0.587202474
899	*bfr*	-0.700853988	973	*trpR*	-0.637540244	1047	*msrA*	-0.585424952
900	*uvrB*	-0.700707125	974	*hcaR*	-0.636823948	1048	*soxR*	-0.584468719
901	*pphA*	-0.70065469	975	*yijP*	-0.63580932	1049	*yqfB*	-0.58416062
902	*sspB*	-0.698208755	976	*yceF*	-0.635796225	1050	*azoR*	-0.582246932
903	*ygiW*	-0.698205176	977	*yeeH*	-0.635498374	1051	*ycaN*	-0.581156656
904	*araH*	-0.697462292	978	*caiF*	-0.635493725	1052	*yeeY*	-0.578937491
905	*ybdL*	-0.696911257	979	*phnF*	-0.635185632	1053	*sthA*	-0.578917619
906	*epd*	-0.696751996	980	*ybbD*	-0.633287126	1054	*uhpB*	-0.57825415
907	*rmuC*	-0.696204762	981	*mlaD*	-0.633104642	1055	*flgC*	-0.577357981
908	*ymcE*	-0.696167317	982	*chiA*	-0.63277212	1056	*nagB*	-0.577037523
909	*aroF*	-0.694640551	983	*yjiV*	-0.632626699	1057	*nudG*	-0.576351107
910	*ecpR*	-0.693929378	984	*tsaD-SPA*	-0.63203459	1058	*yggP*	-0.575375546
911	*psiE*	-0.691195594	985	*sbcB*	-0.632001866	1059	*hemF*	-0.574974947
912	*ygdI*	-0.69086736	986	*fdnG*	-0.631996736	1060	*yjiQ*	-0.573990364
913	*yfbR*	-0.689985329	987	*katE*	-0.631357017	1061	*rzoR*	-0.572980445
914	*sufD*	-0.689474939	988	*ylaC*	-0.630328555	1062	*fhuF*	-0.572502467
915	*agaD*	-0.686921533	989	*fklB*	-0.630216862	1063	*oxc*	-0.572322787
916	*kbaZ*	-0.686250856	990	*dppD*	-0.629615748	1064	*moaD*	-0.572019358
917	*dgoA*	-0.686170018	991	*ycgY*	-0.628966055	1065	*valS-SPA*	-0.571452592
918	*ybeL*	-0.683067097	992	*rfbB*	-0.627831334	1066	*ydeA*	-0.570579511
919	*srlR*	-0.683052625	993	*phoA*	-0.627536369	1067	*yfdL*	-0.569928499
920	*uspF*	-0.679829107	994	*speC*	-0.62723234	1068	*yfaQ*	-0.568465349
921	*yeeL_1*	-0.679723941	995	*yggT*	-0.627029138	1069	*ydcD*	-0.568437627
922	*yghA*	-0.678940455	996	*yaeF*	-0.626816355	1070	*ybjC*	-0.56843279
923	*yegP*	-0.677415105	997	*ynaI*	-0.62633586	1071	*copA*	-0.567849796
924	*glxK*	-0.677047762	998	*yehT*	-0.625615845	1072	*fliN*	-0.567557839
925	*nlpC*	-0.676846969	999	*chiP*	-0.625309472	1073	*nupC*	-0.567513502
926	*mcrC*	-0.676117716	1000	*yfcT*	-0.624979989	1074	*yicR*	-0.564302422
927	*yihI*	-0.675353429	1001	*yhcA*	-0.624102207	1075	*paaF*	-0.563784358
928	*ftnA*	-0.67521956	1002	*allS*	-0.623888133	1076	*ilvD*	-0.563652708
929	*speE*	-0.674366763	1003	*yheS*	-0.62317037	1077	*ygbI*	-0.562903333
930	*cueR*	-0.674133818	1004	*wcaF*	-0.622535059	1078	*ypdC*	-0.562735171
931	*hisP*	-0.67233676	1005	*thiM*	-0.622472728	1079	*hisM*	-0.56259616
932	*yfbM*	-0.672039679	1006	*sdaB*	-0.620547471	1080	*entA*	-0.55984174
933	*yccS*	-0.671174201	1007	*ompG*	-0.618932367	1081	*hokB*	-0.559112816
934	*lrhA*	-0.670945976	1008	*frwC*	-0.617980799	1082	*dinG*	-0.559079885
935	*allR*	-0.670934085	1009	*xanP*	-0.617794478	1083	*nanT*	-0.558770837
936	*frvB*	-0.670913085	1010	*ompL*	-0.615959541	1084	*yhgF*	-0.558599085

1085	*pstC*	-0.557064317	1159	*yhfU*	-0.500552634	1233	*slp*	-0.441164098
1086	*psuT*	-0.556896363	1160	*yhdW*	-0.500485967	1234	*ybiJ*	-0.440848452
1087	*cydX*	-0.556592646	1161	*cof*	-0.499229743	1235	*gcvP*	-0.440592221
1088	*minC*	-0.556330985	1162	*flxA*	-0.496976016	1236	*yigB*	-0.440042791
1089	*mngA*	-0.555556473	1163	*nhaB*	-0.496935054	1237	*wzzE*	-0.440029757
1090	*ydjI*	-0.554424947	1164	*ycjN*	-0.495781816	1238	*yhjC*	-0.439956223
1091	*curA*	-0.552491424	1165	*mhpA*	-0.491873021	1239	*ycbX*	-0.439682206
1092	*rffC*	-0.549828049	1166	*glpQ*	-0.491784491	1240	*rcnR*	-0.439404678
1093	*appY*	-0.549194452	1167	*mcbA*	-0.491113429	1241	*evgA*	-0.439280795
1094	*uhpT*	-0.546114327	1168	*prkB*	-0.490009954	1242	*paaG*	-0.437882381
1095	*fsr*	-0.546109425	1169	*nirD*	-0.48737571	1243	*yhcF*	-0.433872082
1096	*cobS*	-0.544589526	1170	*ygaU*	-0.487163697	1244	*lolA-DAS*	-0.433559705
1097	*rssA*	-0.54458547	1171	*rpsT*	-0.486989823	1245	*ymfP*	-0.433303836
1098	*fabH*	-0.543438556	1172	*omrA*	-0.486333573	1246	*ydiR*	-0.431872137
1099	*yhiK*	-0.543241691	1173	*bolA*	-0.486278757	1247	*ygdG*	-0.430014825
1100	*aidB*	-0.543041509	1174	*ycdX*	-0.485951778	1248	*ytfR*	-0.427258784
1101	*fadJ*	-0.542749635	1175	*ygiV*	-0.484744504	1249	*nei*	-0.427116737
1102	*yfiH*	-0.540471367	1176	*focA*	-0.483583598	1250	*hicA*	-0.426631326
1103	*yebQ*	-0.539905829	1177	*ydaQ*	-0.48231889	1251	*tatE*	-0.424996254
1104	*xseB*	-0.539897369	1178	*yejF*	-0.481814919	1252	*mdtD*	-0.424861375
1105	*kbl*	-0.539113773	1179	*yjbH*	-0.481164694	1253	*zitB*	-0.424295064
1106	*asnA*	-0.538269162	1180	*clpX*	-0.481123711	1254	*ddlA*	-0.42347784
1107	*sra*	-0.537806083	1181	*dnaB-SPA*	-0.480894814	1255	*rffG*	-0.422995105
1108	*pabA*	-0.53733545	1182	*yfaT*	-0.480176742	1256	*msbA{P18S}*	-0.422462382
1109	*frlB*	-0.537304283	1183	*yedP*	-0.478823614	1257	*yfcD*	-0.422156627
1110	*mocA*	-0.537219365	1184	*yfaZ*	-0.478465518	1258	*ygbK*	-0.421585838
1111	*nadE-SPA*	-0.536297317	1185	*yjhG*	-0.477998232	1259	*pphB*	-0.421502848
1112	*yncD*	-0.536113273	1186	*arnT*	-0.477340392	1260	*nac*	-0.420730888
1113	*kptA*	-0.534566206	1187	*yfdR*	-0.475783172	1261	*yedL*	-0.420150083
1114	*ydeO*	-0.534216808	1188	*ydcO*	-0.473488646	1262	*yebZ*	-0.419390322
1115	*sbmC*	-0.533414383	1189	*paoD*	-0.47227437	1263	*moaB*	-0.419053425
1116	*gsiD*	-0.530314203	1190	*yehI*	-0.472046945	1264	*ybiB*	-0.418478271
1117	*galE*	-0.530225573	1191	*eutD*	-0.471058098	1265	*yjbI*	-0.41803509
1118	*yeaW*	-0.52853616	1192	*zapB*	-0.470322765	1266	*qseB*	-0.417812638
1119	*nudE*	-0.527110625	1193	*proX*	-0.468711271	1267	*dctA*	-0.416546528
1120	*spy*	-0.526759675	1194	*galT*	-0.468680341	1268	*lpxA-SPA*	-0.415867508
1121	*clsB*	-0.525486139	1195	*sgcB*	-0.468267869	1269	*ydcI*	-0.415190885
1122	*dosC*	-0.524416421	1196	*ygdB*	-0.467713956	1270	*alpA*	-0.415150473
1123	*ssnA*	-0.523347154	1197	*yiiR*	-0.466915825	1271	*flgK*	-0.414330043
1124	*ydjA*	-0.522961596	1198	*bhsA*	-0.466594697	1272	*fdoH*	-0.41316457
1125	*ecpE*	-0.522940214	1199	*yhfX*	-0.465807641	1273	*flhB*	-0.412347419
1126	*ylcG*	-0.522581024	1200	*exbB*	-0.462891929	1274	*ylcH*	-0.412146425
1127	*ybhQ*	-0.520224675	1201	*csgF*	-0.4627295	1275	*yeaV*	-0.412078246
1128	*fhlA*	-0.519069412	1202	*ytfK*	-0.462307981	1276	*alsC*	-0.411978122
1129	*dipZ*	-0.518507236	1203	*pdxB*	-0.462278081	1277	*hybO*	-0.411693462
1130	*rsuA*	-0.517557159	1204	*yaaX*	-0.461087136	1278	*ydcH*	-0.410380783
1131	*amiA*	-0.517535136	1205	*yjfM*	-0.460847349	1279	*sgcR*	-0.409280082
1132	*ddpB*	-0.5174282	1206	*yqgB*	-0.457894821	1280	*rffA*	-0.408149029
1133	*ydgA*	-0.517145627	1207	*yeiL*	-0.457341969	1281	*fliL*	-0.407747293
1134	*fic*	-0.51619375	1208	*yqiJ*	-0.457249161	1282	*essD*	-0.407443842
1135	*yfdM*	-0.515641831	1209	*lyxK*	-0.457244611	1283	*yciU*	-0.406988613
1136	*ycbK*	-0.514328434	1210	*ttdR*	-0.457101731	1284	*yhbJ*	-0.405742203
1137	*yijF*	-0.514147304	1211	*yecR*	-0.456739988	1285	*tdcB*	-0.405065961
1138	*uacT*	-0.511880639	1212	*yccJ*	-0.456560612	1286	*rnhB*	-0.40430875
1139	*xapA*	-0.511518664	1213	*yiaC*	-0.456152552	1287	*osmB*	-0.40411897
1140	*yjfC*	-0.511424572	1214	*creA*	-0.455698227	1288	*purF*	-0.403788129
1141	*trmL*	-0.511125953	1215	*ygeG*	-0.453551349	1289	*pnuC*	-0.402130587
1142	*fepG*	-0.510254272	1216	*ybcJ*	-0.451333454	1290	*ydcP*	-0.402046146
1143	*sufB*	-0.509934074	1217	*yejG*	-0.45119656	1291	*hcaF*	-0.401034421
1144	*rlmJ*	-0.509399944	1218	*helD*	-0.451177857	1292	*puuC*	-0.400931673
1145	*glpC*	-0.509329868	1219	*atpI*	-0.45071076	1293	*pldB*	-0.399674246
1146	*glpF*	-0.508486024	1220	*sibE*	-0.450677114	1294	*yigL*	-0.399607234
1147	*arpB_1*	-0.508458182	1221	*thiP*	-0.450466184	1295	*treB*	-0.39953612
1148	*aspC*	-0.507864977	1222	*ygfF*	-0.449787859	1296	*pabB*	-0.398790909
1149	*yheU*	-0.507140892	1223	*yhbE*	-0.449652539	1297	*yddE*	-0.398163667
1150	*macA*	-0.507008337	1224	*rhaT*	-0.448782141	1298	*ydiI*	-0.397840492
1151	*tam*	-0.506716621	1225	*arsR*	-0.447128002	1299	*ybjG*	-0.397801631
1152	*dnaE-SPA*	-0.504472284	1226	*umuD*	-0.445000726	1300	*narZ*	-0.397642787
1153	*atoA*	-0.504264771	1227	*pncC*	-0.443755203	1301	*xdhD*	-0.397618692
1154	*ymiA*	-0.503385	1228	*ydgH*	-0.443375485	1302	*yfjH*	-0.397584906
1155	*ygaM*	-0.502686667	1229	*fucO*	-0.442831237	1303	*yigZ*	-0.396501935
1156	*aroM*	-0.502336076	1230	*lldP*	-0.442528657	1304	*hyfG*	-0.396061425
1157	*bglJ*	-0.501760588	1231	*yciT*	-0.441600119	1305	*creB*	-0.390432918
1158	*dauA*	-0.500969563	1232	*ariR*	-0.44145674	1306	*yidD*	-0.390209917

1307	*proW*	-0.389280562	1381	*ydhX*	-0.339924839	1455	*ypdF*	-0.295859966
1308	*yahE*	-0.388265586	1382	*ftsA{R286W}*	-0.339687269	1456	*yecS*	-0.295757875
1309	*rcsA*	-0.3871824	1383	*ybgD*	-0.339653855	1457	*nirB*	-0.294460754
1310	*gntX*	-0.386927882	1384	*dnaQ*	-0.338696675	1458	*sixA*	-0.292651838
1311	*ycgM*	-0.386796018	1385	*ygaQ_1*	-0.337595097	1459	*ycjG*	-0.291391802
1312	*typA*	-0.386682762	1386	*djlA*	-0.337132724	1460	*narJ*	-0.291003216
1313	*phnI*	-0.385275323	1387	*dcuR*	-0.337008153	1461	*yddJ*	-0.289865858
1314	*livJ*	-0.385109467	1388	*tpiA*	-0.33638434	1462	*ykgJ*	-0.289823844
1315	*gpmA*	-0.383659637	1389	*mngR*	-0.33626314	1463	*rsfS*	-0.288434998
1316	*ybfF*	-0.3833857	1390	*yjiP*	-0.335576227	1464	*yjeH*	-0.286079031
1317	*ygjJ*	-0.382785341	1391	*recQ*	-0.335312154	1465	*rssB*	-0.285902503
1318	*pncB*	-0.382197019	1392	*rsxG*	-0.334865976	1466	*psiF*	-0.284515041
1319	*mcrA*	-0.38179794	1393	*folM*	-0.334644869	1467	*sfmD*	-0.284071601
1320	*ycjM*	-0.379752234	1394	*lepA*	-0.333834697	1468	*btuD*	-0.283515753
1321	*alsA*	-0.379575998	1395	*dcd*	-0.333690298	1469	*nfsB*	-0.283194668
1322	*ydbC*	-0.379522578	1396	*allE*	-0.333065259	1470	*waaS*	-0.28310352
1323	*bglH*	-0.379374876	1397	*ahpC*	-0.332999557	1471	*yjhH*	-0.283088467
1324	*tonB*	-0.379298049	1398	*yjcE*	-0.332726991	1472	*rstA*	-0.282669597
1325	*rbsA*	-0.378868165	1399	*ygfT*	-0.332266155	1473	*aldA*	-0.282336503
1326	*flgE*	-0.378801393	1400	*osmY*	-0.331886782	1474	*ampC*	-0.282201681
1327	*wbbJ*	-0.378277006	1401	*hyfE*	-0.328876282	1475	*gcvH*	-0.280961488
1328	*wcaD*	-0.378274239	1402	*gsiC*	-0.328203866	1476	*xapB*	-0.279221742
1329	*setB*	-0.37684768	1403	*agp*	-0.325982986	1477	*yahD*	-0.278899866
1330	*gntU*	-0.376639431	1404	*yhgE*	-0.325034343	1478	*tsgA*	-0.278090852
1331	*lsrG*	-0.376355477	1405	*ytfE*	-0.323500668	1479	*ygfS*	-0.27736594
1332	*yjhC*	-0.376301916	1406	*cynR*	-0.322516687	1480	*yfaU*	-0.277048278
1333	*ilvY*	-0.37621136	1407	*clpP*	-0.322297564	1481	*yebY*	-0.275329476
1334	*exbD*	-0.376160348	1408	*fecA*	-0.321536501	1482	*infA-SPA*	-0.274829031
1335	*yobD*	-0.375198548	1409	*dppB*	-0.320959395	1483	*casB*	-0.274215306
1336	*ansP*	-0.374469017	1410	*yfeK*	-0.320570365	1484	*yegE*	-0.2736366
1337	*rng*	-0.374414563	1411	*ycbB*	-0.319916274	1485	*yidI*	-0.273321837
1338	*idi*	-0.373764561	1412	*yghS*	-0.319020337	1486	*yaeH*	-0.271546392
1339	*uspC*	-0.373585436	1413	*yoeI*	-0.318643211	1487	*xylR*	-0.270201143
1340	*cbrA*	-0.373475074	1414	*hepA*	-0.31769669	1488	*phnH*	-0.270093741
1341	*msbA-kan*	-0.373269613	1415	*ygaX*	-0.316757911	1489	*yfgH*	-0.270006933
1342	*gabP*	-0.372369663	1416	*ynaE*	-0.31553614	1490	*tesA*	-0.269252126
1343	*xdhA*	-0.370394601	1417	*fimZ*	-0.315443689	1491	*ybjQ*	-0.268859893
1344	*yeeS*	-0.367835525	1418	*cadC*	-0.314701562	1492	*yhaI*	-0.268259391
1345	*eutC*	-0.367762677	1419	*pmrD*	-0.314115663	1493	*yieF*	-0.265989082
1346	*yfbK*	-0.367625112	1420	*yjgR*	-0.313856663	1494	*waaA-B*	-0.263872539
1347	*glnQ*	-0.366839584	1421	*nrfF*	-0.313828038	1495	*thiQ*	-0.263656654
1348	*tauA*	-0.365721093	1422	*ppdA*	-0.313328749	1496	*ytfF*	-0.263399256
1349	*mcrB*	-0.364736601	1423	*metK-SPA*	-0.312966514	1497	*yhhN*	-0.262703151
1350	*essQ*	-0.364172689	1424	*ryfA*	-0.312122999	1498	*yagM*	-0.261615735
1351	*hycE*	-0.363563531	1425	*ybdM*	-0.3119757	1499	*ybhC*	-0.260764324
1352	*mzrA*	-0.363541305	1426	*atoD*	-0.31170586	1500	*ytfB*	-0.259329945
1353	*yefM-SPA*	-0.363496922	1427	*dhaM*	-0.311209417	1501	*lacY*	-0.258052896
1354	*gmd*	-0.363336238	1428	*yaiL*	-0.31103265	1502	*nfsA*	-0.256512389
1355	*recF*	-0.363261315	1429	*rnlA*	-0.309655152	1503	*gspJ*	-0.256175716
1356	*yajQ*	-0.361002642	1430	*ybiR*	-0.309225751	1504	*hofC*	-0.256022311
1357	*dcuB*	-0.360655934	1431	*ydeQ*	-0.308345172	1505	*rsmJ*	-0.25520812
1358	*lldD*	-0.360527387	1432	*yqhH*	-0.307930856	1506	*mlrA*	-0.254290035
1359	*yaiU*	-0.359066072	1433	*hycG*	-0.307395985	1507	*puuB*	-0.254241897
1360	*amiB*	-0.35897746	1434	*yfjU*	-0.307223047	1508	*matP*	-0.251678318
1361	*yebF*	-0.358704568	1435	*yeiR*	-0.306675028	1509	*glpT*	-0.250501441
1362	*nupG*	-0.358054431	1436	*yagK*	-0.306412173	1510	*yfcJ*	-0.250019193
1363	*paaY*	-0.354852117	1437	*nrfG*	-0.306261763	1511	*uxaA*	-0.249466005
1364	*ybhA*	-0.354182044	1438	*loiP*	-0.305662896	1512	*cmoA*	-0.249220272
1365	*yqfA*	-0.353681569	1439	*csiR*	-0.304863426	1513	*yjiK*	-0.248372119
1366	*rluF*	-0.353562737	1440	*nadA*	-0.304802006	1514	*ybcD*	-0.248046279
1367	*tolA*	-0.353038388	1441	*ygfM*	-0.30394588	1515	*mnmG*	-0.247904354
1368	*yrdB*	-0.352850279	1442	*yfjZ*	-0.303172287	1516	*fryA*	-0.247692744
1369	*yieP*	-0.352725374	1443	*ymgE*	-0.302237751	1517	*tar*	-0.24758804
1370	*hokA*	-0.352564535	1444	*phr*	-0.302180526	1518	*udk*	-0.246682693
1371	*ybcW*	-0.351609206	1445	*pykF*	-0.302144948	1519	*dpiB*	-0.245870117
1372	*flk*	-0.351243123	1446	*pgk-SPA*	-0.301448763	1520	*ycaM*	-0.245805897
1373	*tauD*	-0.351189915	1447	*csiD*	-0.299467082	1521	*ybcI*	-0.24445223
1374	*yicC*	-0.349786061	1448	*dicF*	-0.298949194	1522	*acpP-SPA*	-0.243987751
1375	*yejM-SPA*	-0.348885799	1449	*ygbM*	-0.298421579	1523	*yfcG*	-0.243771164
1376	*livM*	-0.346374346	1450	*mdtI*	-0.298022336	1524	*ynjA*	-0.243251072
1377	*hslO*	-0.346129743	1451	*paaK*	-0.297967504	1525	*tfaX*	-0.243248643
1378	*rhaM*	-0.344671458	1452	*secG*	-0.297088833	1526	*yjdJ*	-0.242268186
1379	*pflB*	-0.343704688	1453	*ychJ*	-0.29638959	1527	*yrbL*	-0.241282394
1380	*yjjV*	-0.34104441	1454	*ydeM*	-0.296141805	1528	*yehE*	-0.240810292

1529	*menB*	-0.240182197	1603	*phoE*	-0.190374558	1677	*lsrB*	-0.145859918
1530	*puuD*	-0.238634945	1604	*ybcY*	-0.189632611	1678	*hokE*	-0.144939069
1531	*ynaJ*	-0.236109306	1605	*hyaC*	-0.188277731	1679	*yiiE*	-0.143960911
1532	*rrrD*	-0.234802707	1606	*agaW*	-0.187860959	1680	*eutH*	-0.143808189
1533	*phnD*	-0.234427765	1607	*argT*	-0.187613624	1681	*yeiH*	-0.143227224
1534	*yjjG*	-0.233687524	1608	*fimB*	-0.187253984	1682	*ybdG*	-0.142795524
1535	*apt*	-0.233616464	1609	*caiD*	-0.187145351	1683	*ibpB*	-0.14262933
1536	*fumC*	-0.233571166	1610	*yqaE*	-0.186982251	1684	*ulaD*	-0.138432289
1537	*cspG*	-0.232594217	1611	*lpoA*	-0.186643967	1685	*lafU*	-0.138401996
1538	*ispU-SPA*	-0.23186689	1612	*ydgU*	-0.186467562	1686	*mlaC*	-0.137883171
1539	*yifK*	-0.231639179	1613	*yfhM*	-0.185993158	1687	*astB*	-0.137516893
1540	*ydcA*	-0.230333934	1614	*yjeN*	-0.185675118	1688	*lpxC-SPA*	-0.135065761
1541	*rstB*	-0.229838308	1615	*surA*	-0.185394945	1689	*nudI*	-0.134540932
1542	*tmcA*	-0.229515531	1616	*lpxP*	-0.184893393	1690	*gldA*	-0.134176746
1543	*ydbH*	-0.229447333	1617	*ygjH*	-0.184396915	1691	*citG*	-0.133969429
1544	*nth*	-0.228592029	1618	*citT*	-0.184177226	1692	*ilvH*	-0.133664494
1545	*yhgN*	-0.228057928	1619	*ynjF*	-0.183503023	1693	*yfcL*	-0.133419576
1546	*csgG*	-0.227357802	1620	*arnF*	-0.182441295	1694	*yjiE*	-0.132026872
1547	*csrB*	-0.226620192	1621	*manY*	-0.181537441	1695	*recD*	-0.131764624
1548	*cybC*	-0.226527288	1622	*ykgO*	-0.181369666	1696	*trxC*	-0.131359689
1549	*ykfC*	-0.225839486	1623	*abgT*	-0.180493517	1697	*gltL*	-0.131257321
1550	*astE*	-0.225573285	1624	*tabA*	-0.178792208	1698	*ydjH*	-0.130745751
1551	*xdhB*	-0.224375997	1625	*nikC*	-0.178640871	1699	*guaC*	-0.129967577
1552	*csgD*	-0.224331094	1626	*osmF*	-0.178305135	1700	*ypeB*	-0.129581227
1553	*dsbA*	-0.223809042	1627	*patA*	-0.177889095	1701	*ybiV*	-0.129226779
1554	*ymfM*	-0.223081717	1628	*flgJ*	-0.1776482	1702	*hyfH*	-0.128840669
1555	*pmbA*	-0.222620184	1629	*fliG*	-0.176521844	1703	*cusA*	-0.128579723
1556	*hypC*	-0.221674984	1630	*purR*	-0.176506613	1704	*ygiC*	-0.128235463
1557	*pka*	-0.221542787	1631	*yfhR*	-0.176393041	1705	*mrcA*	-0.128196832
1558	*ymjD*	-0.219358351	1632	*rnk*	-0.17600474	1706	*csgB*	-0.126978344
1559	*yqeJ*	-0.219312122	1633	*ychA*	-0.17257452	1707	*metQ*	-0.125696031
1560	*ydcJ*	-0.21763773	1634	*yfdH*	-0.171766941	1708	*rsxD*	-0.123589984
1561	*yafN*	-0.217340884	1635	*htpX*	-0.170076198	1709	*ydiT*	-0.122386663
1562	*slyA*	-0.217021346	1636	*scpC*	-0.168881652	1710	*ybdR*	-0.122345418
1563	*mdtC*	-0.216658636	1637	*fliC*	-0.168293576	1711	*yagL*	-0.118914844
1564	*selD*	-0.216449299	1638	*atoB*	-0.166911201	1712	*potF*	-0.115879507
1565	*lpxc-kan*	-0.215683023	1639	*ydbL*	-0.166525113	1713	*hyaA*	-0.115398437
1566	*yfdN*	-0.215601522	1640	*dppA*	-0.166036781	1714	*garD*	-0.114944134
1567	*ssuA*	-0.214787738	1641	*pcnB*	-0.165253798	1715	*galK*	-0.114732189
1568	*bcsG*	-0.214425464	1642	*acrF*	-0.165012329	1716	*yghW*	-0.114395323
1569	*uidA*	-0.214082277	1643	*yjiA*	-0.16489781	1717	*cueO*	-0.113931873
1570	*purU*	-0.213736177	1644	*pspB*	-0.163622096	1718	*sibABCDE*	-0.112294568
1571	*ydiB*	-0.213637827	1645	*ynfG*	-0.163584079	1719	*hisQ*	-0.111980535
1572	*asr*	-0.213227133	1646	*ydcR*	-0.163393795	1720	*emrY*	-0.111847636
1573	*thiD*	-0.213050437	1647	*bcsF*	-0.163304335	1721	*leuE*	-0.110947447
1574	*potI*	-0.212839184	1648	*potC*	-0.163184663	1722	*bioC*	-0.109432338
1575	*rnhA*	-0.210559751	1649	*wcaK*	-0.162744548	1723	*yfiP*	-0.107608541
1576	*artP*	-0.209390633	1650	*yagF*	-0.162736141	1724	*idnO*	-0.107504735
1577	*recX*	-0.208416266	1651	*ybeZ*	-0.162701024	1725	*yiiX*	-0.107176197
1578	*ybbO*	-0.208156397	1652	*pgaA*	-0.16169183	1726	*rnlB*	-0.106638559
1579	*menA*	-0.207603003	1653	*yjiH*	-0.159036744	1727	*yodD*	-0.105739797
1580	*ssuB*	-0.207276106	1654	*ymdF*	-0.157490909	1728	*yehL*	-0.104712173
1581	*ycaK*	-0.206915294	1655	*ispG-SPA*	-0.157260357	1729	*yfiB*	-0.103371325
1582	*cstA*	-0.206177023	1656	*panE*	-0.156521805	1730	*yjcF*	-0.101381193
1583	*ycbV*	-0.205753951	1657	*rihA*	-0.156455203	1731	*glnP*	-0.099582206
1584	*yjeT*	-0.204953083	1658	*ratB*	-0.156450004	1732	*ynfA*	-0.099577532
1585	*ygjV*	-0.204079978	1659	*yibQ*	-0.156296475	1733	*ybdK*	-0.099264012
1586	*pspG*	-0.20378359	1660	*ybhK*	-0.156064923	1734	*avtA*	-0.097070182
1587	*dgoK*	-0.203597017	1661	*nirC*	-0.15572582	1735	*nagA*	-0.096035573
1588	*ydeE*	-0.202930909	1662	*purD*	-0.155533418	1736	*pqiA*	-0.095975614
1589	*mrr*	-0.202599434	1663	*yjjJ*	-0.154892437	1737	*yceA*	-0.095945927
1590	*ynjB*	-0.20255361	1664	*tdcR*	-0.153579761	1738	*torI*	-0.095711306
1591	*ydfR*	-0.20237664	1665	*yidL*	-0.153379513	1739	*rsxA*	-0.095184419
1592	*yeeN*	-0.199847005	1666	*queE*	-0.15164166	1740	*seqA*	-0.094828563
1593	*gshB*	-0.198633163	1667	*rhaR*	-0.151435691	1741	*glvB*	-0.094567841
1594	*amyA*	-0.197788495	1668	*acpS-SPA*	-0.151167013	1742	*dsdX*	-0.094300038
1595	*yfgF*	-0.196181675	1669	*yidG*	-0.150774912	1743	*renD*	-0.093874586
1596	*yhdV*	-0.195275194	1670	*ymdA*	-0.150140264	1744	*pspC*	-0.093513718
1597	*yihO*	-0.194919547	1671	*yfeW*	-0.148597594	1745	*iscX*	-0.093079384
1598	*yegS*	-0.194906389	1672	*ybfB*	-0.14821857	1746	*galS*	-0.090979172
1599	*ppdD*	-0.193140126	1673	*adrA*	-0.147920673	1747	*yedW*	-0.090963435
1600	*yidE*	-0.193099611	1674	*yfcH*	-0.147311794	1748	*rlmC*	-0.090215526
1601	*yciE*	-0.192120977	1675	*hsdM*	-0.147072776	1749	*ychQ*	-0.089978881
1602	*oppB*	-0.190576835	1676	*yeaE*	-0.14699023	1750	*thiK*	-0.088032455

1751	*yhdH*	-0.087938704	1825	*kduD*	-0.051405213	1899	*ydjK*	-0.015762158
1752	*yegX*	-0.087548002	1826	*yccF*	-0.05100118	1900	*yieK*	-0.015619493
1753	*yjbG*	-0.08737771	1827	*livK*	-0.050405969	1901	*yihN*	-0.015239844
1754	*ykgR*	-0.087216426	1828	*yhaJ*	-0.050382382	1902	*ispA-SPA*	-0.01281832
1755	*yijE*	-0.085718861	1829	*mioC*	-0.050111176	1903	*uhpA*	-0.011648081
1756	*fadI*	-0.085344003	1830	*uspG*	-0.049997876	1904	*frwB*	-0.009983969
1757	*sulA*	-0.085186036	1831	*caiT*	-0.049936528	1905	*pbpC*	-0.009783374
1758	*ulaR*	-0.084887828	1832	*yohK*	-0.049866493	1906	*yhfG*	-0.009106273
1759	*glnK*	-0.084647104	1833	*yicG*	-0.049847392	1907	*alkA*	-0.008726983
1760	*malT*	-0.083464454	1834	*gltB*	-0.049451982	1908	*nikA*	-0.008638956
1761	*recR*	-0.08289575	1835	*yjeM*	-0.049055132	1909	*tdk*	-0.008576636
1762	*rluD*	-0.082134684	1836	*nrdE*	-0.048912867	1910	*yebW*	-0.007724623
1763	*adiA*	-0.081742271	1837	*rdlABC*	-0.048568259	1911	*yqiG*	-0.006506936
1764	*ypjB*	-0.081020113	1838	*ppiA*	-0.048447325	1912	*ansA*	-0.005698685
1765	*ybhN*	-0.080854689	1839	*ppdB*	-0.046802385	1913	*yhaB*	-0.005403432
1766	*gspI*	-0.080838464	1840	*hyfB*	-0.046016582	1914	*idnD*	-0.004812492
1767	*ycaD*	-0.080698883	1841	*ybbA*	-0.045126731	1915	*ispH-SPA*	-0.004770564
1768	*slyX*	-0.080245449	1842	*rna*	-0.044973473	1916	*yihU*	-0.004545204
1769	*mlaA*	-0.079202833	1843	*murA-SPA*	-0.044414991	1917	*yehP*	-0.003081887
1770	*yaaJ*	-0.078697118	1844	*yeeX*	-0.043904927	1918	*ynhF*	-0.001112438
1771	*yajD*	-0.078524992	1845	*mdaB*	-0.043881089	1919	*htgA*	-0.000989142
1772	*grxA*	-0.07774981	1846	*ydaV*	-0.043139593	1920	*metL*	-0.00079906
1773	*hicB*	-0.077659641	1847	*fliY*	-0.042943166	1921	*araJ*	0.00016558
1774	*eutM*	-0.07760649	1848	*pinE*	-0.042358065	1922	*fruA*	0.000327973
1775	*ydfH*	-0.07683715	1849	*clpA*	-0.042108897	1923	*ygbA*	0.000621142
1776	*recA*	-0.076354739	1850	*narQ*	-0.042055411	1924	*yhcC*	0.002016975
1777	*eutL*	-0.076113106	1851	*ybgE*	-0.041404087	1925	*yghD*	0.002024606
1778	*dinQ*	-0.075979969	1852	*uxaB*	-0.041119893	1926	*phnN*	0.002199879
1779	*stfE*	-0.074768039	1853	*yicH*	-0.040642246	1927	*ydaW*	0.00287507
1780	*kbaY*	-0.074108985	1854	*atoE*	-0.040338174	1928	*fimA*	0.004330454
1781	*yhhT*	-0.073533806	1855	*rbfA*	-0.039927509	1929	*yfiE*	0.004430754
1782	*yagH*	-0.073187635	1856	*gutQ*	-0.0398791	1930	*hmp*	0.004570905
1783	*yihS*	-0.070995677	1857	*yicO*	-0.038891926	1931	*yzfA*	0.005425253
1784	*mmuM*	-0.070736346	1858	*fruK*	-0.038138623	1932	*galF*	0.005514879
1785	*yhhS*	-0.070650923	1859	*yaiV*	-0.03516802	1933	*glmS-SPA*	0.005962071
1786	*plaP*	-0.070514525	1860	*iaaA*	-0.034992633	1934	*artI*	0.006995459
1787	*yrfG*	-0.069908989	1861	*yehB*	-0.034641359	1935	*fliQ*	0.007614114
1788	*yodC*	-0.069536884	1862	*mak*	-0.034499492	1936	*ypjF*	0.008879825
1789	*flgL*	-0.068991295	1863	*glnB*	-0.033635401	1937	*yjbL*	0.01039787
1790	*fliS*	-0.067700454	1864	*hybC*	-0.03360506	1938	*kefB*	0.01116726
1791	*gspB*	-0.066792381	1865	*thiS*	-0.033064185	1939	*yodB*	0.012234827
1792	*ypfG*	-0.066513004	1866	*ldhA*	-0.03204491	1940	*yjdC*	0.013757027
1793	*hsrA*	-0.066096893	1867	*mdtM*	-0.030892215	1941	*kdpA*	0.014396906
1794	*corA*	-0.065558115	1868	*yajI*	-0.030844025	1942	*ygeP*	0.014866492
1795	*udp*	-0.065259297	1869	*ynfK*	-0.030641656	1943	*ompW*	0.015398333
1796	*ydhU*	-0.064595124	1870	*wbbL_1*	-0.030142937	1944	*eptA*	0.015430571
1797	*gutM*	-0.064204318	1871	*yjbM*	-0.029143737	1945	*wzb*	0.016021453
1798	*uidB*	-0.063914838	1872	*sapB*	-0.028771855	1946	*yhbP*	0.016143358
1799	*ypdA*	-0.063762738	1873	*fkpB*	-0.02869264	1947	*yqgE*	0.017390288
1800	*yidZ*	-0.062990364	1874	*yccT*	-0.028233185	1948	*lomR_2*	0.017745742
1801	*ypfN*	-0.061449702	1875	*dacB*	-0.027229977	1949	*zntR*	0.017805115
1802	*intE*	-0.061074513	1876	*yeeO*	-0.027193272	1950	*yhfS*	0.018490924
1803	*thiI*	-0.060687115	1877	*yeaG*	-0.027073206	1951	*yihF*	0.018500087
1804	*yafL*	-0.060508486	1878	*trkH*	-0.027014799	1952	*dicC*	0.020176914
1805	*nrfE*	-0.059794053	1879	*yohO*	-0.026802231	1953	*ygbJ*	0.020440987
1806	*napC*	-0.05938281	1880	*gspK*	-0.026714685	1954	*ryfB*	0.02048773
1807	*yraN*	-0.058324767	1881	*yadE*	-0.025813747	1955	*yfjM*	0.021599038
1808	*yhdZ*	-0.058070148	1882	*ddpC*	-0.025775536	1956	*priC*	0.022060062
1809	*aes*	-0.057867322	1883	*murE-C*	-0.025326719	1957	*fldA-SPA*	0.023305841
1810	*acpT*	-0.057108855	1884	*yfaP*	-0.025237006	1958	*flhC*	0.023914645
1811	*obgE-SPA*	-0.056949942	1885	*yicJ*	-0.024527303	1959	*caiC*	0.024562927
1812	*fabZ-kan*	-0.056946668	1886	*bcsZ*	-0.023950128	1960	*tauC*	0.024747664
1813	*mtfA*	-0.056882858	1887	*dgoD*	-0.023731102	1961	*yciQ*	0.025098987
1814	*gspE*	-0.056133201	1888	*yddB*	-0.022941001	1962	*cmoB*	0.025152016
1815	*ybhI*	-0.055804317	1889	*ymgH*	-0.01976528	1963	*glpR*	0.025732517
1816	*ampH*	-0.055296938	1890	*ydcS*	-0.019725754	1964	*tusE*	0.026057029
1817	*fdnI*	-0.053922443	1891	*queD*	-0.019333652	1965	*frmA*	0.026363467
1818	*ymgC*	-0.053689555	1892	*ydaM*	-0.019147699	1966	*ybcO*	0.028266373
1819	*queG*	-0.053515474	1893	*yohC*	-0.019146343	1967	*ynfD*	0.028638208
1820	*ygiN*	-0.052620848	1894	*yfjQ*	-0.018893928	1968	*yfaA*	0.028746525
1821	*yifL*	-0.052619375	1895	*ybfD*	-0.018852571	1969	*rluA*	0.030093481
1822	*fepE*	-0.052521952	1896	*mokC*	-0.018794849	1970	*ydgI*	0.030335068
1823	*yciM*	-0.052393254	1897	*ygeX*	-0.017659695	1971	*hycI*	0.030421782
1824	*sdsP*	-0.0522805	1898	*yphD*	-0.017411428	1972	*ypfJ*	0.030772859

1973	*yhhL*	0.032368076	2047	*yggF*	0.068697907	2121	*yijO*	0.109131809
1974	*fimC*	0.032657854	2048	*rem*	0.069701841	2122	*yggL*	0.109423487
1975	*dinI*	0.033012449	2049	*ryhB*	0.070321444	2123	*sufC*	0.109750898
1976	*intF*	0.034355136	2050	*fixC*	0.070393739	2124	*ygiH*	0.110019454
1977	*rtcR*	0.034909873	2051	*yecF*	0.070877088	2125	*pliG*	0.110189909
1978	*fliD*	0.035745692	2052	*ymfN*	0.071314329	2126	*yfbS*	0.110450644
1979	*cysD*	0.036041252	2053	*ybdH*	0.071498967	2127	*agaC*	0.110763518
1980	*ydfD*	0.039010949	2054	*uidR*	0.071635878	2128	*yghT*	0.111789901
1981	*groS-SPA*	0.039135186	2055	*rpmI*	0.072330054	2129	*melB*	0.112664018
1982	*cdaR*	0.039140281	2056	*yfdK*	0.073578932	2130	*micF*	0.113783082
1983	*yneF*	0.039911392	2057	*ppx*	0.073968322	2131	*yjfK*	0.114086368
1984	*thiE*	0.040269645	2058	*yrbG*	0.075491341	2132	*fnr*	0.114510172
1985	*glcD*	0.040277511	2059	*malI*	0.076238713	2133	*glpA*	0.115066347
1986	*hyaB*	0.040746887	2060	*hybG*	0.076304504	2134	*rsmI-SPA*	0.115314604
1987	*crcB*	0.041249035	2061	*psuG*	0.076710057	2135	*hyaD*	0.115403856
1988	*hypB*	0.041443646	2062	*ryeB*	0.076913643	2136	*gatZ*	0.115727942
1989	*yidR*	0.041624601	2063	*trpS-SPA*	0.078586966	2137	*ugpB*	0.115891083
1990	*purP*	0.041684752	2064	*mntR*	0.079114912	2138	*yhdN*	0.116180303
1991	*yjdL*	0.041838084	2065	*ompA*	0.080245926	2139	*yahC*	0.116221995
1992	*btuC*	0.042734136	2066	*yiaF*	0.0806092	2140	*fabI-SPA*	0.117345649
1993	*pdxY*	0.043148742	2067	*yadH*	0.08086394	2141	*sseB*	0.117778227
1994	*yfaD*	0.043713208	2068	*ydiF*	0.081145124	2142	*thrB*	0.117867106
1995	*hypF*	0.045340086	2069	*yjiJ*	0.083683578	2143	*speB*	0.117897905
1996	*ftsZ-SPA*	0.045585773	2070	*tolR*	0.08371353	2144	*lptA-SPA*	0.118379069
1997	*yhiN*	0.046100749	2071	*pyrH-SPA*	0.083917429	2145	*yihR*	0.12031158
1998	*bioF*	0.046141385	2072	*znuA*	0.083977651	2146	*ygiQ*	0.122327143
1999	*ygeQ*	0.046489843	2073	*yfbP*	0.084636886	2147	*ssuC*	0.122767199
2000	*deoA*	0.046555694	2074	*yeaM*	0.084938498	2148	*cynS*	0.123362776
2001	*ybjE*	0.047210311	2075	*ydiV*	0.085213113	2149	*yncI*	0.123565814
2002	*modE*	0.047426102	2076	*gltX-SPA*	0.085437523	2150	*cydC-SPA*	0.123632719
2003	*ybaY*	0.048732747	2077	*cas1*	0.085664704	2151	*yibI*	0.124746588
2004	*gsk*	0.048767969	2078	*yfdF*	0.085876265	2152	*yliF*	0.125710026
2005	*yqfG*	0.048977087	2079	*ygaC*	0.086028494	2153	*yabP*	0.127506617
2006	*epmC*	0.050128892	2080	*aroA*	0.086451591	2154	*yobH*	0.127905692
2007	*yoeE*	0.050441378	2081	*hslU*	0.086902522	2155	*yneJ*	0.129168501
2008	*rspB*	0.050533189	2082	*fes*	0.088998913	2156	*yeaY*	0.130563639
2009	*hdeA*	0.050957651	2083	*cyaY*	0.089272529	2157	*dsdA*	0.131293138
2010	*fimE*	0.051641507	2084	*yedM*	0.08969798	2158	*yrhA*	0.131534143
2011	*eutS*	0.051972722	2085	*ygfB*	0.090268069	2159	*pdxJ*	0.131857079
2012	*yahL*	0.052169307	2086	*thiG*	0.090491327	2160	*mdfA*	0.131947608
2013	*uhpC*	0.05236583	2087	*pspE*	0.091076576	2161	*yecE*	0.132024827
2014	*purB-SPA*	0.052574474	2088	*yheT*	0.091085261	2162	*frdD*	0.132291322
2015	*ygcP*	0.052767472	2089	*yehM*	0.091583703	2163	*ydfA*	0.132301748
2016	*emtA*	0.052799979	2090	*yfeN*	0.091686928	2164	*yhcG*	0.132319258
2017	*yobI*	0.054166939	2091	*spr*	0.092486041	2165	*ygeY*	0.133041272
2018	*ptsP*	0.054511604	2092	*tyrP*	0.09290393	2166	*ascF*	0.133492024
2019	*ttdB*	0.054861144	2093	*yhbQ*	0.093465894	2167	*yjfI*	0.134137378
2020	*nrfC*	0.054880421	2094	*rhtA*	0.094397413	2168	*intD*	0.134195123
2021	*trpC*	0.05524501	2095	*puuA*	0.094442461	2169	*ugpC*	0.134452777
2022	*frwD*	0.056812894	2096	*cheZ*	0.094576172	2170	*yjhX*	0.134947422
2023	*gcl*	0.056833569	2097	*yqhD*	0.09568081	2171	*pepB*	0.135089069
2024	*yjjN*	0.05695012	2098	*yegV*	0.095713163	2172	*ydjZ*	0.13538379
2025	*dcuC*	0.058475417	2099	*speD*	0.095729388	2173	*yiiD*	0.135602943
2026	*yfbT*	0.059650741	2100	*sgbH*	0.095966568	2174	*yecD*	0.137260085
2027	*ynaA*	0.060597957	2101	*recE*	0.096270902	2175	*ybbY*	0.137928122
2028	*yqeB*	0.060947128	2102	*garP*	0.098310938	2176	*rzpQ*	0.138984773
2029	*ydbJ*	0.061030286	2103	*rimO*	0.09836132	2177	*yahJ*	0.139446502
2030	*ydhO*	0.061118782	2104	*ftsX-SPA*	0.099861127	2178	*flgN*	0.139706104
2031	*hha*	0.06258361	2105	*yeiB*	0.100054827	2179	*ycjS*	0.139775565
2032	*ygeA*	0.063415725	2106	*prmA*	0.100272486	2180	*yiaY*	0.140528083
2033	*metI*	0.063797543	2107	*dmsC*	0.102090844	2181	*psrD*	0.141011629
2034	*nfi*	0.064024572	2108	*malZ*	0.102260469	2182	*yqaB*	0.141409927
2035	*rcnA*	0.064082879	2109	*osmC*	0.102932664	2183	*gltK*	0.141422319
2036	*ypeA*	0.064500662	2110	*yacL*	0.10311294	2184	*nagC*	0.142400459
2037	*yjfY*	0.065212986	2111	*yohF*	0.103217731	2185	*elfG*	0.14256251
2038	*glcG*	0.065532354	2112	*flhE*	0.103963762	2186	*mltD*	0.142945715
2039	*ynfB*	0.065539099	2113	*yajC*	0.103972463	2187	*yqjC*	0.143028024
2040	*yfcV*	0.065575185	2114	*yjjP*	0.104243831	2188	*ybjO*	0.143739128
2041	*prpB*	0.065747306	2115	*yjfF*	0.1047044	2189	*mlc*	0.144500483
2042	*fusA-SPA*	0.065825185	2116	*yaiA*	0.105065615	2190	*holA-SPA*	0.144601139
2043	*yjeJ*	0.06639697	2117	*yedE*	0.105654319	2191	*proQ*	0.144837882
2044	*lhgO*	0.066915079	2118	*basR*	0.105999593	2192	*yhfK*	0.145259449
2045	*ygiL*	0.067774701	2119	*htpG*	0.10723451	2193	*rzpD*	0.145601265
2046	*ydjY*	0.068200795	2120	*pheP*	0.107294819	2194	*entH*	0.146750648

2195	*prlF*	0.147165362	2269	*holE*	0.193681039	2343	*prpR*	0.242180948
2196	*nudC*	0.147779969	2270	*hsdR*	0.19540189	2344	*lysA*	0.242926009
2197	*yigI*	0.148147054	2271	*yciV*	0.195745791	2345	*nikD*	0.24318915
2198	*yciA*	0.149226255	2272	*hisJ*	0.196412807	2346	*modC*	0.243468697
2199	*eco*	0.150727032	2273	*appA*	0.196649177	2347	*ycgR*	0.243772991
2200	*glpB*	0.152599403	2274	*ybfP*	0.197021792	2348	*hycD*	0.244010231
2201	*gntT*	0.152771949	2275	*blr*	0.197204803	2349	*araC*	0.244326507
2202	*fhuE*	0.153229179	2276	*gapA-SPA*	0.198462993	2350	*ysdC*	0.244539644
2203	*holB-SPA*	0.15335636	2277	*yfiO**	0.198914852	2351	*ybgS*	0.245132169
2204	*ygeN*	0.1538438	2278	*ybaS*	0.198930437	2352	*tsr*	0.245182258
2205	*ydcT*	0.153997452	2279	*ybbJ*	0.199072342	2353	*yehU*	0.245507778
2206	*yedJ*	0.154286877	2280	*rpiA*	0.200196929	2354	*mobA*	0.245766067
2207	*yhjE*	0.154563821	2281	*ydjL*	0.20082532	2355	*mppA*	0.246017206
2208	*gspA*	0.155011092	2282	*yejE*	0.200859588	2356	*yniA*	0.246529243
2209	*moaC*	0.156391719	2283	*hcaT*	0.201078495	2357	*yihG*	0.250757951
2210	*waaL*	0.156931747	2284	*etk*	0.201882758	2358	*galR*	0.252193028
2211	*ftnB*	0.158878675	2285	*yneM*	0.203329417	2359	*rutA*	0.252296614
2212	*ratA*	0.159674531	2286	*symE*	0.204293939	2360	*nfrA*	0.253760665
2213	*cdh*	0.161461646	2287	*adhP*	0.204868907	2361	*yaiO*	0.253839187
2214	*eutG*	0.163919154	2288	*ycjX*	0.205564027	2362	*ynbD*	0.255055543
2215	*rnb*	0.164014564	2289	*ydiU*	0.20607498	2363	*erfK*	0.255057026
2216	*yedR*	0.164204092	2290	*menH*	0.206453072	2364	*csdA*	0.255705531
2217	*ygeR*	0.165643162	2291	*mreB-SPA*	0.206692868	2365	*ygfK*	0.256003607
2218	*msrB*	0.16566015	2292	*yihL*	0.207173915	2366	*dut-SPA*	0.256452137
2219	*deoB*	0.165966929	2293	*dtpD*	0.208526956	2367	*eamB*	0.257365191
2220	*uspA*	0.166311096	2294	*ecpA*	0.209404836	2368	*rffT*	0.257856308
2221	*napG*	0.167065992	2295	*entC*	0.210529864	2369	*ugpA*	0.258218255
2222	*lsrA*	0.167827416	2296	*rhsE*	0.21281053	2370	*glcE*	0.258266072
2223	*evgS*	0.16806714	2297	*dusC*	0.214130782	2371	*ycfT*	0.258778604
2224	*ymfO*	0.168221484	2298	*ynfH*	0.214473437	2372	*cas3*	0.259210556
2225	*wzxC*	0.168500507	2299	*glcC*	0.214732303	2373	*yihW*	0.259351784
2226	*gatC*	0.16877474	2300	*yghG*	0.215605714	2374	*ythA*	0.259830596
2227	*rfbX*	0.169952688	2301	*ryeF*	0.21697914	2375	*ampD*	0.259922247
2228	*ggt*	0.172573452	2302	*yjbJ*	0.217195694	2376	*yhiI*	0.261864173
2229	*zwf*	0.172785134	2303	*norR*	0.217478484	2377	*emrA*	0.261949325
2230	*bioB*	0.173018052	2304	*hcaB*	0.218352461	2378	*rpoZ*	0.263672855
2231	*glgB*	0.173911581	2305	*surE*	0.219482215	2379	*malE*	0.263859529
2232	*rseC*	0.174806524	2306	*bglG*	0.219719806	2380	*ytfP*	0.264607338
2233	*potB*	0.174821877	2307	*fecB*	0.220146635	2381	*cysN*	0.265213665
2234	*chbA*	0.174835646	2308	*ugd*	0.220699934	2382	*gnd*	0.265291733
2235	*ybhD*	0.176645823	2309	*yhfY*	0.223537774	2383	*murC-SPA*	0.265755259
2236	*chbB*	0.176903614	2310	*fbaB*	0.225345998	2384	*rlmF*	0.265877214
2237	*ybiU*	0.177086223	2311	*rfbC*	0.227262928	2385	*ypfH*	0.267283639
2238	*luxS*	0.177890739	2312	*pgpB*	0.227571737	2386	*paaI*	0.268450497
2239	*mltC*	0.179620438	2313	*cas2*	0.2276386	2387	*truB*	0.268738298
2240	*micC*	0.180593748	2314	*yoaH*	0.22772908	2388	*mgtA*	0.269492
2241	*dsdC*	0.180768266	2315	*yghR*	0.229438712	2389	*ydaU*	0.270501963
2242	*yadV*	0.18097302	2316	*map-SPA*	0.230070618	2390	*ybcV*	0.271784092
2243	*ycjQ*	0.181372496	2317	*frdB*	0.230580177	2391	*speG*	0.272020552
2244	*yjdM*	0.182129821	2318	*eutQ*	0.230680425	2392	*rhsA*	0.272296809
2245	*ygaY*	0.18216439	2319	*ibaG*	0.230876884	2393	*pal*	0.273017668
2246	*ybhS*	0.18220339	2320	*yfcR*	0.231002731	2394	*yraK*	0.27413107
2247	*tisA*	0.182552993	2321	*mqsR*	0.231844827	2395	*yihT*	0.27501757
2248	*yifE*	0.182622868	2322	*mnmE*	0.232296579	2396	*rpmE*	0.275821835
2249	*iraP*	0.182779822	2323	*dnaA-SPA*	0.232364934	2397	*fliP*	0.276653725
2250	*ccmB*	0.183258545	2324	*yeaQ*	0.232869595	2398	*yhjD*	0.276714499
2251	*ydeJ*	0.183421458	2325	*yhiJ*	0.233183517	2399	*cvpA*	0.276900335
2252	*yhhW*	0.183762753	2326	*ydaG*	0.233504147	2400	*alaC*	0.277450925
2253	*yoaA*	0.183892953	2327	*relE*	0.233579702	2401	*eda*	0.278126494
2254	*abgR*	0.184716252	2328	*nudL*	0.235816775	2402	*rfbA*	0.278244075
2255	*ydgC*	0.185055704	2329	*yphB*	0.236916235	2403	*yfiN*	0.278710647
2256	*kdsA-SPA*	0.186814144	2330	*sdsQ*	0.237029334	2404	*ascB*	0.279682105
2257	*yjjA*	0.187053616	2331	*yraI*	0.237220056	2405	*dppF*	0.280256855
2258	*rimL*	0.188873248	2332	*rybD*	0.237331522	2406	*yafV*	0.280420346
2259	*cspB*	0.189035393	2333	*yjhE*	0.237731935	2407	*yiaG*	0.280811883
2260	*mltA*	0.189926881	2334	*mltF*	0.237749913	2408	*yidX*	0.280869111
2261	*paaE*	0.190008977	2335	*galM*	0.238245461	2409	*artQ*	0.281795242
2262	*yhhX*	0.191205355	2336	*rbn*	0.238846473	2410	*rpoC-SPA*	0.282882082
2263	*yejA*	0.191776141	2337	*yfdG*	0.240178081	2411	*ecpB*	0.284303659
2264	*ybgQ*	0.192017097	2338	*ybhF*	0.240295074	2412	*zapD*	0.284750135
2265	*ybiY*	0.19245359	2339	*acrA*	0.240607677	2413	*xthA*	0.285008384
2266	*nupX*	0.192990469	2340	*phoR*	0.241325084	2414	*iraD*	0.285539149
2267	*yeaJ*	0.193362246	2341	*ade*	0.241552788	2415	*fiu*	0.28633318
2268	*yfiC*	0.193617891	2342	*emrK*	0.241809951	2416	*ycjO*	0.286333853

2417	*rcbA*	0.28756087	2491	*yhaL*	0.34249001	2565	*ygiD*	0.391811062
2418	*ychH*	0.288663315	2492	*yceI*	0.343293485	2566	*yaiT*	0.395009347
2419	*yigE*	0.289549126	2493	*scpB*	0.3438428	2567	*ykfB*	0.395018741
2420	*glpK*	0.290283391	2494	*moeB*	0.344478712	2568	*gudP*	0.396738604
2421	*fepA*	0.291117948	2495	*glgS*	0.344544722	2569	*yahF*	0.398180805
2422	*yggE*	0.291785032	2496	*mmuP*	0.345422821	2570	*slyD*	0.39821701
2423	*hybE*	0.292516546	2497	*tehB*	0.346851165	2571	*yjcH*	0.398259801
2424	*ygcW*	0.293298985	2498	*sfsA*	0.347258362	2572	*pntA*	0.398414569
2425	*apaG*	0.29374678	2499	*arfA*	0.347288704	2573	*cusF*	0.399097083
2426	*proA*	0.293997059	2500	*yhiD*	0.347358364	2574	*yeiQ*	0.400589156
2427	*yraQ*	0.295662007	2501	*yedA*	0.348163412	2575	*sspA*	0.400773145
2428	*rob*	0.296137263	2502	*yfdQ*	0.349602312	2576	*rluB*	0.401086658
2429	*mdtB*	0.296232143	2503	*bdcA*	0.350969655	2577	*yneK*	0.402021947
2430	*yggU*	0.296260674	2504	*ybaN*	0.351835903	2578	*ydhY*	0.40219835
2431	*araF*	0.296284212	2505	*ydjE*	0.351974327	2579	*deoD*	0.402317863
2432	*kdsD*	0.296373945	2506	*ccmD*	0.352415852	2580	*yccA*	0.402467743
2433	*ygiB*	0.296698132	2507	*yfjP*	0.354831203	2581	*csrC*	0.402812004
2434	*rimJ*	0.297337513	2508	*ypjJ*	0.354838417	2582	*sodA*	0.403063458
2435	*bssR*	0.297706001	2509	*yecA*	0.355110468	2583	*rfe*	0.403871637
2436	*asnC*	0.297934154	2510	*upp*	0.355599077	2584	*ydcV*	0.404323026
2437	*bssS*	0.298772541	2511	*nrfD*	0.356234962	2585	*yiaL*	0.404656773
2438	*arnB*	0.298995293	2512	*yfaY*	0.356428333	2586	*fliT*	0.405691461
2439	*ytjC*	0.301706555	2513	*ydiK*	0.357915713	2587	*ycjW*	0.406209113
2440	*trg*	0.302060879	2514	*dcrB*	0.359169534	2588	*nrfB*	0.408337272
2441	*ybcF*	0.302399269	2515	*trxB*	0.359336328	2589	*yfeY*	0.409753596
2442	*bcsC*	0.302730171	2516	*ligT*	0.359636152	2590	*ybdJ*	0.41062783
2443	*ycaL*	0.303393702	2517	*ykgN*	0.360424529	2591	*icdC*	0.410997061
2444	*gspD*	0.303848781	2518	*araG*	0.361336457	2592	*yahK*	0.411192491
2445	*yqhC*	0.304391869	2519	*htrE*	0.361371636	2593	*tdcE*	0.411269765
2446	*artM*	0.305074232	2520	*fadR*	0.36150615	2594	*dppA*	0.412224671
2447	*glgP*	0.305168646	2521	*codA*	0.364331625	2595	*cheB*	0.412254452
2448	*intA*	0.305605894	2522	*wbbK*	0.365276588	2596	*ynbA*	0.41436534
2449	*rrrQ*	0.306357896	2523	*fryB*	0.365698437	2597	*prlC*	0.414655566
2450	*basS*	0.306894724	2524	*glnG*	0.366236814	2598	*pgaC*	0.414937553
2451	*rspA*	0.307956795	2525	*yadG*	0.367237945	2599	*wecH*	0.415640542
2452	*mhpE*	0.308211791	2526	*ycaQ*	0.367760163	2600	*parE-SPA*	0.416094808
2453	*yjcS*	0.309683286	2527	*nlpI*	0.369152066	2601	*ybcQ*	0.416222161
2454	*potG*	0.310272783	2528	*yiaO*	0.369218179	2602	*maeA*	0.417923795
2455	*rluC*	0.31038715	2529	*ptsI*	0.369695886	2603	*lysS*	0.418615544
2456	*ccmG*	0.312479471	2530	*yghB*	0.371236492	2604	*cobU*	0.4204544
2457	*trmJ*	0.312625209	2531	*ybaA*	0.372098896	2605	*napD*	0.420704067
2458	*nepI*	0.312675687	2532	*ybgC*	0.372357735	2606	*ycgZ*	0.420746103
2459	*yphG*	0.313443934	2533	*mdoB*	0.37268402	2607	*lpxH-SPA*	0.421691244
2460	*bamC*	0.313842997	2534	*yggS*	0.372841808	2608	*yqcE*	0.422456717
2461	*yahA*	0.314151181	2535	*ybeT*	0.372890293	2609	*yhfL*	0.422788603
2462	*livH*	0.315268	2536	*afuC*	0.373882369	2610	*bglB*	0.423702256
2463	*pqqL*	0.316536527	2537	*hyaE*	0.374945899	2611	*ldcC*	0.424061429
2464	*elbB*	0.316741699	2538	*gltA*	0.37595714	2612	*hyfF*	0.424180013
2465	*glvC*	0.317166624	2539	*motB*	0.376211882	2613	*recO*	0.42492187
2466	*yjgN*	0.318081946	2540	*ygjP*	0.376343057	2614	*yjhI*	0.425056364
2467	*frc*	0.318094607	2541	*aphA*	0.376478665	2615	*cysE*	0.426577318
2468	*rybB*	0.318962416	2542	*yjjW*	0.380322163	2616	*ybcK*	0.426839998
2469	*flgH*	0.318985546	2543	*yhiM*	0.38059558	2617	*yqjH*	0.427050113
2470	*ydiO*	0.319670577	2544	*yecM*	0.381067017	2618	*malP*	0.428013918
2471	*yhjB*	0.322879656	2545	*ygeF*	0.381609735	2619	*malX*	0.429444012
2472	*ychE*	0.324786527	2546	*arnC*	0.383014909	2620	*nikE*	0.430480367
2473	*sfsB*	0.32487799	2547	*ybhR*	0.383063698	2621	*yhdX*	0.430643503
2474	*moaA*	0.325065374	2548	*yahN*	0.383611194	2622	*motA*	0.430759953
2475	*hinT*	0.327629466	2549	*atl*	0.384093496	2623	*gntK*	0.430890569
2476	*hdhA*	0.327637126	2550	*pagB*	0.385145497	2624	*malK*	0.430912976
2477	*degQ*	0.327647904	2551	*ycgJ*	0.385298501	2625	*marB*	0.430940574
2478	*kdpD*	0.328041375	2552	*yhjG*	0.385675242	2626	*ftsH-SPA*	0.431793966
2479	*intG*	0.328386654	2553	*mdtL*	0.386390368	2627	*grxC*	0.432827116
2480	*mhpC*	0.328670354	2554	*yfiO**	0.386663167	2628	*pepQ*	0.433427476
2481	*yggN*	0.329384463	2555	*phnG*	0.387160986	2629	*yfeS*	0.434561415
2482	*aat*	0.330440799	2556	*rnc-SPA*	0.388192367	2630	*yniB*	0.434697443
2483	*yehX*	0.332060169	2557	*hflD*	0.388731549	2631	*yibG*	0.434790309
2484	*ycdZ*	0.332138543	2558	*nrfA*	0.388743139	2632	*flgG*	0.43617424
2485	*murD-SPA*	0.332157389	2559	*yehY*	0.389034439	2633	*yeaL*	0.43660699
2486	*yaiW*	0.334338245	2560	*purC*	0.389206312	2634	*nanA*	0.436778796
2487	*sdaA*	0.335908399	2561	*mokB*	0.389609501	2635	*tolQ*	0.437466253
2488	*yafU*	0.336718044	2562	*hycB*	0.39107925	2636	*srlE*	0.437682523
2489	*bisC*	0.338735893	2563	*ybbL*	0.391241524	2637	*msyB*	0.437842539
2490	*mhpT*	0.339918874	2564	*phoU*	0.39180435	2638	*hflC*	0.438379873

2639	*yeaI*	0.438769177	2713	*sbcC*	0.512464219	2787	*rlmE*	0.577062857
2640	*rcsB*	0.439368701	2714	*yhcH*	0.512693677	2788	*ddpX*	0.578665034
2641	*ybcL*	0.440015266	2715	*radA*	0.513719902	2789	*tgt*	0.579089638
2642	*yiaV*	0.440604467	2716	*yegL*	0.514238091	2790	*trmH*	0.579159393
2643	*napB*	0.440933591	2717	*tp2*	0.515043722	2791	*ydeH*	0.579262875
2644	*ybjM*	0.442150577	2718	*yeeR*	0.515081125	2792	*yjdA*	0.580660596
2645	*phnJ*	0.443040062	2719	*dinD*	0.515282218	2793	*adiY*	0.581079803
2646	*rraA*	0.443429117	2720	*yggW*	0.51649194	2794	*yebT*	0.5815704
2647	*rbsR*	0.443492603	2721	*talB*	0.516526433	2795	*abgA*	0.582949023
2648	*ttdA*	0.444330499	2722	*aceE*	0.516596521	2796	*ytfA*	0.583103565
2649	*mdtG*	0.447246158	2723	*aldB*	0.516889759	2797	*csgA*	0.583214086
2650	*yjcD*	0.447406562	2724	*fecE*	0.517984652	2798	*ynjD*	0.583502988
2651	*pspF*	0.447902981	2725	*smtA*	0.519025179	2799	*ydiH*	0.585030981
2652	*ansB*	0.449677926	2726	*paaD*	0.523684181	2800	*yicL*	0.58529981
2653	*ebgR*	0.452769466	2727	*yafC*	0.525032119	2801	*yneE*	0.585312641
2654	*moaE*	0.455344123	2728	*yfcE*	0.525609707	2802	*mgrB*	0.586400996
2655	*ydfO*	0.45579519	2729	*murR*	0.526213105	2803	*dtd*	0.586611391
2656	*kgtP*	0.455923815	2730	*glvG*	0.527229657	2804	*patD*	0.587544816
2657	*xdhC*	0.456858615	2731	*yhfT*	0.527415105	2805	*cheW*	0.587746589
2658	*sgrS*	0.457600243	2732	*yigG*	0.527651912	2806	*gpt*	0.587923368
2659	*yqjK*	0.458501478	2733	*fsaA*	0.528861438	2807	*ycaI*	0.588604022
2660	*yqeL*	0.458778285	2734	*mobB*	0.530132875	2808	*sfmC*	0.589622012
2661	*iclR*	0.45928863	2735	*ydeU*	0.530564841	2809	*sxy*	0.593352971
2662	*yghZ*	0.459899265	2736	*fre*	0.531119753	2810	*yhaV*	0.593447855
2663	*wcaE*	0.460323423	2737	*ydfT*	0.531404069	2811	*ybgJ*	0.593800365
2664	*yhbV-SPA*	0.461648028	2738	*htrL*	0.532243194	2812	*yiaW*	0.593828254
2665	*nanE*	0.461663424	2739	*rdgB*	0.532264331	2813	*ybfO*	0.594988154
2666	*yfbU*	0.461673194	2740	*yfeZ*	0.53308124	2814	*yzgL*	0.596793756
2667	*hcaE*	0.463675538	2741	*yfaX*	0.534101199	2815	*yaiI*	0.596921053
2668	*paoC*	0.464677173	2742	*pdxK*	0.536297689	2816	*glyQ-SPA*	0.597368176
2669	*rhlB*	0.46472046	2743	*preA*	0.537018359	2817	*kdsB-SPA*	0.598572941
2670	*yjfJ*	0.465599065	2744	*srlB*	0.537287991	2818	*grcA*	0.600421921
2671	*yhcD*	0.465968594	2745	*yqjI*	0.539329561	2819	*yohP*	0.600989528
2672	*tomB*	0.466378359	2746	*yncG*	0.539890291	2820	*yfcO*	0.601028464
2673	*oppF*	0.469211431	2747	*putP*	0.540199649	2821	*modA*	0.601574682
2674	*yddL*	0.469502097	2748	*alsB*	0.541546956	2822	*ydjX*	0.604916484
2675	*yagI*	0.470787504	2749	*bfd*	0.541792184	2823	*yidP*	0.604960829
2676	*ybcC*	0.472723578	2750	*cysP*	0.541982855	2824	*ppsR*	0.60505234
2677	*fxsA*	0.474337558	2751	*ybiC*	0.545037032	2825	*dcp*	0.606084613
2678	*yqiI*	0.474669717	2752	*cusC*	0.545192762	2826	*rsmC*	0.606149871
2679	*fpr*	0.474811853	2753	*yjgA*	0.546238744	2827	*yaaW*	0.606443257
2680	*tyrR*	0.475163154	2754	*der-SPA*	0.547099185	2828	*gadC*	0.606720067
2681	*citE*	0.476554688	2755	*apbE*	0.548342185	2829	*dacD*	0.607719027
2682	*pbl*	0.476992578	2756	*hscA*	0.54868379	2830	*dhaR*	0.607780453
2683	*ypfM*	0.478120705	2757	*ydgD*	0.549668308	2831	*rhtB*	0.609903674
2684	*arsB*	0.478148337	2758	*ryjB*	0.550050183	2832	*ycbL*	0.61062785
2685	*yfcP*	0.47961973	2759	*yjbQ*	0.551768664	2833	*mscL*	0.611150082
2686	*astC*	0.479719715	2760	*yfeC*	0.551769657	2834	*pqiB*	0.612123354
2687	*glpD*	0.4857158	2761	*rlmL*	0.551819061	2835	*mlaF*	0.612293382
2688	*yagE*	0.486457778	2762	*sapA*	0.553173795	2836	*ykgD*	0.613526448
2689	*ynjI*	0.486604029	2763	*acrD*	0.553855762	2837	*yohJ*	0.614703154
2690	*yihQ*	0.486604407	2764	*dbpA*	0.554621304	2838	*yjcC*	0.614970585
2691	*infC-SPA*	0.487307163	2765	*ykgF*	0.555276582	2839	*hslJ*	0.615835989
2692	*hofQ*	0.487885839	2766	*lsrD*	0.556234842	2840	*nemA*	0.616228444
2693	*arcZ*	0.487922425	2767	*glpG*	0.558116659	2841	*fdoI*	0.616474516
2694	*mutL*	0.489771898	2768	*yccE*	0.558216142	2842	*yibD*	0.616787872
2695	*ydgK*	0.490442045	2769	*yadD*	0.558631904	2843	*ycfS*	0.616814914
2696	*yfcQ*	0.491581933	2770	*xerD*	0.559632041	2844	*yidC-SPA*	0.618928462
2697	*marA*	0.49204225	2771	*mug*	0.562460137	2845	*cspF*	0.619443936
2698	*nadC*	0.493384592	2772	*guaD*	0.563545672	2846	*sgcX*	0.619799439
2699	*cusR*	0.493941713	2773	*ydbD*	0.564065708	2847	*erpA-SPA*	0.61989194
2700	*argK*	0.494352892	2774	*yfcA*	0.566644809	2848	*lfhA*	0.620810916
2701	*ubiC*	0.49555802	2775	*xanQ*	0.566827699	2849	*yoeA*	0.621109228
2702	*yadM*	0.498314013	2776	*hupA*	0.567226927	2850	*lpxB-SPA*	0.621151474
2703	*yibF*	0.500201333	2777	*hcaC*	0.56768987	2851	*yacH*	0.622712434
2704	*macB*	0.501046798	2778	*yebB*	0.56820957	2852	*ygiZ*	0.623727863
2705	*cpsG*	0.502578402	2779	*yfaH*	0.568381015	2853	*ytfI*	0.625309756
2706	*ilvN*	0.503136513	2780	*yhfL*	0.569153826	2854	*hlyE*	0.625679067
2707	*yqeF*	0.504844749	2781	*gltP*	0.57042647	2855	*ryjA*	0.626573253
2708	*ompC*	0.505983519	2782	*bluR*	0.572504772	2856	*rzoD*	0.626998413
2709	*eutA*	0.506184633	2783	*hydN*	0.573199243	2857	*yqhG*	0.627318737
2710	*bglA*	0.507782723	2784	*tamB*	0.575642235	2858	*yciG*	0.627341413
2711	*atoS*	0.509129928	2785	*ampE*	0.575790637	2859	*yghU*	0.627902158
2712	*yjcB*	0.50988009	2786	*kefG*	0.576283249	2860	*rnd*	0.628076965

2861	*melR*	0.628707583	2935	*yjhB*	0.69336179	3009	*yibH*	0.746301942
2862	*mscS*	0.633101866	2936	*tatC*	0.694843853	3010	*yfeX*	0.746953101
2863	*puuP*	0.633442503	2937	*astD*	0.695175804	3011	*yhhJ*	0.747861539
2864	*fliI*	0.634984153	2938	*hokC*	0.695256122	3012	*recT*	0.748076144
2865	*xylH*	0.635478916	2939	*ydcZ*	0.696024343	3013	*yehK*	0.748779791
2866	*fdoG*	0.635579352	2940	*livG*	0.69807743	3014	*miaB*	0.749677792
2867	*yghQ*	0.636984915	2941	*mrp*	0.698801932	3015	*yecC*	0.751442657
2868	*dusA*	0.637139224	2942	*yfiF*	0.699744061	3016	*rihB*	0.751516169
2869	*lsrF*	0.638768804	2943	*yejH*	0.699744322	3017	*yhjV*	0.751657664
2870	*ais*	0.639795248	2944	*sugE*	0.700606521	3018	*wcaA*	0.753653121
2871	*ybiT*	0.639929166	2945	*dusB*	0.701703795	3019	*hybD*	0.754699275
2872	*setC*	0.640377564	2946	*fucU*	0.701733831	3020	*gstB*	0.754723016
2873	*yqjE*	0.641462852	2947	*waaZ*	0.701766127	3021	*idnR*	0.755970818
2874	*puuR*	0.6414961	2948	*ybaL*	0.702879997	3022	*yeeJ*	0.757315541
2875	*aroL*	0.642419924	2949	*fdnH*	0.703537535	3023	*glrK*	0.757936911
2876	*yhjH*	0.643331601	2950	*yjhU*	0.703887214	3024	*actP*	0.75814029
2877	*prpD*	0.643652225	2951	*ykgL*	0.704384869	3025	*nfrB*	0.759621197
2878	*zapA*	0.644229131	2952	*ydcF*	0.708032716	3026	*qseC*	0.759622838
2879	*mdtA*	0.645452917	2953	*pbpG*	0.708265326	3027	*yafQ*	0.759679872
2880	*ygaQ_3*	0.647028632	2954	*tdcC*	0.709797953	3028	*bamB*	0.760469697
2881	*phnE_1*	0.647181907	2955	*glyA*	0.710005472	3029	*xerC*	0.76107993
2882	*yicS*	0.647248855	2956	*djlC*	0.710418412	3030	*cadA*	0.761490608
2883	*lolA-SPA*	0.647290542	2957	*cspA*	0.710591992	3031	*yfeO*	0.761543942
2884	*narW*	0.647618586	2958	*ryeA*	0.710799014	3032	*gmr*	0.762909983
2885	*lplT*	0.648030224	2959	*racC*	0.710958157	3033	*dcuA*	0.763310248
2886	*yeiE*	0.648185538	2960	*ybbM*	0.711213313	3034	*pstA*	0.764238604
2887	*ykfA*	0.649324158	2961	*yheO*	0.711370128	3035	*paaJ*	0.764259751
2888	*ldcA*	0.649878278	2962	*ycbZ*	0.71226555	3036	*acrE*	0.765862272
2889	*istR-2*	0.650000539	2963	*ygeK*	0.71274344	3037	*xylG*	0.766600002
2890	*prfA-SPA*	0.650664769	2964	*leuO*	0.713933993	3038	*gabT*	0.767216998
2891	*dppC*	0.651616874	2965	*ydfB*	0.71423854	3039	*yeeE*	0.768047196
2892	*ybaK*	0.652262801	2966	*agaI*	0.714525081	3040	*dsbG*	0.769335622
2893	*oxyS*	0.654399208	2967	*argA*	0.714586894	3041	*cirA*	0.770155446
2894	*chaC*	0.654528282	2968	*frmR*	0.714937546	3042	*ybgI*	0.770945659
2895	*omrB*	0.654677672	2969	*rpiB*	0.71510261	3043	*nlpA*	0.771098841
2896	*ycjY*	0.655998024	2970	*torY*	0.717764677	3044	*yfdV*	0.771725722
2897	*cbrB*	0.656541278	2971	*mtgA*	0.71968551	3045	*ygaV*	0.771794552
2898	*yebC*	0.657239764	2972	*ydjG*	0.72001704	3046	*exuR*	0.771924573
2899	*allC*	0.657822089	2973	*uvrY*	0.720292234	3047	*phnP*	0.772315251
2900	*ydfJ*	0.658249016	2974	*yhaK*	0.720428232	3048	*rplI*	0.77248028
2901	*sapD*	0.658516045	2975	*fliM*	0.720824474	3049	*mutH*	0.772671825
2902	*fimG*	0.658562634	2976	*betA*	0.721042976	3050	*ybaQ*	0.773541168
2903	*syd*	0.659093623	2977	*queF*	0.722271305	3051	*eutT*	0.774379007
2904	*yafK*	0.661791098	2978	*gadY*	0.722463631	3052	*ypjM_1*	0.774590128
2905	*bax*	0.661926146	2979	*yfjX*	0.723373368	3053	*brnQ*	0.774643976
2906	*yghX_1*	0.662492125	2980	*ydhC*	0.723632104	3054	*acrB*	0.774781355
2907	*ybiO*	0.662761426	2981	*tcdA*	0.723729014	3055	*cysS-SPA*	0.780122063
2908	*fucR*	0.663264696	2982	*slt*	0.724618069	3056	*creC*	0.780494366
2909	*aspS-SPA*	0.663800943	2983	*ccmF*	0.724914191	3057	*dhaL*	0.782677727
2910	*cobB*	0.666463949	2984	*yqiB*	0.725522709	3058	*mdoC*	0.782726741
2911	*tsx*	0.666564377	2985	*ligB*	0.727257228	3059	*pppA*	0.782742783
2912	*nudF*	0.668115186	2986	*yiaN*	0.727728562	3060	*recC*	0.783523954
2913	*pdxA*	0.66815496	2987	*proV*	0.728819853	3061	*yjjQ*	0.784657039
2914	*fucP*	0.668601358	2988	*ybiH*	0.729339084	3062	*yedV*	0.785213144
2915	*yqjD*	0.670743208	2989	*yfeD*	0.729667801	3063	*ybfG*	0.785587798
2916	*yqeG*	0.671244638	2990	*mdlA*	0.731334768	3064	*yjgZ*	0.786195611
2917	*uvrC*	0.671988895	2991	*trkG*	0.732417058	3065	*yeaH*	0.787905975
2918	*uspE*	0.67464448	2992	*intQ*	0.732804376	3066	*folC-SPA*	0.788259592
2919	*yfgM*	0.675990631	2993	*argP*	0.734096588	3067	*hyfJ*	0.78901458
2920	*acrZ*	0.677057784	2994	*ykgH*	0.734783167	3068	*ebgA*	0.79021731
2921	*ydeN*	0.677170589	2995	*smrA*	0.734906581	3069	*rpoH-SPA*	0.790366712
2922	*feoC*	0.677884934	2996	*feaR*	0.734985888	3070	*yidB*	0.791952259
2923	*ysaB*	0.678188122	2997	*sstT*	0.735154921	3071	*cedA*	0.792794855
2924	*psuK*	0.678765946	2998	*ybaT*	0.735303586	3072	*rbbA*	0.793550156
2925	*glgC*	0.679717028	2999	*ydhI*	0.735950576	3073	*rlmB*	0.796925717
2926	*ydhR*	0.680623463	3000	*dld*	0.739290589	3074	*yjfP*	0.798428248
2927	*lsrR*	0.681336025	3001	*sapF*	0.740838249	3075	*gntR*	0.798978951
2928	*alkB*	0.68153017	3002	*yraP*	0.742000451	3076	*ispE-SPA*	0.800313757
2929	*pntB*	0.683240804	3003	*recN*	0.742075374	3077	*hpt*	0.801796124
2930	*ydaF*	0.686160571	3004	*yjgW*	0.742111609	3078	*exoX*	0.801855006
2931	*yciF*	0.687273586	3005	*ybjS*	0.742601771	3079	*yifO*	0.802483561
2932	*galP*	0.688662715	3006	*yjhV*	0.742986954	3080	*focB*	0.802779404
2933	*rsmE*	0.689278304	3007	*aaeA*	0.744122634	3081	*yjjL*	0.802803723
2934	*yhjR*	0.690747406	3008	*rsxE*	0.744198765	3082	*soxS*	0.803484881

3083	*yagA*	0.805471443	3157	*recG*	0.878317578	3231	*acrR*	0.96516354
3084	*ycgH_1*	0.808500159	3158	*yddW*	0.880310396	3232	*ycbF*	0.966519232
3085	*ydjF*	0.808714528	3159	*ycjP*	0.881699177	3233	*fixA*	0.96787769
3086	*mtlD*	0.809911243	3160	*borD*	0.882142922	3234	*eptB*	0.970282768
3087	*ycdT*	0.810643571	3161	*sseA*	0.884038723	3235	*amtB*	0.971459148
3088	*dctR*	0.811971118	3162	*yecN*	0.884556441	3236	*ycgV*	0.971497207
3089	*ygcO*	0.812784327	3163	*cpsB*	0.885541279	3237	*tpkE70*	0.973890584
3090	*ybaM*	0.81318172	3164	*yceM*	0.89046325	3238	*ycfL*	0.975377687
3091	*fixX*	0.813636627	3165	*ygaZ*	0.892262102	3239	*ruvA*	0.976138041
3092	*yedD*	0.813757937	3166	*rbsK*	0.892368378	3240	*lhr*	0.977070639
3093	*ynfL*	0.814680712	3167	*ybjP*	0.893639209	3241	*ulaG*	0.977602643
3094	*yhdP*	0.814945606	3168	*glk*	0.894156588	3242	*cysZ*	0.979835383
3095	*glmY*	0.81724986	3169	*folX*	0.896851235	3243	*aroP*	0.980808664
3096	*gmhB*	0.818901927	3170	*ypjC*	0.897790806	3244	*gluQ*	0.981205832
3097	*ycbU*	0.819515137	3171	*yjiM*	0.898692486	3245	*pagP*	0.98339921
3098	*zntA*	0.819800222	3172	*dadA*	0.89930464	3246	*yjaZ*	0.984929075
3099	*leuC*	0.820417088	3173	*yfcF*	0.901363973	3247	*queA*	0.985637815
3100	*yhfA*	0.820741271	3174	*era-SPA*	0.903001633	3248	*ydhK*	0.987597356
3101	*cmtA*	0.822332979	3175	*tap*	0.904639687	3249	*kdpC*	0.98846184
3102	*rep*	0.822986889	3176	*sgrT*	0.905041408	3250	*dosP*	0.988606264
3103	*ygeV*	0.825803126	3177	*gpmM*	0.905534049	3251	*yjiN*	0.990943421
3104	*ybdO*	0.827015972	3178	*cmk*	0.906780728	3252	*yafT*	0.995517812
3105	*btuF*	0.827022758	3179	*aroG*	0.910460315	3253	*yagU*	0.996633745
3106	*yceJ*	0.82718228	3180	*fhuA*	0.910804652	3254	*hslR*	0.997399986
3107	*yqeH*	0.827385761	3181	*mnaT*	0.911219387	3255	*idnK*	0.998170681
3108	*yoaC*	0.829241084	3182	*ynfF*	0.912468046	3256	*ryfD*	0.998193045
3109	*dsbC*	0.829497288	3183	*purT*	0.913132315	3257	*mdtQ*	0.998681446
3110	*zur*	0.82989775	3184	*ycgI*	0.914085832	3258	*glcA*	1.003000647
3111	*sbmA*	0.833836878	3185	*tldD*	0.914197663	3259	*tusB*	1.003200957
3112	*slyB*	0.834319225	3186	*ppiC*	0.916138036	3260	*rlpA*	1.003212069
3113	*nanS*	0.834364525	3187	*yfiL*	0.916205167	3261	*malG*	1.006005217
3114	*ttdT*	0.834718685	3188	*recB*	0.91652906	3262	*ybfA*	1.006523807
3115	*rprA*	0.834871789	3189	*yjiG*	0.916697551	3263	*hchA*	1.006747899
3116	*scpA*	0.834986706	3190	*icd*	0.916986906	3264	*yidQ*	1.007606337
3117	*eutN*	0.839818288	3191	*fepD*	0.917343036	3265	*ugpE*	1.010111507
3118	*narY*	0.840938856	3192	*flgD*	0.919851148	3266	*csiE*	1.01018087
3119	*kduI*	0.842006804	3193	*selB*	0.922600773	3267	*nhaR*	1.01137869
3120	*mglB*	0.842483448	3194	*paaH*	0.925073516	3268	*tatA*	1.011740286
3121	*ydeP*	0.84272455	3195	*rdgC*	0.927075951	3269	*uspB*	1.013445129
3122	*moeA*	0.843793294	3196	*prpE*	0.929021463	3270	*yhhA*	1.014287347
3123	*deoR*	0.8439415	3197	*lipA*	0.93344826	3271	*ebgC*	1.016618928
3124	*gspH*	0.844520545	3198	*yjiT*	0.934326215	3272	*agaA*	1.017498134
3125	*mntH*	0.844747747	3199	*feoB*	0.934867676	3273	*iadA*	1.018185663
3126	*ynbB*	0.845236665	3200	*edd*	0.935028971	3274	*fhuC*	1.018411699
3127	*ykfF*	0.845968602	3201	*rsmH*	0.935813827	3275	*rffH*	1.019368605
3128	*aroE*	0.846096964	3202	*ykfJ*	0.936058417	3276	*shiA*	1.019562815
3129	*gfcA*	0.847381441	3203	*csrD*	0.936154214	3277	*dmlR*	1.01992673
3130	*yjbB*	0.848065545	3204	*grxD*	0.937385537	3278	*sppA*	1.020155981
3131	*rseB*	0.84836066	3205	*efeO*	0.940307521	3279	*ynfM*	1.024777242
3132	*yqgF-SPA*	0.848572668	3206	*fdhE*	0.940734748	3280	*perR*	1.02561446
3133	*glpE*	0.848840516	3207	*mscK*	0.940816221	3281	*cspE*	1.026083788
3134	*yacG*	0.852674614	3208	*hofB*	0.941522558	3282	*paaB*	1.026343372
3135	*tnaA*	0.855482356	3209	*creD*	0.943150913	3283	*yfbV*	1.02690871
3136	*torD*	0.856467418	3210	*cusS*	0.949003372	3284	*alsK-SPA*	1.027316675
3137	*yjeI*	0.856810598	3211	*yjaH*	0.949111364	3285	*talA*	1.0275838
3138	*thiF*	0.85711473	3212	*yjdF*	0.95081654	3286	*sgrR*	1.02948964
3139	*recJ*	0.857363083	3213	*accD-SPA*	0.951222329	3287	*yciK*	1.030233694
3140	*degP*	0.857399271	3214	*cydB*	0.951674167	3288	*csgE*	1.031156163
3141	*ydjJ*	0.85821434	3215	*prfC*	0.952081411	3289	*ecnAB*	1.032811606
3142	*yhbW*	0.859439368	3216	*ypdK*	0.955154402	3290	*wza*	1.03808507
3143	*hokD*	0.861054548	3217	*higA*	0.955511296	3291	*lrp*	1.039897881
3144	*phnO*	0.862810492	3218	*ybhG*	0.955781525	3292	*ysgA*	1.039913389
3145	*yncM*	0.863352132	3219	*baeR*	0.956475097	3293	*yfgG*	1.040345872
3146	*glgA*	0.864399085	3220	*torZ*	0.957457605	3294	*rimK*	1.041565349
3147	*ilvM*	0.865116681	3221	*rlmG*	0.958141583	3295	*ydfI*	1.041606904
3148	*ahr*	0.865774034	3222	*atoC*	0.958650598	3296	*rtn*	1.043272693
3149	*osmE*	0.866215196	3223	*bamE*	0.95895683	3297	*yidF*	1.043358564
3150	*yecJ*	0.866220313	3224	*yeaX*	0.959186557	3298	*zinT*	1.043924593
3151	*metC*	0.866294514	3225	*folA-SPA*	0.9596527	3299	*miaA*	1.044767313
3152	*tus*	0.870628845	3226	*cysU*	0.959835578	3300	*yeeT*	1.046346763
3153	*yegJ*	0.871713164	3227	*yieE*	0.962322077	3301	*yqeI*	1.047202322
3154	*ruvC*	0.871878647	3228	*ilvI*	0.962527659	3302	*dcyD*	1.04724808
3155	*ymgD*	0.872199474	3229	*gadW*	0.963424388	3303	*damX*	1.049090524
3156	*cutC*	0.874342509	3230	*ygiM*	0.964051758	3304	*yajL*	1.049594238

3305	*yhdY*	1.050713225	3379	*ygdD*	1.12665302	3453	*rplD-SPA*	1.220922625
3306	*dmsD*	1.051864564	3380	*ykgC*	1.126766277	3454	*ydaT*	1.221333488
3307	*rbsC*	1.053571514	3381	*pepN*	1.128895045	3455	*modB*	1.222359728
3308	*frvA*	1.053644903	3382	*ppk*	1.12957762	3456	*ygcU*	1.222713979
3309	*pykA*	1.054127616	3383	*nagZ*	1.130668218	3457	*yigA*	1.224913195
3310	*yoeB*	1.055449152	3384	*yjeO*	1.130907306	3458	*yahI*	1.227924877
3311	*cbpM*	1.055566978	3385	*ydiQ*	1.13338509	3459	*gltF*	1.228964635
3312	*glcB*	1.055625061	3386	*proY*	1.135281459	3460	*ydhT*	1.229861685
3313	*gpp*	1.059815799	3387	*yieH*	1.137093222	3461	*ylbI*	1.231536513
3314	*ridA*	1.06107503	3388	*pspD*	1.137773516	3462	*ssrS*	1.232036125
3315	*uxaC*	1.061874426	3389	*rcsF*	1.138182698	3463	*hcaD*	1.233533866
3316	*ymfI*	1.062139934	3390	*tamA*	1.138558118	3464	*dgt*	1.233862347
3317	*aaeB*	1.063187706	3391	*yfdC*	1.139989467	3465	*ybhM*	1.234578044
3318	*yejL*	1.063513509	3392	*yjhD*	1.140875803	3466	*dkgB*	1.237239588
3319	*clsC*	1.063661752	3393	*paoA*	1.141192221	3467	*abgB*	1.239835523
3320	*yddM*	1.067287468	3394	*yejO*	1.14299226	3468	*ynfC*	1.243060362
3321	*nanC*	1.06780048	3395	*ravA*	1.143356565	3469	*dkgA*	1.243339309
3322	*agaB*	1.06967785	3396	*lsrK*	1.143480422	3470	*yfcC*	1.243556004
3323	*yhfW*	1.069686735	3397	*clpS*	1.145436885	3471	*nsrR*	1.245278048
3324	*lacI*	1.069750002	3398	*tag*	1.146372794	3472	*rutG*	1.246873812
3325	*ydiP*	1.070322373	3399	*garR*	1.146830099	3473	*gltJ*	1.247877297
3326	*ydiE*	1.071186494	3400	*rsmF*	1.148812942	3474	*yadS*	1.252136252
3327	*kdgK*	1.071611961	3401	*ecnA*	1.149177978	3475	*lsrC*	1.253031405
3328	*hpf*	1.072911713	3402	*yhjK*	1.152552958	3476	*hypA*	1.25328115
3329	*add*	1.075085133	3403	*ybbC*	1.154556318	3477	*yaaI*	1.256549377
3330	*exuT*	1.075389404	3404	*ytjB*	1.155059621	3478	*yciH*	1.258111171
3331	*yeaP*	1.075488584	3405	*manX*	1.156376632	3479	*ruvB*	1.260276021
3332	*purE*	1.075949364	3406	*yiaA*	1.157011973	3480	*pyrI*	1.260893475
3333	*frvX*	1.076856054	3407	*caiB*	1.158306637	3481	*lplA*	1.263089464
3334	*yddK*	1.077645271	3408	*dpiA*	1.159769639	3482	*fadH*	1.263670635
3335	*deoC*	1.077997823	3409	*rhtC*	1.159855561	3483	*gspM*	1.266083999
3336	*yggR*	1.078405806	3410	*epmB*	1.163602039	3484	*ninE*	1.267729229
3337	*nudJ*	1.078596258	3411	*ymgA*	1.166999603	3485	*rlmN*	1.270166462
3338	*xylA*	1.078611323	3412	*yoaJ*	1.169802813	3486	*potD*	1.270685475
3339	*dam*	1.08030416	3413	*malM*	1.171129485	3487	*rhlE*	1.271844299
3340	*mfd*	1.081377536	3414	*nemR*	1.172342761	3488	*yhbY*	1.273162934
3341	*ydaE*	1.081523469	3415	*ydhW*	1.17298646	3489	*pnp*	1.274564151
3342	*ubiB-SPA*	1.081911962	3416	*higB*	1.175579298	3490	*wrbA*	1.275275207
3343	*yheV*	1.082306191	3417	*menC*	1.180915185	3491	*rsxB*	1.275988652
3344	*rtcA*	1.084879358	3418	*mtn*	1.181633872	3492	*rpmG*	1.276941092
3345	*narP*	1.085109548	3419	*purA*	1.185050035	3493	*yneH*	1.277616048
3346	*epmA*	1.085749139	3420	*yjiR*	1.185303023	3494	*yjjX*	1.279287914
3347	*tsf-SPA*	1.086039029	3421	*ulaE*	1.185563708	3495	*pyrF*	1.279701184
3348	*hrpB*	1.087511397	3422	*cynT*	1.185961584	3496	*qmcA*	1.282821368
3349	*wcaM*	1.088088904	3423	*endA*	1.189118273	3497	*ybiW*	1.282913174
3350	*ybjD*	1.088761254	3424	*ssuE*	1.191204028	3498	*yjjZ*	1.283402904
3351	*ygcG*	1.088934153	3425	*fabF*	1.191391699	3499	*rybA*	1.284916489
3352	*dcuD*	1.095868382	3426	*yceO*	1.191595175	3500	*eaeH*	1.287046664
3353	*ymfD*	1.096244759	3427	*yjiS*	1.193858661	3501	*envZ*	1.288900922
3354	*yijD*	1.096786523	3428	*kup*	1.19574814	3502	*gapC_2*	1.291001827
3355	*alaE*	1.096832434	3429	*ydaS*	1.196175893	3503	*yqcG*	1.291362696
3356	*ydeI*	1.098949208	3430	*hybA*	1.200079373	3504	*cca-SPA*	1.291919682
3357	*dadX*	1.098973851	3431	*tusC*	1.202699826	3505	*eutP*	1.29298937
3358	*glrR*	1.101609939	3432	*yibN*	1.203121305	3506	*aegA*	1.293085938
3359	*selA*	1.103448557	3433	*frlD*	1.203870365	3507	*nadR*	1.296015928
3360	*yjiY*	1.104771668	3434	*ybiS*	1.203971893	3508	*hcr*	1.296312311
3361	*ybjI*	1.104880905	3435	*alx*	1.204757236	3509	*cbpA*	1.296634244
3362	*thiH*	1.10545921	3436	*kefC*	1.205548262	3510	*hscB*	1.297083862
3363	*mliC*	1.107228862	3437	*yjaA*	1.207456641	3511	*cobT*	1.297694377
3364	*btuE*	1.109708287	3438	*mhpF*	1.208039688	3512	*rfbD*	1.301698621
3365	*malF*	1.110627743	3439	*lpd*	1.208603405	3513	*nanM*	1.301700164
3366	*ygdT*	1.114917991	3440	*yncJ*	1.210270312	3514	*istR-1*	1.304255508
3367	*yphF*	1.11588611	3441	*uxuB*	1.211142065	3515	*iap*	1.305556935
3368	*frr-SPA*	1.117963067	3442	*yedX*	1.211332845	3516	*rlmM*	1.30605547
3369	*uspD*	1.119569183	3443	*xapR*	1.213068059	3517	*pgaB*	1.306076184
3370	*ybiA*	1.120564688	3444	*tyrS-SPA*	1.213200042	3518	*yrhB*	1.309762071
3371	*mtlA*	1.121896095	3445	*ybeU*	1.21446214	3519	*yahH*	1.31020579
3372	*pgi*	1.122570486	3446	*ECK0503*	1.214576061	3520	*pepP*	1.310890994
3373	*yjhQ*	1.122772325	3447	*tesB*	1.214856839	3521	*ytfH*	1.315215503
3374	*arcB*	1.124250568	3448	*yaeR*	1.215964497	3522	*ymgG*	1.317160182
3375	*cynX*	1.124254462	3449	*uup*	1.216594401	3523	*yafD*	1.318519568
3376	*zapC*	1.124725166	3450	*rimI*	1.217144434	3524	*ssrA*	1.319843482
3377	*clcB*	1.125517649	3451	*yjiX*	1.217868896	3525	*yagJ*	1.326705076
3378	*yihX*	1.125977661	3452	*emrD*	1.219190813	3526	*trpA*	1.328989144

3527	*fhuB*	1.330201486	3601	*hyfA*	1.442373339	3675	*zupT*	1.615695221
3528	*yeeZ*	1.33188748	3602	*ykiB*	1.443451596		*bamA{dup(218-*	
3529	*mtr*	1.332842924	3603	*gatY*	1.445327727	3676	*219)}*	1.620138347
3530	*rne-SPA*	1.333184628	3604	*yegU*	1.446063879	3677	*yafS*	1.622153589
3531	*yagP*	1.334959806	3605	*codB*	1.447011292	3678	*gadX*	1.624611246
3532	*ylaB*	1.336178349	3606	*ascG*	1.449380739	3679	*yqcC*	1.626910483
3533	*ypdB*	1.3376729	3607	*ybhU*	1.455247526	3680	*hsdS*	1.628556578
3534	*yqiK*	1.339369276	3608	*rraB*	1.455922675	3681	*fliE*	1.62955954
3535	*ribB-SPA*	1.34067774	3609	*rpmF*	1.458689073	3682	*ygbE*	1.633918795
3536	*mog*	1.342721304	3610	*ydcU*	1.459668492	3683	*maa*	1.645166546
3537	*hybF*	1.343999375	3611	*pheA*	1.459777403	3684	*melA*	1.645908254
3538	*yohH*	1.346289231	3612	*ydhV*	1.464237989	3685	*murF-SPA*	1.647712626
3539	*hipA*	1.346776491	3613	*ypdI*	1.464991966	3686	*yibA*	1.649646999
3540	*pgl*	1.349397497	3614	*yiiQ*	1.465778183	3687	*mglA*	1.651241342
3541	*ygjK*	1.349895144	3615	*dnaX-SPA*	1.468629799	3688	*serC*	1.652903647
3542	*rpsF*	1.351474572	3616	*mdtH*	1.468978346	3689	*yahO*	1.655545331
3543	*znuB*	1.353065998	3617	*ribF-SPA*	1.471228911	3690	*ydhF*	1.658400597
3544	*yrdD*	1.354562573	3618	*lolA-DAS+4*	1.474721184	3691	*rnr*	1.660566198
3545	*gudD*	1.35505956	3619	*mdtJ*	1.475966235	3692	*ygcS*	1.66202138
3546	*sgbU*	1.356940085	3620	*cspC*	1.4764062	3693	*lpp*	1.66774782
3547	*narG*	1.360774495	3621	*allD*	1.484746936	3694	*proP*	1.667802985
3548	*nlpE*	1.361916813	3622	*rpoD-SPA*	1.487766733	3695	*yjjU*	1.668849188
3549	*hupB*	1.362205054	3623	*glmZ*	1.492967937	3696	*ackA*	1.669307657
3550	*spf*	1.364316166	3624	*bsmA*	1.497099276	3697	*smf*	1.669773669
3551	*yehD*	1.364428021	3625	*yqiA*	1.497838328	3698	*frlA*	1.675712035
3552	*rcsD*	1.364901159	3626	*hscC*	1.498474844	3699	*ykgG*	1.676309507
3553	*ydcK*	1.36501261	3627	*ypjA*	1.505428272	3700	*gloA*	1.681943554
3554	*dsrB*	1.368157259	3628	*yqjG*	1.505942136	3701	*argD*	1.682808189
3555	*oppD*	1.372963032	3629	*cytR*	1.505947994	3702	*cheR*	1.682871871
3556	*torC*	1.373782043	3630	*yaeB*	1.507034341	3703	*cspI*	1.688587182
3557	*ykfI*	1.374998303	3631	*ryfB*	1.508769886	3704	*ygiF*	1.690717172
3558	*yhcN*	1.37731538	3632	*kdpE*	1.50954567	3705	*rusA*	1.690873195
3559	*yhiL*	1.377368586	3633	*ynbG*	1.512260698	3706	*poxB*	1.691401747
3560	*yqeC*	1.37774235	3634	*stpA*	1.520423257	3707	*ybeM_1*	1.6968197
3561	*rlmA*	1.381466114	3635	*xisE*	1.522583856	3708	*dedA*	1.699499216
3562	*fdhD*	1.38166215	3636	*gcd*	1.52610241	3709	*hisF*	1.699741948
3563	*yphA*	1.384484945	3637	*paoB*	1.526447162	3710	*mlaE*	1.700916949
3564	*yfgC*	1.387089329	3638	*yobB*	1.529065541	3711	*frdA*	1.702484921
3565	*envC*	1.390141117	3639	*ytfG*	1.532220105	3712	*yobF*	1.706537996
3566	*cheA*	1.391512133	3640	*gabD*	1.532346455	3713	*tyrA*	1.71814579
3567	*yqjA*	1.392010423	3641	*ycaO*	1.53400449	3714	*mdtE*	1.718169512
3568	*ydiJ*	1.393811931	3642	*ada*	1.536768409	3715	*ydhZ*	1.72009722
3569	*phoP*	1.394626003	3643	*mtlR*	1.541900521	3716	*frvR*	1.725100892
3570	*trkA*	1.394869045	3644	*ycgB*	1.543104459	3717	*gnsA*	1.726861018
3571	*flhD*	1.396748815	3645	*mraZ*	1.544658167	3718	*napA*	1.730241174
3572	*arsC*	1.399053992	3646	*ulaB*	1.545407022	3719	*cyaR*	1.731058924
3573	*yfdO*	1.399732559	3647	*pta*	1.545572049	3720	*astA*	1.741346977
3574	*yrdA*	1.401485401	3648	*ulaF*	1.54578023	3721	*lpxL*	1.744989925
3575	*mutS*	1.401586012	3649	*yafO*	1.550406963	3722	*arcA*	1.747417597
3576	*purL*	1.404465263	3650	*waaY*	1.553179351	3723	*ybfC*	1.748976057
3577	*yncE*	1.405078792	3651	*yhaH*	1.554201686	3724	*cysM*	1.750325121
3578	*yfeA*	1.406906308	3652	*yadN*	1.558826539	3725	*bdcR*	1.753264172
3579	*murE-A*	1.409740416	3653	*ypdE*	1.560236415	3726	*ptsN*	1.753306838
3580	*wcaL*	1.412304616	3654	*yhaO*	1.563838175	3727	*gspC*	1.758907497
3581	*hypD*	1.413926722	3655	*sdsR*	1.563986526	3728	*ymfE*	1.766853162
3582	*caiA*	1.414612079	3656	*ybfH*	1.565829491	3729	*cpxA*	1.769076261
3583	*mpl*	1.416815996	3657	*dgoT*	1.566056692	3730	*ndh*	1.777221246
3584	*yadL*	1.417897769	3658	*cbeA*	1.571094539	3731	*sgbE*	1.778165286
3585	*eamA*	1.420692195	3659	*thiC*	1.571386675	3732	*mdtK*	1.779149687
3586	*ybiX*	1.420964946	3660	*hdfR*	1.573030908	3733	*yghE*	1.782663694
3587	*dmlA*	1.424945181	3661	*prfH*	1.573449946	3734	*hflX*	1.792645102
3588	*bcsE*	1.425119391	3662	*xylE*	1.574855349	3735	*ydcX*	1.796690295
3589	*ydfN*	1.425312019	3663	*rppH*	1.576435476	3736	*yceB*	1.800612393
3590	*trmI*	1.426360943	3664	*tusA*	1.578335	3737	*bglX*	1.803271593
3591	*yedI*	1.426749074	3665	*ycfD*	1.578529517	3738	*ygaQ_2*	1.812789662
3592	*manA*	1.42848559	3666	*metJ*	1.581595486	3739	*ycgG*	1.81459427
3593	*ompR*	1.430958373	3667	*yfiO-DAS*	1.58285672	3740	*yhbU*	1.816348904
3594	*pgrR*	1.431209921	3668	*fldB*	1.584826092	3741	*ynjC*	1.827049141
3595	*argO*	1.431728013	3669	*ybbP*	1.591240099	3742	*ymiB*	1.828131968
3596	*diaA*	1.43295845	3670	*yjhP*	1.592635864	3743	*ompN*	1.829095289
3597	*rffM*	1.433323705	3671	*yggM*	1.60743413	3744	*xylB*	1.831795861
3598	*yahG*	1.438014616	3672	*yaiE*	1.6128698	3745	*yjjI*	1.831835394
3599	*narV*	1.44113701	3673	*yfgJ*	1.613652063	3746	*yiaK*	1.834391623
3600	*yhaM*	1.441356965	3674	*betB*	1.614996312	3747	*ykgO*	1.83614105

3748	*ybjH*	1.841356655	3822	*murE-B*	2.077240174	3896	*ytfQ*	2.598342808
3749	*ymfT*	1.841637985	3823	*garL*	2.101206892	3897	*queC*	2.603111572
3750	*nfo*	1.843357288	3824	*setA*	2.101677768	3898	*yjhR*	2.632318275
3751	*ybjJ*	1.849141715	3825	*pyrC*	2.106669633	3899	*truD*	2.648190852
3752	*yhhM*	1.85098211	3826	*rffE*	2.108824116	3900	*yffB*	2.650792107
3753	*acs*	1.851362914	3827	*malS*	2.110715234	3901	*pfkA*	2.66909915
3754	*yfcI*	1.851423659	3828	*yaaY*	2.1110693	3902	*holD*	2.669970279
3755	*yafP*	1.852632889	3829	*zraS*	2.116886543	3903	*trpE*	2.677119719
3756	*ydaN*	1.854844001	3830	*yaaA*	2.11838401	3904	*nrdF*	2.688263658
3757	*yaeQ*	1.856154409	3831	*oppC*	2.122491234	3905	*rpoS*	2.703599014
3758	*treR*	1.857050462	3832	*narU*	2.125483758	3906	*clpB*	2.718353614
3759	*uvrD*	1.857120943	3833	*rpiR*	2.143943442	3907	*dinJ*	2.784585691
3760	*mukE-SPA*	1.867042727	3834	*cydA-SPA*	2.144343945	3908	*blc*	2.803154582
3761	*ykgB*	1.868079901	3835	*yadK*	2.149525267	3909	*raiA*	2.806319316
3762	*yjgL*	1.872873402	3836	*hcp*	2.151737847	3910	*dinF*	2.820861164
3763	*zraP*	1.874582262	3837	*gatB*	2.16072992	3911	*rayT*	2.83080847
3764	*gntP*	1.879805532	3838	*uvrA*	2.175492942	3912	*apaH*	2.857732305
3765	*glnH*	1.885612631	3839	*yjhF*	2.179249328	3913	*ykfG*	2.871819102
3766	*yabI*	1.888098318	3840	*yadI*	2.17985253	3914	*lacA*	2.89265086
3767	*gnsB*	1.888458069	3841	*serB*	2.18386569	3915	*thyA*	2.929105537
3768	*yceG*	1.889176223	3842	*nrdR*	2.186867671	3916	*yafW*	2.933215625
3769	*rdlABCD*	1.891211461	3843	*wcaI*	2.189246621	3917	*cysW*	2.950626351
3770	*ygeL*	1.8972759	3844	*ygaH*	2.189608784	3918	*yajG*	2.952354995
3771	*rutC*	1.897728782	3845	*glnD*	2.194030245	3919	*cnu*	2.986170183
3772	*otsB*	1.901704817	3846	*rpe*	2.209212659	3920	*frsA*	2.993423378
3773	*bioD*	1.908519782	3847	*ycgN*	2.209917951	3921	*yjjK*	3.008013974
3774	*yebO*	1.909593161	3848	*ygjQ*	2.210098499	3922	*mrcB*	3.014466988
3775	*tig*	1.912291514	3849	*yeiI*	2.215064204	3923	*rarD*	3.024921212
3776	*rffD*	1.920159399	3850	*intR*	2.215373319	3924	*crl*	3.02931977
3777	*yfaV*	1.927912275	3851	*iscU*	2.218499141	3925	*ptsG*	3.035601381
3778	*yniC*	1.927983303	3852	*ulaC*	2.226995267	3926	*hisI*	3.050381929
3779	*kdgT*	1.928708561	3853	*bamE*	2.243925799	3927	*citX*	3.058355453
3780	*rlmD*	1.9311126	3854	*yaiX*	2.250498762	3928	*yafE*	3.06322328
3781	*yfdX*	1.933541958	3855	*iscA*	2.252697854	3929	*cysH*	3.095025163
3782	*rph*	1.936572146	3856	*topB*	2.256244418	3930	*ftsA-SPA*	3.139515552
3783	*yieL*	1.946381156	3857	*rpsE-SPA*	2.272280737	3931	*pyrD*	3.162199387
3784	*sroH*	1.948229735	3858	*mutY*	2.273673035	3932	*dacA*	3.209892124
3785	*plsC-SPA*	1.949100199	3859	*tolB*	2.283857542	3933	*amiC*	3.261660206
3786	*ybeY*	1.951199192	3860	*tatB*	2.284962945	3934	*yraH*	3.271959333
3787	*yjiC*	1.951697523	3861	*metA*	2.289056959	3935	*thrA*	3.289089888
3788	*preT*	1.955980132	3862	*ynfE*	2.290432077	3936	*cydD*	3.33027747
3789	*speA*	1.959388223	3863	*artJ*	2.291443823	3937	*cysG*	3.332861066
3790	*ugpQ*	1.9618938	3864	*glgX*	2.291784704	3938	*ftsP*	3.352163843
3791	*can-SPA*	1.967308183	3865	*yegK*	2.294106794	3939	*hisD*	3.35688786
3792	*yhbX*	1.973830381	3866	*argG*	2.301269719	3940	*trpD*	3.454689182
3793	*fliK*	1.985830713	3867	*argH*	2.311569441	3941	*yfdY*	3.457115834
3794	*hisG*	1.987383787	3868	*nanK*	2.314894084	3942	*baeS*	3.461166218
3795	*yehA*	1.994785161	3869	*yqjF*	2.315141975	3943	*arfB*	3.470555831
3796	*proC*	1.997329722	3870	*yccX*	2.324199025	3944	*nudB*	3.474888947
3797	*yadC*	2.00299479	3871	*ygdR*	2.326196365	3945	*sanA*	3.513072865
3798	*yfaL*	2.005001865	3872	*mhpB*	2.328029631	3946	*ykfH*	3.550866918
3799	*rof*	2.008527473	3873	*cheY*	2.333065589	3947	*ppiB*	3.554461555
3800	*iscR*	2.010133512	3874	*rsmG*	2.34152081	3948	*leuA*	3.554953424
3801	*frlC*	2.012048807	3875	*yfjT*	2.354643636	3949	*ychF*	3.56464894
3802	*ybfE*	2.01402993	3876	*pgpA*	2.358016896	3950	*sad*	3.618742887
3803	*plsX*	2.014651563	3877	*purM*	2.404656905	3951	*yajR*	3.619231869
3804	*yaaU*	2.017814518	3878	*ygdQ*	2.431630092	3952	*aroC*	3.632810855
3805	*yfhH*	2.020287117	3879	*cysI*	2.469516253	3953	*yahB*	3.675787799
3806	*gltD*	2.024811972	3880	*pstS*	2.474359723	3954	*eutK*	3.931700791
3807	*metR*	2.027937499	3881	*yggX*	2.475708482	3955	*iscS*	4.212375081
3808	*ydjO*	2.029876609	3882	*yedQ*	2.478600327	3956	*carA*	4.563964212
3809	*afuB*	2.03948908	3883	*cysA*	2.486733193	3957	*ilvA*	4.691765978
3810	*ydfV*	2.04194023	3884	*pncA*	2.499502794	3958	*leuD*	4.768630731
3811	*yahM*	2.043717963	3885	*deaD*	2.505476727	3959	*dapF*	4.7806912
3812	*hisC*	2.044652871	3886	*ybiI*	2.505558895	3960	*ilvE*	4.865858119
3813	*yhjJ*	2.046552815	3887	*ybeD*	2.506827696	3961	*rplA*	4.901910465
3814	*fhuD*	2.050427652	3888	*truA*	2.519972155	3962	*chpB*	5.076033723
3815	*dtpB*	2.051849529	3889	*gadE*	2.526197824	3963	*aceF*	5.185433603
3816	*yicI*	2.054516535	3890	*nlpD*	2.532184798	3964	*pyrB*	5.580314708
3817	*ompT*	2.058644031	3891	*yhfZ*	2.542673512	3965	*hisH*	5.885387029
3818	*ivy*	2.067251707	3892	*yjtD*	2.556207902	3966	*rpoN*	6.244213668
3819	*fdx*	2.069625813	3893	*alr*	2.559519143	3967	*ptsH*	6.413549202
3820	*paaZ*	2.072393075	3894	*yjjY*	2.565870694	3968	*lysR*	6.527648622
3821	*cysC*	2.074286446	3895	*trxA*	2.569422154	3969	*lipB*	7.333729552

3970	*ppc*	11.86087446	3979	*glnA*	N.D.	3988	*leuB*	N.D.
3971	*argC*	N.D.	3980	*pyrE*	N.D.	3989	*purH*	N.D.
3972	*trpB*	N.D.	3981	*hisB*	N.D.	3990	*folB*	N.D.
3973	*metB*	N.D.	3982	*aroB*	N.D.	3991	*cysB*	N.D.
3974	*cysJ*	N.D.	3983	*hisA*	N.D.	3992	*guaA*	N.D.
3975	*serA*	N.D.	3984	*guaB*	N.D.	3993	*yfdS*	N.D.
3976	*argE*	N.D.	3985	*thrC*	N.D.	3994	*rydC*	N.D.
3977	*metF*	N.D.	3986	*ilvC*	N.D.			
3978	*metE*	N.D.	3987	*argB*	N.D.			

Appendix table 1: Relative fitness-scores of Keio library strains in oleate condition compared to a glucose control. Unless otherwise mentioned, the mutations are precise gene deletions from the Keio knockout library. N.D.: Not Determined

Appendix 2:

S. No.	Strain	Position (LCFA dataset)
1	*yqiC*::*kan*	17
2	*yhcB*::*kan*	37
3	*yebK*::*kan*	39
4	*ybhP*::*kan*	48
5	*ybgA*::*kan*	54
6	*yqaA*::*kan*	55
7	*ydeS*::*kan*	66
8	*ygeH*::*kan*	67
9	*yidK*::*kan*	68
10	*ygcR*::*kan*	70
11	*yhbT*::*kan*	72
12	*yjjM*::*kan*	76
13	*yeaN*::*kan*	78
14	*yqiH*::*kan*	79
15	*ydfU*::*kan*	81
16	*yjcZ*::*kan*	82
17	*yegT*::*kan*	87
18	*ybaP*::*kan*	88
19	*ytfL*::*kan*	93
20	*yeaD*::*kan*	98
21	*yfcS*::*kan*	99

Appendix table 2: Position of '*y*' genes among top 100 candidates in the long-chain fatty acid (LCFA) dataset. The genes of unknown function (*y* genes), which were significantly required for growth of *E. coli* in oleate, were selected from top 100 candidates in the LCFA dataset. *yqiC* knockout was first in this list with 17th rank in the LCFA dataset.